

# PRELIMINARY REVIEW COPY

Technical Report Documentation Page

1. Report No. <i>Preliminary Review Copy</i>		2. Government Accession No.		3. Recipient's Catalog No.	
4. Title and Subtitle <i>INSTRUMENTATION SYSTEMS FOR FIELD STUDY OF SEGMENTAL BOX GIRDER BRIDGES</i>				5. Report Date <i>August 1993</i>	
				6. Performing Organization Code	
7. Author(s) <i>J. A. Arrellaga, C. L. Roberts, J. E. Breen, and M. E. Kreger</i>				8. Performing Organization Report No. <i>Research Report 1234-1</i>	
9. Performing Organization Name and Address <i>Center for Transportation Research The University of Texas at Austin 3208 Red River, Suite 200 Austin, Texas 78705-2650</i>				10. Work Unit No. (TRAIS)	
				11. Contract or Grant No. <i>Research Study 3-5-90/3-1234</i>	
12. Sponsoring Agency Name and Address <i>Texas Department of Transportation Transportation Planning Division, Research Section P. O. Box 5051 Austin, Texas 78763-5051</i>				13. Type of Report and Period Covered <i>Interim</i>	
				14. Sponsoring Agency Code	
15. Supplementary Notes <i>Study conducted in cooperation with the U.S. Department of Transportation, Federal Highway Administration. Research Study Title: "Instrumentation of Segmental Box Girder Bridges and Multipiece Winged Boxes"</i>					
16. Abstract  <i>This report is the first in a series reporting the field study of several spans of the San Antonio "Y" Project. The San Antonio "Y" Project is a major urban viaduct comprising segmental concrete box girders post-tensioned with a mix of internal and external tendons and erected using span-by-span techniques.</i>  <i>This report describes the development of the instrumentation systems which were installed in the field project. The major systems were:</i>  <ol style="list-style-type: none"><li>1. External post-tensioning tendon forces,</li><li>2. Span deflections and segment deformations,</li><li>3. Concrete temperatures,</li><li>4. Concrete strains,</li><li>5. Reinforcing steel strains,</li><li>6. Joint openings,</li><li>7. Bearing movements, and</li><li>8. Solar radiation.</li></ol> <i>A comprehensive literature review of each system was performed and the most promising systems were tested in the laboratory and in the field. Recommendations on the best system for each type of measurement were made, and the systems were installed in four spans of the San Antonio "Y" Project. Also in this report the performance of each system in the field is evaluated and recommendations for future field studies are presented.</i>					
17. Key Words <i>post-tensioned, concrete, segmental, box-girder bridges, instrumentation, field measurements, external tendons</i>			18. Distribution Statement <i>No restrictions. This document is available to the public through the National Technical Information Service, Springfield, Virginia 22161.</i>		
19. Security Classif. (of this report) <i>Unclassified</i>		20. Security Classif. (of this page) <i>Unclassified</i>		21. No. of Pages <i>282</i>	22. Price

Technical Report Standard Title Page

4. Title: Instrumentation Systems for Field Study of Segmental Box Girder Bridges
6. Authors: J.A. Arréllaga, C.L. Roberts, J.E. Breen, M.E. Kreger
15. Supplementary Notes: Study conducted in cooperation with the U.S. Department of Transportation, Federal Highway Administration. Research Study Title: "Instrumentation of Segmental Box Girder Bridges and Multipiece Winged Boxes."
16. Abstract:

This report is the first in a series reporting the field study of several spans of the San Antonio "Y" Project. The San Antonio "Y" Project is a major urban viaduct comprising segmental concrete box girders post-tensioned with a mix of internal and external tendons and erected using span-by-span techniques.

This report describes the development of the instrumentation systems which were installed in the field project. The major systems were:

1. External post-tensioning tendon forces,
2. Span deflections and segment deformations,
3. Concrete temperatures,
4. Concrete strains,
5. Reinforcing steel strains,
6. Joint openings,
7. Bearing movements, and
8. Solar radiation.

A comprehensive literature review of each system was performed and the most promising systems were tested in the laboratory and in the field. Recommendations on the best system for each type of measurement were made, and the systems were installed in four spans of the San Antonio "Y" Project. Also in this report the performance of each system in the field is evaluated and recommendations for future field studies are presented.

17. Key Words: post-tensioned, concrete, segmental, box-girder bridges, instrumentation, field measurements, external tendons

# PRELIMINARY REVIEW COPY

1. Report No. <i>Preliminary Review Copy</i>		2. Government Accession No.		3. Recipient's Catalog No.	
4. Title and Subtitle <i>INSTRUMENTATION SYSTEMS FOR FIELD STUDY OF SEGMENTAL BOX GIRDER BRIDGES</i>				5. Report Date <i>August 1993</i>	
				6. Performing Organization Code	
7. Author(s) <i>J. A. Arrellaga, C. L. Roberts, J. E. Breen, and M. E. Kreger</i>				8. Performing Organization Report No. <i>Research Report 1234-1</i>	
9. Performing Organization Name and Address <i>Center for Transportation Research The University of Texas at Austin 3208 Red River, Suite 200 Austin, Texas 78705-2650</i>				10. Work Unit No. (TRAIS)	
				11. Contract or Grant No. <i>Research Study 3-5-90/3-1234</i>	
12. Sponsoring Agency Name and Address <i>Texas Department of Transportation Transportation Planning Division, Research Section P. O. Box 5051 Austin, Texas 78763-5051</i>				13. Type of Report and Period Covered <i>Interim</i>	
				14. Sponsoring Agency Code	
15. Supplementary Notes <i>Study conducted in cooperation with the U.S. Department of Transportation, Federal Highway Administration. Research Study Title: "Instrumentation of Segmental Box Girder Bridges and Multipiece Winged Boxes"</i>					
16. Abstract  <i>This report is the first in a series reporting the field study of several spans of the San Antonio "Y" Project. The San Antonio "Y" Project is a major urban viaduct comprising segmental concrete box girders post-tensioned with a mix of internal and external tendons and erected using span-by-span techniques.</i>  <i>This report describes the development of the instrumentation systems which were installed in the field project. The major systems were:</i>  <ol style="list-style-type: none"><li>1. External post-tensioning tendon forces,</li><li>2. Span deflections and segment deformations,</li><li>3. Concrete temperatures,</li><li>4. Concrete strains,</li><li>5. Reinforcing steel strains,</li><li>6. Joint openings,</li><li>7. Bearing movements, and</li><li>8. Solar radiation.</li></ol> <i>A comprehensive literature review of each system was performed and the most promising systems were tested in the laboratory and in the field. Recommendations on the best system for each type of measurement were made, and the systems were installed in four spans of the San Antonio "Y" Project. Also in this report the performance of each system in the field is evaluated and recommendations for future field studies are presented.</i>					
17. Key Words <i>post-tensioned, concrete, segmental, box-girder bridges, instrumentation, field measurements, external tendons</i>			18. Distribution Statement <i>No restrictions. This document is available to the public through the National Technical Information Service, Springfield, Virginia 22161.</i>		
19. Security Classif. (of this report) <i>Unclassified</i>		20. Security Classif. (of this page) <i>Unclassified</i>		21. No. of Pages <i>282</i>	22. Price

**INSTRUMENTATION SYSTEMS FOR FIELD STUDY OF  
SEGMENTAL BOX GIRDER BRIDGES**

by

**J. A. Arréllaga, C. L. Roberts, J. E. Breen, and M. E. Kreger**

**Research Report No. 1234-1**

**Research Project 3-5-90/3-1234  
"Instrumentation of Segmental Box Girder Bridges  
and Multipiece Winged Boxes"**

***PRELIMINARY REVIEW COPY***

conducted for the

**Texas  
Department of Transportation**

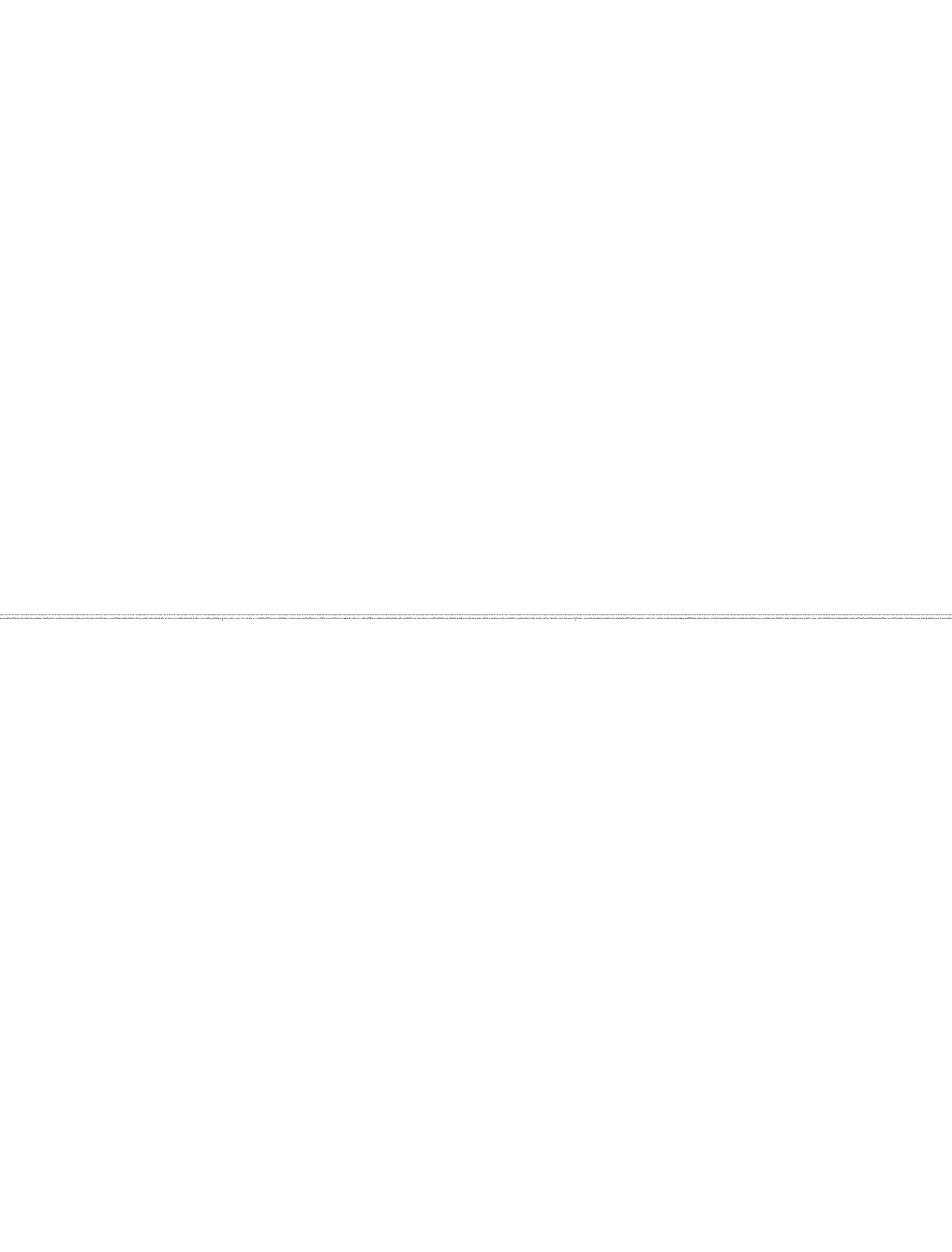
**in Cooperation with the  
U.S. Department of Transportation  
Federal Highway Administration**

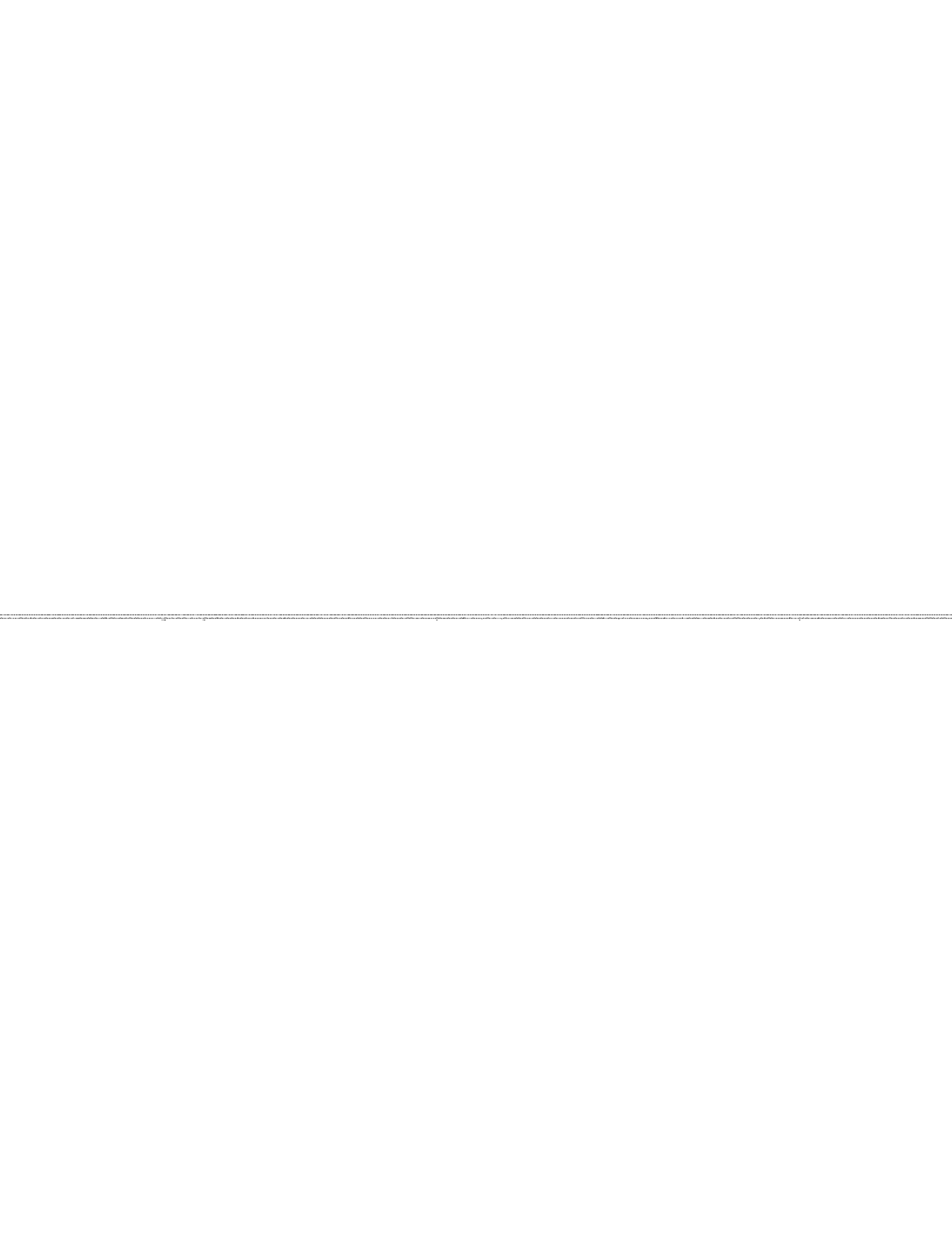
by the

**CENTER FOR TRANSPORTATION RESEARCH  
BUREAU OF ENGINEERING RESEARCH  
THE UNIVERSITY OF TEXAS AT AUSTIN**

**August 1993**







## IMPLEMENTATION

This report provides detailed information on state-of-the-art instrumentation systems for use in the field study of segmental concrete bridges. The recommendations have already been used successfully in the instrumentation of four spans of the San Antonio "Y" Project. The recommendations are readily applicable to the study of similar segmental bridges erected using span-by-span techniques. The information can also be adapted to the field study of other types of segmental and conventional bridge structures. The results of the study should assist bridge engineers and research agencies to efficiently plan instrumentation programs for future bridge projects. Resulting savings from dependable observation programs should be possible through improvement of design and construction standards.

Prepared in cooperation with the Texas Department of Transportation and the  
U.S. Department of Transportation, Federal Highway Administration

The contents of this report reflect the views of the authors, who are responsible for the facts and the accuracy of the data presented herein. The contents do not necessarily reflect the official views or policies of the Federal Highway Administration or the Texas Department of Transportation. This report does not constitute a standard, specification, or regulation.

There was no invention or discovery conceived or first actually reduced to practice in the course of or under this contract, including any art, method, process, machine, manufacture, design or composition of matter, or any new and useful improvement thereof, or any variety of plant which is or may be patentable under the patent laws of the United States of America or any foreign country.

**NOT INTENDED FOR CONSTRUCTION,  
BIDDING OR PERMIT PURPOSES**

John E. Breen, P.E. (Texas No. 18479)  
Michael E. Kreger, P.E. (Texas No. 65541)  
*Research Supervisors*

## PREFACE

This report is the first in a series which presents the results of a field investigation of several spans of the San Antonio "Y" Project, which is a segmental concrete box girder bridge, post-tensioned with a combination of internal and external tendons, and erected using span-by-span techniques. This report reviews the selection of instrumentation systems and presents an evaluation of their field performance. The second report presents the data collected in the field study, compares measured bridge behavior to current design methods, and presents recommendations for the revision of current design and construction criteria.

This work is part of research project 3-5-90-1234 entitled "Instrumentation of Segmental Box Girder Bridges and Multipiece Winged Boxes." The research was conducted at the Phil M. Ferguson Structural Engineering Laboratory and at the casting yard and erection site of the project as part of the overall research programs of the Center for Transportation Research of the University of Texas at Austin. The work was sponsored jointly by the Texas Department of Transportation and the Federal Highway Administration under an agreement with The University of Texas at Austin and the Texas Department of Transportation. Great cooperation was provided by the contractor on Phase IIC of the San Antonio "Y" Project, Austin Bridge and Road of Dallas, Texas.

Liaison with the Texas Department of Transportation was maintained through the contact representative, Mr. Patrick Bachman. Mr. James Craig was the contact representative for the Federal Highway Administration.

The overall study was directed by John E. Breen, who holds the Nasser I. Al-Rashid Chair in Civil Engineering, and Michael E. Kreger, Associate Professor of Civil Engineering. The development of the instrumentation systems was the direct responsibility of José A. Arréllaga, Assistant Research Engineer. The installation of the field instrumentation, the collection and analysis of field data, and the development of final recommendations were the responsibility of Carin L. Roberts, Assistant Research Engineer.

## ABSTRACT

This report is the first in a series reporting the field study of several spans of the San Antonio "Y" Project. The San Antonio "Y" Project is a major urban viaduct comprising segmental concrete box girders post-tensioned with a mix of internal and external tendons and erected using span-by-span techniques.

This report describes the development of the instrumentation systems which were installed in the field project. The major systems were:

1. External post-tensioning tendon forces,
2. Span deflections and segment deformations,
3. Concrete temperatures,
4. Concrete strains,
5. Reinforcing steel strains,
6. Joint openings,
7. Bearing movements, and
8. Solar radiation.

A comprehensive literature review of each system was performed and the most promising systems were tested in the laboratory and in the field. Recommendations on the best system for each type of measurement were made, and the systems were installed in four spans of the San Antonio "Y" Project. Also in this report the performance of each system in the field is evaluated and recommendations for future field studies are presented.

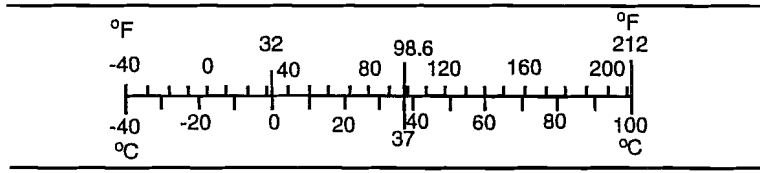
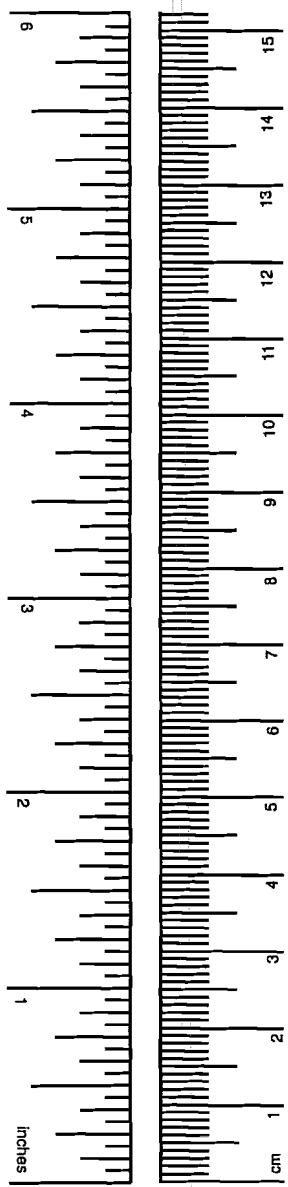
# METRIC (SI\*) CONVERSION FACTORS

## APPROXIMATE CONVERSIONS TO SI UNITS

## APPROXIMATE CONVERSIONS FROM SI UNITS

Symbol	When You Know	Multiply by	To Find	Symbol
<b>LENGTH</b>				
in	inches	2.54	centimeters	cm
ft	feet	0.3048	meters	m
yd	yards	0.914	meters	m
mi	miles	1.61	kilometers	km
<b>AREA</b>				
in <sup>2</sup>	square inches	645.2	millimeters squared	mm <sup>2</sup>
ft <sup>2</sup>	square feet	0.0929	meters squared	m <sup>2</sup>
yd <sup>2</sup>	square yards	0.836	meters squared	m <sup>2</sup>
mi <sup>2</sup>	square miles	2.59	kilometers squared	km <sup>2</sup>
ac	acres	0.395	hectares	ha
<b>MASS (weight)</b>				
oz	ounces	28.35	grams	g
lb	pounds	0.454	kilograms	kg
T	short tons (2,000 lb)	0.907	megagrams	Mg
<b>VOLUME</b>				
fl oz	fluid ounces	29.57	milliliters	mL
gal	gallons	3.785	liters	L
ft <sup>3</sup>	cubic feet	0.0328	meters cubed	m <sup>3</sup>
yd <sup>3</sup>	cubic yards	0.0765	meters cubed	m <sup>3</sup>
<b>TEMPERATURE (exact)</b>				
°F	Fahrenheit temperature	5/9 (after subtracting 32)	Celsius temperature	°C

Symbol	When You Know	Multiply by	To Find	Symbol
<b>LENGTH</b>				
mm	millimeters	0.039	inches	in
m	meters	3.28	feet	ft
m	meters	1.09	yards	yd
km	kilometers	0.621	miles	mi
<b>AREA</b>				
mm <sup>2</sup>	millimeters squared	0.0016	square inches	in <sup>2</sup>
m <sup>2</sup>	meters squared	10.764	square feet	ft <sup>2</sup>
m <sup>2</sup>	meters squared	1.20	square yards	yd <sup>2</sup>
km <sup>2</sup>	kilometers squared	0.39	square miles	mi <sup>2</sup>
ha	hectares (10,000 m <sup>2</sup> )	2.53	acres	ac
<b>MASS (weight)</b>				
g	grams	0.0353	ounces	oz
kg	kilograms	2.205	pounds	lb
Mg	megagrams (1,000 kg)	1.103	short tons	T
<b>VOLUME</b>				
mL	milliliters	0.034	fluid ounces	fl oz
L	liters	0.264	gallons	gal
m <sup>3</sup>	meters cubed	35.315	cubic feet	ft <sup>3</sup>
m <sup>3</sup>	meters cubed	1.308	cubic yards	yd <sup>3</sup>
<b>TEMPERATURE (exact)</b>				
°C	Celsius temperature	9/5 (then add 32)	Fahrenheit temperature	°F



These factors conform to the requirement of FHWA Order 5190.1A.

\* SI is the symbol for the International System of Measurements

# TABLE OF CONTENTS

	<b>Page</b>
CHAPTER 1 INTRODUCTION . . . . .	1
1.1 Introduction . . . . .	1
1.2 Areas of Uncertainty in the AASHTO Guide Specification . . . . .	1
1.3 Required Instrumentation Systems . . . . .	2
1.4 Project Objectives . . . . .	2
1.5 Report Organization . . . . .	3
CHAPTER 2 PRESTRESSING STEEL STRAINS/FORCES . . . . .	5
2.1 Review of Available Systems . . . . .	5
2.1.1 Strain Measuring Devices. . . . .	5
2.1.2 Load Measuring Devices. . . . .	10
2.2 Trials of Instrumentation Systems . . . . .	19
2.2.1 Electrical Resistance Strain Gages. . . . .	20
2.2.2 Epoxy Sleeves. . . . .	48
2.3 Recommendations for Use with the San Antonio Y Project . . . . .	70
2.3.1 Electrical Resistance Gages. . . . .	70
2.3.2 Epoxy Sleeves. . . . .	76
2.4 Field Installation . . . . .	79
2.4.1 Prefabrication. . . . .	79
2.4.2 Job Site Activities. . . . .	79
2.5 Performance . . . . .	84
2.6 Instrumentation Layouts . . . . .	85
2.7 Recommendations for Future Projects . . . . .	88
CHAPTER 3 SPAN DEFLECTIONS . . . . .	89
3.1 Review of Available Systems . . . . .	89
3.1.1 Objectives. . . . .	89
3.1.2 Baseline Methods. . . . .	89
3.1.3 Hydrostatic Methods. . . . .	94
3.1.4 Surveying Methods. . . . .	97
3.2 Trials of Instrumentation Systems . . . . .	98

3.2.1	Line Tensioning Systems. . . . .	100
3.2.2	Reading Systems. . . . .	108
3.2.3	Short-Span Performance of Final System. . . . .	110
3.2.4	Field Performance Test of Final System. . . . .	111
3.3	Recommendations . . . . .	125
3.3.1	System Description and Selection. . . . .	125
3.3.2	Field Installation. . . . .	128
3.3.3	Operation and Storage. . . . .	128
3.4	Field Installation in the San Antonio Y Project . . . . .	129
3.4.1	Span Deflections. . . . .	129
3.4.2	Truss Deflection System. . . . .	130
3.4.3	Wingtip Deflection System. . . . .	130
3.4.4	Segment Deformations during Match Casting. . . . .	132
3.5	Performance . . . . .	133
3.6	Layouts . . . . .	134
3.7	Recommendations for Future Projects . . . . .	134
<b>CHAPTER 4 CONCRETE TEMPERATURES . . . . .</b>		<b>137</b>
4.1	Review of Available Systems . . . . .	137
4.1.1	Objectives. . . . .	138
4.1.2	Thermocouples. . . . .	139
4.1.3	Thermistors. . . . .	141
4.1.4	Other Systems. . . . .	143
4.2	Recommendations for Use with the San Antonio Y Project . . . . .	144
4.3	Field Installation . . . . .	146
4.3.1	Prefabrication. . . . .	146
4.3.2	Casting-Yard Operations. . . . .	146
4.3.3	Job-Site Operations. . . . .	147
4.4	Performance . . . . .	147
4.5	Instrumentation Layouts . . . . .	148
4.6	Recommendations for Future Projects . . . . .	148
<b>CHAPTER 5 CONCRETE STRAINS . . . . .</b>		<b>151</b>
5.1	Review of Available Systems . . . . .	151
5.1.1	Objectives. . . . .	153
5.1.2	Embedment Systems. . . . .	154
5.1.3	Surface Strain Systems. . . . .	162



5.2	Trials of Instrumentation Systems . . . . .	167
5.2.1	Demec Gages: Bonding Methods. . . . .	167
5.2.2	Demec Gages: Increases in Operating Speed. . . . .	172
5.2.3	Demec Gages: Repeatability. . . . .	175
5.3	Recommendations for Use with the San Antonio Y Project . . . . .	176
5.3.1	Installation of Locating Points. . . . .	176
5.3.2	Corrections for Temperature Differentials. . . . .	177
5.3.3	Operating Instructions. . . . .	178
5.4	Field Installation . . . . .	180
5.5	Performance . . . . .	180
5.6	Instrumentation Layouts . . . . .	181
5.7	Recommendations for Future Projects . . . . .	181
CHAPTER 6 OTHER MEASUREMENTS . . . . .		185
6.1	Reinforcing Steel Strain Gages . . . . .	185
6.1.1	Recommendations. . . . .	185
6.1.2	System Installation in the San Antonio Y Project. . . . .	186
6.1.3	Performance. . . . .	187
6.1.4	Instrumentation Layouts. . . . .	187
6.1.5	Recommendations for Future Projects. . . . .	190
6.2	Joint Openings . . . . .	190
6.2.1	Recommendations. . . . .	190
6.2.2	Field Installation in the San Antonio Y Project. . . . .	191
6.2.3	Performance. . . . .	192
6.2.4	Instrumentation Layouts. . . . .	192
6.3	Bearing Movements . . . . .	196
6.3.1	Recommendations. . . . .	196
6.3.2	Field Installation. . . . .	197
6.3.3	Performance. . . . .	197
6.3.4	Instrumentation Layouts. . . . .	198
6.3.5	Recommendations for Future Projects. . . . .	198
6.4	Solar Radiation . . . . .	198
6.4.1	Recommendations. . . . .	198
6.4.2	Field Installation on the San Antonio Y Project. . . . .	199
6.4.3	Performance. . . . .	199
6.4.4	Recommendation for Future Projects. . . . .	200

CHAPTER 7 DATA ACQUISITION SYSTEMS . . . . .	201
7.1 Review of Available Systems . . . . .	201
7.2 System Selection . . . . .	203
7.3 System Installation in the San Antonio Y Project . . . . .	207
7.4 Performance . . . . .	207
7.5 Recommendations for Future Projects . . . . .	207
CHAPTER 8 COMPANION MATERIAL TESTS . . . . .	209
8.1 Recommendations . . . . .	209
8.1.1 Concrete. . . . .	209
8.1.2 Prestressing Steel. . . . .	211
8.1.3 Reinforcing Steel. . . . .	213
8.2 Field Applications in the San Antonio Y Project . . . . .	214
8.2.1 Concrete. . . . .	214
8.2.2 Prestressing Steel and Reinforcing Steel. . . . .	215
CHAPTER 9 CONCLUSIONS AND RECOMMENDATIONS . . . . .	217
APPENDIX A . . . . .	219
APPENDIX B . . . . .	243
REFERENCES . . . . .	259

## LIST OF FIGURES

		<b>Page</b>
Figure 2.1	Electrical resistance foil gage bonded to single wire of strand. . . . .	7
Figure 2.2	Stress-strain plot of single prestressing strand with 6 ER-gages (after Yates <sup>54</sup> ). . . . .	7
Figure 2.3	Principle of reference optical fiber sensors. . . . .	10
Figure 2.4	Calibrated hydraulic jack for field measurement of tendon loads. . . . .	11
Figure 2.5	Electrical resistance load cells with central holes (from Geokon's catalog). . . . .	12
Figure 2.6	Schematic of a typical electrical resistance load cell (after Dunningcliff <sup>15</sup> ). . . . .	13
Figure 2.7	Freyssinet's Tensiomag system (from Freyssinet's catalog). . . . .	15
Figure 2.8	Operation principle of Tensiomag (from Freyssinet's catalog). . . . .	16
Figure 2.9	DynaTension System (from DynaTension's catalog). . . . .	17
Figure 2.10	Cable Tensiometer (after Dunningcliff <sup>15</sup> ). . . . .	17
Figure 2.11	Fulmer Tension Meter (after Hanna <sup>20</sup> ). . . . .	18
Figure 2.12	Kuhlman Beam from California D.O.T. (after Richardson <sup>45</sup> ). . . . .	18
Figure 2.13	Installation of the electrical resistance strain gages for TEST 1S (similar to TEST 4S). . . . .	28
Figure 2.14	Analytical approximation of a prestressing strand's apparent modulus of elasticity, as determined by electrical resistance strain gages bonded to individual wires. . . . .	29
Figure 2.15	Stress-strain curves for TEST 2S on first 1/2" $\phi$ strand specimen from roll "B". . . . .	30
Figure 2.16	Summary of stress-strain average curves of single-strand tests with ER-gages. . . . .	31
Figure 2.17	Statistical analysis of electrical resistance strain gage results from tests on 1/2" $\phi$ strand specimens from roll "B". . . . .	33
Figure 2.18	Statistical analysis of electrical resistance strain gage results from tests on 0.6" $\phi$ strand specimen from roll "C". . . . .	34
Figure 2.19	General schematic of TEST 1T and TEST 2T. . . . .	37
Figure 2.20	General schematic of TEST 3T and TEST 4T. . . . .	38
Figure 2.21	Schematic representation of data-reduction procedure. . . . .	40
Figure 2.22	Stress-strain plots of individual ER-gages for TEST 1T. . . . .	41
Figure 2.23	Stress-strain plots of individual ER-gages for TEST 2T. . . . .	42
Figure 2.24	Statistical analysis of electrical resistance strain gage results from tendon TESTs 1T and 2T with 1/2" $\phi$ strands. . . . .	44
Figure 2.25	Comparison of average stress-strain plots of the ER-gages of TESTs 3T and 4T. . . . .	46
Figure 2.26	Statistical analysis of ER-gage results from tendon TESTs 3T and 4T on 19-0.6" diameter strands. . . . .	47
Figure 2.27	Schematic of the epoxy sleeve system used in single-strand tests. . . . .	50

Figure 2.28	Summary of stress-strain average plots of single-strand tests with epoxy sleeves. . . . .	52
Figure 2.29	Statistical analysis of epoxy sleeve results from tests on 1/2" $\phi$ strand specimens from roll "B". . . . .	53
Figure 2.30	Statistical analysis of epoxy sleeve results from tests on the 0.6" $\phi$ strand specimen from roll "C". . . . .	53
Figure 2.31	Construction steps of the epoxy sleeve system used in TEST 2T: molds for the epoxy sleeve; installed epoxy sleeve assembly; and final gaged epoxy sleeve system. . . . .	55
Figure 2.32	Epoxy leaks in TEST 2T. . . . .	57
Figure 2.33	Stress-strain plots of individual epoxy sleeve reading locations for TEST 1T. . . . .	59
Figure 2.34	Stress-strain plots of individual epoxy sleeve reading locations for TEST 2T. . . . .	60
Figure 2.35	Statistical analysis of epoxy sleeve results from tendon TESTs 1T and 2T with 12" $\phi$ strands. . . . .	61
Figure 2.36	Possible stress distributions in a typical epoxy collar. . . . .	63
Figure 2.37	Epoxy sleeve measuring systems. . . . .	63
Figure 2.38	Stress-Strain plots of individual epoxy sleeve reading locations for TEST 3T. . . . .	65
Figure 2.39	Stress-strain plots of individual epoxy sleeve reading locations for TEST 4T. . . . .	66
Figure 2.40	Statistical analysis of epoxy sleeve results from tendon TESTS 3T and 4T on 19-0.6" diameter strands. . . . .	67
Figure 2.41	Short-term creep TEST 1C. . . . .	69
Figure 2.42	Grouting component of the epoxy sleeve system for multi-strand tendons. . . . .	71
Figure 2.43	Schematic of the final epoxy sleeve system for multi-strand tendons. . . . .	77
Figure 2.44	Forms for epoxy sleeves. . . . .	81
Figure 2.45	Clamping system for ER gages on tendon bundles. . . . .	83
Figure 2.46a	Grout by-pass system for span C11. . . . .	85
Figure 2.46b	Grout by-pass system for spans A43 and A44. . . . .	85
Figure 2.47a	Tendon force instrumentation layouts. . . . .	86
Figure 2.47b	Tendon force instrumentation layouts. . . . .	87
Figure 3.1	Pauw-Breen original baseline system. . . . .	91
Figure 3.2	Bradberry-Breen modifications of the baseline system. . . . .	93
Figure 3.3	Law of communicating vessels. . . . .	94
Figure 3.4	Sample layouts and final measuring pot of the hydrostatic leveling system (after Markey <sup>28</sup> ). . . . .	95
Figure 3.5	Basic operation of surveying methods for measuring span deflections (after Bradberry <sup>11</sup> ). . . . .	97
Figure 3.6	Live end tensioning mechanism type I. . . . .	101
Figure 3.7	Live end tensioning mechanism type II. . . . .	102
Figure 3.8	Live end tensioning mechanism type III. . . . .	103

Figure 3.9	Live end tensioning mechanism type IV. . . . .	104
Figure 3.10	Typical dead end anchorage. . . . .	105
Figure 3.11	Typical short span test setup of deflection measuring systems. . . . .	106
Figure 3.12	Comparison of performances of line tensioning methods. . . . .	107
Figure 3.13	Portable reading unit of deflection measuring system (during installation to reading position). . . . .	109
Figure 3.14	Portable reading unit of deflection measuring system (located in reading position). . . . .	110
Figure 3.15	Overall performance of final deflection measuring system during short-span test. . . . .	112
Figure 3.16	Reading errors of final deflection measuring system during short-span tests. . . . .	113
Figure 3.17	Repeatability errors of final deflection measuring system during short-span test using two different operators. . . . .	114
Figure 3.18	System setup inside box girder bridge. . . . .	115
Figure 3.19	Live end anchor and calibrated weight inside the box girder bridge. . . . .	116
Figure 3.20	Digital scale measuring unit, mini-printer-processor, and voltmeter during sample reading operation inside box girder bridge. . . . .	116
Figure 3.21	Repeatability of errors of final deflection measuring system during field test. . . . .	118
Figure 3.22a	Measured and calculated deflections of span C-35. . . . .	120
Figure 3.22b	Measured and calculated deflections of span C-35. . . . .	121
Figure 3.23a	Measured and calculated vertical movements of span C-35 at different construction stages. . . . .	123
Figure 3.23b	Measured and calculated vertical movements of span C-35 at different construction stages. . . . .	124
Figure 3.24	Truss deflection system. . . . .	130
Figure 3.25	Truss schematic. . . . .	131
Figure 3.26	Wingtip deflection measurement system. . . . .	131
Figure 3.27	Deformation Measurement System . . . . .	132
Figure 3.28	Segment deformation measurement system. . . . .	133
Figure 3.29	Deflection measurement system layouts. . . . .	135
Figure 4.1	Factors influencing the thermal response of segmental box girder bridges. . . . .	138
Figure 4.2	Typical thermocouple system for field instrumentation projects. . . . .	140
Figure 4.3	Principle of operation of thermocouples. . . . .	141
Figure 4.4	Typical thermistor for concrete embedment (from B.R. Jones Catalog). . . . .	144
Figure 4.5	Installation of a series of thermocouple wires across the thickness of a concrete member. . . . .	145
Figure 4.6	Thermocouple. . . . .	146
Figure 4.7	Positioning thermocouples with fishing line. . . . .	147
Figure 4.8a	Thermocouple layouts. . . . .	148
Figure 4.8b	Thermocouple layouts. . . . .	149
Figure 4.8c	Typical horizontal thermocouple layout . . . . .	150

Figure 5.1 Strain errors produced from *inclusion effect* of different materials and sizes (after Bakoss<sup>9</sup>). . . . . 155

Figure 5.2 Typical commercial embedment-type vibrating wire gages. . . . . 157

Figure 5.3 Typical sister bar vibrating wire strain gage (after Dunicliff<sup>15</sup>). . . . . 157

Figure 5.4 Concrete embedment strain gages based on the electrical resistance technology. . . . . 159

Figure 5.5 Typical Carlson Elastic Wire Meter (courtesy of B.R. Jones and Associates, Inc.). . . . . 160

Figure 5.6 Demec extensometer (after Dunicliff<sup>15</sup>). . . . . 162

Figure 5.7 Principle of interferometric fiber optic sensors. . . . . 166

Figure 5.8 Concrete embedment method. . . . . 169

Figure 5.9 Inserts for drilled concrete methods. . . . . 170

Figure 5.10 Modified Demec extensometer. . . . . 173

Figure 5.11 Location of Demec points on test span C-35. . . . . 174

Figure 5.12 Comparison of reading speed of modified and standard Demec gages. . . . 175

Figure 5.13 Installation of recommended Demec guiding system. . . . . 177

Figure 5.14 Proper and improper Demec point attachment. . . . . 181

Figure 5.15a Demec point layouts. . . . . 182

Figure 5.15b Demec point layouts. . . . . 183

Figure 6.1a Reinforcing steel strain gage layouts. . . . . 187

Figure 6.1b Reinforcing steel strain gage layouts. . . . . 188

Figure 6.1c Reinforcing steel strain gage layouts. . . . . 189

Figure 6.2a Avongard calibrated crack monitor: typical dimensions. . . . . 190

Figure 6.2b Avongard calibrated crack monitor: appearance. . . . . 191

Figure 6.3 Grid crack monitor and Demec points. . . . . 192

Figure 6.4 Grid crack monitor at offset joint. . . . . 193

Figure 6.5a Joint movement instrumentation layouts. . . . . 194

Figure 6.5b Joint movement instrumentation layouts. . . . . 195

Figure 6.6 Bearing measurement details. . . . . 197

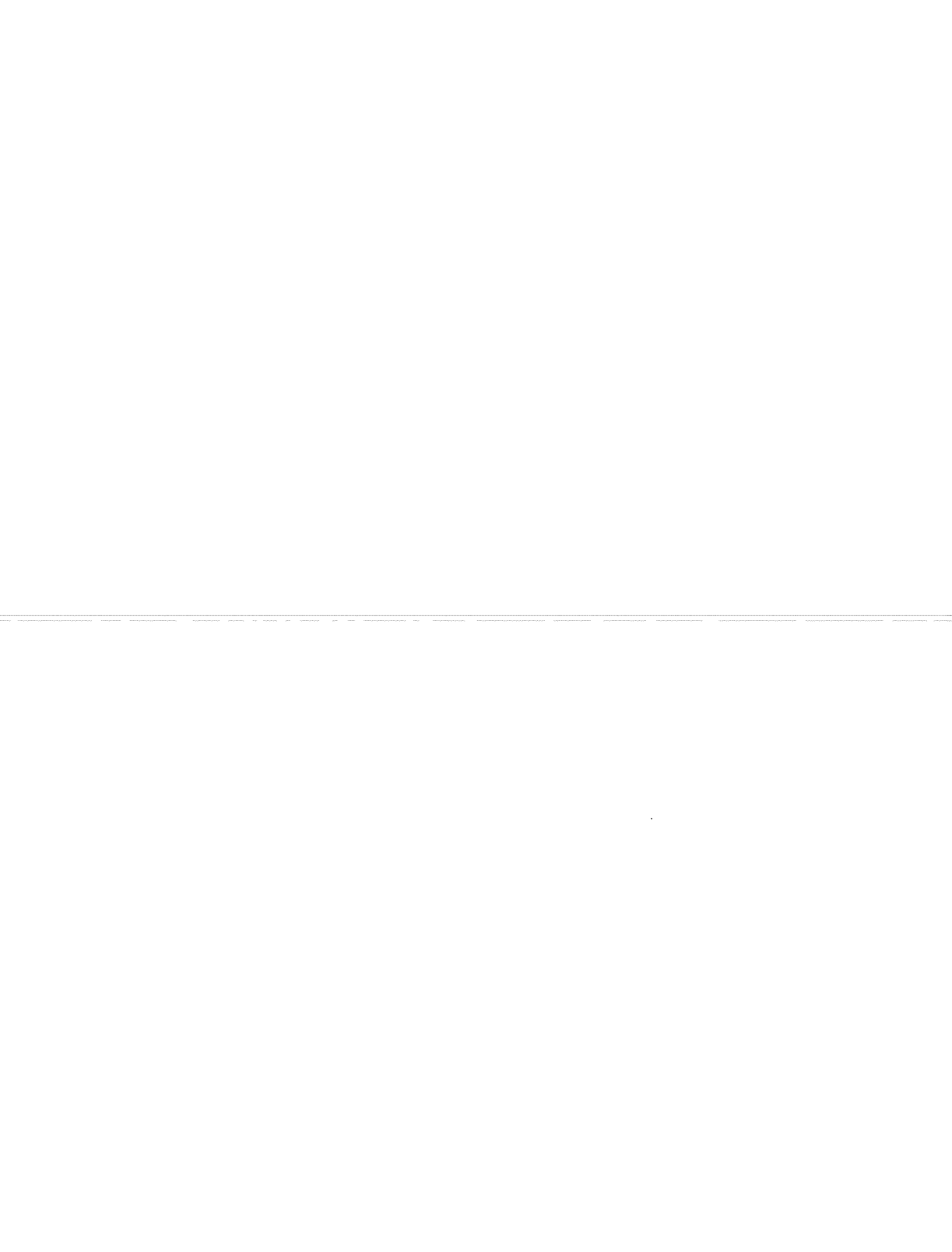
Figure 6.7 LI-200SZ Pyranometer. . . . . 199

Figure 7.1 Three-leadwire, quarter-bridge Wheatstone completion circuit typically needed for most data-loggers. . . . . 205

Figure 8.1 Schematic of finished single-strand epoxy sleeve systems. . . . . 212

## LIST OF TABLES

	<b>Page</b>
Table 2.1	Technical data for ER-load cells. . . . . 12
Table 2.2	Descriptions of single strand tests. . . . . 27
Table 2.3	Suggested ER-Gage systems. . . . . 72
Table 4.1	Commonly available thermocouple wires, insulations, and overbraidings (from Omega Eng., Inc.). . . . . 142
Table 4.2	Typical costs of a thermocouple system for use in concrete structures (from Omega Eng., Inc., prices from late 1990). . . . . 143
Table 5.1	Technical data of typical vibrating wire strain gages for embedment in concrete. . . . . 155
Table 5.2	Technical data of original Mustran Cells. . . . . 156
Table 5.3	Technical data of other strain gages for embedment in concrete. . . . . 161
Table 5.4	Technical data for typical Demec extensometers. . . . . 163
Table 5.5	Current prices of Whittemore gages (from Soiltest, Inc.). . . . . 164
Table 5.6	Technical data for typical surface-mounted vibrating wire strain gages. . . 164
Table 5.7	Technical data of surface bonded foil electrical resistance strain gages. . . 165
Table 5.8	Ease of installation of different bonding methods of Demec locating points. . . . . 168
Table 5.9	Description of systems tested for long-term stability. . . . . 170
Table 5.10	Final report on long-term stability of Demec guiding systems. . . . . 171
Table 7.1	Late 1990 prices for data-acquisition components offered by Campbell Scientific, Inc. . . . . 202





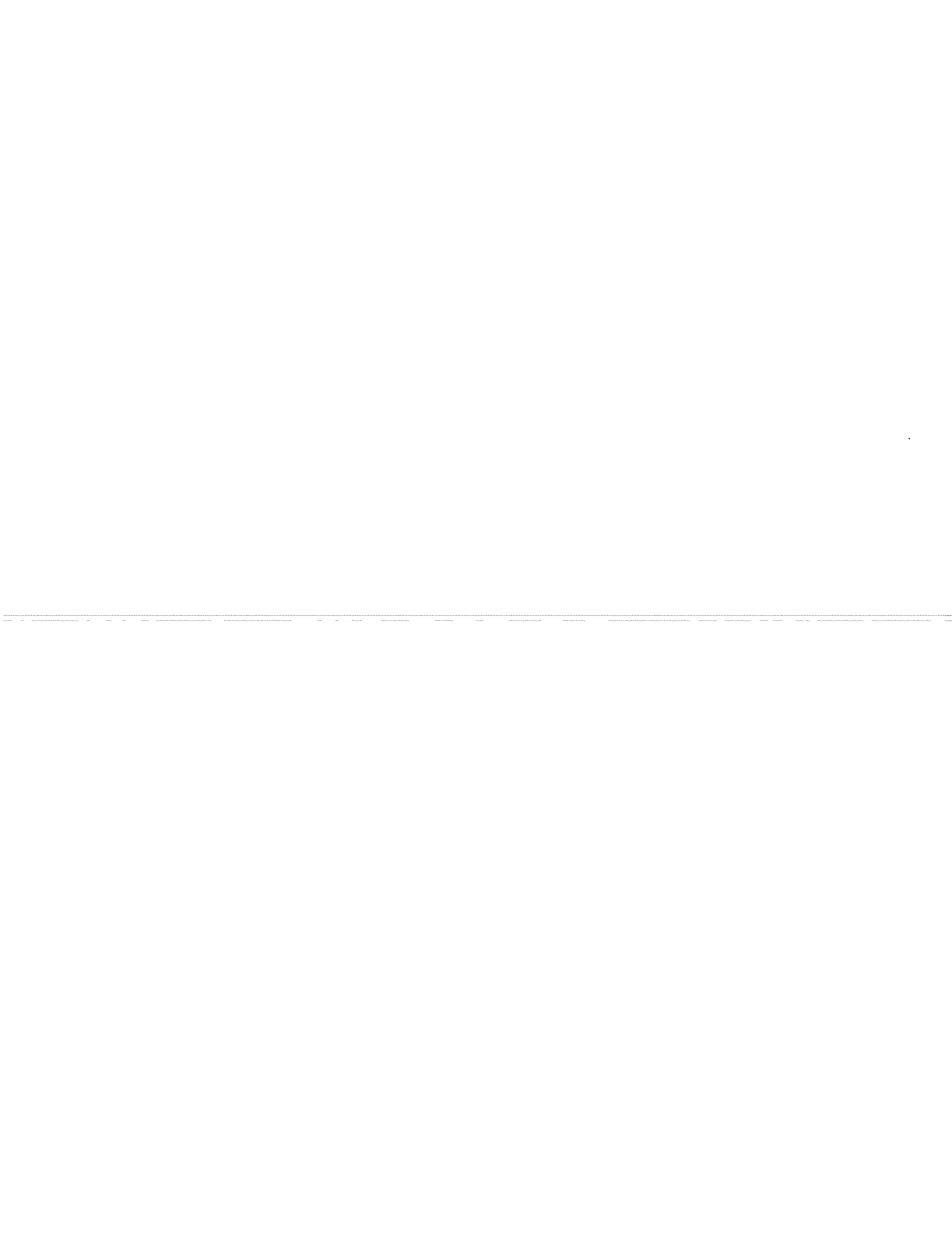
## SUMMARY

This report is the first in a series reporting the field study of several spans of the San Antonio "Y" Project. The San Antonio "Y" Project is a major urban viaduct comprising segmental concrete box girders post-tensioned with a mix of internal and external tendons and erected using span-by-span techniques.

This report describes the development of the instrumentation systems which were installed in the field project. The major systems were:

1. External post-tensioning tendon forces,
2. Span deflections and segment deformations,
3. Concrete temperatures
4. Concrete strains,
5. Reinforcing steel strains,
6. Joint openings,
7. Bearing movements,
8. Solar radiation.

A comprehensive literature review of each system was performed and the most promising systems were tested in the laboratory and in the field. Recommendations on the best system for each type of measurement were made, and the systems were installed in four spans of the San Antonio "Y" Project. Also in this report the performance of each system in the field is evaluated and recommendations for future field studies are presented.



# CHAPTER 1 INTRODUCTION

## 1.1 Introduction

The State of Texas, as well as many other states, is currently making substantial use of precast segmental concrete box girder bridges on urban freeways. The San Antonio "Y" Project comprises six phases of segmental viaducts erected using span-by-span techniques. The US-183 Project in Austin, Texas will also entail several miles of segmental concrete box girders erected with both span-by-span and balanced cantilever construction. In these designs a number of assumptions had to be made regarding the design and behavior of the structures.

These construction systems reflect the rapid development and implementation of many high technology ideas. Even greater utilization is envisioned in coming years as designers and constructors gain in familiarity and experience with these methods. With this relatively new and unusual form of construction, in which Texas and other states have invested a great deal of time and money, additional studies are warranted to examine those areas of design and construction which are still uncertain and to check the validity of design assumptions.

A unique opportunity existed in Texas in connection with the major segmental projects planned and underway to obtain field information to allow confirmation or revisions of many design uncertainties. A well-planned and -executed field instrumentation study could provide valuable information during the initial erection operations and with time. A consistent measurement program could also assist in the long-term maintenance of the structure, and future designs would certainly benefit from data collected in a comprehensive field instrumentation project.

## 1.2 Areas of Uncertainty in the AASHTO Guide Specification

The *AASHTO Guide Specification for the Design and Construction of Segmental Concrete Bridges*<sup>1</sup>, published in 1989, provides guidelines for the design of segmental concrete bridges. It represents the current state-of-the-art design and construction techniques and incorporates the findings of most research on segmental bridges which had been published at that time. There were a number of areas, however, where professional judgement had to be used to develop specification provisions where actual data was scarce or non-existent. Some of these key areas of uncertainty are:

1. Prestress losses in external tendons,
2. Transverse diffusion of external post-tensioning forces,
3. Temperature gradients and their effects,

4. Joint efficiency, and
5. Anchorage zone and deviator behavior.

A comprehensive field instrumentation program could provide considerable data on these specific areas of uncertainty.

### 1.3 Required Instrumentation Systems

Based on the previously mentioned areas of uncertainty, as well as other topics of interest to TxDOT designers, the following measurements were deemed necessary:

1. Post-tensioning tendon forces,
2. Span deflections,
3. Segment deformations,
4. Concrete temperatures,
5. Concrete strains,
6. Reinforcing steel strains,
7. Joint movements,
8. Bearing movements, and
9. Solar radiation.

### 1.4 Project Objectives

The overall project was initiated with the objective of collecting data from a field study which would provide new information on areas of uncertainty in segmental design and construction. Four spans of the San Antonio "Y" Project were targeted for field instrumentation. The initial concern, however, was to develop an efficient, hardy instrumentation program which could be installed with a minimum disruption of contractor activities. This report deals specifically with the instrumentation systems, their selection, installation and performance. This phase of the project was organized into a series of intermediate objectives:

1. Review existing state-of-the-art instrumentation systems,
2. Select promising systems for laboratory and field evaluations,
3. Test promising systems in the laboratory and field,
4. Evaluate tests and recommend the best systems for the field study,
5. Install the systems in the San Antonio "Y" Project, Phase IIC,
6. Evaluate the field performance of the instrumentation systems, and
7. Recommend improvements for future field study.

A separate phase of this research program reports the results of the instrumentation study.<sup>46</sup> Many recommendations are presented for the improvement of the *AASHTO Guide Specification*.

## 1.5 Report Organization

This report is divided into 9 chapters. Each of chapters 2 through 7 presents a specific instrumentation need, the evaluations and recommendations for that system, the field installation process and layouts of the instrumentation in the San Antonio "Y" Project, the field performance, and recommendations for future projects. Chapter 8 presents recommendations for companion material tests. The chapters are as follows:

- Chapter 2. Post-tensioning tendon forces,
- Chapter 3. Span deflections and segment deformations,
- Chapter 4. Concrete temperatures,
- Chapter 5. Concrete strains,
- Chapter 6. Other measurements,
  - Reinforcing steel strains,
  - Joint movements,
  - Bearing movements,
  - Solar radiation,
- Chapter 7. Data acquisition system,
- Chapter 8. Companion material tests, and
- Chapter 9. Recommendations and conclusions.

This report provides comprehensive information on instrumentation systems and should be of substantial assistance for future field projects. Continued study of segmental bridges in the lab and in the field is vital to the continued success and improved long term performance of this attractive and adaptable bridge system.



## CHAPTER 2 PRESTRESSING STEEL STRAINS/FORCES

### 2.1 Review of Available Systems

Accurate field measurements of initial and especially long term-strains or forces at different cross-sections of internal prestressing steel strands embedded in grout or concrete and external tendons at deviators are extremely important but have been difficult to achieve in an effective manner. However, several devices have been used in the past with acceptable levels of success.

This section reviews some of the devices that have been commonly used for the measurement of strain or force in prestressing strands. The objective is to help select the most appropriate instruments for the measurement of loads at different cross-sections of external and internal prestressing tendons used in concrete segmental box girder bridges. Section 2.2 reports the evaluation of the systems chosen and their refinement in laboratory and field trials. Final recommendations are given in Section 2.3.

In most cases, the load level in prestressing steel strands is measured indirectly by strain gages or directly (only at live or dead ends) by load cells or calibrated hydraulic jacks. Available instrumentation systems can thus be separated into two groups: indirect strain measuring devices and direct load measuring devices. A description of several commonly-used instruments corresponding to each one of these two groups is included in this section. Although load cells and some of the other mechanical systems cannot be used for measuring stresses at intermediate cross sections of multi-strand tendons (essential in studies of local stress losses), they are presented here to complement the information in this broad area of measurements.

**2.1.1 Strain Measuring Devices.** Two factors complicate the accurate measurement of the prestressing strand stress level by use of strain gages. These factors, influencing all types of strain measuring devices surveyed in this section, are:

1. Inaccurate modulus of elasticity of the prestressing strand, and
2. Inability to measure stress losses due to steel relaxation.

**Inaccurate Modulus of Elasticity.** Due to manufacturing tolerances in the diameter of each wire of a 7-wire strand and in the pitch of the six outer wires, a strand's modulus of elasticity can vary up to 2.4% among two different specimens. Since fabricators usually provide load-elongation curves based on the average of the last 30 to 50 tests of similar strands, a maximum error of 2.5% has been suggested in their reported modulus of elasticity.<sup>43</sup> This error can be increased considerably when a different instrumentation system is used for measuring strains in the field. If the manufacturer-furnished modulus of elasticity based on a measuring system which determines axial elongation over a fairly long length is used to interpret strains measured with standard bonded foil electrical resistance strain gages applied over a very short

length of a single wire and parallel to the wire's axis (which is inclined to the strand axis), load errors of up to 10% can be experienced. It is therefore suggested that individual strand measurement systems be calibrated in known load tests using the same type of instrumentation system to be utilized in the field.

**Losses from Steel Relaxation.** Using strain gages or mechanical elongation instruments will, by definition, not measure the load changes due to steel relaxation. According to its definition, steel relaxation is a time-dependent loss of prestress which occurs under a constant state of strain in the strands. An accurate supplementary analytical procedure should be followed to calculate such unmeasured steel relaxation losses at different time stages when using strain gages for measuring a strand's load. Previous research studies from the University of Queensland in Australia have reported differences of the magnitude of 0.5 to 2.75% between code-established relaxation losses and their test results.<sup>24</sup> The relaxation losses occurring in the first one or two minutes after stressing were ignored.

**2.1.1.1 Electrical Resistance Strain Gages.** These are the most popular devices used for the measurement of strains in structural elements. The electrical resistance gaging technology is briefly reviewed to highlight the most important factors regulating the sensitivity, accuracy, and long term stability of this type of measuring device.

Electrical resistance gages are basically formed by an electrical conductor bonded to a backup matrix material. This material is in turn bonded to the element to be instrumented. As this element deforms, the matrix material and conductor are strained causing a resistance change in the conductor. This resistance change is measured when a current is sent through the conductor. The change in resistance is directly proportional to the change in length. This relationship between initial resistance ( $R_o$ ), resistance change ( $\Delta R$ ), initial length ( $L_o$ ), and change in length ( $\Delta L$ ) is provided by the gage factor (GF) as follows:

$$\frac{\Delta R}{R_o} = \frac{\Delta L}{L_o} * GF$$

The gage factor is a measure of sensitivity of the strain gage. Very strict guidelines for installation and moisture protection methods must be followed to achieve satisfactory long-term stability. Many types of strain gages are presently available. They vary according to size, geometry, materials, and rated electrical resistance. A large selection of gages, completion circuits, data acquisition systems, and bonding methods have been previously used in research and field applications. Exact description of the gages, their method of installation, and other technical data is avoided in the present report due to the large differences among each application.

As shown in Figure 2.1, a foil electrical resistance gage is generally bonded to an individual wire of a 7-wire prestressing strand. A problem evident with this arrangement is that the gage gives the measurement of strains experienced by an individual outer wire in a direction parallel to the orientation of the axes of that wire, as opposed to the average cross-sectional



strains in the strand. With standard stressing equipment used in construction operations, the gripping force exerted on individual wires of a prestressing strand can vary widely. This is generally understood to be the cause of different levels of stress in each wire of a strand, especially at initial stressing loads.

Yates<sup>54</sup> reviewed the degree of influence of this factor on sets of fully-instrumented strands. In Figure 2.2, the nominal strand stress is plotted against measured strain from gages bonded on each exterior wire of a 1/2"  $\phi$  Grade 270, stress-relieved strand gripped with standard three jaw prestressing anchors at each end. Loads were obtained with a pair of center-hole load cells provided at each end of the calibrating bench.

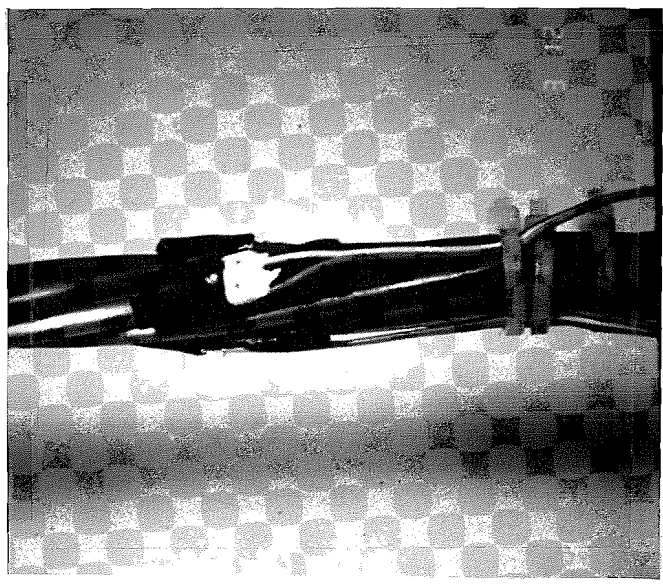


Figure 2.1 Electrical resistance foil gage bonded to single wire of strand.

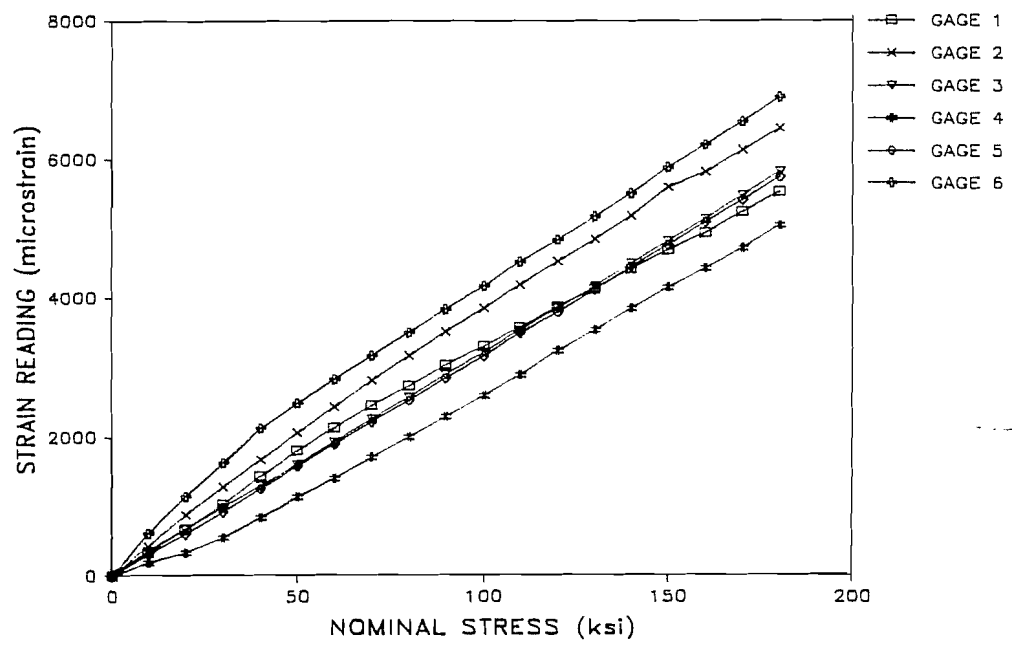


Figure 2.2 Stress-strain plot of single prestressing strand with 6 ER-gages (after Yates<sup>54</sup>).

Figure 2.2 indicates that each wire experiences a different level of strain during the initial stressing operation (0-50 ksi). Once each wire is fully anchored, the subsequent strain increases

are more linear and stable. The slopes of each wire are approximately equal. The measurement of strain of a single wire can thus produce considerable levels of error in the average or nominal stress in the strand if the absolute values are used. To reduce these errors when determining strand stress based on placement of a strain gage on a single wire, Yates ignored all readings corresponding to low stress levels. He suggested that only the readings for stresses higher than 50 ksi ( $\approx 0.20f_{pu}$ ) should be used in the preparation of a linear calibration curve.<sup>54</sup> In a study of a box-girder bridge model, MacGregor<sup>30</sup> followed Yates' procedure of ignoring low stress readings. He also performed a linear regression of average gage data values with respect to live end loads obtained during stressing operations. These lines were transformed into straight lines of equal slope passing through the origin of the coordinates giving initial offset values. With this method he was able to correct for the offset in the individual strain data value.<sup>30</sup> After using this procedure to correct initial strain readings, MacGregor established the level of stress in the tendons based on the calibrated values of modulus of elasticity that he previously obtained from his material tests (different than manufacturer data).

Other researchers further suggested the installation of two ER-gages bonded to diametrically opposed wires of a single strand. This was thought to provide a more representative average modulus of elasticity for the actual field tests.<sup>8</sup>

In multi-strand tendons the acceptability of average tendon stresses determined from measurement of strain on a single wire becomes even less acceptable than for single prestressing strands. Individual stresses on each strand of a multi-strand tendon can vary considerably. The stress level on each strand varies according to the efficiency of the live end grips, the total strand length (in turn dependant on the degree of twisting of each strand), and the amount of frictional losses across path changes. Obviously, an increase in the number of instrumented strands at each tendon cross-section will increase the accuracy of the modified average tendon stresses. However, for large instrumentation projects this is an expensive alternative.

Another problem associated with electrical resistance gages is related to their long-term stability. Several factors can influence the long-term performance of ER-gages. Among the most important ones are:

- a. Partial debonding of gages with time due to large temperature differentials, attacks from aggressive environments, and/or fatigue loadings;
- b. Variation of electrical resistance due to accidental grounding of leadwires or moisture increases;
- c. Temperature variation on long leadwires, gages and connectors; and
- d. Variation of parasitic resistance in switches or connectors (influenced by moisture or temperature differentials).

Each one of the above-listed topics should be carefully addressed in any serious long-term instrumentation program which includes electrical resistance strain gages. The overall performance of strain gages based on measurements of variation of electrical resistance signals has not been very successful for long periods of time. A large number of research studies have reported serious problems with their electrical resistance strain gages (either Carlson elastic wire meters or bonded foil gages).

A major advantage of using electrical resistance strain gages is the possibility of automated multi-channel data acquisition, remote recording, and automated data reduction. This type of gage is also quite sensitive. Sensitivities of  $1\mu\epsilon$  are possible with most gages and standard reading units. Short-term accuracy of  $5\mu\epsilon$  can be achieved with proper gage installation and operation. Strain ranges of up to  $3000\mu\epsilon$  are typical with most strain gages suited for prestressing strands. Finally, the cost of electrical resistance strain gages is relatively low, although the backup equipment such as portable readout units, extra wire, bridge completion circuits, or any multi-channel automated readout unit can be expensive.

**2.1.1.2 Other Systems.** Most of the other systems for measuring strains in prestressing strands are mechanical. Due to their high costs these mechanical extensometers are mainly used by strand manufacturers for their modulus of elasticity and ultimate strength tests. One of the major problems with these devices is related to the mechanical method of gripping each test strand. Any slip or rotation of the strand's wires at the end of the extensometers will throw off the accuracy of the measurements. Two mechanical extensometers were mentioned to be the best performers and most widely-used devices.<sup>43</sup> These are known as the *50" Double Dial Extensometer* and the *Tinius Olsen Extensometer*. The first extensometer uses a pair of dial indicators with sensitivities of 0.001 inch thus providing an accuracy of  $20\mu\epsilon$  for the 50-inch gage length system. Replacing the dial indicators by more sensitive devices of 0.001 mm resolution ( $\approx 0.00004$  inch) can substantially improve their accuracy to a few microstrains. Although not investigated, the accuracy of the other device should be quite similar. Preston<sup>43</sup> also provided several details of the *50" Double Dial Extensometer* which can be easily fabricated at a machine shop.

A newer device known as the *Wallace No-Contact Extensometer* has also been reported by Preston.<sup>43</sup> This expensive equipment is based on optical reading devices which lock the contact points without any influence from slip or rotation of individual strand wires. In 1984 Preston was quoted a price of \$16,565.00 (plus freight and installation) for 7-wire strand testing equipment of this type. Values for level of accuracy of these machines were not investigated. They have been distributed in the United States by: Testing Machines Inc., 400 Bayview Ave., Amityville, New York 11701; telephone: (516) 842-5400.<sup>43</sup>

An approach to fiber optical strain gage measurements was developed by Strabag Bau-AG in Germany.<sup>35</sup> Since optical fibers have excellent light permeability, the amount of light attenuation due to mechanical constraints in bonded parts of the fibers is used for measuring strains. A graphical description of the main components of this system is shown in Figure 2.3. The optical fiber is bonded to the material to be instrumented at a certain location along its

length. Infrared light rays are emitted from one end of the fiber while a receiver at the other end measures the amount of light that passes through. Elongation of the bonded part of the fiber causes transverse shortening according to Poisson's law. This decrease of the wire's diameter is measured by the amount of light that passes to the receiver, provided that no other physical damage caused any additional light passage restriction. This technology has been tested in full-scale structures. However, these were prototypes with new optical fiber prestressing tendons that incorporated the gages at their center.<sup>53</sup>

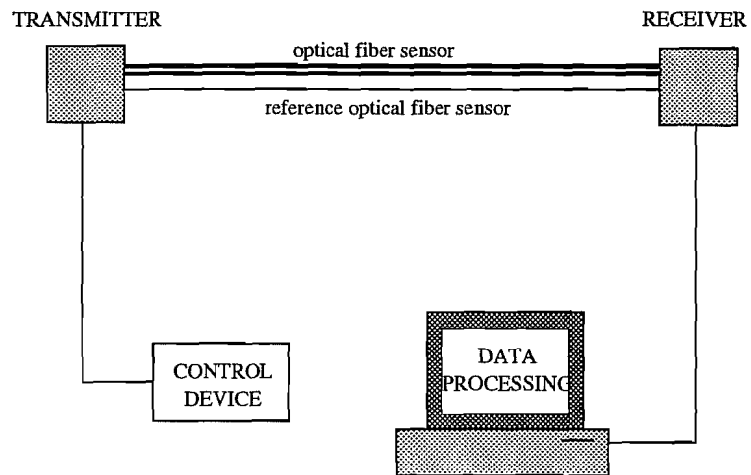


Figure 2.3 Principle of reference optical fiber sensors.

The greatest advantage of this type of fiber optical gage is their suitability for long-term instrumentation projects, and their adequacy for automated data recording. Presently these gages are only included as part of the optical fiber prestressing strands manufactured by the same company. This approach to a workable fiber-optical strain gaging system is also growing at a fast pace. Further developments for standard structural applications should come in the near future.

**2.1.2 Load Measuring Devices.** As mentioned earlier, the largest problem with these systems is related to their geometric requirements. In most cases these instruments must be positioned at the ends of the prestressing strands or tendons, thus limiting their versatility. Because of cost they are usually not left in place. The tendons must be prestressed to remove them. There are many recent innovative techniques within this area of measurements, but the efficiency of most of these novel systems is still uncertain. This section reviews some of the most important devices available currently. Other devices were also investigated due to their unusual and innovative measuring techniques.

**2.1.2.1 Calibrated Hydraulic Jacks.** These are the most commonly used tools for measuring strand or tendon forces during normal construction operations by recording hydraulic pressures. It is customary when using hydraulic jacks to also check the elongation of the strand. A sample field use of a calibrated hydraulic jack with a single pressure dial gage is shown in Figure 2.4. Problems directly influencing the degree of accuracy achieved by this form of measurement were reported by Dunicliff.<sup>15</sup> They consist of load misalignments, off-center loading, internal friction in the jack, hydraulic pressure losses at higher loads, temperature

changes, and resolution of dial gages. In addition, an incorrect calibration of the jack can further reduce the accuracy of measurements.

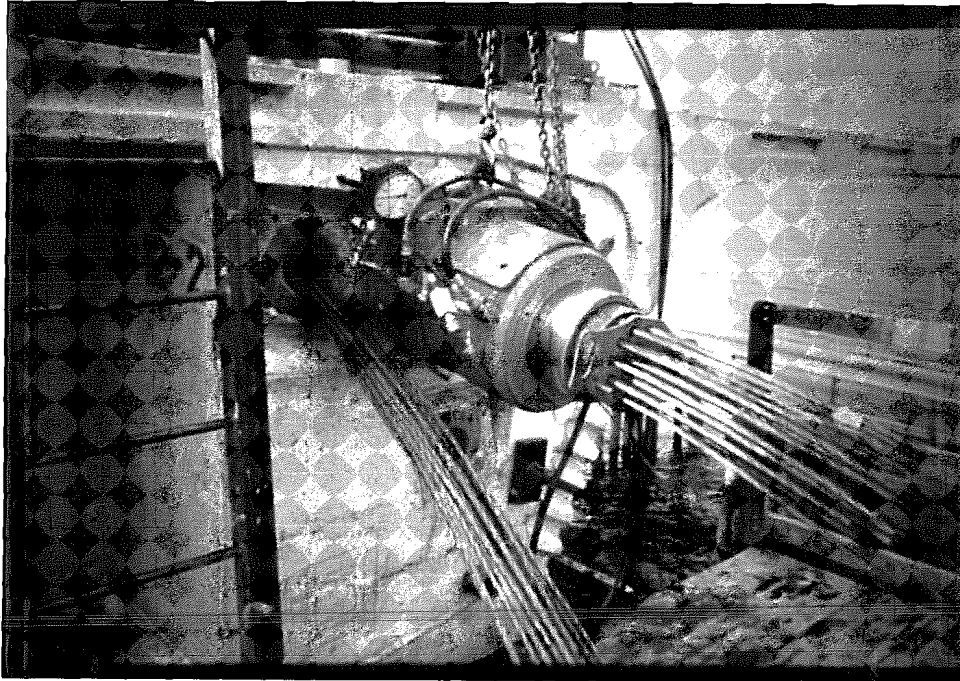


Figure 2.4 Calibrated hydraulic jack for field measurement of tendon loads.

Hydraulic jack calibration under laboratory conditions can be substantially different than a normal field application. One important difference is that in the laboratory, and on a high-quality vertical loading machine, the jacks are loaded with spherical swivel heads and rigid bearing plates. In the field, the centerline of the tendons being stressed can be at an angle with respect to the centerline of the loading jack. This will therefore produce a higher degree of internal friction between the piston and the cylinder of the jack, and thus a variation from the "real" load in the prestressing tendons. In the field of geotechnical engineering there are several reports of errors introduced by load misalignment and eccentric loading on calibrated hydraulic jacks. Fellenius<sup>18</sup> claimed that overestimations of up to 15% of the applied load can be found when comparing hydraulic jack loads with load cell data. This seems quite high compared to previous experience at Ferguson Structural Engineering Laboratory (FSEL). Probably the calibration of the jacks and load cells used by Fellenius were not accurate and this contributed to such a high error percentage. In any case, the existence of some errors in estimating forces from hydraulic pressure when using jacks is obvious but can be minimized by proper system calibration. Littlejohn<sup>25</sup> suggested an ideal method for calibrating hydraulic jacks and load cells.

The resolution of readings with calibrated hydraulic jacks directly depends on the resolution of the pressure dial indicators. Higher resolution dial indicators or pressure transducers

can improve the resolution of the readings. Remote readouts and automated systems for data acquisition, retrieval, and analysis can also be implemented with most types of pressure transducers. Pressure transducers, along with the complete system to be utilized for stressing and readouts, should be properly calibrated in order to achieve useful levels of accuracy.

**2.1.2.2 Load Cells.** These are popular for most loading operations of prestressing strands or tendons in laboratory testing operations. They obviously present the same geometric inconveniences as calibrated hydraulic jacks. Their level of accuracy also depends on their proper calibration, so load cells should be calibrated according to the same guidelines previously mentioned for hydraulic jacks. There are many different types of load cells and they vary according to their basic method of operation. Load cells can be based on electrical resistance technology, hydraulic pressure, mechanical methods, vibrating wire technology, and even photoelastic principles.

#### Electrical Resistance Load Cells.

These are the most popular type of load cells, probably due to their high accuracy and low cost. Cells used for measuring loads on prestressing strands and tendons are of the center-hole type (Figure 2.5). A typical schematic for commercial designs of electrical resistance load cells is shown in Figure 2.6. Individual ER-gages of the foil type are usually connected in a full Wheatstone bridge configuration, with some of the foil gages positioned to measure tangential strains. This is done to reduce errors from load-misalignments and off-center loadings.

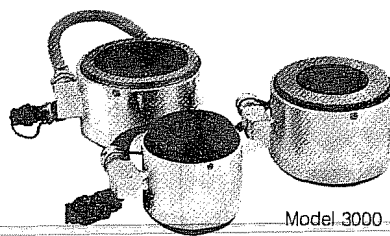


Figure 2.5 Electrical resistance load cells with central holes (from Geokon's catalog).

The cost of these cells is considerable and can limit their field application (see Table 2.1). These cells can be reused if the tendons are destressed or if they are used only as a check of stressing forces at the live end of the tendons. However, they must be left in place when installed at the dead end of tendons or when monitoring vertical reactions at the supports of bridge structures unless considerable provisions are made for their removal. Allowance for proper fitting must be made in box-girder bridges when they are to be left on site permanently. Their size is a limiting factor since minimum heights of greater than 3 inches are necessary even for

Table 2.1 Technical data for ER-load cells.

<b>Load Cell Manufacturer:</b>	Geokon, Inc.	
<b>Distributor:</b>	Geokon, Inc.	
<b>Current Cost (p/unit):</b>	≈\$700.00	≈\$1200.00
<b>Load Cell Model:</b>	3000-400-4.0	3000-400-6.0
<b>Load Range (Tons):</b>	181	200+
<b>Sensitivity (kg):</b>	13	45
<b>Central Hole Diameter (in):</b>	4	6
<b>System Accuracy Range (%):</b>	±2-5	

the small type of cells. Most of the problems previously outlined with respect to the long-term stability of electrical resistance foil gages are also applicable to ER-load cells. Although moisture protection is better achieved in load cells, some manufacturers do not provide waterproofed equipment which is essential for long-term projects.

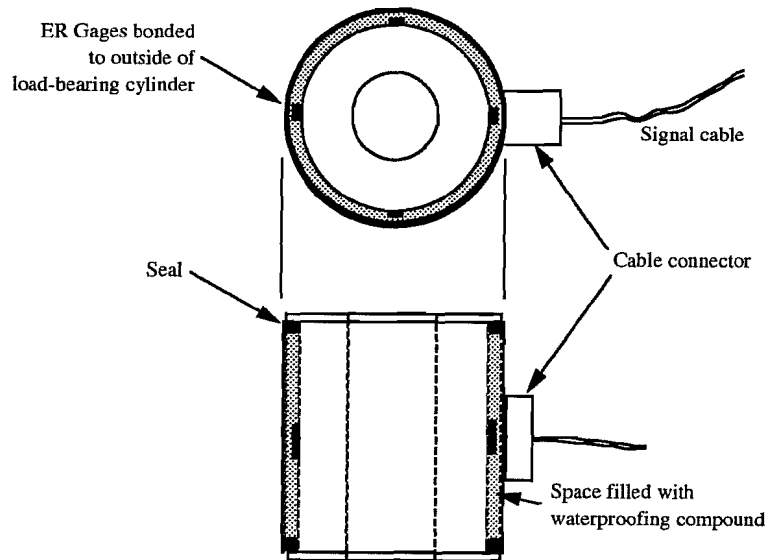


Figure 2.6 Schematic of a typical electrical resistance load cell (after Dunnicliff<sup>15</sup>).

This type of load cell is strongly recommended for use during stressing as a check of calibrated hydraulic jack loads but not as an instrument to monitor the load variations in tendons over the life of a structure. With somewhat lesser accuracy, some electrical resistance based load cells can also be custom manufactured and tested in laboratory conditions. Barker, Reese et al. built a simple load cell called a *bottomhole cell* that provided good results for measuring loads at the bottom of drilled shafts.<sup>10</sup>

**Hydraulic Load Cells.** Most hydraulic load cells are similar in size to electrical resistance load cells. The largest difference is in their method of operation. Hydraulic load cells use pressure transducers to measure loads. These transducers can vary in type of operation including pneumatics, semiconductor strain gages, electrical resistance strain gages, or vibrating wires. Their degree of accuracy is much higher than that of the load cells themselves. Larger errors are introduced from internal friction of the cell components and from eccentric loadings. Due to their lower accuracy, these cells are usually not recommended as the sole device for measuring jacking loads.

**Other Load Cells.** There are also reports of load cells based on photoelastic fringes and mechanical methods. These load cells do not allow for remote reading operations, have stricter geometric requirements, and are usually less accurate. However, advantages of these systems consist of their extra stiffness for field operations, and their good performance for long-term measurements.

**2.1.2.3 Cable Tensiometers.** Systems designed to measure the tension in a cable are the Tensiomag, DynaTension, Cable Tensiometer, and the Fulmer Tension Meter. Most of these instruments are made for single strands or cables. Some of them are not readily available in this country. However, an understanding of their behavior is important for avoiding past errors and enhancing future developments.

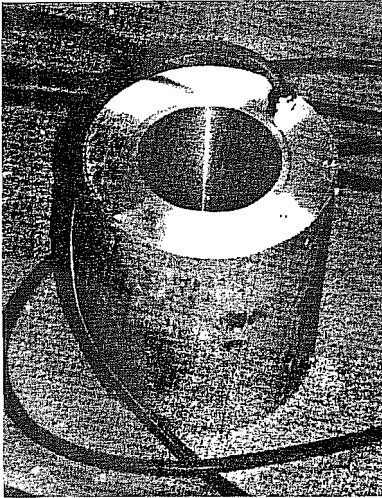
**Tensiomag.** These devices are offered by Freyssinet International. They are the only ones (within the present category) that can be used in multi-strand tendons. They consist of steel jackets with a central hole and a separate readout unit (Figure 2.7). The operation of the Tensiomag is based on the variation of the incremental magnetic permeability of steel with respect to applied mechanical stress. The sensing device is made of a special transformer. When steel (such as a prestressing strand) is placed in its inner core, it serves as a connection between the primary and secondary windings of the transformer (Figure 2.8). When the primary winding is supplied with an electric current, it produces a magnetization in the steel and an electric signal is emitted from the secondary winding. This signal is dependant on the magnetic state of the tendon and thus on the stress imposed on it.<sup>37</sup>

The reported sensitivity of this system is on the order of  $\pm 25 \text{ N/mm}^2$  ( $\pm 145 \text{ psi}$ ).<sup>37</sup> The main advantage is that it can be placed at several cross sections along the length of the longitudinal (internal as well as external) prestressing tendons of segmental box girder bridges. It is of sturdy construction and is reported to have good long-term stability. Another interesting characteristic is that it measures the average tendon stress at each cross-section, and not single stresses related to individual wires of a strand. Laboratory accuracy for multi-strand tendon tests were reported between 2% to 3% when using 12-0.6"  $\phi$  strands.<sup>37</sup>

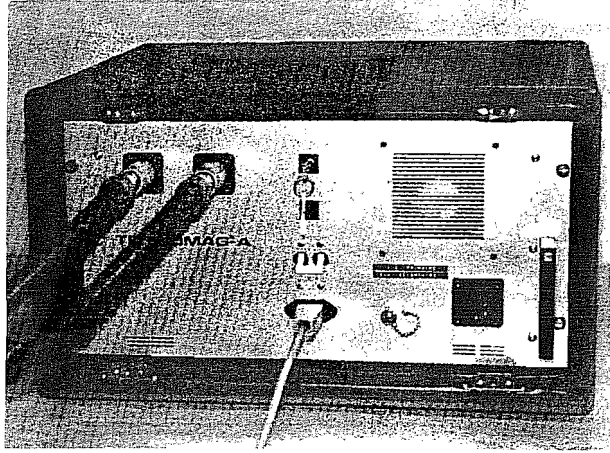
Costs and availability of devices able to measure tendons made of up to 19 - 0.6"  $\phi$  strands could not be obtained from the manufacturers. However, it seems that a complete set of sensor, power unit, and readout box can be expensive. No reports of previous use in field studies in the U.S. were found in the literature review prepared for this study. It is also possible that for long-term use the amount of magnetic permeability creep of prestressing strands can introduce much larger errors than originally reported in the manufacturer's catalog. The system is also not readily portable because it cannot be removed from a tendon without first destressing the tendon. A final disadvantage of the system is the need for preparing calibration curves according to each configuration where it is designed to be installed.

**DynaTension.** These are made for measurements of loads on single strands or cables. The method of operation consists of relating the fundamental frequency of vibration of strands and cables to the applied tension. This is based on the principle that the natural frequency of a length of cable between two nodes is directly proportional to the tension in the cable. It is simple to install and use. A proximity-type or a contact-type transducer is installed near or around the single strand or cable. Information regarding the free length of the strand and its

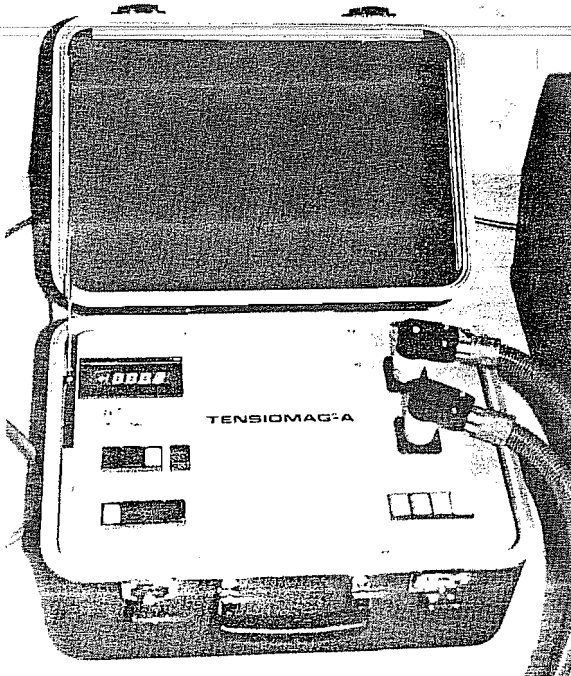




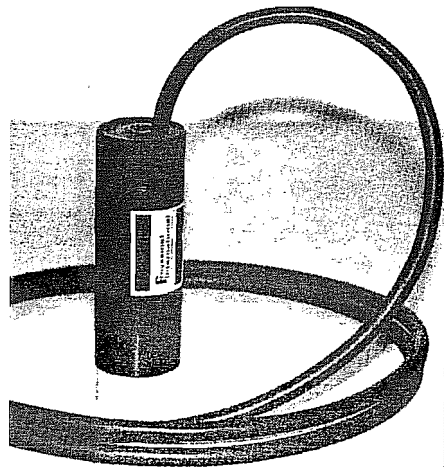
a. Sensor for multi-strand tendons.



b. Power supply unit.



c. Readout unit.



d. Sensor for single strands.

Figure 2.7 Freyssinet's Tensiomag system (from Freyssinet's catalog).

weight per unit length is introduced in the portable readout unit. A scale and a multiplying factor are selected according to the expected level of measurements. A simple tap on the free length of cable will produce a vibration that is in turn measured by the *DynaTension* and related to tension according to the input data. These devices do not need recalibration with use, and are unaffected by weather, cable lubricants, dirt, or overloads. The workable range is rated up to 4,000 kips and can accept cables weighing up to 80.5 lb/ft. The manufacturer reported accuracies of  $\pm 2\%$  and resolutions of 0.33% with this system. A sample portable readout box and two different types of sensors are included in Figure 2.9.

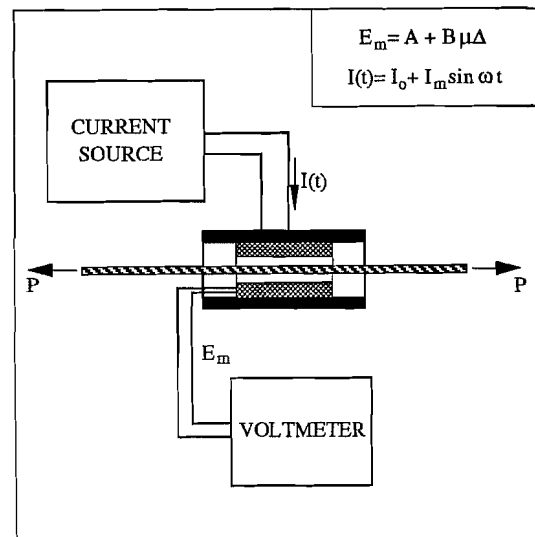


Figure 2.8 Operation principle of Tensiomag (from Freyssinet's catalog).

An original version of the *DynaTension* was used on extensive tests performed by the California Department of Transportation in 1984.<sup>45</sup> Their system, then known as *Vemco*, was reported to work well, with an initial accuracy of 2% at 100% confidence level. The *Vemco* and the *DynaTension* systems do not have the portability problem associated with the *Tensiomag*, since both can be clamped and removed from any location along the free length of a single strand. However it has the disadvantage that the strand must not be in contact with anything between the nodes of the free length.

Unfortunately, *DynaTension* is not adaptable to measure loads on multi-strand tendons. Its cost is quite high; the complete system (including two sensors and a portable readout box) has been rated at \$7,000.00 in late 1990. It can be purchased from Smiser Industries, Inc., 9215 Solon Unit D-2, Houston, Texas 77064; current telephone: (713) 890-6007.

**Cable Tensiometer.** This device was manufactured by Roctest, Inc. It is currently unavailable due to certain operational irregularities found by the manufacturer. However, the method of operation is quite innovative. Load measurements are determined from a calibration curve based on the travel velocity of a wave generated by impact. An impactor and a detecting sensor are attached to a single cable at a distance of five feet (Figure 2.10). The time of travel is then measured in a portable readout unit that is provided with the system. The original manufacturer's claim of accuracy and resolution is not repeated herein due to the failure reported in the original system. Evidently, this device is also limited to measurements in single cables or prestressing strands. Initial cost of the complete system and reports of previous use are not available. It is probable that a new instrumentation system based on this technology may appear in the future. This system also has the same type of portability mentioned for the *DynaTension*.

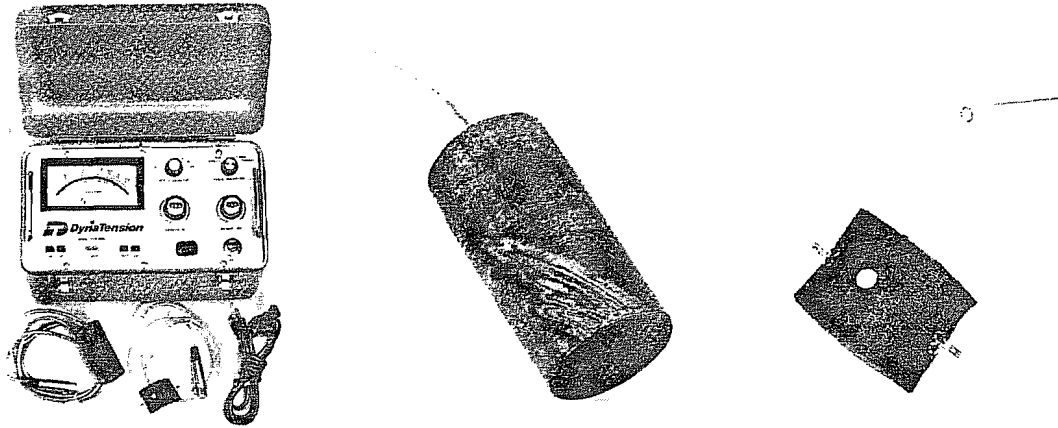


Figure 2.9 DynaTension System (from DynaTension's catalog).

**Fulmer Tension Meter.** This is an example of a simple mechanical device that can be used for the measurement of loads on single prestressing strands or cables. The system in operation is shown in Figure 2.11. The eccentric wheel applies a deflecting force on a single strand causing the frame of the meter to bend in direct proportion to the applied force.<sup>20</sup> A calibration chart must be prepared for each strand type in order to obtain load measurements from the values of the dial indicator. The system accuracy has been rated at 5% on prestressing strands.<sup>15</sup> Besides its inability to measure multi-strand tendon loads, there are also severe geometric restrictions for its proper use. As originally designed, the system does not allow for remote reading operations. Similar devices evolved from the original *Fulmer Tension Meter*. One instrument known as the *Kuhlman Beam* - named to honor its creator - was fabricated and successfully used in field tests of the California Department of Transportation (Figure 2.12). Several improvements were introduced by the *Kuhlman Beam*. The most important ones are related to the reduction in size and the allowance for remote reading operations. Values for the initial level of accuracy of this device were reported around 6.5% and 2.8% for field tests with 100% and 95% confidence levels respectively.<sup>45</sup> However, the rated accuracy is strictly limited to the skill of the operators and the stability of the electrical resistance signals.

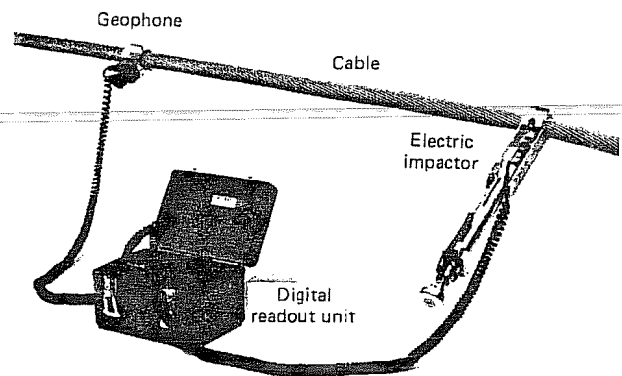


Figure 2.10 Cable Tensiometer (after Dunnicliff<sup>15</sup>).

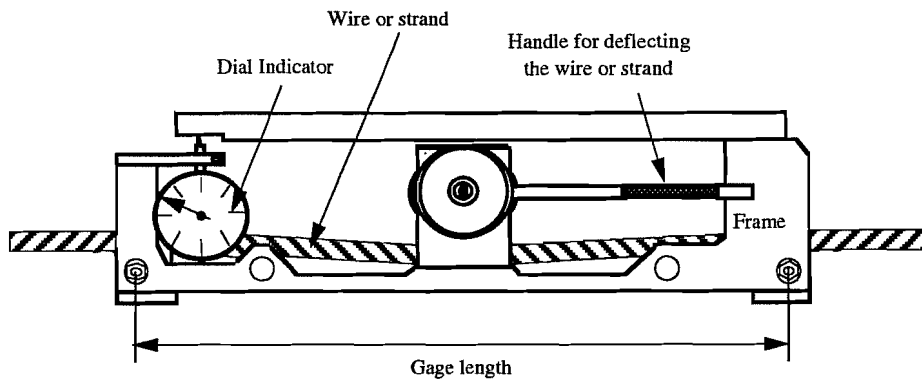


Figure 2.11 Fulmer Tension Meter (after Hanna<sup>20</sup>).

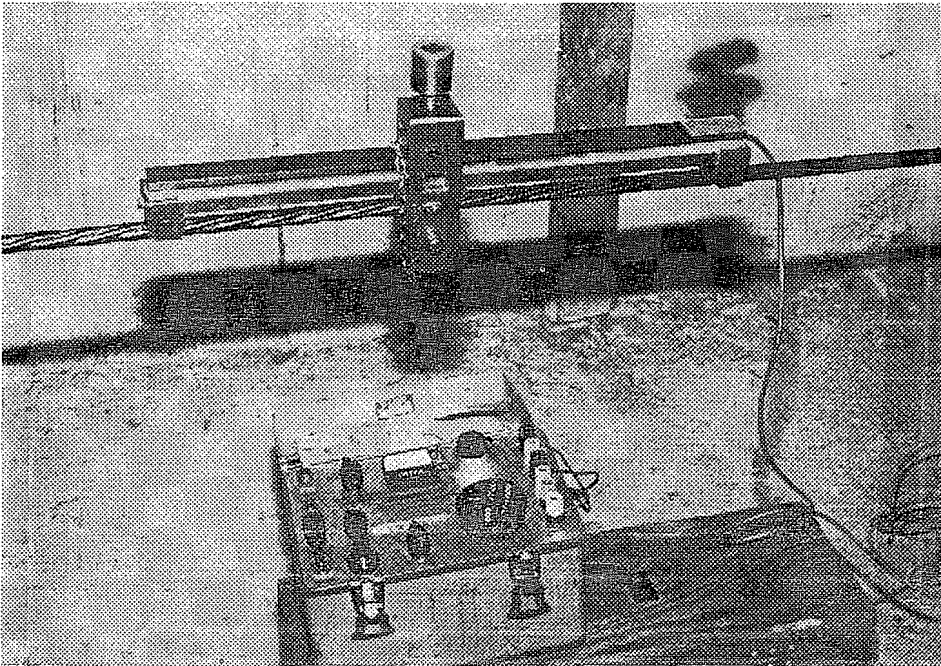


Figure 2.12 Kuhlman Beam from California D.O.T. (after Richardson<sup>45</sup>).

## 2.2 Trials of Instrumentation Systems

In the preliminary survey, only two devices were found to be even possibly useful for the present applications for measuring strains or loads at different cross-sections of multi-strand tendons. These devices consisted of the Tensiomag load-measuring system and the bonded foil type of electrical resistance strain gages.

More information about Freyssinet's Tensiomag was sought. Representatives of Freyssinet International in the United States were contacted several times to obtain information about their product's accuracy, geometric requirements and price. A few months later, only basic information was provided by the manufacturer's representative in this country. A catalog and a published report of tests and explanation of behavior were later obtained from other sources.<sup>37</sup> Although conversation was established several times with Freyssinet's technical engineers, no information on costs and availability was obtained.

The article published in IABSE Proceedings reported that Tensiomag cells have not been used in tendons composed of more than 12 - 0.6"  $\phi$  7-wire prestressing strands. However, most of the external and internal tendons for the San Antonio Y bridges were designed for 12 to 19 - 0.6"  $\phi$  7-wire strands. Another problem related to this system is the lack of portability of the cells, since the only method for moving these devices is by detensioning the tendons to which they are installed.

Without a field report of system reliability, lack of portability, and no serious interest from the manufacturers, the possibility of using Tensiomag load cells for the San Antonio Y Project was eliminated.

The only other system with proven reliability and behavior is electrical resistance strain gages. Although several complications are tied to this technology, advances in this field of measurements have been remarkable and some workable system was thought possible. Another factor leading to interest in this technology was that trial test costs were expected to be minimal since all completion circuits, portable readout boxes, automated scanning units, and data reduction software were readily available at the research facility.

The awareness of the poor long-term performance of electrical resistance gages made it imperative to find a secondary "back-up" system for measuring in-place, long-term tendon stresses. Tensiomag cells were considered an unreliable and probably expensive possibility. Since no other commercially manufactured devices were available, a new device (known as the Epoxy Sleeve System) was developed. Final manufacturing details, operation and trial tests of this new system are included in Section 2.2.2.

**2.2.1 Electrical Resistance Strain Gages.** Electrical resistance (ER) gages were selected as the primary system for obtaining stresses at different cross-sections of prestressing tendons. Trial tests were performed in order to better understand the current technology and to improve the application of bonded foil type electrical resistance strain gages. The studies were concentrated in the following areas:

- a. Improvements necessary for acceptable long-term stability of signals,
- b. Stress differences between wires of a single prestressing strand, and
- c. Stress differences among strands in multi-strand tendons.

Final recommendations with respect to the most appropriate type, installation and use of this system of measurements in field studies of segmental box girder bridges with internal and external tendons are included in Section 2.3.

**2.2.1.1 Improvements in Signal Stability.** Reports of previous instrumentation projects which utilized electrical resistance strain gages were carefully reviewed. Factors that directly affected the resulting stability of these gages were studied individually. A thorough investigation of manufacturer technical reports on electrical strain gaging technology helped considerably in the preparation of this section.<sup>31</sup>

The following conditions can influence the long-term behavior of bonded foil electrical resistance strain gages:

- a. Width of backup gage matrix,
- b. Material of gage matrix and conductor,
- c. Gage rated resistance and excitation level,
- d. Bonding system and installation,
- e. Moisture protection system for aggressive environments,
- f. Gage completion circuit,
- g. Leadwires, and
- h. Connectors used for automated multi-channel scanning systems.

**a. Gage Size.** The most important dimension regulating maximum size is the width of the backup matrix of the resistors. Most previous researchers at Ferguson Laboratories have used Measurements Group gages of the size type 062AP (matrix size: 6.6 mm L x 4.1 mm W). TML gages size type FLE-1 (matrix size: 5 mm L x 2.5 mm W) were also popular for laboratory applications. In the present trial tests, three different types of gages were compared. Measurements Group gages of sizes 062AQ (6.6 mm L x 3.8 mm W), 125BZ (7.4 mm L x 3.3 mm W) and the previously mentioned 062AP were studied for ease of installation on individual wires of 0.6"  $\phi$  7-wire prestressing strands. After individual applications for the experimental trials, narrower gages were found easier to install and are recommended for future use. Although slightly longer, the 125BZ gages performed the best during the installation process and had the fewest problems with improper bonding to the sharply curved wires. TML

manufactured gages were not investigated. However, the size type FLE-1 should also provide acceptable results.

**b. Gage Material.** It is important to choose the most appropriate material for the gage's conductor and backup matrix in order to reduce errors associated with temperature differentials. Obviously, the more accurate conductor materials will be those for which temperature differentials have smaller effects on their electrical resistance properties. These special low temperature effect gages are available for a considerable increase in cost. Their price can be as much as double the price of conductors of "moderate" accuracy.

Changes in strand length due to temperature fluctuations can induce error. The increase or decrease in strand length is measured as stress-induced strain by the bonded foil gages unless it is properly accounted for. The resistivity of the strain gage's conductor wire also varies with temperature, and this is also measured as stress-induced strain by the gage readout units. Temperature-induced strains in the strand and in the gages are commonly known as *apparent strains*.

One method of compensating for temperature is the use of a "dummy" unstressed strain gage bonded to the same material (but unstressed) and at the same environmental condition as the principal gages. Compensation is then achieved by installing both gages on opposite legs of a Wheatstone bridge circuit in order to cancel their strains. It is possible to implement this approach with measurements in prestressing strands by gaging a small unstressed strand specimen located next to each instrumented cross section of the stressed strand. However, this procedure would increase final instrumentation costs considerably due to the addition of the extra gage, and the additional Wheatstone bridge circuits in the data acquisition system.

Another method for avoiding apparent strains is to use temperature-compensated strain gages currently offered by most gage manufacturers. Measurements Group offers two types of temperature self-compensating materials, constantan (A-alloy) and a more expensive modified karma (D-alloy). To compensate for strains suffered by the material where these gages are to be installed, strain manufacturers use an S-T-C (Self-Temperature-Compensation) number. This number matches the linear coefficient of expansion of most structural materials. For prestressing strands, an S-T-C factor of 09 approximates well the linear coefficient of expansion of high-strength steel (with a  $\approx 8 \mu\epsilon/^\circ\text{F}$ ).

Temperature compensated constantan gages provide the best behavior for smaller temperature variations. Inside the box-girders of the San Antonio Y segmental bridges a temperature differential of 80°F is the most expected between top summer heat and the coolest measurement day in the winter. When bonded to high-strength steel, errors due to *apparent strains* from temperature differentials in the order of 80°F will only represent about 10 $\mu\epsilon$  for 09 S-T-C constantan gages. When high precision measurements are required, compensation for even such small differences can be done with the formula provided on each individual package of strain gages. Calibration formulas for 09 S-T-C gages are usually prepared from manufacturer tests on 304 Stainless Steel. They have a thermal expansion coefficient of about

9.6  $\mu\epsilon/^\circ\text{F}$ , which is slightly higher than for the low-relaxation prestressing strands. The difference of 1.6  $\mu\epsilon/^\circ\text{F}$  should not matter for the smaller temperature differentials expected for the present project. However, it was found that better performance can be provided by 06 S-T-C gages. Their calibration tests are usually made on 1008-1018 Steel with 6.7  $\mu\epsilon/^\circ\text{F}$  thus providing an S-T-C mismatch of only 1.3  $\mu\epsilon/^\circ\text{F}$ . These gages are therefore recommended for the present instrumentation project.

**c. Gage Resistance and Excitation Level.** Another inconvenience with electrical resistance measurements is that signals are usually quite small. This is worsened when the physical property to be measured varies only slightly, as is expected for the long term tendon stress fluctuations of the San Antonio Y structures. Even in cases of overloading of this type of structure, the stress variations on the tendons are expected to be small. MacGregor's model study of an external tendon segmental box-girder bridge found a maximum stress increase of only 5 ksi for factored design live load plus impact, and up to 8 ksi for cracking loads.<sup>30</sup> To successfully measure and distinguish these small movements with electrical resistance strain gages it is necessary to have stronger electrical signals. An easy way to achieve this is by using slightly higher resistance strain gages and their corresponding higher excitation levels. Most previous short-term static testing of structures used lower 120 $\Omega$  strain gages, but the next standard gage resistance of 350 $\Omega$  was selected for this project. Gage resistances above 350 $\Omega$  are not standard but still available at higher prices and longer delivery times.

The most appropriate excitation for strain gages depends on gage rated resistance, gage size, and type of material to be instrumented. For Measurements Group gages of the type EA-125BZ-350 (Option LE) bonded to high-strength steel of prestressing strands (which provide a good level of heat dissipation) an optimum excitation level of 4 to 5V was calculated from manufacturer tables.<sup>32</sup> Conservatively, an excitation level of 4.5V would prevent self-heating strains in these gages.

**d. Bonding System.** Cyanoacrylate (i.e. Super Glue) type of adhesives are usually the preferred bonding system due to their ease of installation. Most previous short-term laboratory tests investigated have used the M-Bond 200 cyanoacrylates from Measurements Group. As easy and fast as they are to use, cyanoacrylates are not recommended for long-term projects due to their lower bond life. More durable epoxy-based glues should be used when stability for longer periods of time is desired. Besides higher costs, added complications of epoxy glues are their slower drying period and stricter installation requirements. During installation of gages with epoxy adhesives, an evenly distributed surface pressure over the strain gages must be exerted in the drying period to obtain proper bond. This is complicated by the small curved surfaces of individual prestressing strand wires and the tight arrangements of strands in a tendon.

Use of epoxy adhesives was investigated for the instrumentation of the San Antonio Y structure. The final type of adhesive selected for testing was Measurements Group's AE10 since it dries faster (at normal temperatures) than other epoxies. For proper gage installation, a method of providing even drying pressure on the surface of the strain gages bonded to single wires of prestressing strands was also investigated. Small plastic molds of individual 0.6"  $\phi$



7-wire prestressing strands were prefabricated with a special silicone. The product used for these molds was General Electric RTV-620 Silicone. Plastic silicone molds of  $\approx 1" \phi$  were precast around small prestressing strand pieces and dried (keeping a vertical position of the strand pieces) at normal temperature for a period of 4 to 7 days. Cutting a longitudinal line on one side of the dried plastic molds enabled them to be easily pulled out in jackets of 1" to 1 1/2" lengths. For tests on individual strands, these small jackets were fitted at the strain gage's location and even pressure was applied by tightening a small hose clamp around each jacket. The hose clamp tightening procedure should be carefully applied since high pressures can squeeze too much epoxy resin from underneath the foil gages. Ideally, the clamping pressure on the gages should be between 5 and 20 psi. When using strain gages with pre-attached leadwires (Measurements Group Option LE) a small piece of Teflon tape or clear plastic sheet was placed between the leadwires and the instrumented surface of the strand. This was done before the installation of the silicone jackets in order to prevent bonding of the leadwires to the prestressing steel.

For multi-strand tendons the procedure was slightly different. Since the silicone jackets could not be wrapped all around individual strands, they were cut in three sections. These cuts were done in a way which ensured that a full wire's cross section would be in the middle of each piece. These smaller silicone pieces were later placed on top of each previously installed strain gage. A larger hose clamp placed around the full tendon bundle was used for the application of even surface drying pressure on each strain gage. Trial tests with these systems performed well and installation was not difficult to carry out. However, practical experience and strain gage handling care of the operators played an important role for optimum installation. The biggest problem with this bonding method was the long time period needed for proper epoxy drying. At normal temperatures ( $\approx 75^\circ\text{F}$ ) the clamped gages must be dried for no less than five hours.

**e. Moisture Protection System.** Humidity protection of the gage is one of the most important factors because it has serious influences on the initial stability of the system. If excess humidity is present, three different effects are possible: an electrical short of lead wires, a gage resistance change due to electrochemical corrosion of the lead wires or foil, or a breakdown of the bonding material. Waterproofing must therefore provide a high degree of bond to the strain gage, and at the same time should not be stiff enough to cause resistance to movements of the instrumented surface.

Several methods for avoiding moisture intrusion in the strain gages have been used in the past. Yates achieved good performance by unwinding each individual wire of a strand, installing the gage and its protection scheme and later rewinding the whole system.<sup>54</sup> This is impractical for the present project where great lengths and number of strands are expected. Other methods have been used less successfully and are based on standard manufacturer recommendations. These performed poorly on most long-term projects. The combination of grouting of tendons and the very small, tightly-curved surfaces of individual wires of each strand creates a highly aggressive environment for a proper gage protection scheme. Since prevention is a better technique for avoiding physical or moisture damage to strain gages, a method for maintaining

a dry atmosphere around the gages by blocking off certain sections of external tendons during the grouting process was developed. The blocked sections of external tendons were protected against corrosion (after mounting of the gages) with high-quality greases. Greases have the added benefit of enhancing the moisture protection of the strain gages, and they can be easily removed if a strain gage needs to be replaced in the future.

More elaborate schemes were investigated for protecting strain gages placed in areas that necessarily have to be grouted. Epoxy-based coatings were found to work satisfactorily. The M-Coat J system from Measurements Group was characterized as having enough consistency to stay in place after placement. It also spread well in tight areas between strand wires. Before coating gages with M-Coat J epoxy a small piece of Teflon tape was usually placed on top of the installed gages to prevent a bond to their epoxy cover. After placement of the epoxy, liberal amounts of microcrystalline wax in a larger area around the epoxy was found to help the moisture protection scheme. These small wax plates were easily liquefied with air blow driers. Other moisture protection schemes based on nitrile rubbers did not work well in grouted environments.

**f. Gage Completion Circuit.** Different Wheatstone bridge completion circuits provide varying degrees of accuracy and cost. The most popular system for laboratory applications due to cost and ease of configuration consists of the quarter bridge circuits. Quarter bridge Wheatstone networks can have two or three leadwires attached to a single strain gage. This is important when long lead-wires are necessary, or when large temperature differentials are expected to occur during the test schedule, as in the San Antonio Y instrumentation project. Leadwire lengths of up to 60 feet are necessary and temperature differentials of up to 80°F are possible. Three-leadwire quarter bridge completion circuits directly compensate for temperature differentials in the length of the wires, provided that both wires connected to the single strain gage terminal have the same length and undergo the same temperature differentials. This is a proven electrical characteristic of the Wheatstone bridge and no tests were performed between two- and three-leadwire quarter bridge circuits. Temperature compensation systems are strongly recommended for long-term instrumentation projects. A detailed explanation of the benefits and complications related to each possible completion circuit configuration was presented by Dunnicliff<sup>15</sup> and should be consulted when other circuits are under consideration.

**g. Leadwires.** Their selection is also important for final system stability. Factors influencing proper leadwire selection are physical protection and electrical noise reduction. Jackets around individual leadwires are necessary for physical protection. Electrical noise produced from large currents or electromagnetic sources can be diminished by threading individual leadwires in winding arrangements. This type of leadwire can be obtained from most electrical wire manufacturers. Trial tests were successfully performed with Belden conductors of the type 8771. These consisted of stranded tinned copper, polyethylene insulated conductor cables of size 22AWG (American Wire Gage). Added electrical noise reduction of the stranded three-leadwires was provided by an encapsulation of aluminum-polyester shield, and physical protection was provided by a chrome PVC jacket.

An important concern related to long lengths of leadwires is the introduction of an extra electrical resistance that dampens the readings of strain-induced resistances. For the selected type of leadwires and strain gages, the original gage factor should be desensitized to account for long leadwire lengths. Strain gage manufacturers suggest the following procedure to quantify the effect of leadwire lengths:<sup>31</sup>

$$GF_D = GF_o * \frac{R_G}{R_G + R_W}$$

$GF_D$	=	desensitized value of gage factor
$GF_o$	=	original gage factor (provided by manufacturer)
$R_G$	=	gage resistance in Ohms
$R_W$	=	effective leadwire resistance (for a three-leadwire quarter-bridge configuration this should be the resistance of one single leadwire).

For the suggested gages of the type Micro Measurements EA-06-125BZ-350, Belden type 8771 leadwires, and for average lengths of 35 feet expected for the present applications in the San Antonio Y bridges, the desensitized factor becomes:

$$\begin{aligned} GF_o &= 2.085 \\ R_G &= 350\Omega \\ R_W &= 35 * 0.01474 = 0.5159\Omega \\ GF_D &= 2.082 \end{aligned}$$

Neglecting this correction factor only implies an error of 0.14% on each strain reading.

**h. Connectors.** Another source of *parasitic resistances* comes from electrical resistance variations due to different connections of strain gage leadwires. A good connection of two electrical wires (with minimum losses in resistance) is difficult to achieve. Moreover, an exact reproduction of a connection of two electrical wires is difficult to replicate. Factors affecting these two complications are not only related to physical differences in the connections but also due to temperature differentials. The electrical resistance related to an individual connection at a point in time with one certain temperature will be different than the resistance of the same connection at a later time with a different temperature. This is because the resistivity of the connector's materials varies with temperature. One solution is to establish a "permanent" connection of all leadwires to each strain gage channel. Although this does not fully eliminate all *parasitic resistances*, it avoids the introduction of electrical resistance differentials due to varying physical connections. However, this is ineffective to achieve in multi-channel systems, since no connectors would imply a permanent readout unit for each channel. To make the system more effective, a high quality multi-channel switching device was purchased. This electronic device had the characteristic of reducing differences in electrical resistance variations during different scans by using gold-plated connectors. Temperature induced differentials were also minimized with these systems. The multi-channel switching device purchased was the

*AMD-416 Multiplexer* manufactured by Campbell Instruments, Inc. This was also compatible with the electronic data-acquisition system and is further described in Chapter 7 of this report.

**2.2.1.2 Single Strand Tests.** Electrical resistance strain gages measure strains of individual wires of the prestressing strands to which they are bonded. Yates<sup>54</sup> indicated that the strains experienced by each wire of a 7-wire prestressing strand can vary substantially. A plot of his results for one particular strand test was previously included as Figure 2.2. Although each wire behaved differently at low stresses, the slopes of the best-fit lines of high-stress data points seemed to be approximately the same. In most of these and other previous single-strand tests, the "apparent" modulus of elasticity defined by the slope of the best-fit line of the stress-strain plot obtained from each electrical resistance strain gage was slightly larger than the manufacturer-provided modulus.

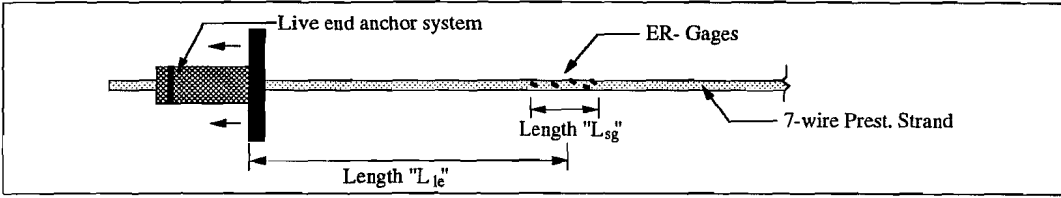
Several additional tests with electrical resistance strain gages bonded to single wires of prestressing strands were performed to better understand their overall behavior. These tests were also performed to investigate the performance of various types of strain gages and bonding methods. It was also desired to suggest a more standardized procedure for the data-reduction process.

**a. Test Descriptions.** A total of four single-strand tests were performed. Three strand specimens of approximately 3.5-foot lengths were used in the first three tests. These specimens were taken from two different rolls of  $\frac{1}{2}$ " $\phi$  7-wire low-relaxation prestressing strands manufactured by Florida Wire and Cable Company. A 7-foot specimen was used in the fourth single-strand test. This specimen was taken from a roll of 0.6" $\phi$  7-wire low-relaxation strand also manufactured by Florida Wire and Cable Company. Two loading cycles were performed in the final single-strand test. Standard anchorage equipment used in all single-strand tests consisted of 3-wedge anchor systems manufactured by Supreme Industries Inc. General descriptions related to the strain gages, their physical position, and the stressing system used for each test are included in Table 2.2.

Electrical resistance strain gages of the foil type were bonded to each one of the six external wires of each strand specimen. In TEST 1S and TEST 4S each set of six gages was carefully installed in one particular cross-section of the strands, as shown in Figure 2.13. The cross-sections passing through the middle of each gage had a longitudinal separation of less than 5 mm (0.2 inches). However, in the specimen used for TEST 2S and TEST 3S the gages were spread over a length of 10 cm (4 inches). Only gage #1 of TEST 1S was damaged during installation.

In most tests, strand strains were automatically scanned with a computer-controlled data-acquisition system. However, a portable strain indicator box connected to a switch and balance unit was used in TEST 3S. Load levels were obtained either from the scale readings of a 60 kip vertical loading machine (TESTs 1S and 2S) or from readings of an electrical resistance load cell (TESTs 3S and both loadings of TEST 4S) installed at one of the anchoring ends of the strands. All electrical measuring devices (strain gages and occasional load cell) were connected to the

Table 2.2 Descriptions of single strand tests.



	TEST 1S	TEST 2S	TEST 3S	TEST 4S (a & b)
<b>Strand Characteristics:</b>				
a. Strand Roll	A	B	B	C
b. Diameter [in]	½	½	½	0.6
c. Type	7-wire, low-lax	7-wire, low-lax	7-wire, low-lax	7-wire, low-lax
<b>ER- Gages:</b>				
a. Manufacturer	Measurements Group	Measurements Group	Measurements Group	TML
b. Description	EA-06-125BZ-350	EA-06-062AQ-120	EA-06-062AQ-120	FLE-1 (120Ω)
c. Length "L <sub>sg</sub> " [in]	0.5	4	4	0.5
d. Length "L <sub>le</sub> " [in]	23	8	4	20
<b>Stressing Method</b>	Loading Machine	Loading Machine	Hydraulic Jack	Loading Machine

data-acquisition system for the complete duration of each test. Errors due to temperature differentials were minimal due to the short duration of each test. Moreover, no errors due to existence of *parasitic resistances* were assumed to be present since the gages were permanently connected to the data-acquisition system (i.e. for the complete duration of each test).

**b. Data Reduction Method.** Stress values of each strand were obtained by considering the nominal areas of 0.153 inch<sup>2</sup> and 0.215 inch<sup>2</sup> for the ½"φ and the 0.6"φ strands respectively. Since no stress losses can be reasonably expected to occur between the instrumented section of the strand and the section where loads were measured, the corresponding values of stress and strain were plotted on a single  $\sigma$ - $\epsilon$  graph. A best-fit line was defined considering the data points of the  $\sigma$ - $\epsilon$  graph that corresponded to stresses between 0.20 $f_{pu}$  and 0.80 $f_{pu}$ . This procedure thus avoided the consideration of initial nonlinearities in the graph (usually occurring during seating of the strand specimen at the anchor ends). The slopes of the best-fit lines corresponding to each workable electrical resistance strain gage installed in each specimen were recorded. The prestressing strand's apparent modulus of elasticity was determined by the average of these slopes.

Since electrical resistance strain gages are installed at a certain angle from the longitudinal axis of a strand, a slightly different modulus of elasticity than determined by strand manufacturers was expected. To help quantify the possible value for the "apparent" modulus defined by an electrical resistance strain gage, an analytical study of the phenomena was performed. This study is summarized in Figure 2.14. The drawing in this figure represents a 7-wire prestressing strand specimen (drawn with an exaggerated high pitch and small wires to better show the extreme behavior). If this sample specimen were completely anchored at the

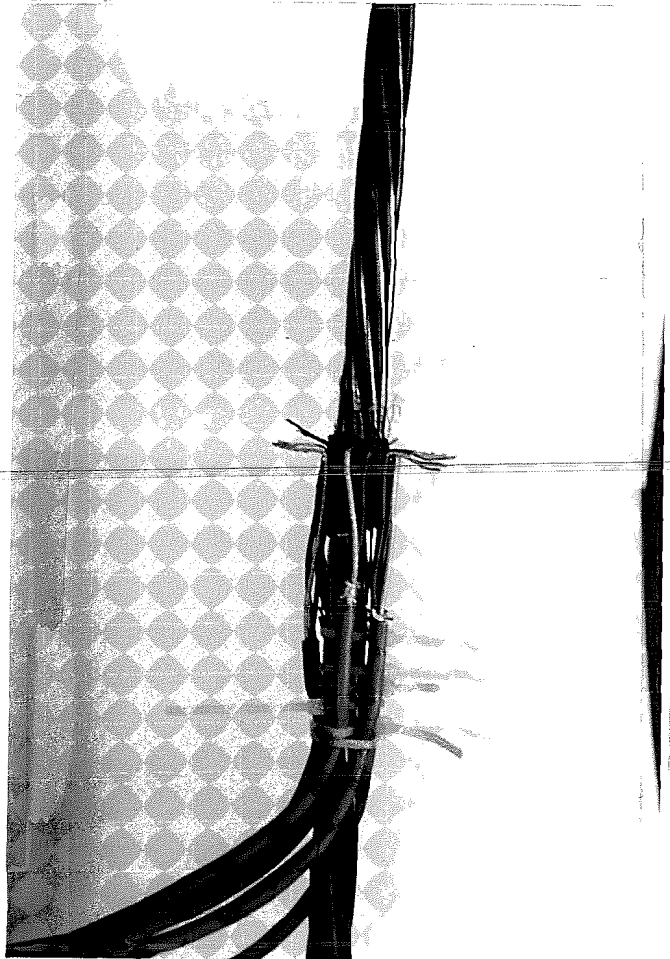
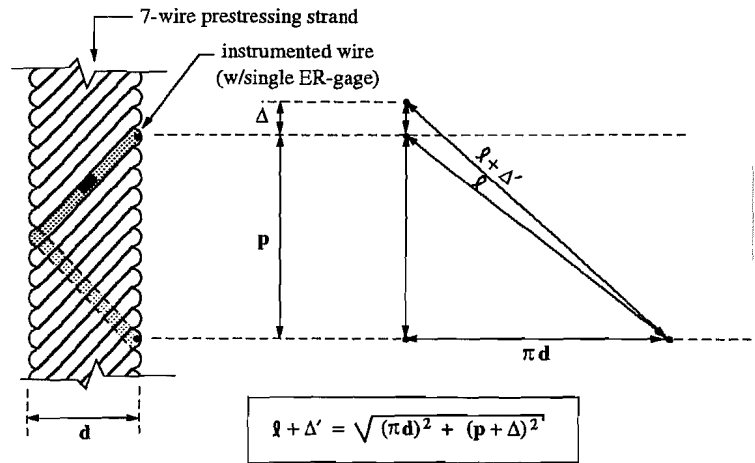


Figure 2.13 Installation of the electrical resistance strain gages for TEST 1S (similar to TEST 4S).

better show the extreme behavior). If this sample specimen were completely anchored at the beginning and at the end of the instrumented wire's single loop, the strand strains would be 3.7% to 6.4% higher than the single wire's strains (for the same stress level). This implies that the strand's modulus of elasticity is slightly smaller than the single wire's modulus due to their different geometric conditions.

The modulus of elasticity tests performed by strand manufacturers measure average strains of the whole strand, whereas the electrical resistance strain gage measures a single wire's strain. This difference in testing devices combined with the theoretical example of Figure 2.14 show that it is expected that strands will have a slightly larger apparent modulus of elasticity when performing measurements with electrical resistance strain gages. It is difficult to accurately predict how much larger the apparent modulus would be (because other factors different than the strand pitch influence the results). However, to avoid a potential source of error it is strongly recommended to always perform calibration material tests of the prestressing strand specimens with the same instrumentation devices that will be used either in the laboratory or in the field. In the data-reduction process the "apparent" modulus determined by each instrumentation device should be used accordingly.



where:  
 $l + \Delta'$ : length of instrumented wire corresponding to 1 revolution around the strand.  
 $\Delta$ : strand elongation.  
 $\Delta'$ : wire elongation.  
 $\epsilon$ : strand strain.  
 $\epsilon'$ : wire strain.  
 $p$ : pitch of the strand.  
 $d$ : nominal strand diameter.

\* Manufacturer tolerance in strand's pitch: 12 to 16 strand diameters.

\* Effect on apparent modulus determined by electrical resistance strain gages: (same for 1/2"  $\phi$  and 0.6"  $\phi$  strands)

Pitch	$(\frac{\epsilon'}{\epsilon})$
12 d	0.936
16 d	0.963

Figure 2.14 Analytical approximation of a prestressing strand's apparent modulus of elasticity, as determined by electrical resistance strain gages bonded to individual wires.

**c. Interpretation of Results.** The measured behavior of the strand wires in a typical single-strand test is plotted in Figure 2.15. A summary of the average values in each test is shown in Figure 2.16. Final statistics of the results from both tests performed with the

**TEST 2S**  
**Electrical Resistance Strain Gages**

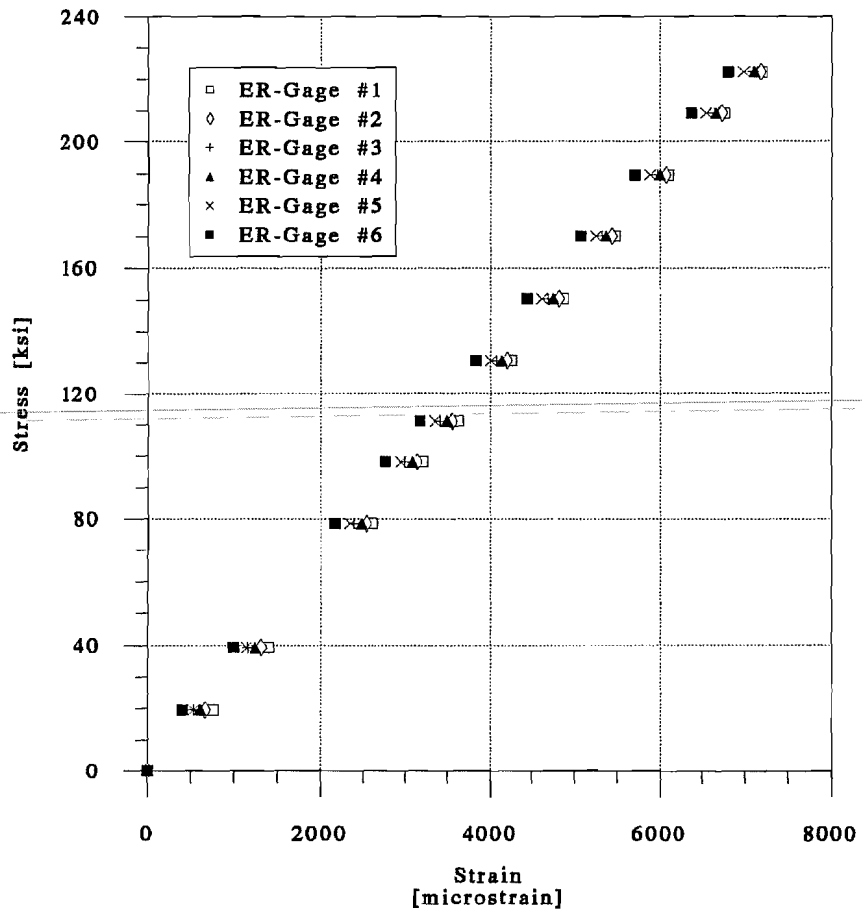


Figure 2.15 Stress-strain curves for TEST 2S on first 1/2"  $\phi$  strand specimen from roll "B".



**Summary of Average Results of the  
Electrical Resistance Strain Gages  
in Single Strand Tests**

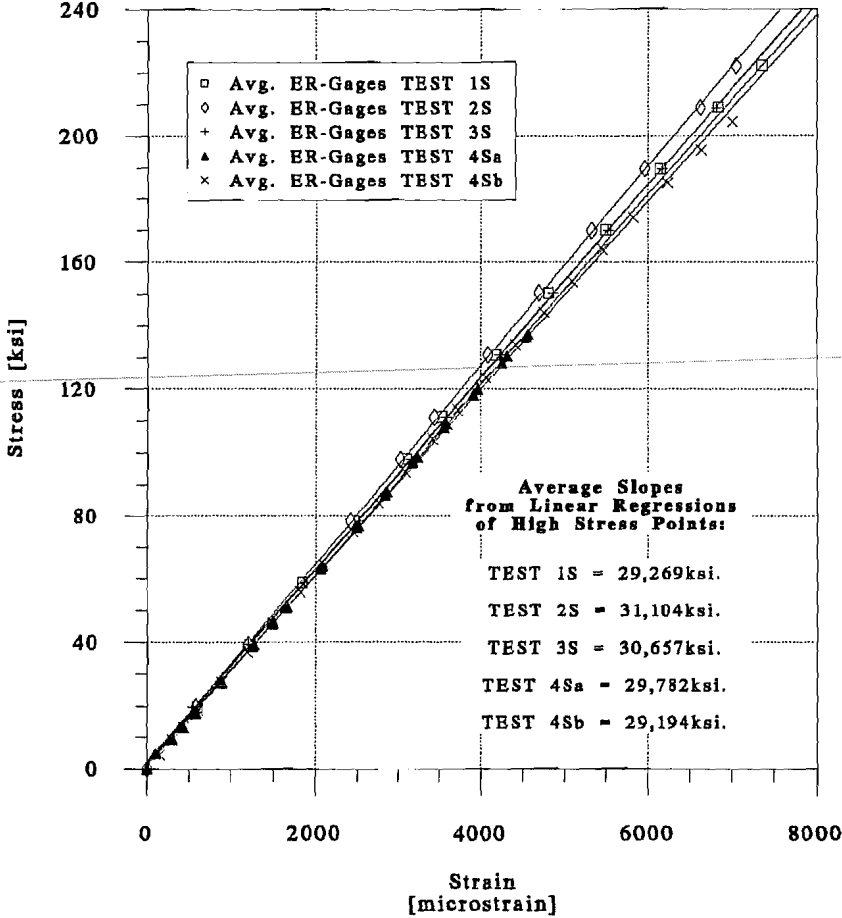


Figure 2.16 Summary of stress-strain average curves of single-strand tests with ER-gages.

specimens taken from strand roll "B" ( $\frac{1}{2}\phi$  strand) are included in Figure 2.17. The statistics of the results from both tests with the single specimen from strand roll "C" ( $0.6\phi$  strand) are included in Figure 2.18.

In general, it was found that the variation of strain readings among the wires of each individual strand was considerably lower than the values obtained by Yates. Differences between the present test results and those from Yates' are probably caused by a combination of the following factors:

- type of strand,
- type of anchorage,
- type of stressing system,
- distance from ER-gage to anchorage (" $L_{1e}$ " on Table 2.2), and
- separation of ER-gages (" $L_{sg}$ " on Table 2.2).

As mentioned earlier in this report, during initial stressing operations the wires of a prestressing strand are engaged at varying degrees of tightness by the stressing hardware. It is therefore logical to find large differences of stresses between wires. However, the authors believe that due to the helical arrangement of the wires the stress gradient between them should decrease at sections farther away from the anchorage ends. According to this train of thought, the wires should experience similar strains at sections beyond the "stress distribution length" from either end of the strand. The present test results agree with this hypothesis. TEST 1S and TEST 4SB (second loading of the strand specimen of TEST 4S) had longer *stress distribution lengths* during testing. They also had very linear placement of the strain gages on a single cross-section of each strand specimen. The results from these two tests indicate quite similar behavior of the wires of each strand, even at low stress levels. Results from the other single-strand tests indicate slightly more irregular behavior at low stress levels.

An interesting observation can be drawn from the results of TEST 4SA. One of the single-strand anchorages of this test was accidentally left at an angle from the longitudinal axis of the strand thus causing certain wires to be stressed at a higher level than the others. The severity of this stress differential between wires was not corrected by the long *stress distribution length* of this particular test setup. During the second loading of the same specimen (with the only difference of correcting the anchorage's positioning) the wires behaved quite similarly.

The theory of stress distribution among the wires of a strand can thus be different in most practical applications of prestressing. Friction between strands and deviation ducts in multi-strand tendons, uneven strand lengths between anchor assemblies, and variations in the positioning of end anchors can all modify the redistribution of stresses among wires of each strand. But even with these unfavorable conditions, at high stress levels each wire should still behave similarly. This is partially addressed in the following section, where tests on multi-strand tendons deviated at small angles were performed.

**Summary of results from tests of specimens from strand roll "B" (1/2" diameter):**

		Computed Modulus of Elasticity *		
		[ksi]		
		TEST 2S	TEST 3S	
	ER-Gage #1	31470	31838	
	ER-Gage #2	31087	30172	
	ER-Gage #3	30720	29548	
	ER-Gage #4	31238	30796	
	ER-Gage #5	31098	30743	
	ER-Gage #6	31010	30846	
<b>Statistics of ER-Gages</b>				<b>Statistics of ER-Gages</b>
<b>(per TEST):</b>				<b>(from both TESTS):</b>
	Min.:	30720	29548	29548
	Max.:	31470	31838	31838
	St. Dev.:	248	765	590
	Avg.:	31104	30657	30881
	Variability of Avg.**:	±0.80%	±2.49%	±1.91%

**Notes:**

\* To obtain each computed modulus of elasticity, a best-fit line was performed only considering the measured data points that corresponded to stresses between 0.20fpu and 0.80fpu. No other manipulation of raw data was performed.

\*\* The values corresponding to the variability of each given average were considered to be equal to the percentage of the ratios between the standard deviation of each set of slope observations and their corresponding average slope.

Figure 2.17 Statistical analysis of electrical resistance strain gage results from tests on 1/2"  $\phi$  strand specimens from roll "B".

**Summary of results from tests of specimen from strand roll "C" (0.6" diameter):**

		Computed Modulus of Elasticity *		
		[ksi]		
		TEST 4Sa	TEST 4Sb	
ER-Gage #1		29538	28860	
ER-Gage #2		30112	29433	
ER-Gage #3		29778	29220	
ER-Gage #4		29323	28969	
ER-Gage #5		29915	29351	
ER-Gage #6		30023	29330	
<b>Statistics of ER-Gages (per TEST):</b>				<b>Statistics of ER-Gages (from both TESTS):</b>
	Min.:	29323	28860	28860
	Max.:	30112	29433	30112
	St. Dev.:	302	229	399
	Avg.:	29782	29194	29488
	Variability of Avg.**:	±1.01%	±0.79%	±1.35%

**Notes:**

\* To obtain each computed modulus of elasticity, a best-fit line was performed only considering the measured data points that corresponded to stresses between 0.20fpu and 0.80fpu. No other manipulation of raw data was performed.

\*\* The values corresponding to the variability of each given average were considered to be equal to the percentage of the ratios between the standard deviation of each set of slope observations and their corresponding average slope.

Figure 2.18 Statistical analysis of electrical resistance strain gage results from tests on 0.6"  $\phi$  strand specimen from roll "C".

A further analysis of the single-strand test results was carried out to find the stress level at which all wires became engaged to the stressing hardware. Gradually eliminating low stress points and performing best line fits of the results from the single-strand tests suggested that  $0.20f_{pu}$  was a conservative low stress mark after which all wires strain more similarly. All data reductions were thus performed between this low level of stress and a stress level just below  $0.80f_{pu}$  (to safely avoid measuring the plastic behavior of prestressing steel).

From the twelve statistical observations it was found that the variabilities of the average modulus of elasticity of the  $\frac{1}{2}"\phi$  and the  $0.6"\phi$  strand specimens were  $\pm 1.91\%$  and  $\pm 1.35\%$  respectively. In the tests with the  $0.6"\phi$  strand specimen the loads were computed from readings of a high definition electrical resistance load cell that was simultaneously scanned with the strain gages. This must have been one of the main reasons for improving the variability of the apparent modulus to under  $\pm 1.5\%$ . Future material tests are thus recommended to be performed with calibrated load cells scanned simultaneously with the electrical resistance strain gages.

Another comment from the statistical analysis of the test results is the slightly larger apparent modulus recorded by the electrical resistance strain gages. A manufacturer-obtained modulus of elasticity of 29,100 ksi was supplied with the prestressing strand roll "B" (used to take the two specimens for TESTs 2S and 3S). The statistics of Figure 2.17 indicate an apparent average modulus of 30,881 ksi for the two specimens from this strand roll. This is 6.1% larger than the manufacturer-supplied value and still within the analytical range previously computed in Figure 2.14. No manufacturer value was obtained from the prestressing strand roll "C" (corresponding to the  $0.6"\phi$  strand specimen). However, the average apparent modulus (29,488 ksi) is still slightly larger than the 28,900 ksi to 29,100 ksi typical range of manufacturer modulus.

**d. Conclusions.** The following conclusions can be drawn from the electrical resistance strain gages bonded to single prestressing strands:

- a. When all electrical resistance strain gages are installed at one particular cross-section and at an equal distance of no less than 24 inches from the anchorage ends, the gages were found to measure similar values of strains (even at low stress levels).
- b. Calibrated load cells scanned at the same time as the electrical resistance strain gages were found to improve the variability of the average apparent modulus of elasticity obtained in the data-reduction process. With calibrated load cells, the apparent modulus of elasticity determined by a single ER-gage was found more likely to be within  $\pm 1.35\%$  of the average strand modulus.
- c. When computing the linear regression of measured data points on a  $\sigma$ - $\epsilon$  graph, it was found better to consider only the points that corresponded

to stresses between  $0.20f_{pu}$  and  $0.80f_{pu}$ . This prevented any consideration of errors related to the initial differential seating of the wires, or to the plastic behavior of the prestressing steel.

- d. The slopes of individual  $\sigma$ - $\epsilon$  lines (the "apparent" modulus of elasticity) obtained from the electrical resistance strain gages were found repeatedly higher than manufacturer-given values. This is mainly attributed to the different measurement system used by strand manufacturers. Since most single-strand tests are performed as material checks of the modulus of elasticity and the overall behavior of the strands from a particular structure, the measured "apparent" modulus of elasticity should be consistent with the instrumentation device to be used in the actual tests of the structure.

**2.2.1.3 Multi-Strand Tendon Tests.** These tests were developed to check the performance of electrical resistance strain gages on multi-strand tendons. A technique for reducing the amount of stress differences among strands of typical prestressing tendons was also investigated.

Laboratory tests using short lengths of tendons can produce stress differentials among each instrumented strand. This is mainly due to the following factors:

- Small differences in initial strand length. This is usually produced from irregular twisting of the strands as they are threaded through the test specimens.
- Small sliding movements of seating wedges before a strand is fully engaged by the anchorage hardware. During initial stressing it is unlikely that all strands will seat simultaneously in the stressing hardware. Small stress variations are thus expected.

Most laboratory instrumentation projects with prestressing tendons are carefully prepared so as to avoid overstressing individual strands. This is usually accomplished by initially stressing and seating each strand against the back of the multi-strand tendon jacking system. Stressing operations of most stay cables composed of multiple prestressing strands are usually performed in a similar way. However, this practice is not followed in field applications of prestressing tendons, where small variations in length among individual strands should not cause a major overstressing problem.

Four tests of multi-strand tendons in two different testing setups were performed with electrical resistance strain gages of the bonded foil type. The description of each test, along with the most important findings follows.

a. **Test Descriptions.** The first two tendon tests (TEST 1T and TEST 2T) were developed in connection with a different study related to bonding of external tendons at deviators.<sup>44</sup> A tendon made of  $7\text{-}\frac{1}{2}\text{"}\phi$  prestressing strands was used in TEST 1T, and a tendon made of  $12\text{-}\frac{1}{2}\text{"}\phi$  prestressing strands was used in TEST 2T. A general description of the test setup is shown in Figure 2.19, where the position of the instrumentation system under study is also indicated. The epoxy sleeves (also shown in Figure 2.19) were a candidate instrumentation system investigated as a backup to the electrical resistance strain gages. This system is described fully in Section 2.3. One expected influence of the epoxy sleeves in the present tests was a "clamping" action on the strands, making them behave much more similarly during stressing operations. Thus, only a few ER-gages would be needed to accurately determine the average tendon stress of each instrumented section. The strain gages used in these tests were of the type EA-06-062AP-120 Option LE, made by Measurements Group. Three ER-gages were bonded to easily accessible strands at a particular tendon cross-section of TEST 1T. Four ER-gages of the same type were used in TEST 2T. All of these electrical resistance strain gages performed satisfactorily during both tendon tests. No complicated provisions for long-term stability were implemented in these gages due to the short duration of the tests. Strand strains were automatically scanned with a computer-controlled data-acquisition system. Corresponding live end load levels were scanned simultaneously by the data-acquisition system. They were computed from readings of an electrical resistance pressure transducer installed in the pressure line of the hydraulic jack used for stressing the tendons.

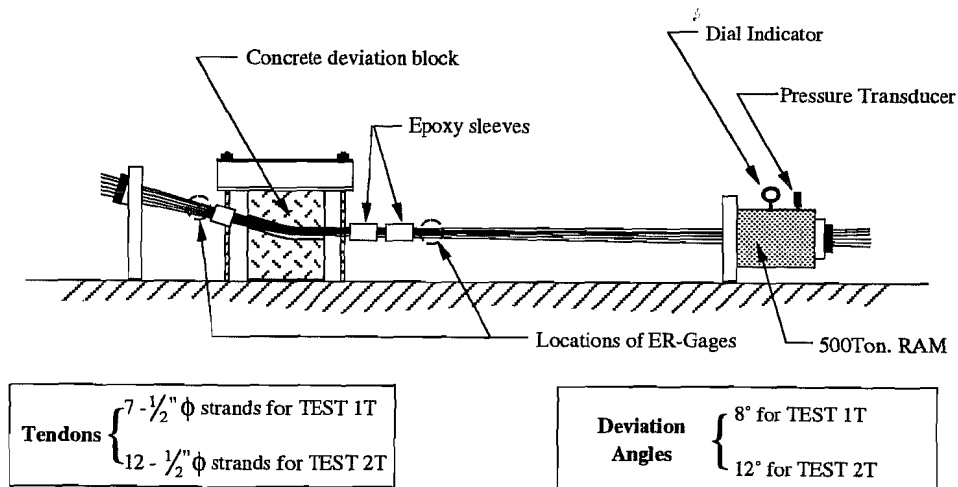


Figure 2.19 General schematic of TEST 1T and TEST 2T.

TEST 3T and TEST 4T were performed to observe the more complicated behavior of tendons composed of  $19\text{-}0.6\text{"}\phi$  strands. Actual field operations were simulated in the threading and stressing operations of these tendons. In each test, the tendons were loaded in three different cycles from zero stress to about  $0.85f_{pu}$ . These tests were performed in San Antonio, on a testing setup (shown in Figure 2.20) built by Austin Bridge Co. to perform their regular

modulus of elasticity tests. Austin Bridge Co. extended the use of their equipment, and also donated all the prestressing strands needed for these two tests. Two types of electrical resistance strain gages and the final version of the epoxy sleeves were implemented. The strain gages used were of the type EA-06-125BZ-350 Option LE and EA-06-062AQ-350 Option LE, both manufactured by Measurements Group. In each one of these last two tendon tests, three ER-gages were bonded to selected strands at a particular tendon cross-section. Only one gage (ER-gage #2 of TEST 3T) was damaged before performing the actual tendon test. Strand strains were monitored using a portable strain indicator box that was coupled to a portable multi-channel switching device. Both were connected to the electrical resistance strain gages for the complete duration of each test. Loads were computed at the live ends from pressure readings of a calibrated hydraulic jack instrumented with a pair of dial indicators. As in the previous tendon tests, no provisions for long-term gage stability were necessary.

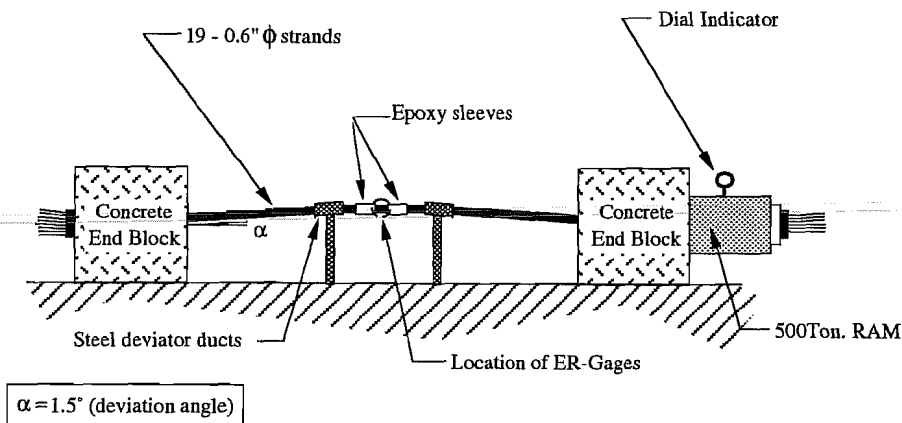


Figure 2.20 General schematic of TEST 3T and TEST 4T.

**b. Data Reduction Method.** In most laboratory and field investigations with instrumented tendons, load levels are measured at the live ends from readings of calibrated hydraulic jacks equipped with pressure transducers (usually of the electrical resistance type). However, better accuracy of the stressing loads imposed on the tendons can be obtained with calibrated center-hole load cells. But these expensive devices must be permanently left in each one of the instrumented tendons when performing field measurements of actual structures.

Stressing loads of the instrumented spans of the San Antonio Y project were to be obtained with electrical resistance pressure transducers installed in the calibrated hydraulic jacks. These pressure transducers were to be scanned simultaneously with the electrical resistance strain gages located at selected intermediate cross-sections of the external tendons. The information available will therefore consist of live end loads and corresponding cross-section strains of instrumented strands. The stress loss from the live end to each intermediate tendon cross-section is unknown but were to be estimated using live end loads and cross-section strains. Another

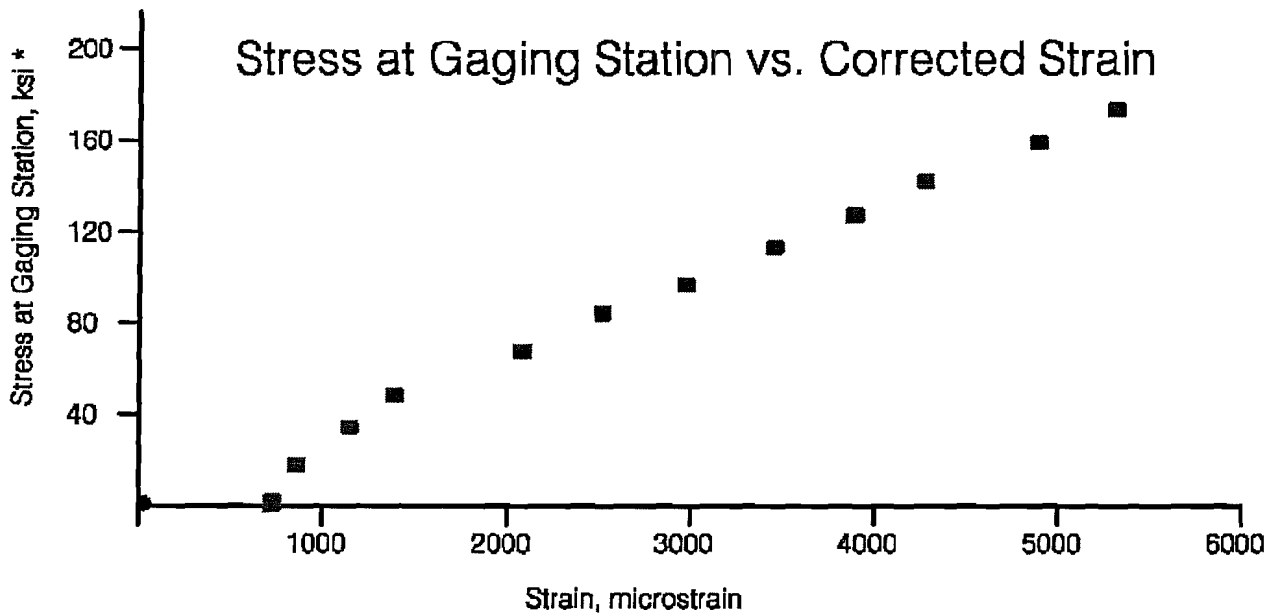
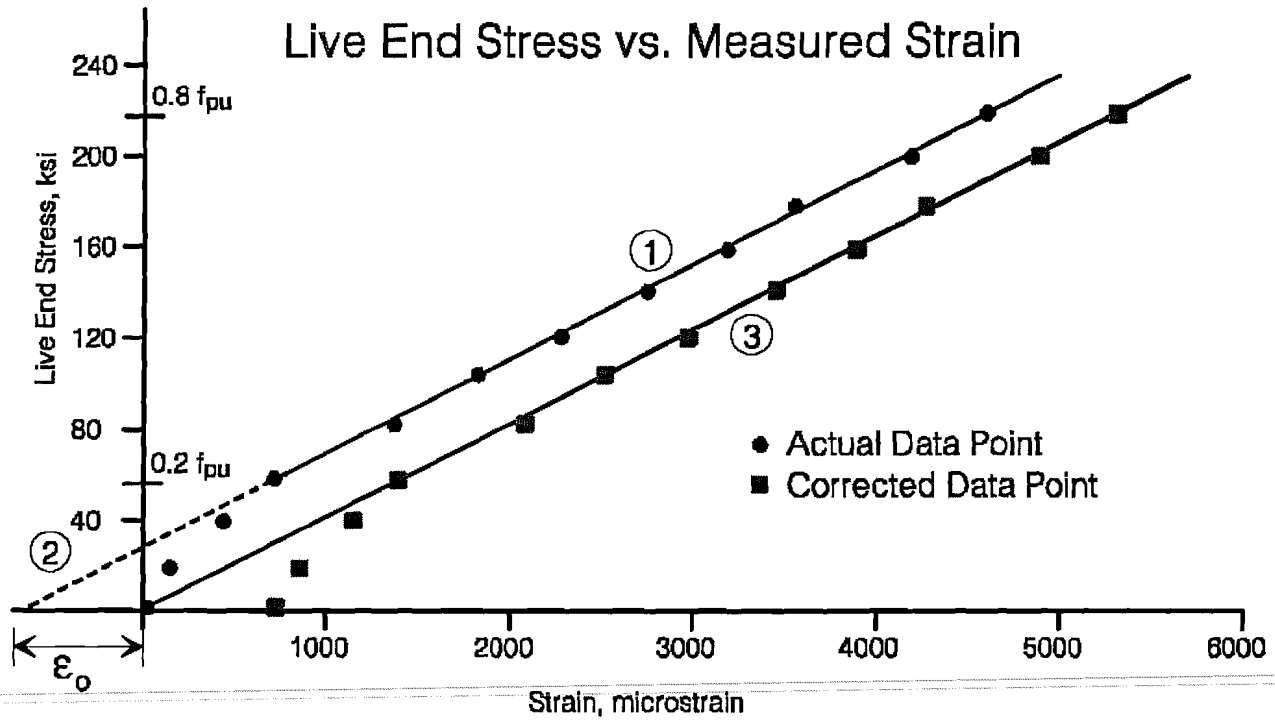


expected field complication is that the strands of each multi-strand tendon will probably behave erratically at low stress levels (mainly because of uneven strand anchorage and varying strand lengths).

Given these conditions, it was necessary to determine the best method for reducing the measured data. Several complicated procedures were investigated in the present project. The most accurate data-reduction method resulted in one of the simplest to understand. A description of this data-reduction procedure which was utilized for the present tendon tests and suggested for future investigations is included here and is shown schematically in Figure 2.21.

Average tendon stress values at the live ends were obtained by considering the nominal areas of  $0.153 \text{ inch}^2$  and  $0.215 \text{ inch}^2$  for each one of the  $\frac{1}{2}\text{"}\phi$  and the  $0.6\text{"}\phi$  strands respectively. Strain readings from each ER-gage and their corresponding live end stresses computed from the pressure transducer (or dial indicator) readings were plotted on the  $\sigma$ - $\epsilon$  graph in the upper part of Figure 2.21. For each ER-gage, a best fit line (shown as solid line 1) was computed considering the data points that corresponded to stresses between  $0.20f_{pu}$  and  $0.80f_{pu}$ . The intersection of this best-fit line when extended to its intersection with the  $\epsilon$ -axis (shown as dashed line 2) was also computed. This value (labeled " $\epsilon_o$ ") was considered to be the strain reading that corresponded to the zero stress level. Each measured value of strain was thus corrected by algebraically subtracting the computed initial strain value ( $\epsilon_o$ ) (resulting in the points shown along solid line 3). Stress values at the tendon locations away from the end were then obtained by multiplying each corrected strain value by the apparent modulus of elasticity (previously obtained in the prestressing strand calibration tests). The resulting stresses at the gaging station are shown in the lower plot in Figure 2.21. Stress losses between the live end and the gaging station produced in each loading step were estimated by comparing reduced stresses (of the intermediate ER-gages) with corresponding live end stresses (measured by the calibrated hydraulic jack). An estimate of the average tendon stress loss was calculated by averaging the intermediate loading step losses registered by each ER-gage (only comparing the intermediate stresses located between  $0.20f_{pu}$  and  $0.80f_{pu}$ ). However, a more accurate average of the stress loss from live end to each instrumented tendon cross-section was obtained by computing the ratio between the slope of the calculated best-fit line of each ER-gage with the slope obtained from the material tests of the prestressing strands (the apparent modulus of elasticity). When using more than a single ER-gage on an intermediate tendon cross-section, an even better estimate of the tendon stress loss was given by averaging the stress losses determined from the individual strain gages.

**c. Interpretation of Results from TEST 1T and TEST 2T.** Strain readings of each ER-gage of TEST 1T and TEST 2T were plotted against corresponding stress values computed from readings of a pressure transducer located at the live end. These plots are shown in Figures 2.22 and 2.23. The  $\sigma$ - $\epsilon$  curves of both plots are shifted away from the origin of coordinates because each prestressing strand was independently stressed to 20 ksi in TEST 1T and to 40 ksi in TEST 2T before the ER-gages were installed. The best-fit lines (along with their calculated slopes) defined by the high stress data points of the  $\sigma$ - $\epsilon$  graphs of each ER-gage are also included in the plots of Figures 2.22 and 2.23.



\* Stress at gaging station is equal to corrected strain times calibrated strand modulus of elasticity from companion material test

Figure 2.21 Schematic representation of data-reduction procedure.

**TEST 1T**  
**\* 7-0.5in. strands \***  
**Electrical Resistance Strain Gages**

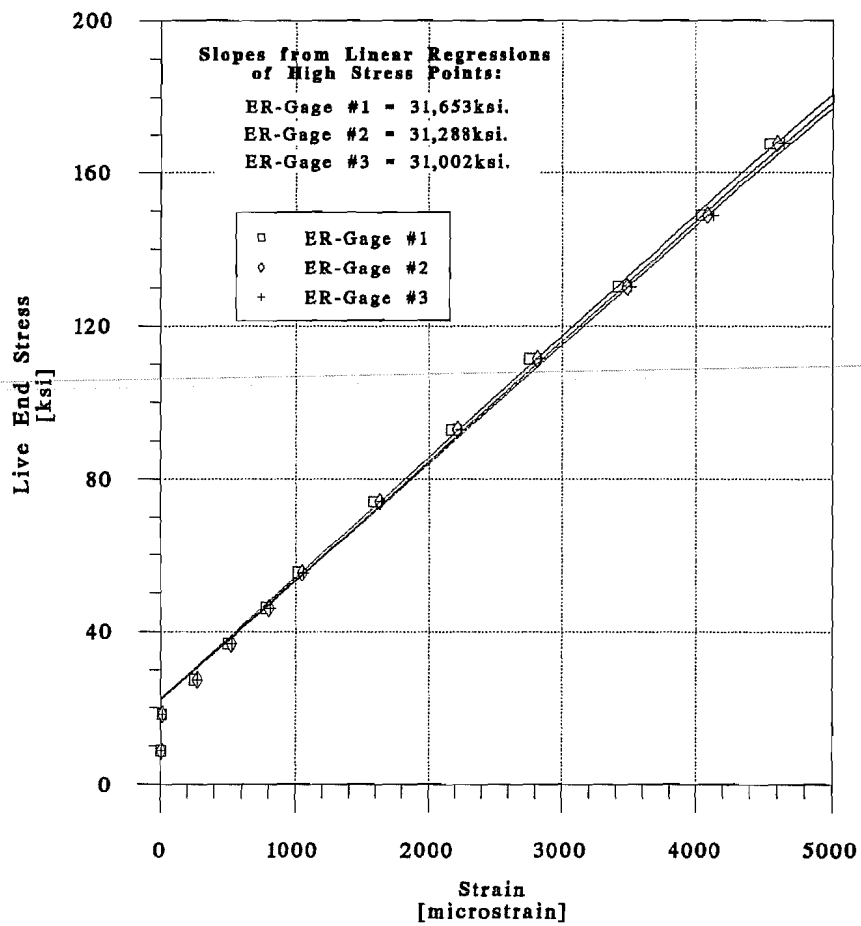


Figure 2.22 Stress-strain plots of individual ER-gages for TEST 1T.

**TEST 2T**  
**\* 12-0.5in. strands \***  
**Electrical Resistance Strain Gages**

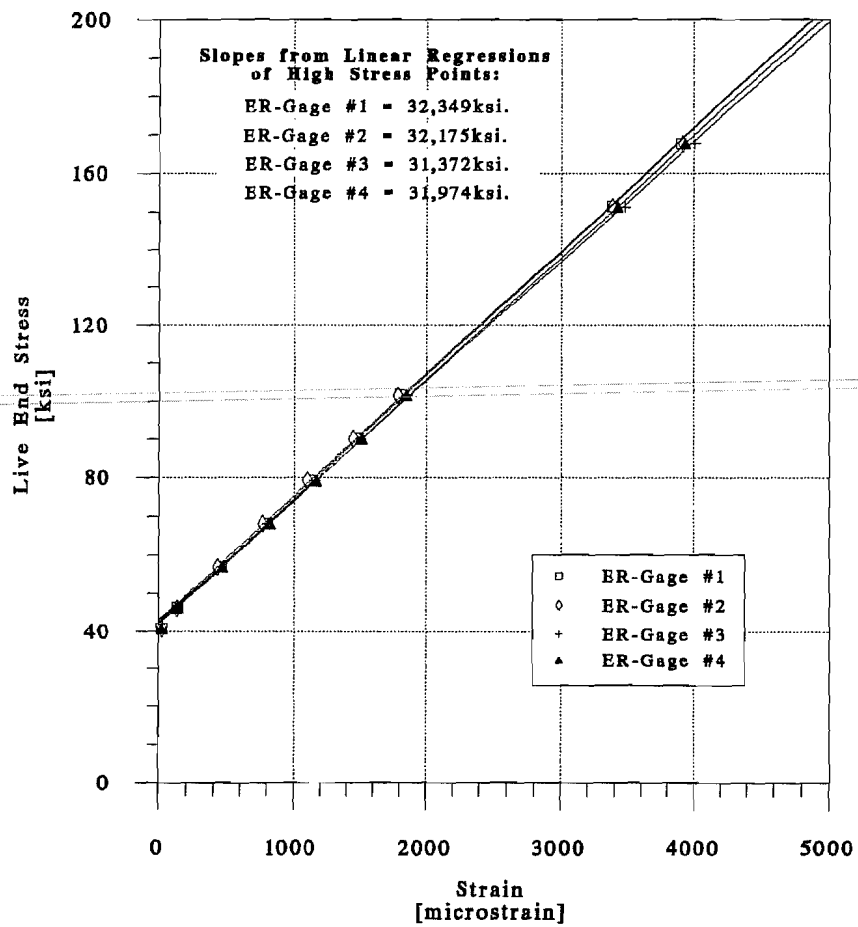


Figure 2.23 Stress-strain plots of individual ER-gages for TEST 2T.

Calibration tests of a specimen taken from the same prestressing strand roll used for tendon TESTs 1T and 2T were described as strand TESTs 2S and 3S in the previous section. The average apparent modulus of elasticity obtained from the calibration test specimens was found to be equal to 30,900 ksi. As explained in the data-reduction process, this apparent modulus was the one used for determining the average stress losses occurring from the live end to the instrumented cross-section of each tendon.

Figures 2.22 and 2.23 show the very similar strain levels at a given live end stress for the instrumented strands of each tendon test. The combined statistical analysis of the results from these first two tendon tests are shown in Figure 2.24. Interestingly, the variability of the combined average slope of all seven statistical observations from TESTs 1T and 2T was  $\pm 1.57\%$  (as defined by the percentage of the ratio between the combined standard deviation and the average of all slope observations). This is a better level of variability than the  $\pm 1.91\%$  previously obtained in the single strand tests.

**d. Conclusions from TEST 1T and TEST 2T.** The following conclusions can be drawn from the electrical resistance strain gages installed in the first two tendon tests (composed of  $\frac{1}{2}$ " $\phi$  prestressing strands):

- a. In most cases, the measured data of a field instrumentation program with multi-strand tendons is comprised of live end stresses and corresponding strains of individual prestressing strands located at intermediate tendon cross-sections. An appropriate data-reduction method must be followed to obtain valuable information from the measured data. A data-reduction method was suggested and successfully employed in multi-strand tendon tests.
- b. The average stress losses occurring between instrumented tendon cross-sections was measured with a  $\pm 1.57\%$  accuracy when electrical resistance strain gages were only installed on 25% of the  $\frac{1}{2}$ " $\phi$  strands of a tendon. However, this occurred when: (a) the suggested data-reduction method and accompanying calibration tests were performed, and (b) the strands were individually pretensioned to a similar stress level.
- c. Absolute stress losses of 2.61% ( $\pm 1.61\%$ ) were found to occur due to internal friction of the stressing equipment used in the first two tendon tests. Although difficult to determine with great accuracy, these stress losses seem to be present in most stressing equipment and are recommended to be more carefully investigated in future projects.

**e. Interpretation of Results from TEST 3T and TEST 4T.** As mentioned earlier, three loading cycles from zero stress to  $0.85f_{pu}$  were performed in tendon TESTs 3T and 4T. The ER strain gages used were installed without an initial tendon stress. The method of threading

**A. Summary of results from tests on tendons composed of 1/2" diameter strands:**

		Slope of Best-Fit Line *		Statistics of ER-Gages (from both TESTS):
		[ksi]		
		TEST 1T	TEST 2T	
ER-Gage #1		31653	32349	
ER-Gage #2		31288	32175	
ER-Gage #3		31002	31372	
ER-Gage #4		(-)	31974	
Statistics of ER-Gages (per TEST):	Min.:	31002	31372	31002
	Max.:	31653	32349	32349
	St. Dev.:	326	426	498
	Avg.:	31314	31968	31688
Variability of Avg.**:		±1.04%	±1.33%	±1.57%

**B. Summary of stress losses from tests on tendons composed of 1/2" diameter strands:**

		Stress loss from live end ***		Statistics of ER-Gages (from both TESTS):
		[%]		
		TEST 1T	TEST 2T	
ER-Gage #1		2.50%	4.75%	
ER-Gage #2		1.32%	4.19%	
ER-Gage #3		0.39%	1.59%	
ER-Gage #4		(-)	3.54%	
Statistics of ER-Gages (per TEST):	Min. Loss:	0.39%	1.59%	0.39%
	Max. Loss:	2.50%	4.75%	4.75%
	St. Dev.:	1.06%	1.38%	1.61%
	Avg. Loss:	1.40%	3.52%	2.61%

**Notes:**

- \* The best-fit line of each ER-gage was computed only considering the measured data points that corresponded to stresses located between 0.20fpu and 0.80fpu. No other manipulation of raw data was performed.
- \*\* The values corresponding to the variability of each average slope were considered to be equal to the percentage of the ratios between the standard deviation of each set of slope observations and their corresponding average slope.
- \*\*\* Losses were obtained by the ratio between the modulus of elasticity given on "A" and the "apparent" modulus determined from the material tests of strand specimens taken from the same prestressing strand roll used for these tendons ( $E_{app}=30,881\text{ksi}$ ).

Figure 2.24 Statistical analysis of electrical resistance strain gage results from tendon TESTs 1T and 2T with 1/2"  $\phi$  strands.

the tendons closely simulated the actual field operations to be followed in the San Antonio Y project. The strains measured from the workable ER-gages were plotted against live end stress values computed from readings of pressure gage

The final average results from both tendon tests with 0.6"  $\phi$  strands are shown in a single graph (shown in Figure 2.25). Finally, a detailed statistical analysis from the results of both tendon tests is included in Figure 2.26.

No material calibration tests were performed on specimens taken from the same prestressing strand roll used in TEST 3T and TEST 4T. Instead, the results obtained from material tests performed on a different 0.6"  $\phi$  strand specimen (taken from a different strand roll) were used as background information for these last two tendon tests. The average apparent modulus of elasticity was found to be equal to 29,488 ksi. This apparent modulus of elasticity was used for the determination of the average stress losses that occurred from the live end to the instrumented cross-section of each tendon. The test results are still helpful for reaching important conclusions about the overall ER-gage performance, differences in the behavior of each instrumented strand, and performance of the backup tendon strain measuring system (the *epoxy sleeve* system described in Section 2.2.2).

The data showed that each instrumented strand from the same test behaved similarly and this agreement seems to be related principally to the use of the epoxy sleeve system. As mentioned earlier, this novel tendon strain measuring system has the added benefit of producing a certain form of "clamping" action among all the prestressing strands of the instrumented tendon especially at lower stress levels below about 100 ksi.

The comparisons of average tendon behavior for each loading cycle of each test indicated approximately equal average slopes of the best-fit lines. The combined statistical analysis of the results from both tendon tests (shown in Figure 2.26) indicated a  $\pm 2.61\%$  variability of the average of the slopes obtained from all best-fit lines. This seems to be an acceptable instrumentation behavior for predicting the average stresses of a tendon composed of 19 prestressing strands.

**f. Conclusions from TEST 3T and TEST 4T.** The following conclusions can be drawn from the electrical resistance strain gages installed in the final tendon tests (composed of 19-0.6"  $\phi$  prestressing strands):

- a. The backup instrumentation system for measuring average tendon strains (the epoxy sleeve system) was found to improve the consistency of comparable ER-gage results by exerting a certain degree of "clamping" to all the prestressing strands of the tendon. This was particularly true for strands located in the outer periphery of the tendon and for stresses up to about 110 ksi. However, it was also apparent that occasional strands disengaged from the epoxy "clamps" at lower stresses.

**Comparison of Results from  
Tendon Tests of 0.6in. Strands**

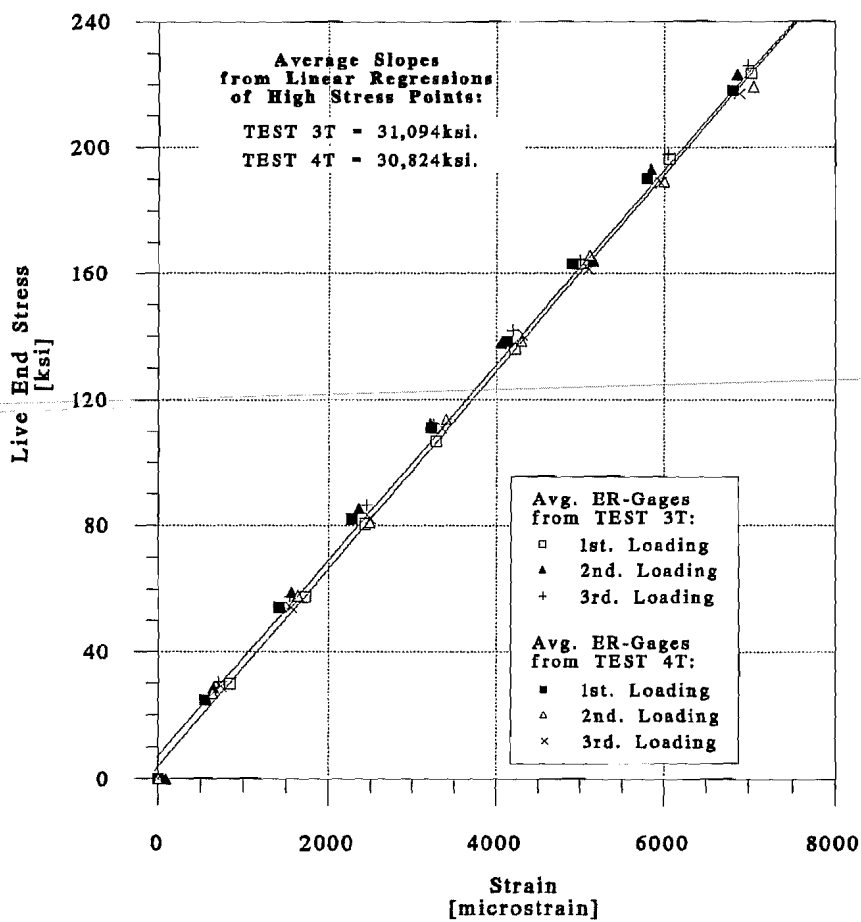


Figure 2.25 Comparison of average stress-strain plots of the ER-gages of TESTs 3T and 4T.



**A. Summary of results from tests on tendons composed of 0.6" diameter strands:**

		Slope of Best-Fit Line [ksi.]						Statistics of ER-Gages (from both TESTS):
		TEST 3T			TEST 4T			
		1st. Loading	2nd. Loading	3rd. Loading	1st. Loading	2nd. Loading	3rd. Loading	
ER-Gage #1		30568	30009	29625	30171	30097	30463	
ER-Gage #2		(-)	(-)	(-)	31492	31056	30827	
ER-Gage #3		32498	31733	32133	31118	31092	31100	
Statistics of ER-Gages (per TEST):	Min.:		29625			30097		29625
	Max.:		32498			31492		32498
	St. Dev.:		1189			477		809
	Avg.:		31094			30824		30932
	Variability of Avg.:		±3.82%			±1.55%		±2.61%

**B. Summary of stress losses from tests on tendons composed of 0.6" diameter strands:**

		Stress loss from live end (using $E_{app}=29,488$ ksi.) [%]						Statistics of ER-Gages (from both TESTS):
		TEST 3T			TEST 4T			
		1st. Loading	2nd. Loading	3rd. Loading	1st. Loading	2nd. Loading	3rd. Loading	
ER-Gage #1		3.66%	1.77%	0.46%	2.32%	2.07%	3.31%	
ER-Gage #2		(-)	(-)	(-)	6.80%	5.32%	4.54%	
ER-Gage #3		10.21%	7.61%	8.97%	5.53%	5.44%	5.47%	
Statistics of ER-Gages (per TEST):	Min. Loss:		0.46%			2.07%		0.46%
	Max. Loss:		10.21%			6.80%		10.21%
	St. Dev.:		4.03%			1.62%		2.74%
	Avg. Loss:		5.45%			4.53%		4.90%

Figure 2.26 Statistical analysis of ER-gage results from tendon TESTs 3T and 4T on 19-0.6" diameter strands.

- b. The average stress losses occurring between instrumented tendon cross-sections were measured with a  $\pm 2.74\%$  accuracy when electrical resistance strain gages were only installed to 16% of the  $0.6''\phi$  strands of a tendon. However, this occurred when: (a) the suggested data reduction method was performed, and (b) all the electrical resistance strain gages were bonded between the epoxy sleeves. The accuracy was further improved to  $\pm 2.0\%$  by performing a data reduction considering only the data points located between  $0.20f_{pu}$  and  $0.50f_{pu}$ .

**2.2.2 Epoxy Sleeves.** A mechanical backup system envisioned as an alternative method for measuring strand strains, and ultimately tendon loads at intermediate cross-sections was highly desirable. Since no available system satisfied the backup requirements of the present instrumentation project, the epoxy sleeves were investigated as a new device for measuring loads in multi-strand tendons.

Tests were first performed using single strands so as to easily address the effectiveness of the system. After an analysis of the initial problems, slightly modified epoxy sleeve systems were investigated in further strand tests. For the San Antonio Y instrumentation project, these single-strand tests with epoxy sleeves were only performed as part of the material tests of prestressing strands. The final recommendations for these tests are therefore included with the recommended Material Tests in Chapter 8.

Larger epoxy sleeve systems were tested with the electrical resistance strain gages in the previously described multi-strand tendon tests. These tests also provide a check of the behavior of the new instrumentation system under large loads and stress differentials among strands. As explained previously, the first two tests were performed with tendons composed of 7 and  $12\frac{1}{2}''\phi$  low relaxation strands loaded to about  $0.80f_{pu}$ . After these initial tests, a final modified epoxy sleeve system was tested in the tendon tests of 19- $0.6''\phi$  low relaxation prestressing strands loaded to  $0.85f_{pu}$ . An analysis of the results related to the epoxy sleeve system used in multi-strand tendons is included in Section 2.2.2.3. The final epoxy sleeve system is also described in Section 2.3 and 2.4 as applied in the field tests of the San Antonio Y structures.

**2.2.2.1 Single-Strand Tests.** The envisioned operation of the epoxy sleeve system was based on the measurement of the elongations of a completely clamped section of a prestressing strand. The "clamping" of each wire of a prestressing strand was envisaged to be performed by high strength epoxy collars precast on two locations of the strand specimens. The gage length of the epoxy sleeve system was given by the center-to-center distance of the precast epoxy collars. Initial single-strand tests were performed to check the overall system behavior and to determine the required diameter and gage length of the epoxy collars. The last three single-strand tests were performed with the final version of the epoxy sleeve system. These last three tests (TESTs 1ES, 2ES and 3ES) are reported here.

**a. Test Descriptions.** TESTs 1ES and 2ES were performed on  $\frac{1}{2}''\phi$  7-wire low relaxation prestressing strand specimens taken from the same prestressing strand roll. The two

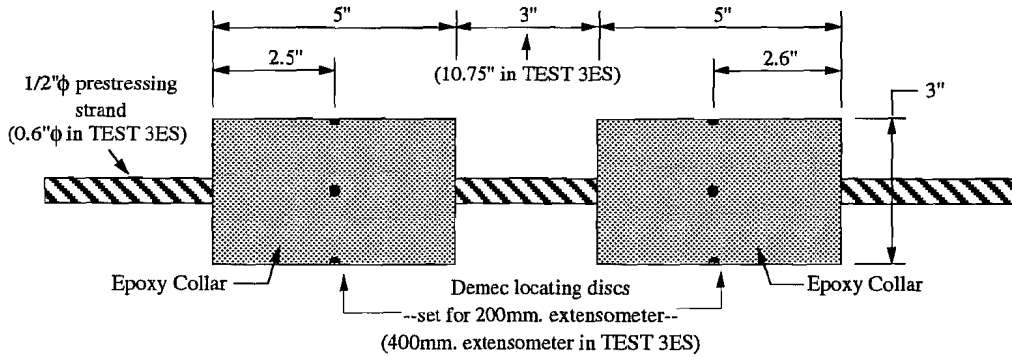
loading cycles of the single specimen (TESTs 3ESa and 3ESb) were performed on a 0.6"  $\phi$  7-wire low relaxation prestressing strand specimen.

Descriptions of the precast operations and dimensions of the epoxy sleeve systems used in these tests are shown in Figure 2.27. The only difference between the two epoxy sleeve systems described in Figure 2.27 is that a 200 mm Demec extensometer was used in TESTs 1ES and 2ES, and a 400 mm extensometer was used on both loadings of TEST 3ES.

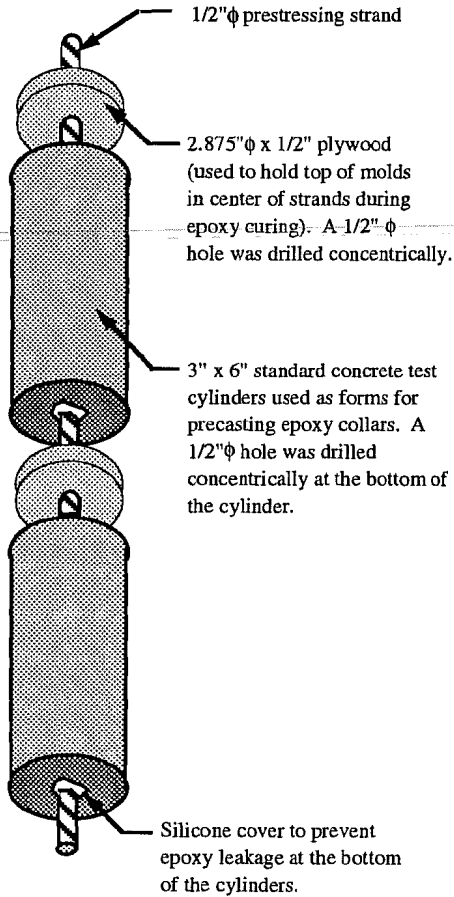
Several types of two-part epoxy products were compared in the single-strand tests. Two products with good performance were: Industrial Coating A-103 and Sikadur 32 Hi-Mod. Both of these epoxies comply with the requirements for a Type V Epoxy according to the Material Specifications of the Texas State Department of Highways and Public Transportation (TSDHPT).<sup>49</sup> Most of the epoxy products used for these tests were donated by the Material Testing Laboratories of TSDHPT. A smaller amount of epoxy was also donated by the Testing Laboratory of Sika, Inc. from New Jersey. The epoxy sleeves of TEST 1ES were made with A-103 epoxy mixed with sand, and those of TEST 2ES and 3ES were made with Sikadur 32 Hi-Mod epoxy.

Testing was performed using a vertical loading machine, and the strand specimens were anchored with standard 3-wedge single-strand anchorages. Strain readings from the epoxy sleeve system of TESTs 1ES and 2ES were taken with a 200 mm Demec extensometer which had a resolution of  $8\mu\epsilon$ . Loads for TEST 1ES were registered from the scale readings of a 60 kip vertical loading machine. In TEST 2ES, loads were computed from strain readings of an electrical resistance load cell. The strain readings from the epoxy sleeve system of TEST 3ES were taken with a 400 mm Demec extensometer of  $4\mu\epsilon$  resolution. Load levels on both cycles of this final single-strand test were also computed from strain readings of an electrical resistance load cell.

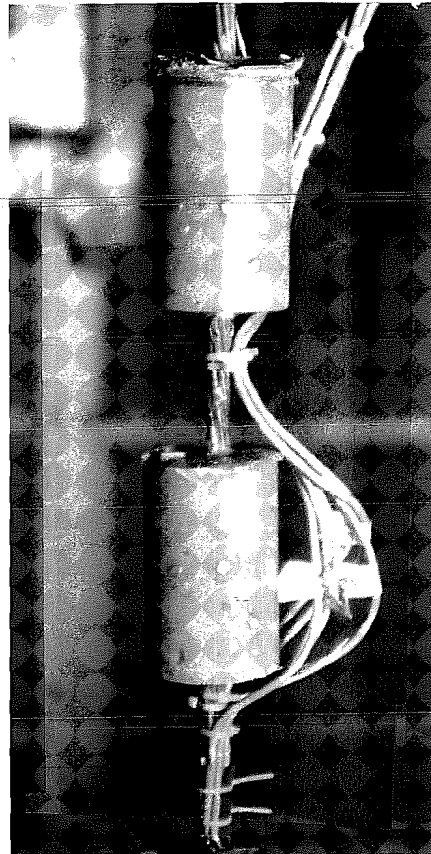
**b. Data-Reduction Method.** A similar method to that described previously in Section 2.2.1.2 was used for the data reduction of the measured epoxy sleeve strains. This method is explained here for the particular case of epoxy sleeve readings. Stress values in each strand were obtained by considering the nominal areas of 0.153 inch<sup>2</sup> and 0.215 inch<sup>2</sup> for the  $\frac{1}{2}$ "  $\phi$  and the 0.6"  $\phi$  strands respectively. Since no stress losses can be reasonably expected to occur between the instrumented section of the strand and the section where loads were measured, the corresponding values of stress and strain were plotted on a single  $\sigma$ - $\epsilon$  graph. A best-fit line was defined considering the data points of the  $\sigma$ - $\epsilon$  graph that approximately corresponded to stresses between  $0.20f_{pu}$  and  $0.80f_{pu}$ . This procedure thus avoided the consideration of initial nonlinearities in the graph (usually occurring during seating of the strand specimen at the anchor ends). As shown in Figure 2.27, one to four pairs of demec locating discs were installed in diametrically opposed locations around the epoxy collars. At each loading step, up to four different strain readings were thus obtained in each epoxy sleeve system according to the location of the Demec reference discs. The slopes of the best-fit lines corresponding to each epoxy sleeve reading location were recorded. The prestressing strand's apparent modulus of elasticity was determined by the average of these slopes.



**a. Final schematic of the single strand epoxy sleeve system used in TESTS 1ES and 2ES.**



**b. Precasting operations of TESTS 1ES and 2ES.**



**c. Close-up of specimen of TEST 1ES.**

**Figure 2.27 Schematic of the epoxy sleeve system used in single-strand tests.**

Prestressing strand manufacturers usually perform their modulus of elasticity tests using a similar method (but with longer gage lengths) as the epoxy sleeve system. It was therefore expected to find much closer values between the apparent modulus of elasticity determined from the epoxy sleeve system and that given by the strand manufacturer.

**c. Interpretation of Results.** A plot showing the averages of the epoxy sleeve readings of each single-strand test is shown in Figure 2.28. Statistics of the results from the tests performed with the  $\frac{1}{2}$ " $\phi$  strand specimens (TESTs 1ES and 2ES) are included in Figure 2.29. Similarly, the statistics of the results from the tests performed with the 0.6" $\phi$  specimen (both loading cycles of TEST 3ES) are included in Figure 2.30. In each one of the tests with the  $\frac{1}{2}$ " $\phi$  strand specimens (TESTs 1ES and 2ES), the apparent modulus of elasticity determined by each epoxy sleeve reading was smaller than the apparent modulus determined by the average of the ER-gages. Although significantly reduced, a similar trend of differences was found with the 0.6" $\phi$  strand specimen. It is thus evident that the type of instrumentation system used in the single-strand tests plays an important role in the determination of the apparent modulus of elasticity. The average apparent modulus determined by the epoxy sleeve readings of TEST 1ES ( $E_{app}=27,571$  ksi) was found to be 5.3% lower than the manufacturer modulus that was provided with the prestressing strand roll ( $E=29,100$  ksi). This difference was unexpectedly high and was presumably related to the use of a lower-strength epoxy mix in the epoxy collars used for this particular test. The quality of the Industrial Coating A-103 two-part epoxy was considerably altered by the mixing of sand. The lower-strength epoxy collars suffered several small tension cracks that may have caused the measurement of larger strains at each loading step.

Sand mixes were avoided in the following single-strand tests. A strand specimen taken from the same roll as the specimen used in TEST 1ES was tested with a stronger epoxy mix in TEST 2ES. The average modulus of the epoxy sleeve readings of this second test ( $E_{app}=29,504$  ksi) was in better agreement with the manufacturer-provided modulus ( $E=29,100$  ksi).

No accurate conclusions can be drawn from the apparent modulus determined by the average of the epoxy sleeve readings from both loadings of the 0.6" $\phi$  strand. This is because no manufacturer modulus of elasticity was obtained with the prestressing strand roll from which this specimen was taken. However, the results of TESTs 3ESa and 3ESb were quite similar, as indicated by the low 334 ksi standard deviation of the eight different statistical observations (shown in Figure 2.30). The general average of the apparent modulus of these two tests was 29,261 ksi. This average is just 227 ksi smaller than the apparent modulus determined by the average of the ER-gages (29,488 ksi, shown previously in Figure 2.18).

**d. Conclusions.** The following conclusions can be drawn from the epoxy sleeve systems installed in single prestressing strands:

- a. Low-strength epoxy mixes (especially those with sand in the mix) were found to provide unreliable performance.

**Summary of Average Results of the  
Epoxy Sleeves  
in Single Strand Tests**

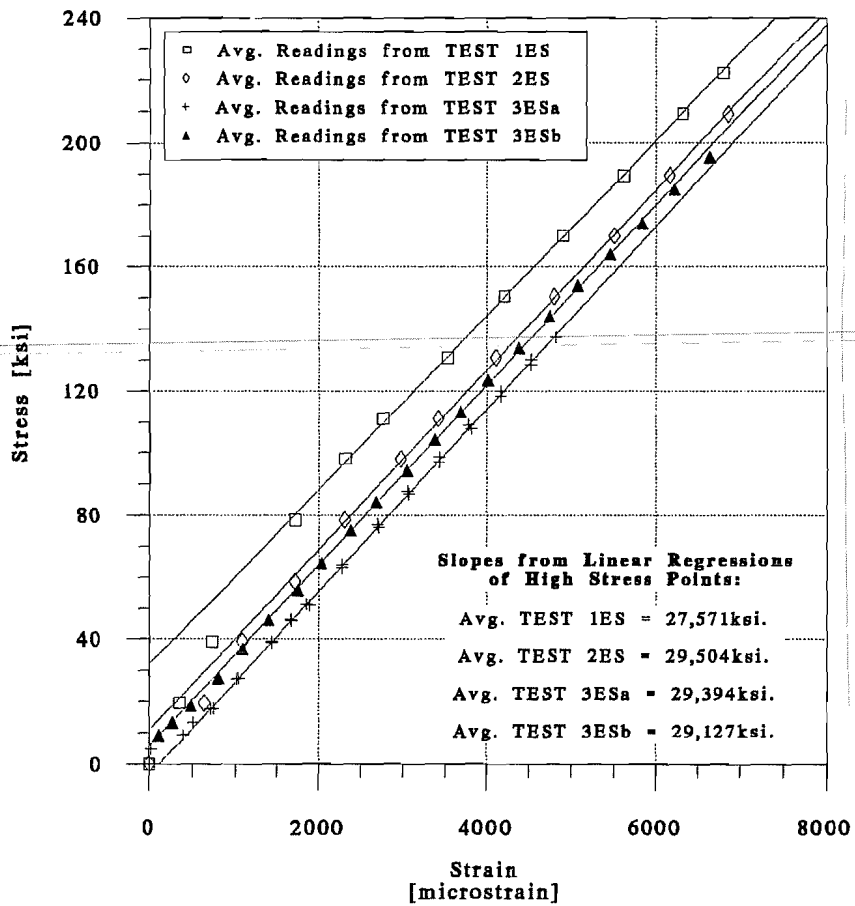


Figure 2.28 Summary of stress-strain average plots of single-strand tests with epoxy sleeves.

**Summary of results from tests of specimens from strand roll "B" (1/2" diameter):**

		Computed Modulus of Elasticity *	
		[ksi]	
		TEST 1ES	TEST 2ES
Epoxy Sleeve @Location A-1		28088	28956
Epoxy Sleeve @Location A-2		27053	30052
Final Statistics (from both TESTS):	Min.:	27053	
	Max.:	30052	
	St. Dev.:	1275	
	Avg.:	28537	
	Variability of Avg.**:	±4.47%	

Figure 2.29 Statistical analysis of epoxy sleeve results from tests on 1/2"  $\phi$  strand specimens from roll "B".

**Summary of results from tests of specimen from strand roll "C" (0.6" diameter):**

		Computed Modulus of Elasticity *		Final Statistics (from both TESTS):
		[ksi]		
		TEST 3ESa	TEST 3ESb	
Epoxy Sleeve @Location A-1		29258	29392	
Epoxy Sleeve @Location A-2		29383	28979	
Epoxy Sleeve @Location A-3		29157	28670	
Epoxy Sleeve @Location A-4		29778	29467	
Final Statistics (per TEST):	Min.:	29157	28670	28670
	Max.:	29778	29467	29778
	St. Dev.:	272	373	334
	Avg.:	29394	29127	29261
	Variability of Avg.**:	±0.93%	±1.28%	±1.14%

**Notes:**

\* To obtain each computed modulus of elasticity, a best-fit line was computed considering only the measured data points that corresponded to stresses between 0.20fpu and 0.80fpu. No other manipulation of raw data was performed.

\*\* The values corresponding to the variability of each given average were considered to be equal to the percentage of the ratios between the standard deviation of each set of slope observations and their corresponding average slope.

Figure 2.30 Statistical analysis of epoxy sleeve results from tests on the 0.6"  $\phi$  strand specimen from roll "C".

- b. The apparent modulus of elasticity determined from the epoxy sleeves was generally found similar to the manufacturer-given values. In some cases, the epoxy sleeve apparent modulus was also found close to the apparent modulus determined by the electrical resistance strain gages. However, on average the measured results indicated that the type of instrumentation system used makes a difference in the determination of the apparent modulus of elasticity of the prestressing strand.
- c. The modulus of elasticity obtained from the data reduction of the readings from one location around a particular epoxy sleeve was very similar to the results obtained from other reading locations around the same epoxy sleeve. A single epoxy sleeve reading location was found to provide results that were around  $\pm 1.14\%$  of the average apparent modulus of elasticity.
- d. Judging from the results and the repeatability of the epoxy sleeve readings in single-strand tests, it was concluded that the epoxy sleeves provided an accurate instrumentation system for determining the load level at intermediate cross-sections of individual prestressing strands.

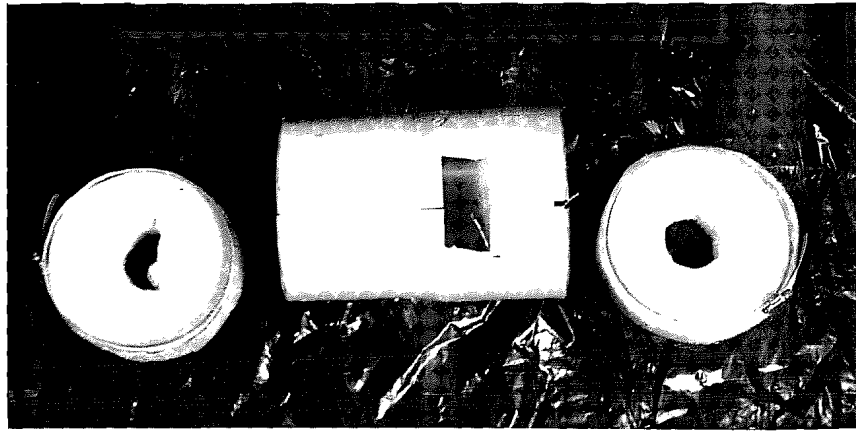
**2.2.2.2 Multi-Strand Tendon Tests.** As explained previously each strand of a multi-strand tendon can experience a different level of stress in most field applications. The epoxy sleeve system would then have to bond to each strand and adequately average their stresses for it to be successful in measuring tendon loads. Tests were performed on multi-strand tendons to check the performance of various sizes of epoxy sleeves. Initial tests were performed in 7- and 12-  $\frac{1}{2}$ " $\phi$  strands, and final tests were implemented on 19-0.6" $\phi$  strands.

**a. Test Descriptions.** A sample preparation process for one of the epoxy sleeve systems used in the multi-strand tendon tests is included in Figure 2.31. Recommendations about the precast process and the installation of the final epoxy sleeve system in multi-strand tendons are included in Section 2.3.

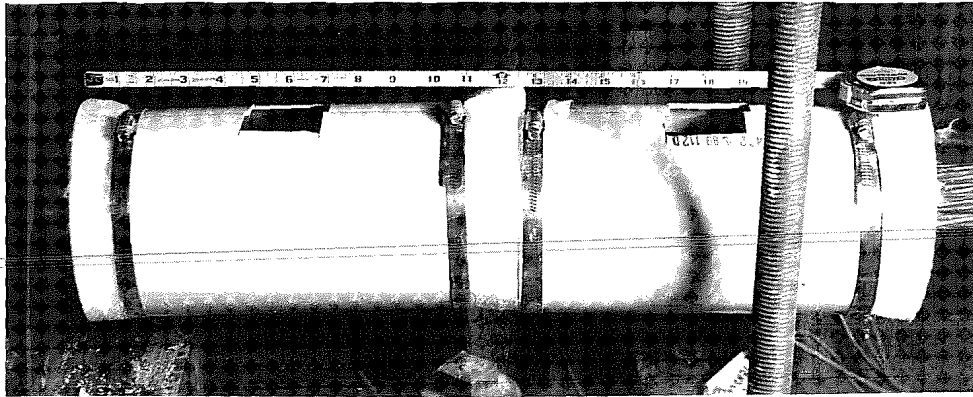
The first two tendon tests of the epoxy sleeve system were TEST 1T and TEST 2T reported previously in the section of electrical resistance strain gages. For organizational purposes these tests were split according to the two measurement systems investigated. A general sketch of the testing setup is shown in Figure 2.19. The epoxy sleeves used in both of these tests were made with Industrial Coating A-103 Epoxy donated by the Material Testing Laboratories of TSDHPT.

The last two tendon tests, TEST 3T and TEST 4T, were also the same as those mentioned previously in the section on electrical resistance strain gages. The corresponding test setup is shown in Figure 2.20. The epoxy resin used in TEST 3T consisted of Industrial Coating A-103 (Type V Epoxy Resin) also donated by the Materials Testing Laboratories of TSDHPT. The epoxy resin of TEST 4T was Sikadur 32 Hi-Mod. donated by Sika, Inc.

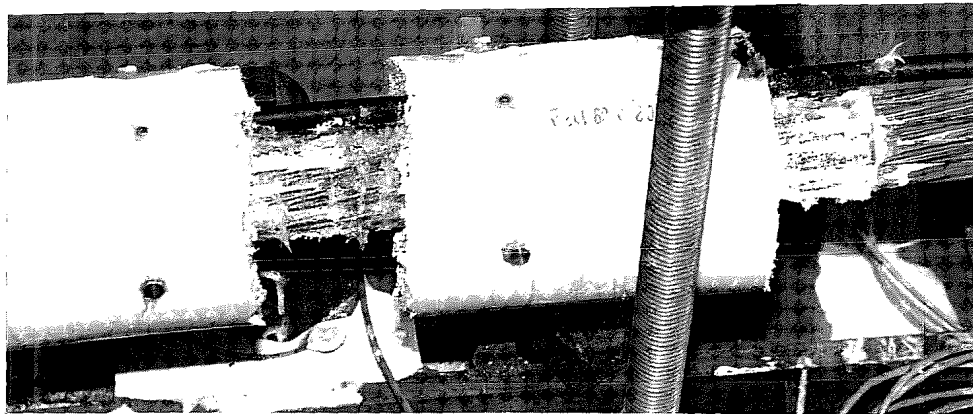




a. Molds for the epoxy sleeve.



b. Installed epoxy sleeve assembly.



c. Final gaged epoxy sleeve system.

Figure 2.31 Construction steps of the epoxy sleeve system used in TEST 2T: molds for the epoxy sleeve; installed epoxy sleeve assembly; and final gaged epoxy sleeve system.

The molds for the epoxy collars consisted of 6-inch o.d. standard PVC drainage pipes of 10-inch, 10-inch, 13-inch, and 13-inch lengths corresponding to the 7-, 12-  $\frac{1}{2}$ "  $\phi$ , and the two sets of 19-0.6"  $\phi$  strands respectively (TESTs 1T, 2T, 3T and 4T). Each mold had a single longitudinal splitting cut and two 2-inch x 1-inch rectangular cuts located approximately in the middle of the cylinder, on both sides of the longitudinal cuts.

A pair of plastic foam pieces of 2-inch thickness were cut in circular shapes of 6-inch o.d. The middle of these pieces were in turn cut into the approximate shape of the tensioned tendons, but at a reduced size. These were used as end covers of the PVC cylinders. The final locations of the foam molds in the tendon were then calculated and marked. These marks indicated the cross-sections where silicone was to be injected between and around the prestressing strands. This process was found to be critical and should be done very carefully. A large screwdriver was used as an aid for separating the strands to allow for the installation of silicone in the tight spaces at the center of the tendon. Once the silicone was placed between all the strands, the molds were installed in their marked locations. The ends of the PVC cylinders were in turn placed around the foam molds, making sure that the square holes of the cylinders were facing up. Large-diameter hose clamps were finally used to tighten the PVC cylinders to the foam molds.

The strong tightening pressure of the hose clamps against the foam molds and the strands spread the silicone to less accessible areas between the strands. The excess silicone outside the foam molds was spread evenly around the outer surfaces of the strands. A one-hour drying period was the minimum allowed for curing time of the silicone in the strands. After proper mixing of the epoxy resins, they were poured into the square holes on the top part of the PVC cylinders. Lack of careful spreading of the silicone between strands resulted in several leaks in the epoxy collars of TEST 2T (see Figure 2.32). However, it was found that small leaks usually stopped quickly due to the quick hardening of the epoxy resins (caused by the overheating effect created by large volumes of epoxy).

The epoxy sleeves were given an average eight-hour drying period at normal summer temperatures of  $\approx 80^{\circ}\text{F}$ . Once hardened, the PVC molds were separated from the epoxy collars in certain sections. Pairs of Demec locating points were installed directly on the epoxy collars and on the PVC molds to compare measurements. The lack of longer gage lengths of Demec extensometers limited the tendon tests to a combination of 100 mm and 200 mm gage lengths. The 400 mm Demec extensometer designed for the San Antonio Y field tests was received too late for use in these trials.

Tendon loading was performed up to  $0.80f_{pu}$  for the  $\frac{1}{2}$ "  $\phi$  strands, and up to  $0.85f_{pu}$  for the 0.6"  $\phi$  strands. The loading steps were mostly done in 10 kip increments for TEST 1T and 2T, and in 100 kip increments for TEST 3T and 4T. At the time of each mechanical measurement of the strains at each instrumented location of the epoxy sleeves of TESTs 1T and 2T, the corresponding live end load levels were automatically scanned by a computer-controlled data-acquisition system. Load levels were determined from readings of an electrical resistance pressure transducer installed in the pressure line of the hydraulic jack used for stressing the



Figure 2.32 Epoxy leaks in TEST 2T.

tendons. In TESTs 3T and 4T, loads were computed at the live ends from pressure readings of a calibrated hydraulic jack instrumented with a pair of dial indicators.

**b. Data-Reduction Method.** A similar method to that described previously was used for the data reduction of the measured epoxy sleeve strains. This method is explained here for the particular case of the epoxy sleeve readings.

As mentioned earlier, stressing loads of the instrumented spans of the San Antonio Y project were to be obtained with electrical resistance pressure transducers installed in the calibrated hydraulic jacks. These pressure transducers were to be scanned at regular time intervals and were to be related to the mechanical strain readings of the epoxy sleeves located at selected intermediate cross-sections of the external tendons (the stressing load was to be maintained for about 20 minutes on each reading operation). The information available to the researcher will therefore consist of live end loads and corresponding cross-section strains of instrumented tendons. The stress loss from the live end to each intermediate tendon cross-section is unknown but will be estimated using live end loads and cross-section strains. Another expected field complication is that the strands of each multi-strand tendon will probably behave erratically at low stress levels (mainly because of uneven strand anchorage and varying strand lengths).

The data reduction process suggested in this report was based on the same field conditions and available information expected for the San Antonio Y instrumentation project. Average tendon stress values at the live ends were obtained by considering the nominal areas of  $0.153 \text{ inch}^2$  and  $0.215 \text{ inch}^2$  for each one of the  $\frac{1}{2}''\phi$  and the  $0.6''\phi$  strands respectively. Strains from each reading location of each epoxy sleeve and their corresponding live end stresses computed from the pressure transducer (or dial indicator) readings were plotted on a  $\sigma$ - $\epsilon$  graph.

For each reading location of each epoxy sleeve, a best-fit line was computed considering the data points that corresponded to stresses located between  $0.20f_{pu}$  and  $0.80f_{pu}$ . The intersection of this best-fit line with the  $\epsilon$ -axis was also computed. This value (labeled " $\epsilon_0$ ") was considered to be the strain reading that corresponded to the zero stress level. Each measured value of strain was thus corrected by algebraically subtracting the computed initial strain value ( $\epsilon_0$ ). Stress levels were then obtained by multiplying each corrected strain value by the apparent modulus of elasticity (previously obtained in the prestressing strand material tests). Stress losses produced in each loading step were estimated by comparing reduced stresses (of the intermediate epoxy sleeve system) with corresponding live end stresses (measured by the calibrated hydraulic jack). An estimate of the average tendon stress loss was calculated by the average of the intermediate loading step losses registered at each reading location of each epoxy sleeve (only comparing the intermediate stresses located between  $0.20f_{pu}$  and  $0.80f_{pu}$ ). However, a more accurate average of the stress loss from live end to each instrumented tendon cross-section was obtained by computing the ratio between the slope of the calculated best-fit line of each epoxy sleeve reading location with the slope obtained from the material tests of the prestressing strands (the apparent modulus of elasticity). When using more than a single reading location on each epoxy sleeve, an even better estimate of the tendon stress loss was given by averaging the stress losses determined from the individual reading locations.

The strain reading corresponding to the zero stress value ( $\epsilon_0$ ) of each epoxy sleeve system is particularly difficult to determine without a regression analysis of the measured data. A proper data-reduction process is thus very important for the case of strain readings from epoxy sleeve systems.

**c. Interpretation of Results from TEST 1T and TEST 2T.** Strains from each the epoxy sleeves were plotted against corresponding live end stress values as shown in Figures 2.33 and 2.34. The  $\sigma$ - $\epsilon$  curves of both plots are shifted away from the origin because each prestressing strand was independently stressed to 20 ksi in TEST 1T, and to 40 ksi in TEST 2T before the ER-gages were installed. The best-fit lines (along with their calculated slopes) defined by the data points for stresses above  $0.2 f_{pu}$  are also included. A detailed statistical analysis is included in Figure 2.35.

The average apparent modulus of elasticity obtained from the material test specimens was found to be equal to 28,537 ksi. This apparent modulus was used for determining the average stress losses occurring from the live end to the instrumented cross-section of each tendon.

In TEST 2T although strains were similar at each loading step, the  $\sigma$ - $\epsilon$  curves were highly non-linear. This was caused by tension cracks that appeared around the epoxy sleeves of TEST 2T. This second test was performed on a tendon composed of a larger number of strands than the first tendon ( $12\text{-}\frac{1}{2}$ "  $\phi$  strands instead of the  $7\text{-}\frac{1}{2}$ "  $\phi$  strands used in TEST 1T). The length of each epoxy collar of TEST 2T (about 7 inches) and the type of epoxy resin employed (Industrial Coating A-103) were exactly the same as for TEST 1T. The results of

**TEST 1T**  
 \* 7-0.5in. strands \*  
 Epoxy Sleeve

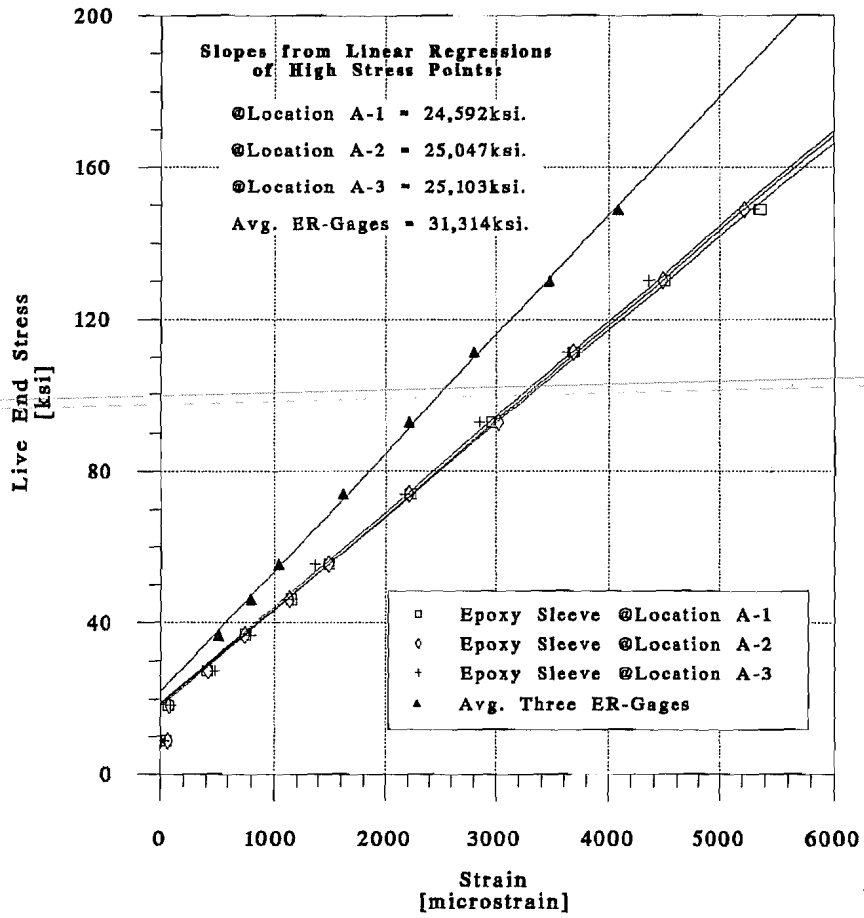


Figure 2.33 Stress-strain plots of individual epoxy sleeve reading locations for TEST 1T.

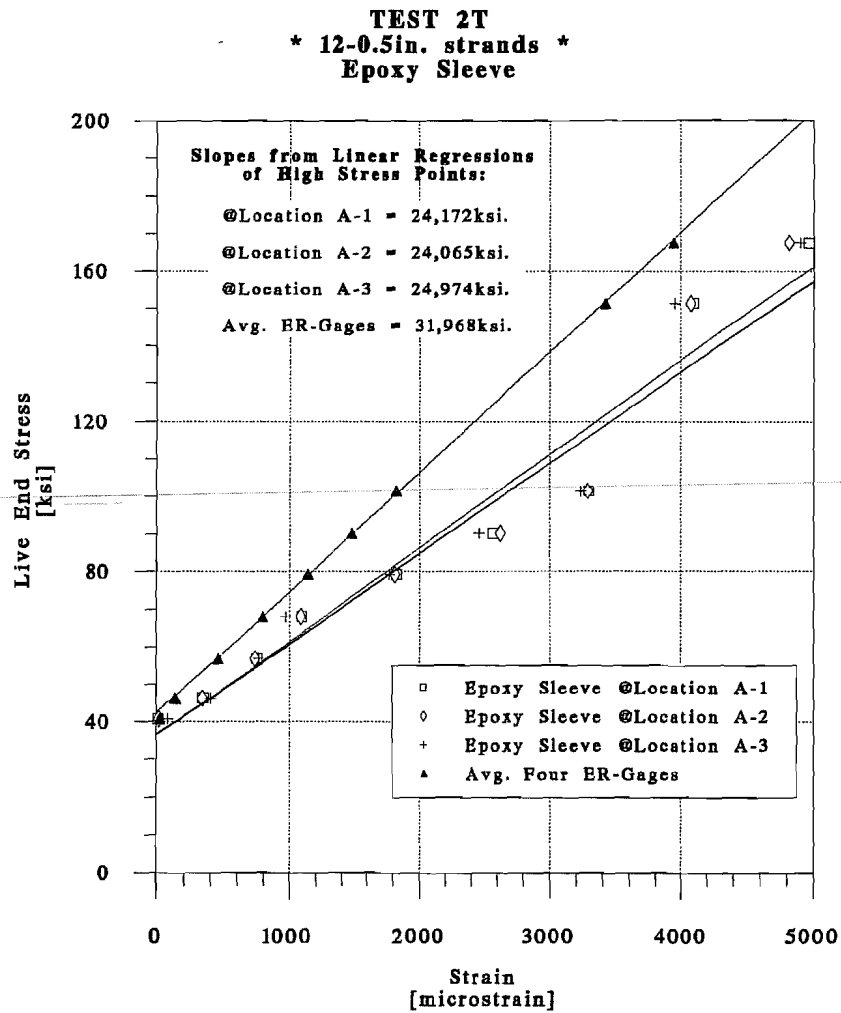


Figure 2.34 Stress-strain plots of individual epoxy sleeve reading locations for TEST 2T.

**A. Summary of results from tests on tendons composed of ½" diameter strands:**

		Slope of Best-Fit Line *		Statistics of Epoxy Sleeves (from both TESTS):
		[ksi]		
		TEST 1T	TEST 2T	
Epoxy Sleeve @ Location A-1		24592	24172	
Epoxy Sleeve @ Location A-2		25047	24065	
Epoxy Sleeve @ Location A-3		25103	24974	
Statistics of Epoxy Sleeves (per TEST):	Min.:	24592	24065	24065
	Max.:	25103	24974	25103
	St. Dev.:	280	497	456
	Avg.:	24914	24404	24659
	Variability of Avg.**:	±1.12%	±2.04%	±1.85%

**B. Summary of stress losses from tests on tendons composed of ½" diameter strands:**

		Stress loss from live end ***		Statistics of Epoxy Sleeves (from both TESTS):
		[%]		
		TEST 1T	TEST 2T	
Epoxy Sleeve @ Location A-1		-20.37%	-21.73%	
Epoxy Sleeve @ Location A-2		-18.89%	-22.07%	
Epoxy Sleeve @ Location A-3		(-)	-19.13%	
Statistics of Epoxy Sleeves (per TEST):	Min. Loss:	-20.37%	-22.07%	-22.07%
	Max. Loss:	-18.89%	-19.13%	-18.89%
	St. Dev.:	1.04%	1.61%	1.45%
	Avg. Loss:	-19.63%	-20.98%	-20.44%

**Notes:**

- \* The best-fit line of each epoxy sleeve reading location was computed considering only the measured data points that corresponded to stresses located between 0.20fpu and 0.80fpu. No other manipulation of raw data was performed.
- \*\* The values corresponding to the variability of each average slope were considered to be equal to the percentage of the ratios between the standard deviation of each set of slope observations and their corresponding average slope.
- \*\*\* Losses were obtained by the ratio between the modulus of elasticity given on "A" and the "apparent" modulus determined from the material tests of strand specimens taken from the same prestressing strand roll used for these tendons ( $E_{app}=28,537\text{ksi.}$ ).

Figure 2.35 Statistical analysis of epoxy sleeve results from tendon TESTs 1T and 2T with 12"  $\phi$  strands.

these initial tests thus influenced certain modifications of the epoxy sleeve systems to be used in the future 19-0.6"  $\phi$  tendon tests: (a) the length of each epoxy collar should be increased to about 10 inches, and (b) a stronger epoxy resin (such as Sikadur 32 Hi-Mod) should be used.

An important characteristic of the behavior of the epoxy sleeves in TESTs 1T and 2T can be determined from the comparisons of the slopes of the best-fit lines of the epoxy sleeves and the corresponding best-fit lines of the ER-gages (Figures 2.33 and 2.34). The statistical analysis of the results from the epoxy sleeve readings (shown in Figure 2.35), it is indicated that the slopes of the best-fit lines indicate average stress increases of 20% from the live end to the intermediate section instrumented with the epoxy sleeves. This obviously could not have occurred. In the data reduction process, it was found later that the strain increases measured in the epoxy sleeves must have been directly related to: (a) the incorrect positioning of the Demec extensometers, and (b) the linear stress distribution occurring through the epoxy collars. The probable distribution of stresses in a typical epoxy collar is shown in Figure 2.36. The epoxy sleeve strains of TEST 1T and 2T were not measured from the center-to-center distance between the two epoxy collars but rather from about their nearest quarter points (as shown in Figure 2.37a). The internal strains between these points and the center points were thus not measured in these tests and caused an "apparent" increase in stress. The system shown in Figure 2.37b was used in the following tendon tests (since the 400 mm Demec extensometer was not yet available for testing). For the actual San Antonio Y field measurements, the system shown in Figure 2.37c was used with the 400 mm Demec extensometers.

**d. Conclusions from TEST 1T and TEST 2T.** The following conclusions can be drawn from the epoxy sleeves used in the first two tendon tests (composed of  $\frac{1}{2}$ "  $\phi$  prestressing strands):

- a. Strains were found to be very similar in different locations around the epoxy sleeves. According to results from TEST 1T, the measurement of strains in a single location of the epoxy sleeve will more likely give results that are within  $\pm 1.12\%$  of the average strains.
- b. The strength and the length of the epoxy used for the collars is critical for applications in tendons with a large number of strands. It was found that an epoxy collar length of 7 inches was too small for 12- $\frac{1}{2}$ "  $\phi$  strands. From the test results, a 10-inch length was suggested as the minimum for the epoxy collars of tendons composed of 19-0.6"  $\phi$  strands. It was also found important to carefully measure the right mixing amounts of each epoxy product.
- c. Absolute measurements from the epoxy sleeves of both initial tendon tests showed inconsistent strains when compared to the ER-gage measurements. A theoretical stress distribution in each epoxy collar was considered. This



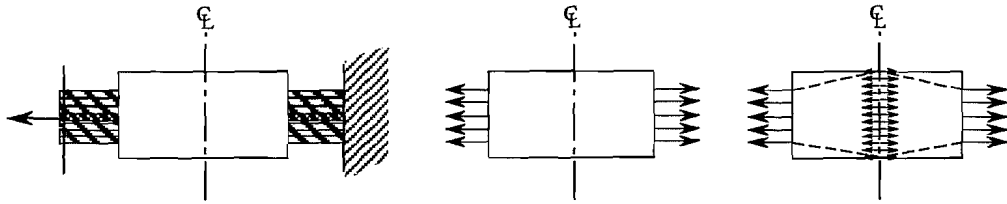
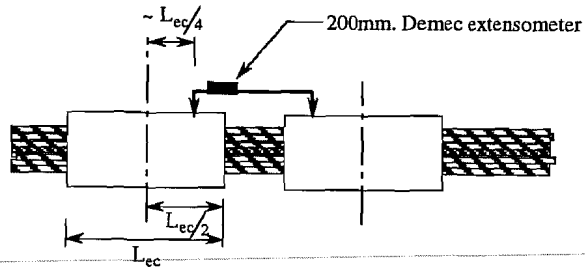
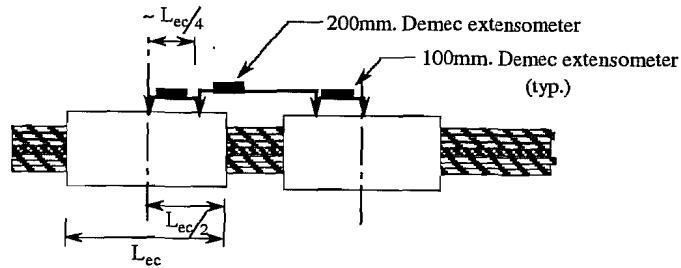


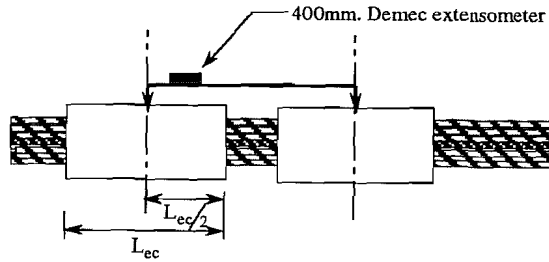
Figure 2.36 Possible stress distributions in a typical epoxy collar.



a. System used in TESTS 1T and 2T



b. System used in TESTS 3T and 4T



c. System planned for the San Antonio Y project

Figure 2.37 Epoxy sleeve measuring systems.

distribution suggested that future epoxy sleeve strains should be measured with a gage length equal to the center-to-center distance between each pair of epoxy collars.

**e. Interpretation of Results from TEST 3T and TEST 4T.** Three loading cycles from zero stress to  $0.85f_{pu}$  were performed in tendon TESTs 3T and 4T. In each one of these two tendon tests, the strains measured from two epoxy sleeve reading locations were plotted against corresponding stress values computed from readings of a pressure gage located at the live end. Since the strains were found previously to be similar at different locations around each epoxy sleeve, readings from only two locations were taken in the first loading cycles of TESTs 3T and 4T. The  $\sigma$ - $\epsilon$  plots corresponding to each epoxy sleeve reading location and to each loading cycle of TESTs 3T and 4T are shown in Figures 2.38 and 2.39 respectively.

The epoxy sleeves used on these two tests were installed without an initial tendon stress. The plots of Figures 2.38 and 2.39 show irregular strain variations corresponding to the initial stress increases. Also included are the corresponding average ER-gage results obtained for each test. Calculated values for the slopes of each one of the best-fit lines (for "high stress" data points) are also shown in the same figures. Finally, a detailed statistical analysis of the results from both tendon tests with  $0.6''\phi$  strands is included in Figure 2.40.

The method of threading of the tendons and installing the instrumentation devices during the present tests were performed with a close simulation of the actual field operations to be followed in the instrumented spans of the San Antonio Y project. As suggested by the first two tendon tests, the proper length of epoxy collars (of  $\approx 10$  inches) and Demec extensometers were used in the final tendon tests. Instead of the 400 mm Demec extensometers, a proper gage length was achieved by using a combination of 200 mm and 100 mm Demec extensometers.

**f. Conclusions from TEST 3T and TEST 4T.** The following conclusions can be drawn from the epoxy sleeves installed in the final tendon tests (composed of 19- $0.6''\phi$  prestressing strands):

- a. The data-reduction process for epoxy sleeve readings of large multi-strand tendons was found to perform best when limited to consideration of the data points that approximately increased linearly in the  $\sigma$ - $\epsilon$  graphs. In most cases, linear behavior of the epoxy sleeve readings started around 50 ksi. However, in some special cases linearity did not occur until 80 ksi.
- b. A very small variability of results was found among the epoxy sleeve readings. Eight statistical observations only produced a standard deviation corresponding to a  $\pm 1.52\%$  variation of the average slope of the best-fit line in the  $\sigma$ - $\epsilon$  graph. This resulted in better instrumentation behavior than for the ER-gages.

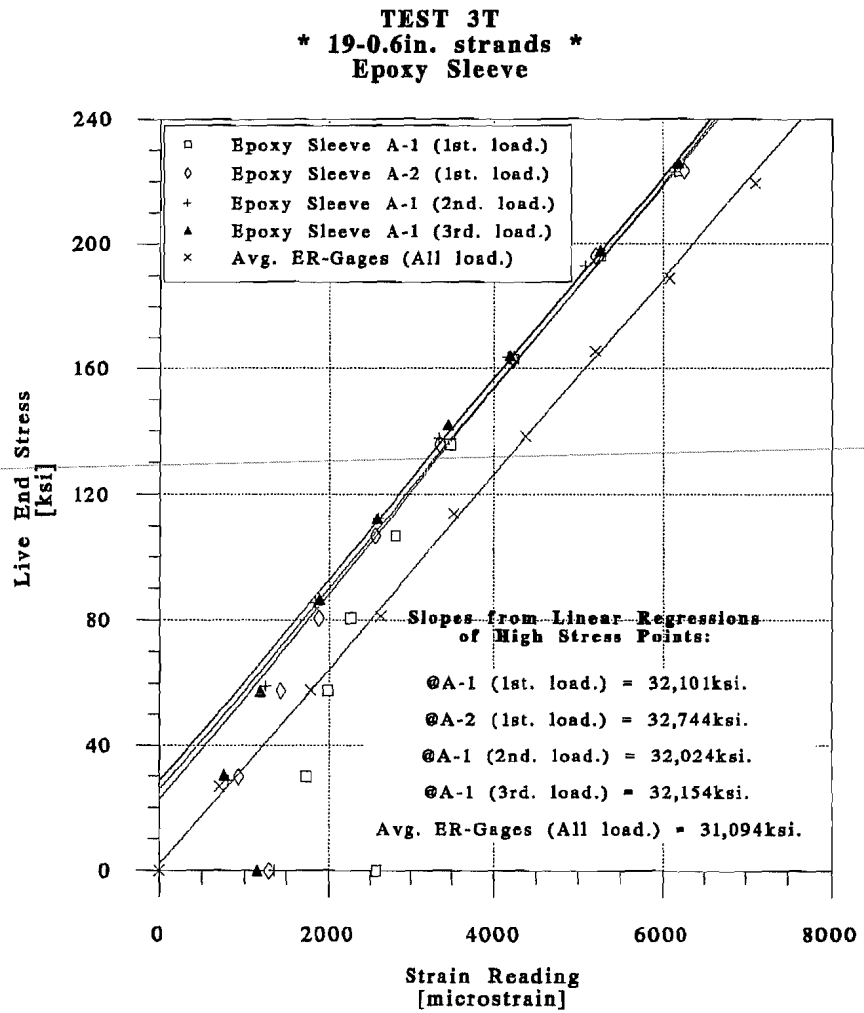


Figure 2.38 Stress-Strain plots of individual epoxy sleeve reading locations for TEST 3T.

**TEST 4T**  
**\* 19-0.6in. strands \***  
**Epoxy Sleeve**

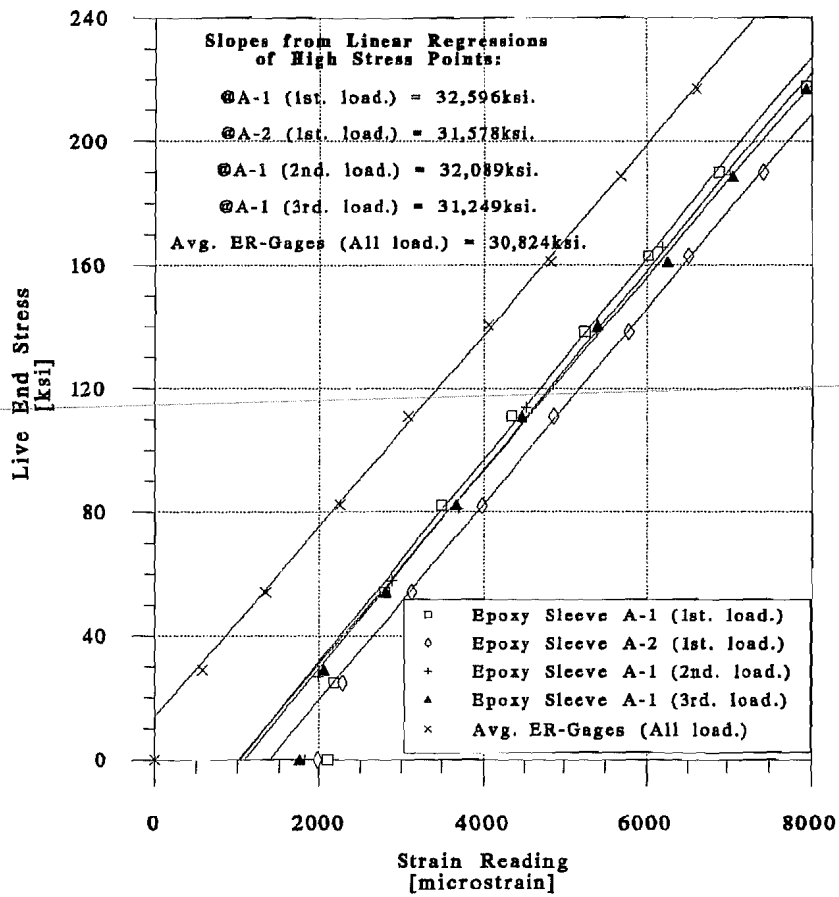


Figure 2.39 Stress-strain plots of individual epoxy sleeve reading locations for TEST 4T.

**A. Summary of results from tests on tendons composed of 0.6" diameter strands:**

		Slope of Best-Fit Line [ksl.]						Statistics of Epoxy Sleeves (from both TESTS):
		TEST 3T			TEST 4T			
		1st. Loading	2nd. Loading	3rd. Loading	1st. Loading	2nd. Loading	3rd. Loading	
Epoxy Sleeve @ Location A-1		32101	32024	32154	32596	32089	31249	
Epoxy Sleeve @ Location A-2		32744	(-)	(-)	31578	(-)	(-)	
Statistics of Epoxy Sleeves (per TEST):	Min.:		32024			31249		31249
	Max.:		32744			32596		32744
	St. Dev.:		330			590		487
	Avg.:		32256			31878		32067
	Variability of Avg.:		±1.02%			±1.85%		±1.52%

**B. Summary of stress losses from tests on tendons composed of 0.6" diameter strands:**

		Stress loss from live end (using $E_{app}=29,261\text{ksl.}$ ) [%]						Statistics of Epoxy Sleeves (from both TESTS):
		TEST 3T			TEST 4T			
		1st. Loading	2nd. Loading	3rd. Loading	1st. Loading	2nd. Loading	3rd. Loading	
Epoxy Sleeve @ Location A-1		9.71%	9.44%	9.89%	11.40%	9.66%	6.79%	
Epoxy Sleeve @ Location A-2		11.90%	(-)	(-)	7.92%	(-)	(-)	
Statistics of Epoxy Sleeves (per TEST):	Min. Loss:		9.44%			6.79%		6.79%
	Max. Loss:		11.90%			11.40%		11.90%
	St. Dev.:		1.13%			2.02%		1.66%
	Avg. Loss:		10.23%			8.94%		9.59%

Figure 2.40 Statistical analysis of epoxy sleeve results from tendon TESTS 3T and 4T on 19-0.6" diameter strands.

- c. The epoxy sleeve systems seemed to provide a better estimate of the average tendon stress than did the ER-gages. However, to reach a better conclusion further tests are recommended to be performed using multi-strand tendons instrumented with a larger number of ER-gages.

**2.2.2.3 Other Tests.** Two final development stage tests were performed on the epoxy sleeves system: one related to creep behavior, and the other one to check the performance of the epoxy sleeves during grouting of the external tendons.

**a. Creep Test.** After consultations with epoxy manufacturers, particularly with technical engineers from Sika,<sup>48</sup> they recommended that a check of the stability of the epoxy sleeve strain readings be performed. This was suggested since epoxy materials are known to strain plastically under stress. A single creep test was therefore performed on a  $\frac{1}{2}$ "  $\phi$  7-wire low-lax prestressing strand specimen, instrumented with 6 standard ER-gages and epoxy sleeves. The specimen was loaded to  $0.80f_{pu}$  and properly seated, with the load cell registering a residual load of  $0.70f_{pu}$  after seating. Nine readings of all ER-gages, epoxy sleeves, load cell, and ambient temperature were taken for a time period of 15 days after initial loading. A portable data-acquisition system with multi-channel switching devices was connected to the load cell and strain gages for the duration of the experiment. A 200 mm Demec extensometer with a resolution of  $8\mu\epsilon$  was used for the epoxy sleeve readings.

Results from this test are shown in Figure 2.41. Epoxy sleeve readings were corrected for temperature differentials between the linear expansion of prestressing steel ( $\alpha \approx 8.0 \times 10^{-6}/^{\circ}\text{F}$ ) and Invar steel ( $\alpha \approx 0.8 \times 10^{-6}/^{\circ}\text{F}$ ). The electrical resistance strain gages were of the temperature-compensated type (Measurements Group S-T-C type 06), thus no corrections for temperature were necessary for such small temperature variations.

The maximum error reading of  $36\mu\epsilon$  in the epoxy sleeves system marked on the first measurement day of Figure 2.41 corresponds to only 1.05 ksi in the prestressing strand. For a  $0.70f_{pu}$  stress level in the strand, the highest epoxy sleeve measurement error implies only a 0.55% variation of stress, which is acceptable for field measurements. However, it was found that the measured error level of the epoxy sleeves is highly dependent on the reading resolution of the Demec extensometers. With Demec gages of higher resolutions (either 400 mm or modified gages with high resolution digital indicators) the results from this test would have indicated smaller errors than with the standard 200 mm Demec extensometer.

As shown in Figure 2.41, the electrical resistance strain gages behaved well during the creep test. The largest measurement error of the ER-gages also occurred in the first measurement day and only corresponded to  $10\mu\epsilon$ . For practical matters, the ER-gages were not affected by creep of the gages and of the bonding agents during the short-term creep test.

**b. Grouting Test.** A secondary benefit of the epoxy sleeves system consists of their tight blocking of grout at intermediate sections of multi-strand tendons where electrical resistance

**TEST 1C**  
**Creep Induced Errors in**  
**Epoxy Sleeves System**

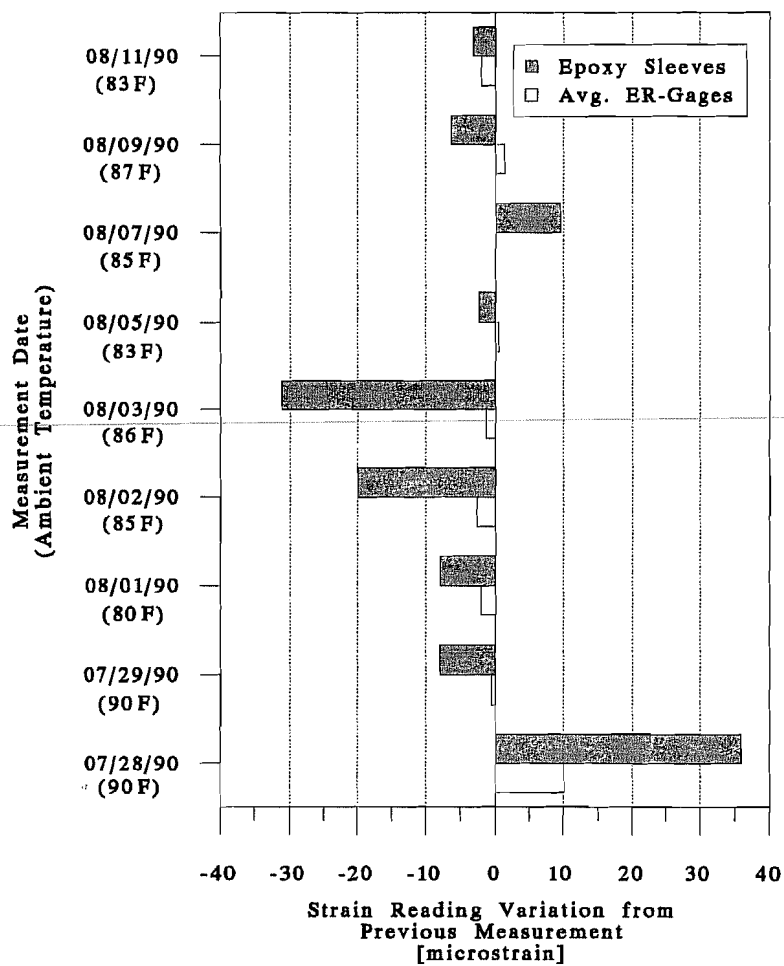


Figure 2.41 Short-term creep TEST 1C.

strain gages are to be applied. It has always been difficult to provide a good mechanism for blocking grout at such intermediate sections of external tendons. However, the epoxy sleeve system seemed ideal for this purpose. It was therefore necessary to design and test a grouting by-pass system that could be implemented in external tendons of segmental concrete bridges.

The final version of the epoxy sleeves have an outer diameter of approximately 6 inches. However, the external tendons of the San Antonio Y bridges are designed to be protected by 4-inch o.d. polyethylene ducts (PE ducts). A 6-inch to 4-inch o.d. rubber reducer used for standard drainage pipes was thus designed to be used with the epoxy sleeves to be placed in the San Antonio Y external tendons. These reducers are attached to the epoxy sleeves and PE ducts with hose clamps. A grouting test was performed to check how well the hose clamps of the reducers avoided any leakage during the high-pressure grouting operations of the tendons. The tests were performed on a 7-foot section of 12-  $\frac{1}{2}$ "  $\phi$  strands instrumented with a standard epoxy sleeve system. Pressure was checked with a special gage. Water was used instead of grout. It was found that the hose clamp connections and the reducers performed well up to  $\approx 40$  psi. At higher pressures, failure was actually induced by a modeling error in the test setup and not by a poor connection. Due to the test setup problem, it was assumed that the grouting by-pass system could have still worked well for a 50% increase in pressure. It was finally safely suggested that a  $\gg 50$  psi pressure should be the maximum allowed during the grouting operations of the instrumented tendons.

Further innovations of the grouting components of the epoxy sleeves produced the final system that is shown in Figure 2.42. For each epoxy collar, a 1"  $\phi$  hole was drilled on top of the PE duct, just before the 6-inch to 4-inch reducer. A standard 90° grouting attachment hose and valve system was then clamped on top of the drilled hole of the PE duct. This final setup is designed to allow normal grouting operations to be performed from any of the two grouting vents of each epoxy sleeve system. As mentioned earlier, the section of the tendons located between the epoxy sleeves will be later protected with a high-quality grease.

### 2.3 Recommendations for Use with the San Antonio Y Project

**2.3.1 Electrical Resistance Gages.** The most important consideration investigated for strain gage technology was the reliability of measurements for long-term testing applications. Several sources of literature about the electrical resistance strain gaging technology were reviewed. Short-term testing was performed to address problems with installation, moisture protection, and actual performance in single strands and multi-strand tendons. The late completion of the purchasing and assembling of the data-acquisition system prevented any long-term performance tests of the complete electrical resistance strain gaging system. In fact, the lack of long-term testing influenced the decision for accommodating a mechanical backup system for measuring multi-strand tendon loads.

Nevertheless, a detailed analysis of most of the factors related to long-term signal stability was made. This section presents a guideline for the proper ER-gage system selection



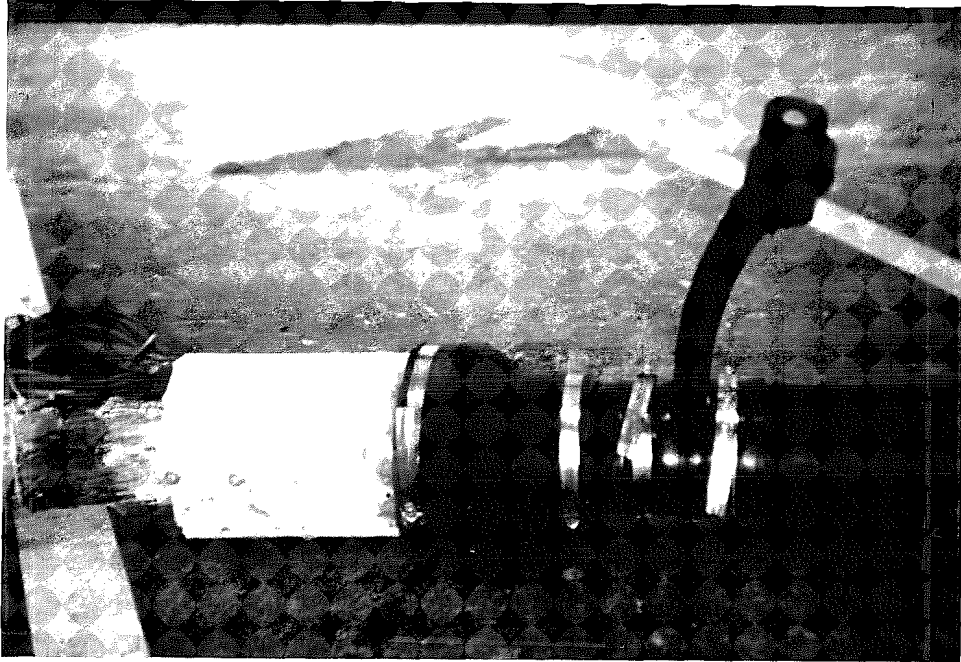


Figure 2.42 Grouting component of the epoxy sleeve system for multi-strand tendons.

and installation. Suggestions for a data reduction method are also mentioned. Electrical resistance strain gages were planned to be used in selected spans of the San Antonio Y project for the following objectives:

- long-term measurements of strains in steel tendons composed of 19- and 12- 0.6"  $\phi$  prestressing strands, and
- short-term measurements of strains in #3 to #7 steel reinforcing bars.

**2.3.1.1 System Selection.** It is important to select the most adequate gage, bonding agent, protection, wiring, and data-retrieval systems according to the particular type of test to be performed. Literature from gage manufacturers concerning these factors is strongly recommended for applications different from those reviewed in this project. Table 2.3 shows the final systems recommended for the San Antonio Y project, and a summary of important guidelines.

#### **2.3.1.2 Installation.**

1. **Epoxy Preparation.** The bottles of epoxy type AE-10/15 supplied by Micro Measurements come in volumes that produce large amounts of waste when installing a group of gages, especially if installation is done under hot Texas summer temperatures. This is because the adhesives completely harden in 10 to 20 minutes, therefore providing only short

Table 2.3 Suggested ER-Gage systems.

<b>I. GENERAL GUIDELINES</b>	
ER-Gages:	
Length	≥0.29in. (7.4mm)
Width	≤0.13in. (3.3mm)
Material	Constantan (A-alloy)
Bonding agents	cyanoacrilates (short-term tests), epoxy (long-term tests).
Resistance	350Ω
Leadwires	stranded, shielded, three-leadwire conductors.
Completion circuit	quarter-bridge Wheatstone.
Connectors	simple (short-term tests), gold-plated (long-term tests).
Data Acquisition System	Battery operated (for field tests), permanently switched (throughout testing), multi-channel scanners.
<b>II. FINAL SYSTEM</b>	
ER-Gage	EA-06-125BZ-350 (Micro Measurements).
Leadwires	8771 (Belden Wire).
Bonding Agent	M-Bond 200 (short-term tests), M-Bond AE10 (long-term tests).
Excitation level	4.5V

workable times. It is recommended to separate each bottle of AE-10/15 resin (bottle with larger volume) into four other smaller, clean glass containers. Proper mixing can then be accomplished with one-fourth the volume of the hardener component, at the 5 ml mark on the provided calibrated droppers.

2. **Surface Preparation.** This should be done according to technical suggestions from gage manufacturers.<sup>34</sup> A summary of the steps suggested for applications in prestressing wires follows:
  - 2.1 Surface degreasing with CSM-1 degreaser sprayed on a strand section of 3- to 4-inch length should be the first procedure.
  - 2.2 Initial sanding with 120-grid sanding paper.
  - 2.3 Final sanding with a smoother 400-grid silicon-carbide sanding paper.

- 2.4 Apply the cleaning solution (Conditioner A), avoiding drying on the finished surface. For drying purposes apply single strokes of clean cotton swabs.
- 2.5 Apply the surface conditioner (Neutralizer 5), also avoiding drying on the finished surface.

\* Gage installation should follow as soon as possible.

3. **Gage Installation.** More detailed procedures are usually included in each package of epoxy adhesives. A modified summary from technical literature follows.<sup>33</sup>

3.1 Remove the gage from the plastic envelope by carefully grasping the attached leadwires. Place the gage on a chemically clean surface with its top side up.

3.2 Bond a piece of cellophane tape to the top of the gage and carefully detach it from the clean surface by lifting it at a shallow angle, making sure the gage is glued to the tape.

3.3 Position the gage/tape assembly on the cleaned surface of the strands and tack down one end of the tape to the strand.

4. **Epoxy Mixing and Placing.** The instructions included with the adhesives<sup>33</sup> should be slightly modified to accommodate the approximate distribution of epoxy resin that was previously prepared. The following steps are now recommended:

4.1 Use calibrated droppers to insert 5 ml of the epoxy hardener in the center of the bottle of epoxy resin. Use the provided stirring rods to mix both solutions for a period of 3 to 5 minutes.

4.2 Lifting one end of the cellophane tape (at a shallow angle), coat the back of the gage and wire with a thin layer of mixed epoxy solution.

4.3 With a clean gauze sponge slowly make a single wiping to bring the tape/gage assembly back to the final gage position.

4.4 Lifting the end of the tape that corresponds to the pre-attached gage leadwires, position a small piece of Teflon tape to prevent a strong bond of the leadwires with the prestressing steel wire.

5. **Gage Clamping.** Use precast silicone pieces of the proper strand size to completely cover the installed gage (fabrication previously reviewed). Apply an approximate pressure of 5 to 20 psi with a standard hose clamp. The epoxy solution should achieve good curing in five hours at 75°F (for higher temperatures consult charts included in gage packages).
6. **Soldering and Gage Protection.** The following instructions are suggested for gage protection in aggressive environments:
  - 6.1 Cover each one of the three leadwires (usually red, white and black) with the M-Coat B Solvent (white-colored solution).
  - 6.2 Cut a piece of the FB rubber sealant (black-colored) and install next to the end of the gage, under the gage's leadwires. This is done to prevent shorting with the prestressing steel wires. The size of the piece of rubber sealant should be enough to cover the spaces up to the middle of the two adjacent wires to the wire being gaged. Make sure that the rubber sealant covers the grooves between prestressing wires.
  - 6.3 Twist two conductors of the leadwires together (usually the red and white conductors) and cut all three conductors to a length of about ¼ inch. Bend the conductor ends in 90° angles and place them tight against the previously-installed rubber sealant.
  - 6.4 With small tweezers wrap each one of the two leadwires coming from the gage to each conductor placed on the rubber sealant surface. Make sure that no shorting of wires and specimen occurs. Finally, solder both terminals.
  - 6.5 Cover the complete assembly strain gage/soldered terminals with a coating of epoxy type M-Coat J-1. Let the coat cure for a day at normal 75°F temperature, or for two hours at 150°F (when using a blow drier).
  - 6.6 Use a larger layer of rubber sealant to cover the hardened system. Cover the gage system with a final coating of wax (Microcrystalline Wax W-1, melted with a blow drier).
7. **Data Reduction.** The following procedures are suggested for the data-reduction process of each electrical resistance strain gage bonded to an individual prestressing strand located at an intermediate tendon cross-section:

- 7.1 Record the live end loads according to the readings obtained from pressure transducers installed in the calibrated hydraulic jacks used for initial stressing of the tendon. Compute the average tendon stresses at the live end by considering the nominal areas of the prestressing strands.
- 7.2 Simultaneously scan the ER-gage and the live end pressure transducer at load intervals of no more than  $0.08f_{pu}$  (about 20 ksi). Plot the strain readings from the ER-gage and the corresponding live end stresses computed from the pressure transducer on a  $s-\epsilon$  graph. In this graph, find the best-fit line through the data points corresponding to live end stresses between  $0.20f_{pu}$  and  $0.80f_{pu}$ . Find the intersection of the best-fit line with the strain axis (this is the strain reading that corresponds to the zero stress level). Subtract this zero strain reading algebraically from each one of the originally-measured strain readings. The corrected strain values multiplied by the apparent modulus of elasticity (determined in the previously-performed material tests with ER-gages) gives an approximate indication of the stress level of the intermediate tendon cross-section where the ER-gage is installed.
- 7.3 A good approximation of the stress loss that occurs between the live end and the instrumented tendon cross-section is given by the ratio between the slope of the best-fit line (computed above in 7.2) and the apparent modulus of elasticity (computed from the material tests with ER-gages).
- 7.4 To establish stress losses from one ER-gage instrumented section to another, follow a different data-reduction procedure. Compute the average difference between each strain reading pair corresponding to each stress load level from  $0.20f_{pu}$  to  $0.80f_{pu}$  during the initial loading of the tendon. To find the average stress loss multiply the final averaged strain difference by the apparent modulus of elasticity of the prestressing strand (determined from the material tests with ER-gages, following Section 5.7.2.2).
- 7.5 In long-term tests, the effects of steel relaxation with time should be estimated according to current AASHTO<sup>2</sup> formulas (see Section 3.2.2).

When using epoxy sleeves, install the ER-gages in between each pair of epoxy collars. The epoxy collars were found to produce a certain degree of clamping to the prestressing strands and thus help averaging the tendon stresses between the strands. In the data reduction process, instead of considering the data points located between  $0.20f_{pu}$  and  $0.80f_{pu}$ , only consider the

linear data points that were obtained before the strands slipped in the epoxy sleeves. In the reported tendon tests, the stress level when strand slippage usually occurred was  $\approx 110$  ksi.

**2.3.2 Epoxy Sleeves.** This is the mechanical system envisioned as a backup for measuring loads at intermediate sections of typical external tendons used in segmental box girder bridges. The system was selected due to the following benefits:

- it has a relatively low cost,
- it probably provides a better estimate of average tendon cross-section stresses (at intermediate tendon sections) than the ER-gages,
- it is a good method for blocking grout and protecting ER-gages, and
- it produces an averaging effect of the stresses on the strands located between the epoxy collars (which helps ER-gages in the sense that a few instrumented strands can still provide a good approximation of the average tendon stresses).

At the same time, it is equally important to mention some of the problems related to this new measurement system:

- long-term stability of the system was not tested properly with fully-modeled effects of creep, and temperature,
- epoxy fumes can become a problem for installation inside box girder bridges (especially when instrumenting several tendons), and
- tendon segments have to be grouted carefully at each intermediate location between epoxy sleeves.

**2.3.2.1 Installation.** A step-by-step procedure for precasting and preparing the epoxy sleeves on 19-0.6"  $\phi$  prestressing strands is described in this section. Final dimensions of the finished epoxy sleeves system are included in Figure 2.43. The following steps are recommended to be followed in the fabrication and installation of multi-strand epoxy sleeves:

1. Cut two 12-inch long pieces of 6-inch o.d. PVC drainage pipe to be used as cylinder molds for the epoxy collars. Standard 6-inch x 12-inch plastic cylinder molds for standard concrete compression tests also work well for this purpose (after cutting off the bottom of the mold).
2. Make a single longitudinal cut in the 12-inch axis of each PVC mold. Also make rectangular cuts of approximately 2 inches x 1 inch at the middle of the cylinders, and on each side of the longitudinal cuts.

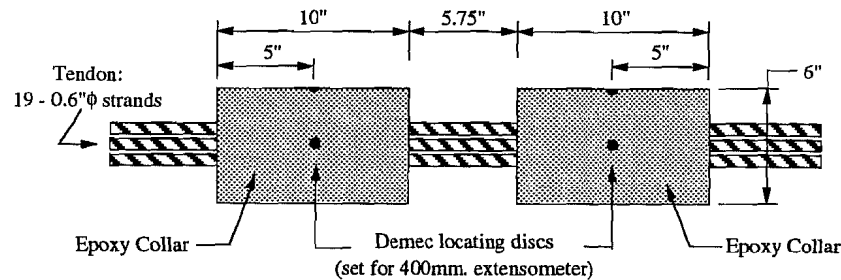


Figure 2.43 Schematic of the final epoxy sleeve system for multi-strand tendons.

3. End caps of the molds for the epoxy collars should be prepared from 2-inch thick foam panels. Two circles of 6-inch o.d. should be cut from the foam panels, and an approximate shape of the cross section of the tendons to be instrumented should be cut from the center of each one of these end covers.
4. A small initial load corresponding to  $0.05f_{pu}$  should be applied to the tendons before installing the epoxy sleeves. This is necessary to shape the tendons according to the approximate configuration that they will take in their final loading stage.
5. The first step in the installation process of the epoxy collars is to mark the approximate places where the foam caps will be located. This should be done carefully to obtain the final dimensions of epoxy sleeves shown in Figure 2.43. The strands located at the cross-sections corresponding to the location of the foam caps should be well covered with silicone.
6. Foam caps should be placed in their final marked positions around the strands. The PVC cylinders should be placed around each pair of end caps, covering about an inch of each cap. This is necessary to allow enough room for a 10-inch length between the inner faces of a pair of end caps.
7. A pair of hose clamps should be used for tightening the PVC molds against each foam cap and against the strands. This will further help spreading the silicone to the areas between strands that were not accessed during their initial installation. A final coating of silicone should be spread around the ends of each epoxy collar and strand. The silicone should be cured for no less than one hour before pouring the epoxy.

8. Epoxy should be poured in the top rectangular access holes of each collar. The large volume of epoxy contained in each collar induces a fast hardening process of the epoxy (due to self-heating effects produced by the high temperatures of large volumes of epoxy). However, the epoxy should be allowed to cure according to manufacturer-recommended periods.
9. After taking the PVC molds from the epoxy collars, the proper Demec locating discs should be installed as close as possible to the positions shown in Figure 2.43. The suggestions for assuring the long-term stability of Demec locating discs included in Chapter 5 of this report should be followed. Also, 400 mm Demec extensometers are recommended highly due to their higher reading resolution.

**2.3.2.2 Data Reduction Process.** A good recording of live end loads and corresponding epoxy sleeves strains is necessary for determining stress losses from the live end to the location of each pair of epoxy sleeves. The following procedures are suggested for the data-reduction process of each pair of epoxy sleeves installed at an intermediate tendon cross-section:

- a. Record the live end loads according to the readings obtained from pressure transducers installed in the calibrated hydraulic jacks used for initial stressing of the instrumented tendon. Compute the average tendon stresses at the live end by considering the nominal areas of the prestressing strands.
- b. Record the epoxy sleeve strain and the corresponding live end pressure transducer readings at load intervals of no more than  $0.08f_{pu}$  (about 20 ksi). Plot the strain readings from the epoxy sleeve and the corresponding live end stresses computed from the pressure transducer on a  $s-\epsilon$  graph. In this graph, find the best-fit line through the data points that show approximately linear increases of stress and strain (these points usually corresponded to stresses between  $0.20f_{pu}$  and  $0.80f_{pu}$ ). Find the intersection of the best-fit line with the strain axis (this is the strain reading that corresponds to the zero stress level). Algebraically subtract this zero strain reading from each one of the originally measured strain readings. The corrected strain values multiplied by the apparent modulus of elasticity (determined in the previously-performed material tests with epoxy sleeves) gives an approximate indication of the stress level of the intermediate tendon cross-section where the epoxy sleeve system was installed.
- c. A good average approximation of the stress loss that occurs between the live end and the instrumented tendon cross-section is given by the ratio between the slope of the best-fit line (computed above in "b") and the



apparent modulus of elasticity (computed in the material tests with epoxy sleeves).

- d. To establish stress losses from one epoxy sleeve instrumented section to another follow a different data-reduction procedure. Compute the average difference between each strain reading pair corresponding to each load level stress from  $0.20f_{pu}$  to  $0.80f_{pu}$  during the initial loading of the tendon. To find the average stress loss, multiply the final averaged strain difference by the apparent modulus of elasticity of the prestressing strand (determined from the material tests with epoxy sleeves).
- e. In long-term tests, the effects of steel relaxation with time should be estimated according to current AASHTO<sup>2</sup> formulas.

## 2.4 Field Installation

This section describes the actual process of installing the tendon strain measurement system at the San Antonio Y Project.

**2.4.1 Prefabrication.** Well ahead of the beginning of erection, many components of the system were prepared in the laboratory. These include:

1. *Forms for Epoxy Sleeves* - Plastic cylinder molds were used as side forms and styrofoam was used for the end forms. On spans A43 and A44 additional stay-in-place PVC side forms were prefabricated.
2. *Lead Wires for Electrical Resistance Gages* - Amphenol connectors were used to attach the lead wires to the data-acquisition systems. All lead wires were cut to length, labeled, and soldered to the connectors.
3. *Data-Acquisition System* - The three complete systems were assembled and tested in the laboratory before erection.

**2.4.2 Job Site Activities.** At the job site three days were required for the installation of all systems in a given span. The contractor proceeded as usual with erection until the tendons were threaded. At this point the external tendons were slightly stressed to take out the slack. After this, the contractor's crews vacated the span and the investigators were allowed three days to prepare for stressing. This section outlines the installation of the tendon measurement system during those three days.

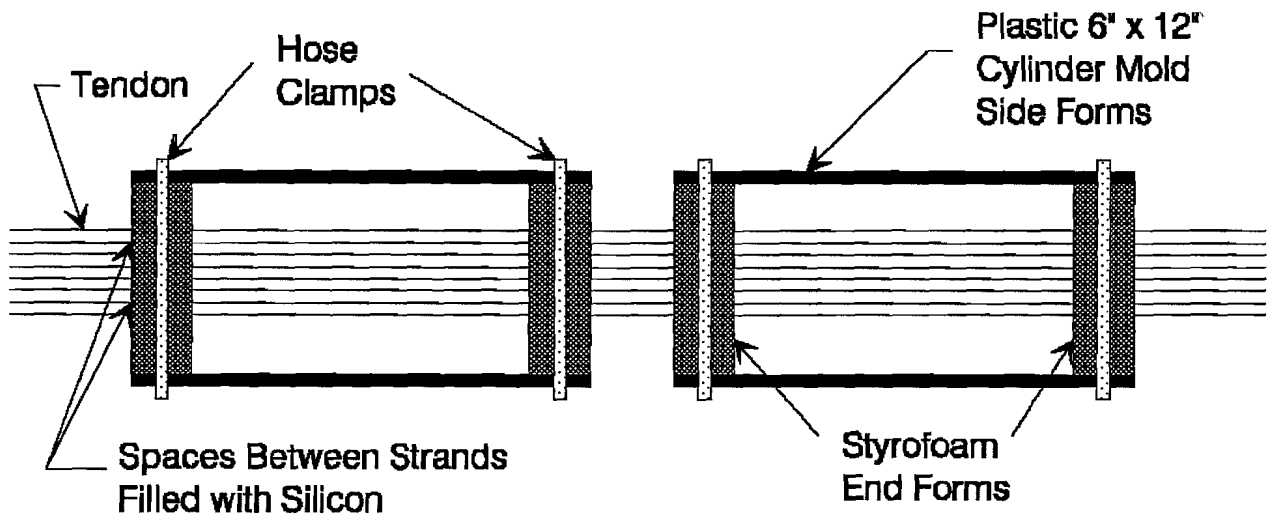
***Day Before:***

After the contractor had measured and installed the PE pipe for the external tendons, gaps were cut to allow for access to the tendons. All reducers and couplers required for the grout bypass system were installed at this time. While the tendons were threaded, investigators monitored the gaps to insure smooth threading operations.

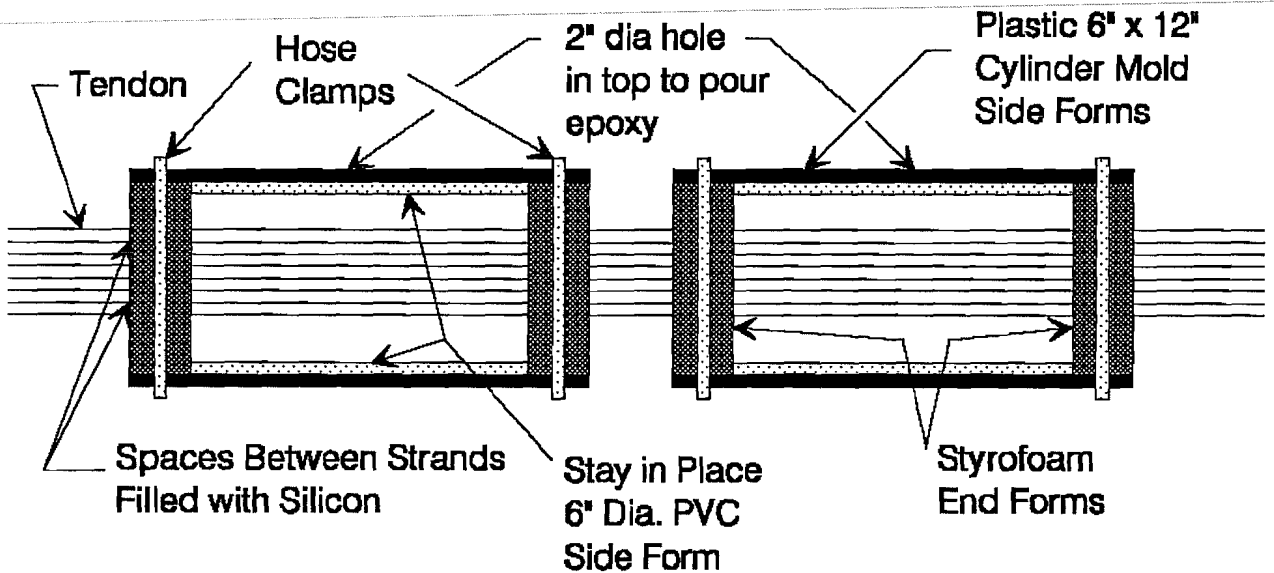
***Day 1:***

After the tendons were snugged a team of 4 to 6 students began to work to place the forms for the epoxy sleeves. This involved the following steps:

1. The strands were marked for the location of the styrofoam end forms.
2. The gaps between strands were sealed at the location of each end form with silicon sealant. This was a crucial step to prevent leakage of epoxy during the pouring operation. The strands were snug but could be pried apart to inject the silicon between them.
3. End forms were positioned.
4. Side forms, cylinder molds, were pulled into place and hose clamps were used to tighten the side forms against the end forms (see Figure 2.44).  
  
*Note:* This operation required approximately one-third man-hour per form. Span C11 had 24 forms and Spans A43 and A44 had 36 forms each.
5. The silicon sealant was allowed to dry for approximately one hour. During this time, preparations were made for the epoxy mixing operations.
6. Sheets of black plastic were placed under the molds to catch epoxy leaks.
7. An exhaust fan was positioned near the open end of the box to remove fumes generated by the reacting epoxy.
8. The epoxy was mixed in four-gallon batches and poured into the molds.
9. The molds were carefully monitored to discover any leaks. Leaking forms were repeatedly "topped-off" with epoxy as the leaking drained the forms. Eventually the leaks plugged themselves.



Forms for Span C11



Forms for Spans A43 and A44

Figure 2.44 Forms for epoxy sleeves.

10. When it was confirmed that all leaking had ceased and the epoxy was reacting, the team evacuated the box.

### *Day 2:*

On the second day the forms were removed and the first step of strain gage application was accomplished. The following activities were performed by 2 to 4 people:

1. The epoxy sleeve forms were removed.
2. Two strands between each pair of sleeves were selected to be gaged and were cleaned and sanded.
3. The surface was prepared and the gage positioned using cellophane tape.
4. When a group of gages (four or six) was prepared, a small batch of two-part epoxy was mixed and applied to each of the gages.
5. The gages were then clamped into position using preformed rubber pads and hose clamps (see Figure 2.45). This clamping was required for at least six hours to ensure proper adhesion of the gage to the strand.

*Note:* The entire operation took about one man-hour per set of gages. Span C11 had six sets of 4 gages and Spans A43 and A44 had six sets of six gages each.

Other tasks performed on day two by workers not involved in strain gage application were:

1. The lead wires were threaded through previously-installed conduit. The conduit was placed in the segments when they were in the storage yard.
2. The security lock-box for the data acquisition system was installed.
3. Demec gages were attached to the epoxy sleeves.

### *Day 3:*

On the third day the lead wires were soldered to the strain gages and connected to the data-acquisition system. This involved the following tasks, performed by two people:

1. Clamping system was removed. The gages which had not adhered properly were replaced using a fast-setting super glue. Quite a few gages (18 of 24) failed to adhere in span C11, due to low temperatures. In span

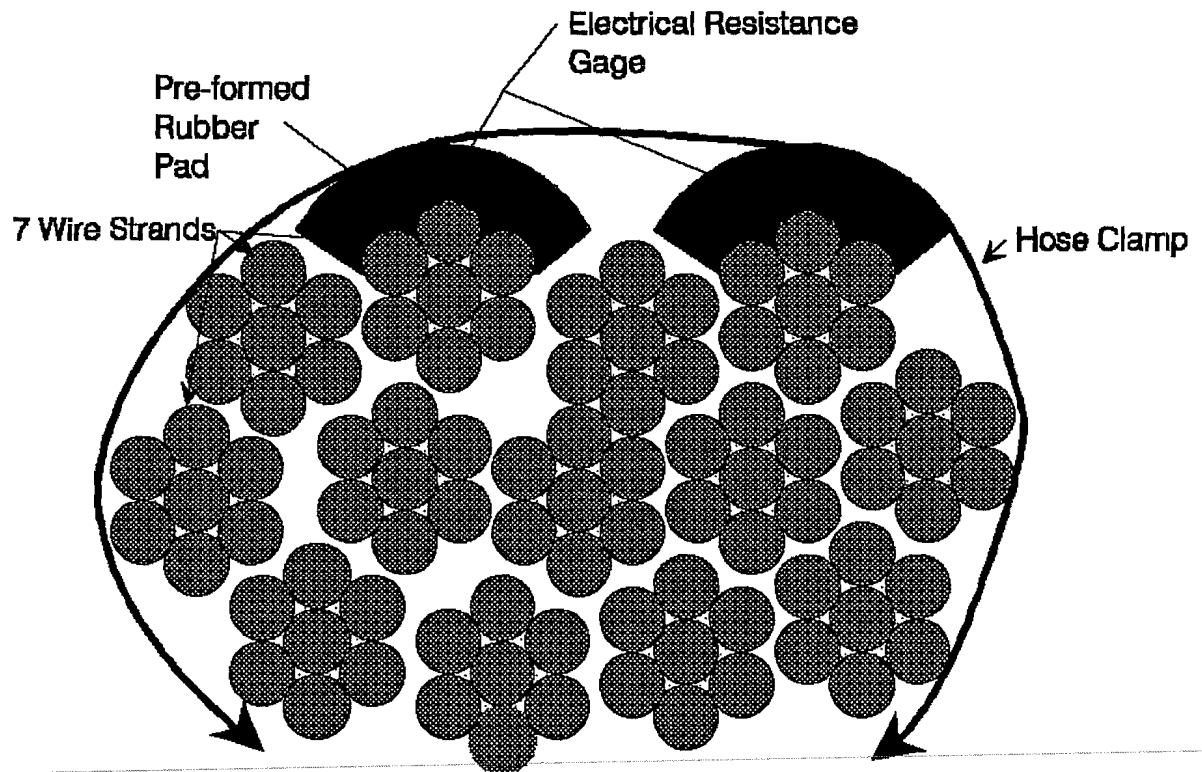


Figure 2.45 Clamping system for ER gages on tendon bundles.

A43, 11 of 36 failed to adhere and in A44 only 3 gages of 36 failed to adhere with the two-part epoxy.

2. The lead wires were soldered to the gages.
3. The gages were covered with waterproofing protection, and lead wires were firmly tied to the tendons to prevent accidental breaking of the soldered connections.
4. The data-acquisition system was positioned in its lock box and all leads were connected using preassembled amphenol connections.
5. The system was checked to see if any gages were not responding. Gages were repaired or replaced as time allowed.

#### **Day 4:**

On the fourth day the stressing operations took place and tendon readings were made during those operations. As recommended, the several readings were taken during the course of stressing (as opposed to simply recording a before and after reading) in order to compensate for initial irregularities in strain readings. Normally during stressing operations the TxDOT

inspectors require pauses, when the ram pressure is held constant, to take elongation readings. At each elongation reading pause, the investigators also took tendon Demec readings. The pause also allowed for several ER-gage readings, since the data-acquisition system was operating at a 20-second interval during stressing. The Demec readings were taken at 20%, 40%, 60%, and 77% of the ultimate strength of the tendon. A reading was also made after seating. When the stressing operations were completed, the data acquisition system program was altered to read the gages every 1-1/2 hours.

## 2.5 Performance

The epoxy sleeve/ER-gage combination system worked quite well in the field, but was very labor intensive.

The day spent installing the epoxy sleeves was very strenuous and uncomfortable. Working in the cramped and hot conditions inside of the box invoked many well-founded complaints from the volunteer staff. The spans were erected in February and in early April when the temperatures were relatively low. The conditions would have been extremely uncomfortable in July.

The biggest problem encountered with the ER strain gages was temperature-related as well. For the two part epoxy to set properly, a uniform pressure must be applied and the epoxy must cure for 6 hours at no less than 70°F. The first span was erected in February when the temperatures were quite cool. The span was sealed and space heaters were used to warm the air, but apparently the prestressing steel itself remained too cold and a majority of the gages did not adhere properly. They were replaced using the less-reliable super glue. For future projects, the availability of a two-part epoxy which reacts at lower temperatures should be investigated.

The grouting operations had a few problems as well. The original system (see Figure 2.46a) utilized a flexible rubber reducer to transition from the six-inch diameter sleeve to the four and one-half inch PE duct. This reducer deformed considerably during the pressure grouting and in many cases leaks occurred. The problem was solved by coating the sleeves with high-strength epoxy. It was messy but effective.

The second two spans incorporated a modification to this system. Rigid PVC reducers were used instead of the flexible rubber. This also required the addition of a stay-in-place PVC mold to ensure a snug fit between the epoxy sleeve and the rigid reducer (see Figure 2.46b). This system proved to be a bit more clumsy to install, but much more reliable in the grouting operations.

The Campbell system performed very well. The programming was quite straightforward as were the interface programs which allowed data to be retrieved from the system and programs to be downloaded. The large marine slow-cycle battery proved to be more of a hinderance than

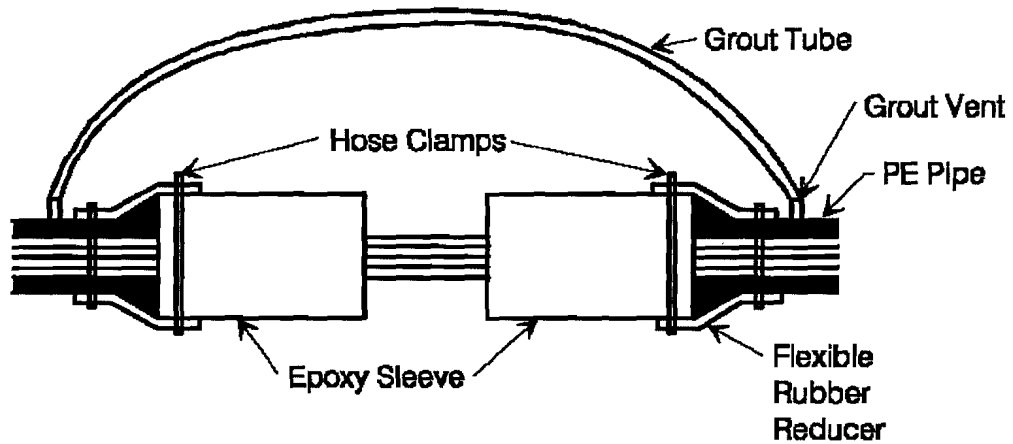


Figure 2.46a Grout by-pass system for span C11.

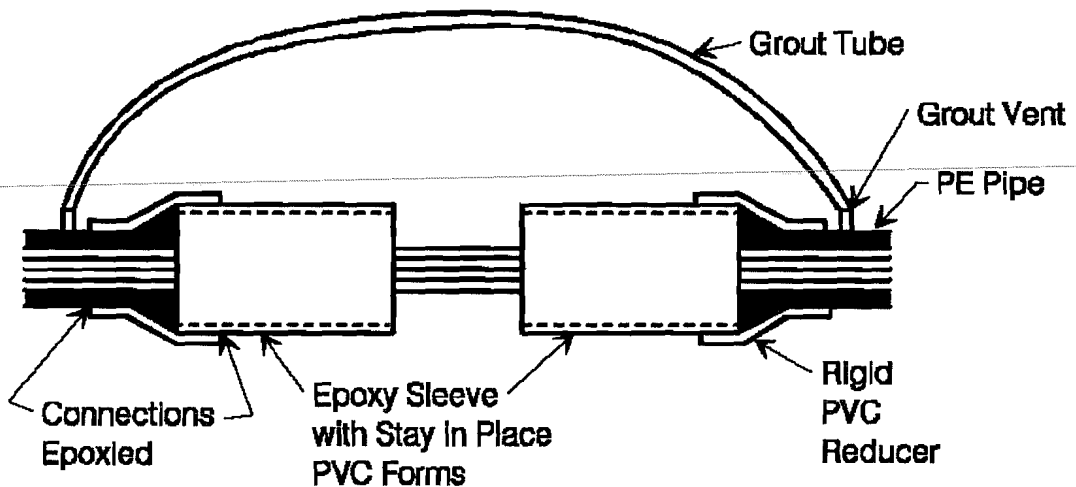


Figure 2.46b Grout by-pass system for spans A43 and A44.

a help. The batteries are very heavy and difficult to manage in the cramped quarters inside the box. The batteries lasted almost one full year before requiring replacement, but several replacements of a smaller-size battery would have been much easier.

## 2.6 Instrumentation Layouts

Figures 2.47a and 2.47b show the basic layout of the field tendon strain measurements. Each external tendon comprises three straight lengths of tendon. It was assumed that the strain would be constant along each straight length of tendon, so only one reading location was required. In this way each tendon provided a live end, middle, and dead end reading. The

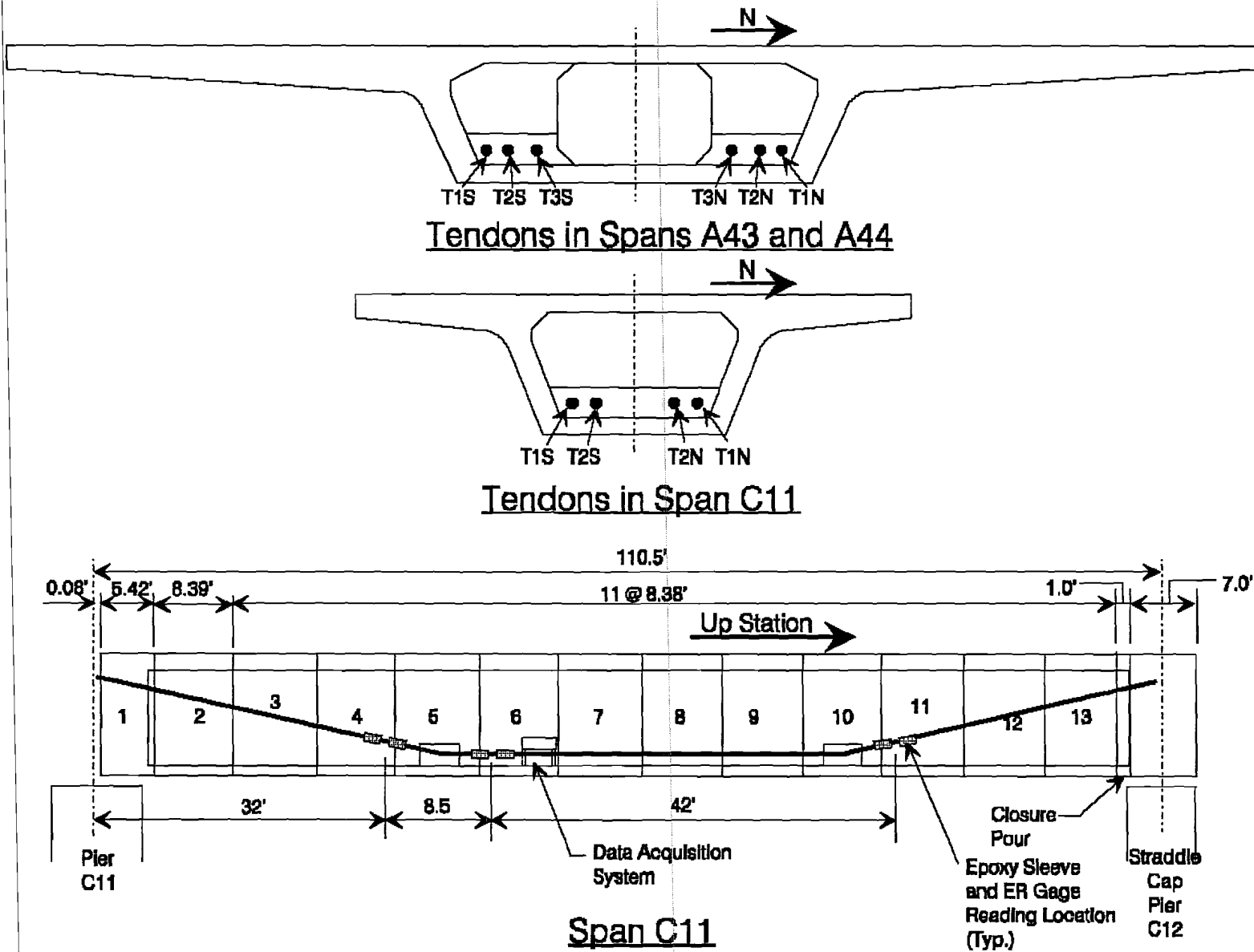
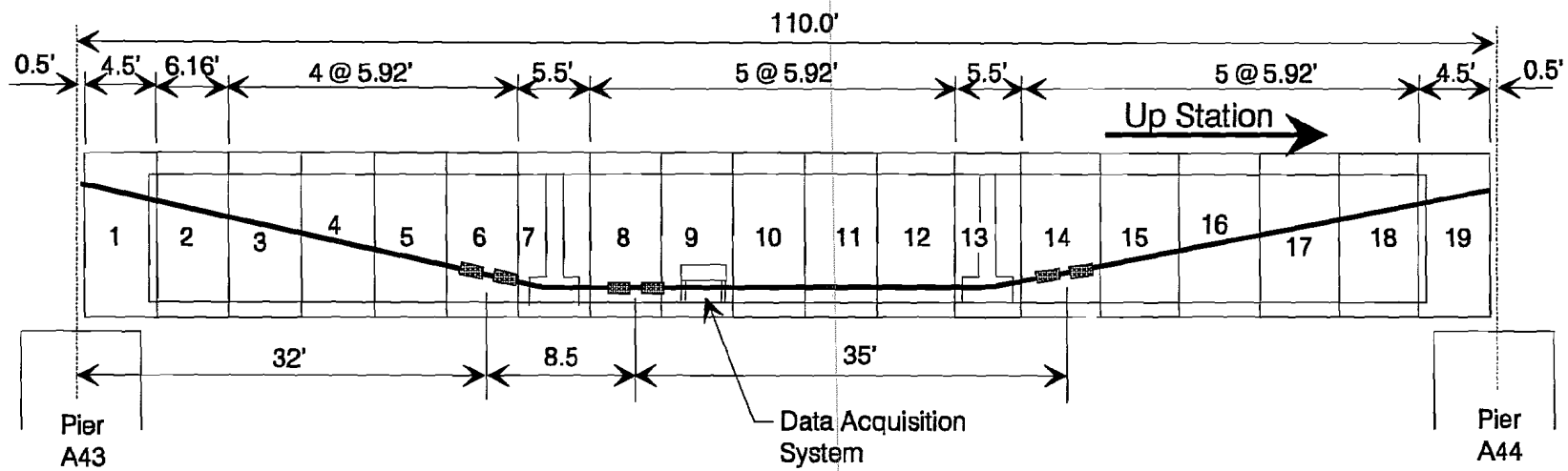
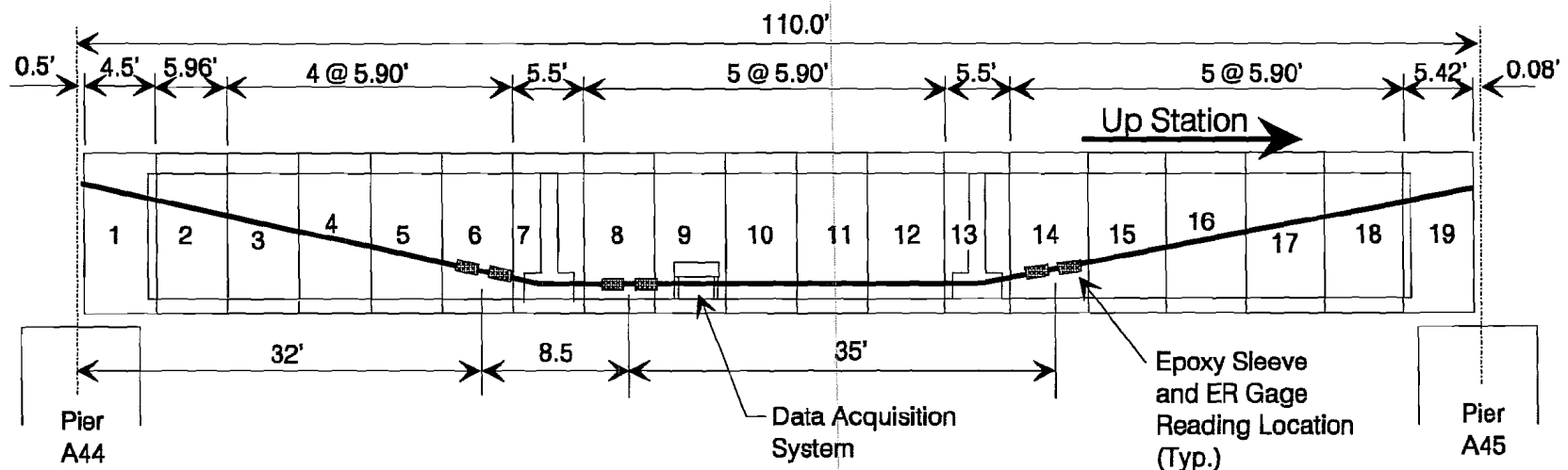


Figure 2.47a Tendon force instrumentation layouts.





### Span A43



### Span A44

Figure 2.47b Tendon force instrumentation layouts.

figure also shows the locations of the Campbell data acquisition systems, which were placed in specially-fabricated lock boxes. The lock boxes were designed to position the data-acquisition system just above the external tendons which run at 4 inches above the top of the bottom slab of the box. This placed the data-acquisition system approximately 10 inches above the top of the bottom slab. A severe rain storm caused flooding inside two of the spans and in one span the data-acquisition system was damaged by the water. In future instrumentation projects, the system should be placed in a safer location.

## **2.7 Recommendations for Future Projects**

The system used in the current project provided very good initial stressing data. The long-term data was apparently affected by thermal fluctuations and possibly creep of the epoxy sleeves. The electrical resistance strain gages worked well when applied with the two-part epoxy, and less reliably when applied with the fast-setting super glue. The following recommendations should improve the performance of the system:

1. Perform laboratory studies on the influence of temperature changes on the epoxy sleeve system.
2. Re-evaluate the grout bypass method to devise a more leak proof method.
3. Investigate other two-part epoxy glues for the electrical resistance gages which will react at temperatures less than 70°F.
4. Place the data-acquisition system in a position which will be safe from damage during construction and from rainwater inside of the box before the deck joints are made watertight.
5. Investigate the possibilities of connecting a modem by phone line or radio to the data-acquisition system so that the data can be collected from a computer in the laboratory.
6. Investigate the use of smaller batteries to power the data-acquisition system. A solar collector might also be used to constantly recharge the batteries.
7. The completed data-acquisition system introduces parasitic resistances which alter the gage factor of the electrical resistance gages. It is imperative that the difference between the gage factor with the data-acquisition box and the gage factor when reading from a strain gage box be known.

## CHAPTER 3 SPAN DEFLECTIONS

### 3.1 Review of Available Systems

Accurate measurements of span deflections are vital in the study of bridge behavior. Individual measurements of span deflections are useful for checking certain design assumptions for segmental concrete bridges, and to verify their structural safety and strength (through load tests which can be performed at any time during the life of the structures).

This type of measurement is not too difficult to perform, especially when compared to the cases of detecting strains or loads in concrete and prestressing strands. A variation in height is a relatively simple quantity to measure. However, some complications are usually added due to the large distances between the points that determine the reference line for vertical movements and the small magnitudes of expected displacements and access problems inside curved box girder bridges. The deflections of selected cross-sections of a segmental bridge structure are mainly taken with respect to reference points located in the abutments or pier segments. The longitudinal distance between these two reference points is thus usually equal to several thousand times the maximum expected vertical movements of the instrumented cross-section. For example, vertical movements of less than 1/10 inch usually have to be measured during load tests with bridge spans of over 100 feet in length.

Measurements of vertical deformations of prestressed concrete bridges have been frequently performed with surveying techniques (sometimes called *optical methods*). The results have often been poor or marginal.<sup>52</sup> The need for a higher level of accuracy has spurred studies of new methods within this area of measurements. Both mechanical and hydrostatic techniques have emerged as candidates for future deflection measuring systems. New devices (based on these two technologies) not only proved to be reliable and accurate, but also came with a reduction in the total cost of the surveyor's leveling technique.

**3.1.1 Objectives.** An investigation of some devices used for measuring vertical deformations in spans of concrete bridge structures is introduced here. Existing techniques can be separated into three different classes, according to their basic method of measurements: baseline methods, hydrostatic methods, and surveying methods.

Devices based on the first two methods were more carefully investigated due to their innovation, relatively good accuracy levels, and cost-effectiveness.

**3.1.2 Baseline Methods.** The original baseline method used for measuring the relative vertical movements of certain points of a bridge span was developed in late 1959 by A. Pauw and J. Breen.<sup>38</sup> The method has the advantage of simplicity, good accuracy, and ease of use. It basically consisted of the mechanical measurement of vertical movements of specific span points from a firmly-set reference line. Two slightly different systems were originally designed

according to the needs for short- and long-term measurements of vertical movements of two prestressed concrete girders. The difference between the two measuring systems only consisted of the better protection techniques designed for the long-term readings.

The overall schematic of the original baseline system is shown in Figure 3.1. The reference line for vertical movements was a tensioned wire stretched between two end brackets. In the temporary system, special plug inserts were cast into the top surface of the girders and above the bearing plates. These inserts were used to hold the bases of the anchorage brackets that were leveled to a fixed height between the mounting surface on the girder and the baseline (as shown in Figure 3.1a). The bracket at the dead end was used as an anchorage for the wire, while the bracket at the live end had an arm and two grooved pulleys from which a calibrated 50-pound weight was suspended. This was the method used to provide constant tension in the baseline wire. The wire originally used consisted of #23 gage steel music wire (piano wire), stretched to 100 ksi by the 50-pound weight.

The only variation for the permanent system (used after the girders were in place on the abutments) was that the dead and live end brackets were installed in anchorage boxes precast in the inner faces of the end piers. The live end box had a detachable part with an additional grooved bearing that was used as a wire guide to hang the calibrated weight for the deflection readings (as shown in Figure 3.1b). The other notable characteristic was that both boxes had cover plates with rubber gasket seals to protect the anchorage parts from environmental conditions. A package of silica gel dehydrator was also placed inside each box to prevent rusting and corrosion of the moving parts.

Reference brass inserts were cast into the girders on top (for temporary readings) and bottom (for permanent readings) surfaces at the quarter- and center-points. For the deflection readings, the deflection meter (shown in Figure 3.1c) was installed on a precast set of brass inserts, and leveled with the third adjustable screw. The deflection meter consisted of a standard 12-inch *Starrett* gage with a micrometer adjustment and with a vernier that allowed for a measurement accuracy of 1/1000 inch. The gage's extension arm and vibrating reed were used as a method for more accurately determining the contact of the gage with the base wire. When the movable head of the reed was brought into contact with the wire, the vibration of the reed was damped, thus giving a sensitive indication of position. The base plate of the deflection meter had a bubble level that was used to level the meter assembly to reproduce its previous measuring positions.

One system-related problem described by Pauw and Breen consisted of the movements of the baseline wire on windy days. A secondary source of errors, mainly for long term measurements, was that any variation of the friction of the pulleys implied a variation of the catenary shape of the reference line. Despite the inconveniences, the original investigators claimed to have reproduced measurements on the order of 2/1000 inch.<sup>38</sup> However, this high level of accuracy is probably related to reproductions of a series of readings from each set position of the baseline wire and deflection meter. The repeatability of readings at varying positions of the

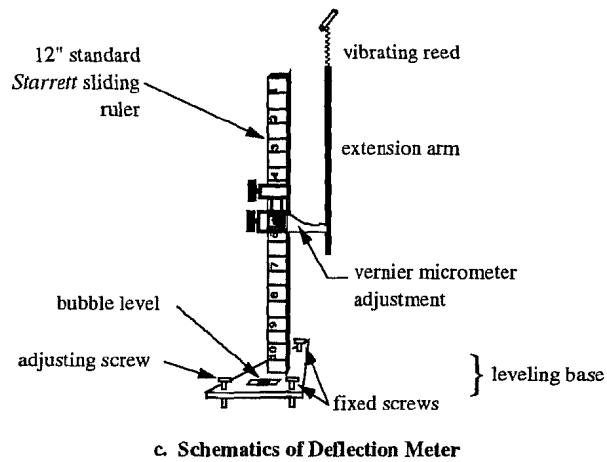
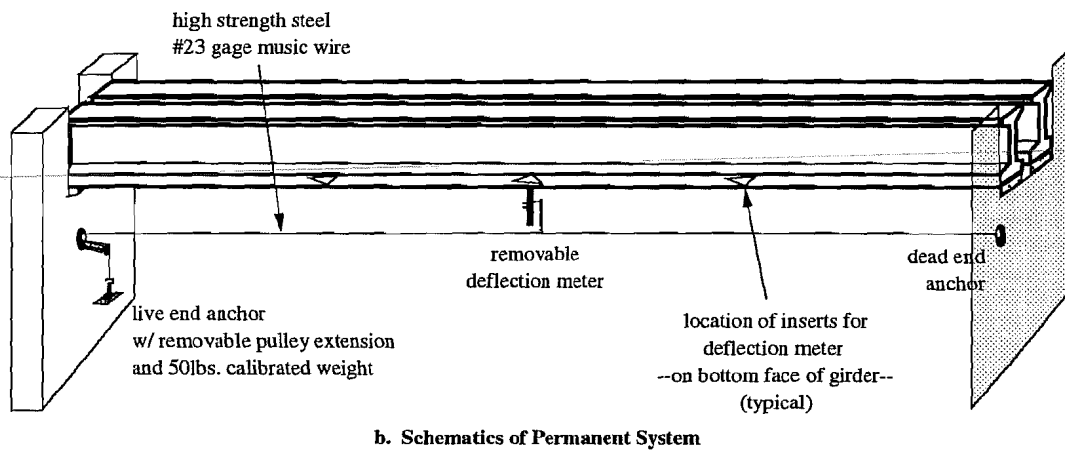
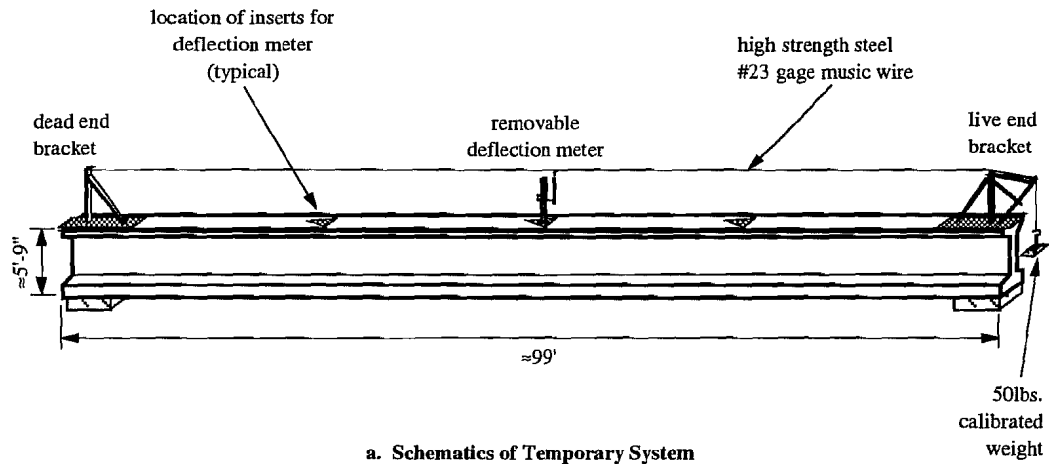


Figure 3.1 Pauw-Breen original baseline system.

deflection meter must have been limited by the small angular movements of the base plate. The bubble level has a lower degree of accuracy than the vernier ruler, and small inclinations of say  $0.25^\circ$  at the base plate can produce height differentials of 0.0065 inch at a set height of 10 inches from the base plate.

However, the method still seems to be highly accurate and even with pessimistic observations it should be able to determine 1/100-inch movements on still days and for long-term readings.

A slightly-modified version of the original baseline deflection method was later used on a field measurement of deflections of a prestressed concrete girder bridge during load testing operations.<sup>42</sup> However, one of the most detailed investigations for improvements of the original baseline method was developed by Bradberry in 1986.<sup>11</sup> Bradberry presented a good comparison of different systems available for measuring span deflections of prestressed concrete girders. After determining the general adequacy of the baseline method for his particular tests, he proceeded to evaluate possible modifications of the original system in order to eliminate the pulleys and the 50-pound weight while making it possible to easily reposition the baseline. His final suggestions involved modifications of the baseline tension adjusting method, and of the reading devices.

Bradberry designed wire anchorages that were ideal for imposing small load increments to the wire during the tension-adjusting procedures. The live end anchor consisted of a  $\frac{1}{2}$ "  $\phi$  x  $2\frac{1}{2}$ " bolt with a  $\frac{3}{4}$ " H x  $\frac{1}{8}$ " D shank recess, and a  $\frac{1}{8}$ "  $\phi$  hole for the passage of the baseline wire. The recess provided a winding area for the excess wire obtained during the adjustment of tension. To adjust deflection readings according to the small movements of the wire at the live end, Bradberry installed an additional deflection measuring station next to the live end anchorage.

As an accurate method for reproducing the tension of the baseline wire he suggested the following steps (refer to Figure 3.2):

- a. Initially adjust the baseline wire tension by turning the live end anchor bolt like the frets of a guitar, controlling the tension initially "by sound."
- b. Hang a small calibrated load at mid-span section of the tensioned line and measure the resulting deflection increment.
- c. Repeat procedures a. and b. until obtaining a pre-determined line deflection increment for the calibrated load.

The reading devices used by Bradberry consisted of small mirrors located next to short pieces of calibrated rulers (with divisions of 1/64"). These two pieces were bonded to quarter-, center-, and live end-points on a side face of the girders. Two-part epoxy products were used for the surface bond of the mirror and tape assembly to the concrete. Accurate readings were

obtained with this simple system by aligning the mirror image of the taut baseline wire with the position of the wire itself (see Figure 3.2).

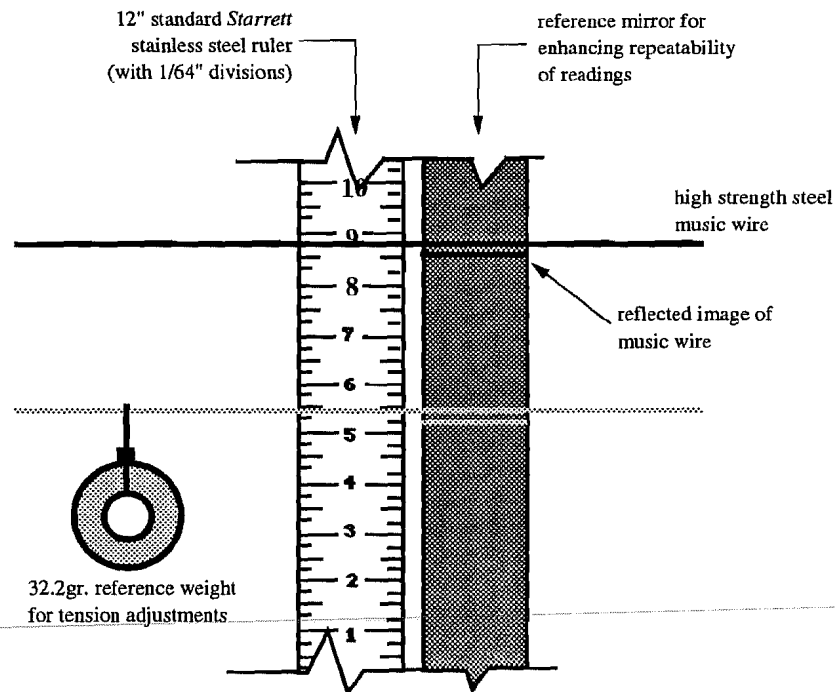


Figure 3.2 Bradberry-Breen modifications of the baseline system.

Bradberry's evaluation of the overall performance of his instrumentation system indicated it highly satisfactory, recommending that it be used in future similar projects.<sup>11</sup> Although Bradberry considered that the final system had high levels of accuracy, an overall field accuracy value was not provided. However, this value was estimated to be close to half of the reading resolution of the system. This is approximately equal to half of the resolution of the calibrated rulers, or 8/1000 inch.

Some possible complications of Bradberry's baseline method are:

- Long-term problems can result from loosening of the epoxy bond of the ruler and mirror assemblies.
- The tension adjusting method suggested by Bradberry seems to be time consuming (mainly due to the trial and error procedures that need to be followed to obtain accurate tension adjustments of the base wire).
- To anchor the dead and live end of the base wire, Bradberry installed bolts on the actual formwork of the girders. These bolt inserts attached

to the formwork can be damaged during concrete vibration and depend on the approval of the contractors. The present project researchers investigated alternative solutions to this problem during the testing of anchoring systems for the locating discs of the Demec Extensometer. It was found that the best system consisted of a combination of mechanical stainless steel anchors and two-part epoxies (refer to Chapter 5).

- Wind-induced vibration of the reference wire still presents an occasional inconvenience for this modified baseline system.
- Baselines are difficult to use with curved girders if the girder sweep causes the chord between ends to be greater than the box width.

Bradberry's reference to the difficulties in uncoiling long lengths of piano wire under time-restricted situations is another complication that should also be considered in future applications of this modified baseline system.

Finally, a common inconvenience of both baseline methods is related to their basic incompatibility for allowing remote or automatic data recording operations. Despite this and the other previously-mentioned problems, both systems evidently provide affordable levels of accuracy.

**3.1.3 Hydrostatic Methods.** Extensive research related to hydrostatic methods for measuring vertical deformations were investigated in Switzerland by Markey and Favre.<sup>28,17</sup> Their final system suggested for field installation in box girder bridges is presented here.

The principle of operation of their system is based on the hydrostatic law of communicating vessels (Figure 3.3). This law is basically that at a state of equilibrium and when certain physical parameters are ideally equal, interconnected liquid surfaces lie at the same horizontal level. The most rudimentary case of a deflection measuring system based on this principle is the traditional hose level. A quite advanced version of the hose level is represented by the Swiss

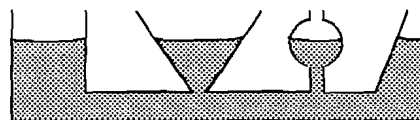
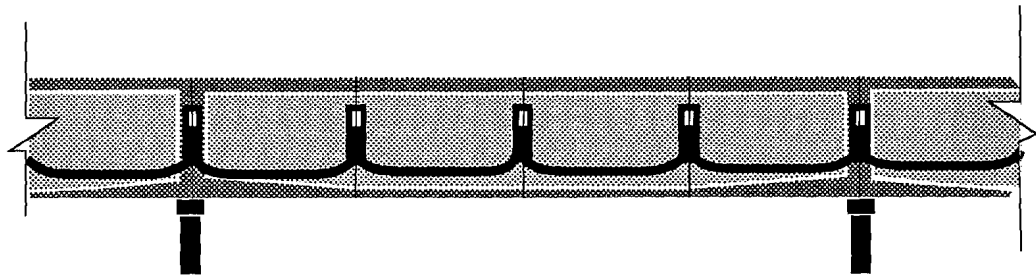


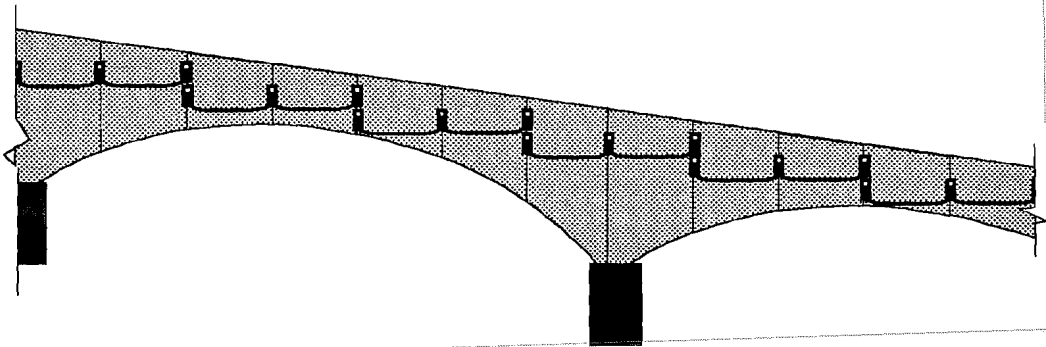
Figure 3.3 Law of communicating vessels.

hydrostatic leveling system, which was specifically designed for field measurements in box girder bridges. The system is made of reading pots firmly installed in the inside face of the box girders and interconnected to each other by clear plastic tubing (as illustrated in Figure 3.4). Each reading pot is formed by a calibrated glass cylinder (2 mm thick and 20 mm internal diameter) mounted to a metal stand that is in turn fixed to the internal walls of the box girder segments. The pots are hose clamped (with some type of rubber gaskets and adaptors) to a clear plastic PVC tubing of 2 mm thickness and 11 mm internal diameter. Varying distances to the

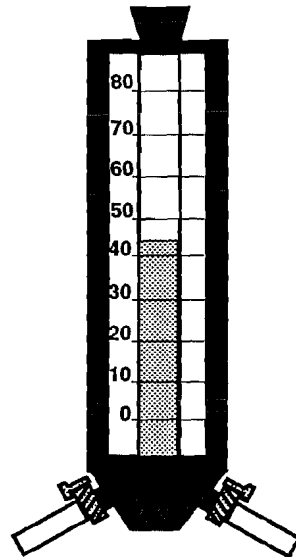




a. Sample installation on box girder bridge with zero gradient and constant section.



b. Sample installation on box girder bridge with a gradient and varying section.



c. Schematics of measuring pot.

Figure 3.4 Sample layouts and final measuring pot of the hydrostatic leveling system (after Markey<sup>28</sup>).

reference pots (usually installed at the pier segments) can be obtained by splicing lengths of tubing through tapered hard plastic connectors and pairs of hose clamps. Circuit lengths of up to 100 m were found to be reasonable limits to avoid complications of the measuring systems. However, the actual length of a circuit is usually regulated by the bridge geometry, as shown in the sample layouts of Figure 3.4. The communicating liquids suggested for use consist of clean, demineralized water, isopropyl alcohol, or a 50/50 mix of both liquids.

Actual field applications of several models of the hydrostatic leveling concept imposed certain alterations of the original design envisioned by the developers of the system.<sup>28</sup> Their most adequate model was the one introduced in the present review. However, some important areas of concern still mentioned by system investigators were:<sup>28</sup>

*a. The communicating liquid.* This needs to be non-homogeneous, preferably with a low variation of density with temperature, clear, and with a low freezing point and a high evaporation point. Non-homogeneous liquids introduce errors due to their unknown densities. Similarly, when temperature varies during a measurement, all liquids expand or contract, thus introducing movements that must be accounted for during the data reduction process. Clear tubing and liquids are needed to help locate trapped air bubbles (which in certain cases can throw off the deflection readings). Finally, low freezing points are obviously necessary for preventing the liquid from freezing in low-temperature areas. On the other hand, a high point of evaporation is also desired to slow the rate of evaporation of the liquid during the summer temperatures of certain regions. Isopropyl alcohol was successfully used in the last applications of the leveling system. However, the investigators still recommended a search for more appropriate liquids.

*b. The reading system of the level of the liquid.* Some physical properties of the liquids complicate the efficiency of an acceptable reading system for the hydrostatic leveling method. The first problem is the irregular surface of liquid levels in small tubes (property known as *capillary action*). This introduces some approximation to the exact location of the "meniscus" of the liquid level. A secondary problem is the need for using a high-resolution scale or ruler that can accurately measure the small variations of the level of the meniscus of the liquid surface. The solution recommended by the Swiss researchers consisted of a calibrated clear glass cylinder (probably to the 1 mm division marks) from where measurements are taken by sighting a horizontal level at the plane at which the meniscus touches the glass walls.

*c. Infiltration of air bubbles in the liquids.* When air bubbles are trapped in vertical lengths of the tubing, they introduce vertical height differentials in the measuring systems. This is due to the negligible density and compressibility of air. Bubbles were found to be usually formed during the filling of the plastic tubes. This process was thus recommended to be performed at a laboratory, where the tubes can be pre-filled with the liquid and tightly corked to assure no entrained air in the system. When this process needs to be performed on site, however, all visible air bubbles must be carefully removed. To further avoid having air bubbles in longitudinal sections, an inverted "Y" shape of the plastic tubes at their connection to each measuring pot was recommended. This is because a natural evacuation of air bubbles can occur

in vertical lengths. A secondary option only available when using water as the interconnecting fluid is to deaerate it by previous boiling.

*d. Movement of the liquid surface.* Certain problems were reported due to the oscillations of the liquid after its installation in the tubes. On the other hand, traffic movement on top of the instrumented bridges did not cause oscillations in the liquid. Moreover, with the final hydrostatic leveling system the investigators reported that equilibrium of water was usually obtained within a matter of a few minutes.

The Swiss investigators claimed to have reached an accuracy of 0.5 mm ( $\approx 2/100$  inch) in their field applications on actual box girder bridges.<sup>17</sup> However, it is not clearly described how this accuracy was obtained nor the method for computing the "true" measurements of vertical movements of the instrumented spans. Most of the report about the field tests<sup>17</sup> deals with "deflection trends" and not with relative movements from specific reference points (such as the bridge abutments or the pier segments). However, it is still possible that a slightly-modified hydrostatic leveling system could become an alternative for measuring relative vertical movements with a 1/100-inch accuracy level.

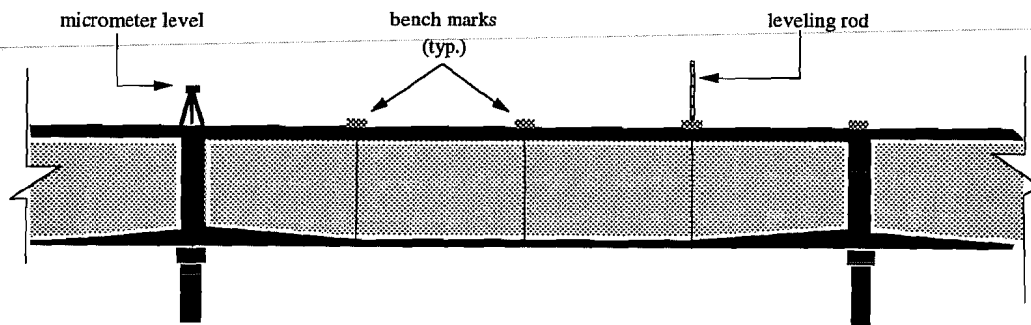


Figure 3.5 Basic operation of surveying methods for measuring span deflections (after Bradberry<sup>11</sup>).

**3.1.4 Surveying Methods.** These are probably the most traditional methods used for field monitoring of span deflections in bridges. The basic operation principle of the majority of these methods is illustrated in Figure 3.5. It consists of sighting leveling rods located on bench marks at different points along the top surface of the bridge. This is usually accomplished with high precision optical micrometer levels or theodolites. The accuracy of this type of measurement depends on several factors:

- Resolution of the surveying instruments, either precision theodolites or electronic levels.
- Type of reference points used as guidance for the leveling rod.

- Experience of the survey crew.
- Efficiency of the surveying technique utilized by the crew.

A previous field investigation of vertical movements of two 100-foot spans of a composite winged-girder concrete bridge at Bear Creek, Austin, Texas using experienced surveyors reported accuracies only to the 12/100-inch level.<sup>52</sup> This is obviously a very large error when compared to the other methods previously investigated in the present survey.

In conclusion, the most important problems with this method of measurement are related to:

- Cost. Accurate bridge deflection measurements require surveying instruments of high resolution along with an experienced crew. Both of these requirements are costly.
- Accuracy. Even with state-of-the-art instruments and an experienced surveying crew it is highly unlikely that the method could reach an accuracy level of 1/100 inch.
- Weather protection. Readings during extreme temperatures (with substantial distortions due to heat reflections) and on rainy days can further limit the effectiveness of the measurements.

### 3.2 Trials of Instrumentation Systems

Only small ranges of deflections are anticipated during construction operations, service load conditions, and long-term behavior of concrete segmental box girder bridges. Vertical movements during construction operations and due to long-term behavior were estimated by TxDOT's computer analysis based on current AASHTO recommendations for the design of segmental concrete bridges. For the 110-foot span A-44 of the San Antonio Y project, TxDOT's computer-aided analysis calculated 0.182 inch and 0.210 inch mid-span upward camber variations after stressing each one of the following two continuous spans, A-43 and A-42 respectively. The analysis also predicted that the initial deflected shape of span A-44 should move a total of 0.571 inch at the mid-span cross-section after finishing all construction operations on continuous spans, after adding dead loads (including a 2-inch overlay and the rails), and after accounting for prestress losses (at 199 days after erection). However, the mid-span vertical movement from day 200 to day 4000 was calculated at only 0.049 inch.

The temperature-induced vertical movements calculated by TxDOT's computer program showed only small variations. Results indicated a maximum daily movement of only 0.050 inch at the center of the 110-foot span.

Ranges of vertical movements due to high loadings were also investigated. Results from recent tests on a scale model of a segmental box girder bridge<sup>30</sup> found maximum service load deflections in the order of  $l/6000$ . If the same behavior occurs at the instrumented 110-foot span of the San Antonio Y project, a 0.220-inch mid-span downward deflection should be expected for full service loads.

For measuring vertical movements during construction operations or high service loadings it would appear that an accuracy of about 0.02 inch may be acceptable. However, movements due to high loadings are rare and perhaps only present during specific load tests of a structure.

On the other hand, the very small vertical movements due to daily temperature variations and due to long-term effects can only be adequately measured with an instrumentation system of high accuracy and repeatability. The present testing trials were therefore seeking an instrument that would be able to provide a final accuracy of approximately 1/100 inch and that can be reliable over a long period of time. Secondary concerns for economics also influenced the final selection of the most adequate instrumentation system.

Only two of the systems reviewed in Section 3.1 complied with the present requirements of accuracy, stability, and cost (directly related to availability). The two acceptable systems were based on hydrostatic leveling techniques and on the modified baseline methods. Hydrostatic devices were later canceled from further trial tests for the following reasons:

- lack of familiarity with the different aspects of this technology (i.e. construction, installation, and operation of the measuring devices),
- concerns over evaporation and leakage problems in the very hot climate of San Antonio,
- the long-term accuracy of hydrostatic devices is still doubtful, and
- concerns over thermal effects.

With these considerations in mind, the present researchers opted to enhance the accuracy and ease of operation of the reviewed baseline methods, and to check their performance in actual concrete structures.

Two components of the reviewed baseline methods needing improvement were the method for adjusting the tension of the baseline wire, and the type of measuring device used for the recording of small movements. Modifications of the line tensioning systems along with new measuring devices were investigated in trial tests. The overall performance of the most adequate system was finally checked in a short-span, short-term deflection test, followed by an actual field installation and test on a finished span of the San Antonio Y bridge project.

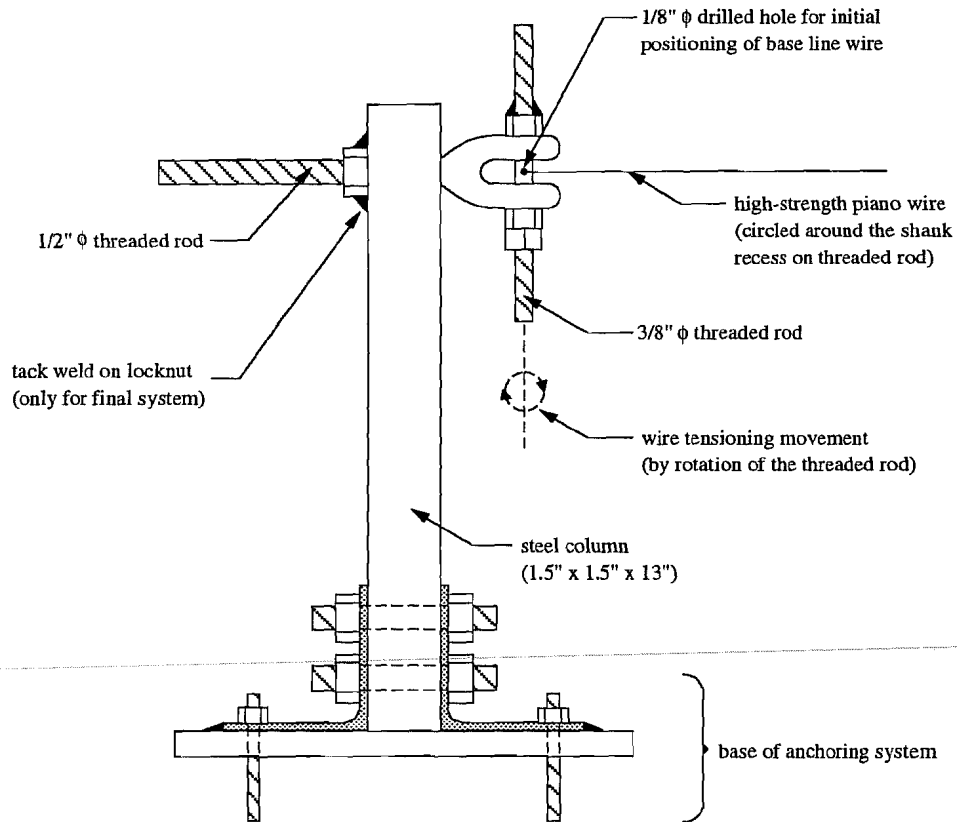
**3.2.1 Line Tensioning Systems.** As reviewed earlier, two baseline tensioning methods were used in past investigations with varying degrees of success. The first method consisted of the tension adjusting procedure introduced by Bradberry.<sup>11</sup> With this method, the tension of the base wire is adjusted according to the deflection imposed by a calibrated weight hung at mid-span. Although it was reported to have worked well in Bradberry's applications, the time needed to accurately adjust the tension in the wire was envisioned to be a major drawback when speed of measurements is a factor of concern. Adding to the total measurement time required by this method is the need for checking vertical movements of the base wire at the live end anchor. These extra measurements are needed when using Bradberry's drilled bolt-tensioning method because the height of the base wire usually varies at each turn of the bolt. All deflection readings are therefore corrected according to the initially-measured position of the base wire at the live end anchor. The recording of this extra station reading thus increases the time required for taking all the deflection measurements and for carefully reducing the data.

The second system under consideration consisted of the constant weight method used by Pauw-Breen with the original baseline system.<sup>38</sup> In this system, the catenary shape of the base wire is kept constant by the force produced from a calibrated weight hung at the live end station. From previous tests, it was found that the calibrated weight needs to be such that it stresses the base wire to 80% or 90% of its breaking strength. One problem mentioned by Pauw-Breen was the wind-induced oscillations of the base wire. However, when applied to measurements inside box girder bridges, climatic factors (especially wind) should not impose severe movements on the calibrated weight and base wire assembly. A second inconvenience to this method, however, was that any variations in the friction of the moving parts will produce a different catenary shape in the base wire. To decrease the degree of influence of this problem, high-quality sealed bearings were purchased for the present trial tests. The outer circumference of each bearing was machined with a narrow groove that was used as a guide for the base wire.

Several line-tensioning methods based on the two previously-mentioned applications were investigated. The following sections describe the systems investigated, their test setup, and the findings from the trial tests performed in the laboratory (on short-span, short-term configurations).

**3.2.1.1 Systems Investigated.** Four devices were manufactured and tested in short-span trial test configurations (22.7 feet and 18.3 feet). Although originally based on the two previous applications of the baseline method, each tested line-tensioning device evolved from observed behavioral errors found in the previous trial test. General schematics, along with the main problems and advantages of all the line-tensioning systems investigated are included in Figures 3.6 through 3.10.

**3.2.1.2 Short-Span Test Setup.** The short-span tests were performed at the setup of an on-going investigation of bond behavior of prestressing strands in prestressed concrete girders.<sup>57,27</sup> The schematic of a typical short-span test setup is included in Figure 3.11. Each baseline deflection system under consideration was installed on the top surface of the girder,



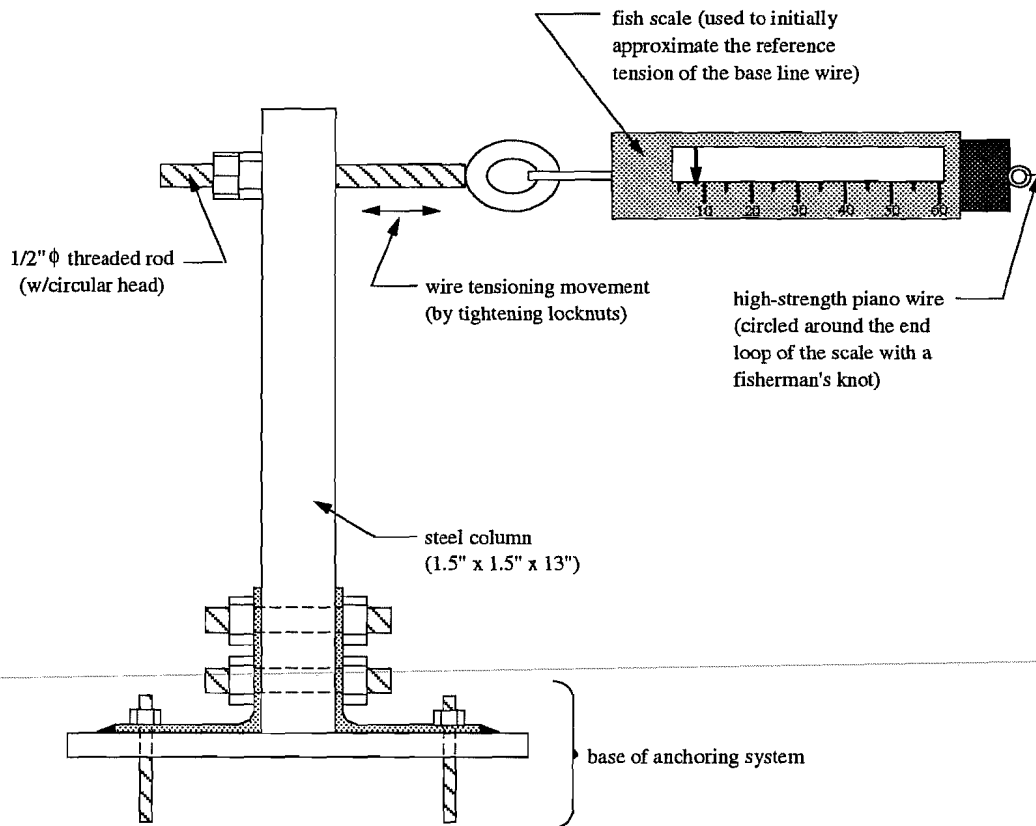
#### Inconveniences:

- vertical movements of the base wire at the tensioning end.
- very difficult anchoring process of the piano wire. The geometry of the anchoring system requires excessive bending of the piano wire. This in turn produces a low strength section in the wire, causing it to fail during the tensioning process.

#### Advantages:

- easy to manufacture.
- low cost.
- fast setup.
- fast tensioning mechanism.

Figure 3.6 Live end tensioning mechanism type I.



**Inconveniences:**

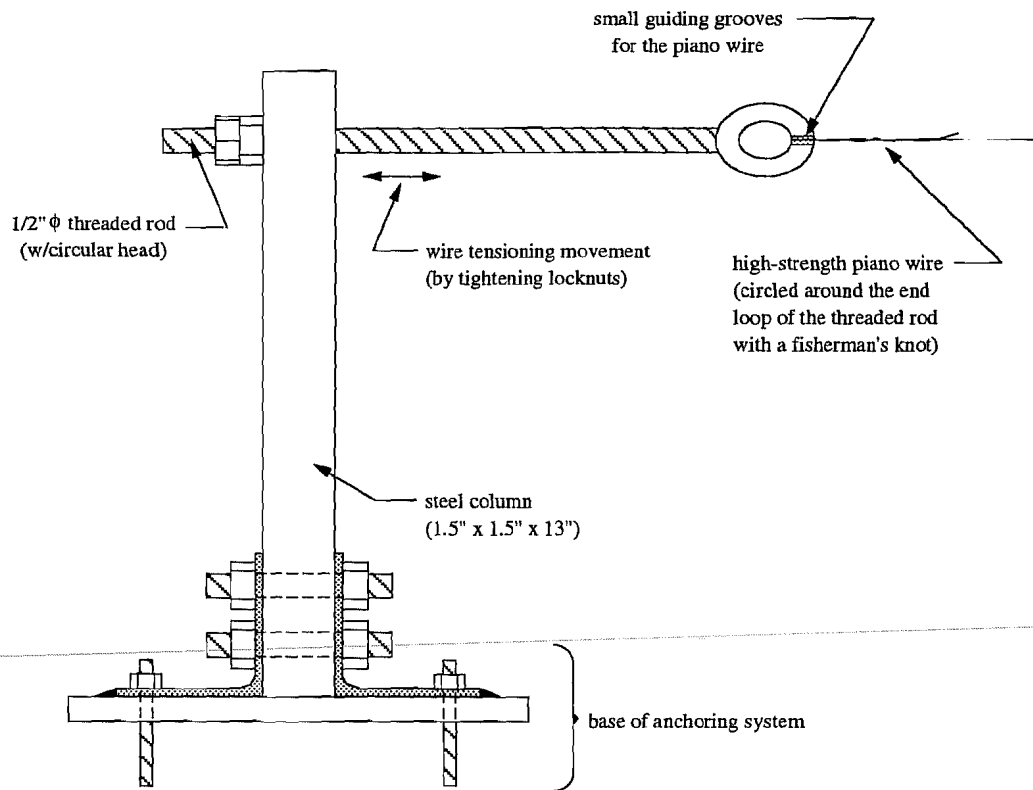
- small vertical movements of the base wire at the tensioning end.
- low accuracy in measurements obtained through fish scale (does not improve the speed for adjusting the tension of the base wire).

**Advantages:**

- easy to manufacture.
- low cost.
- fast setup.
- fast tensioning mechanism.
- allows for an efficient wire anchoring knot (fisherman's knot).

Figure 3.7 Live end tensioning mechanism type II.





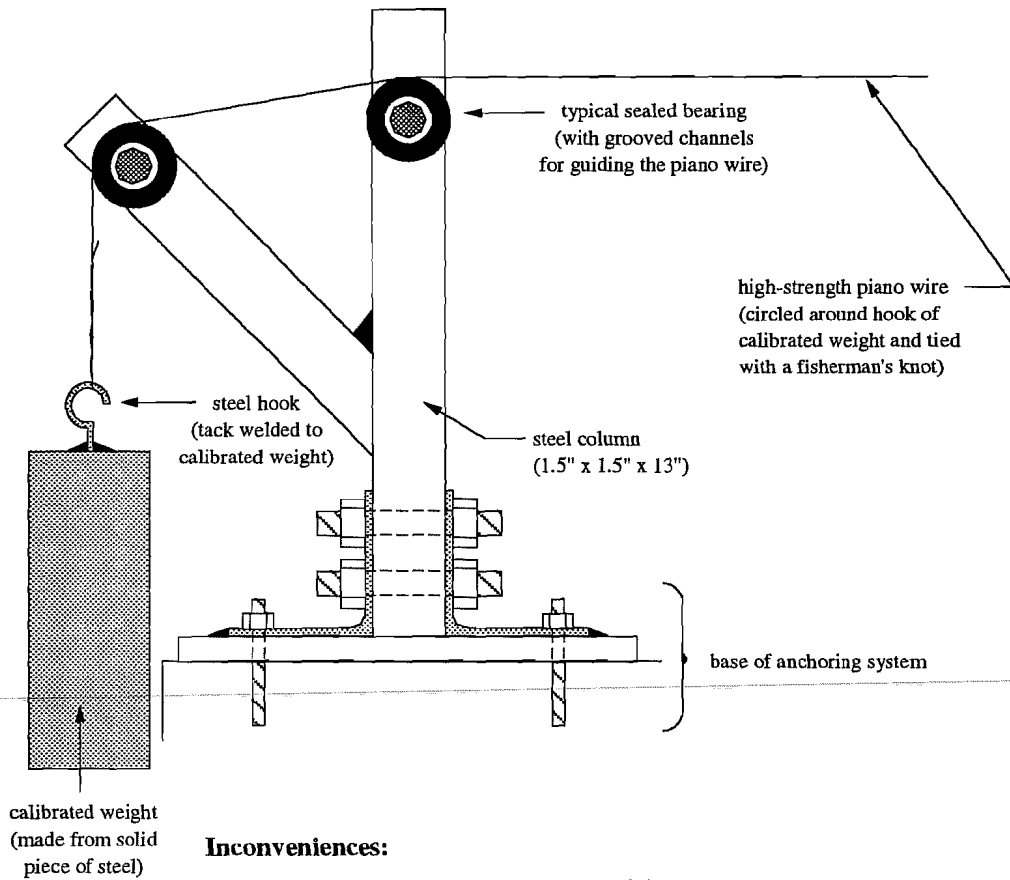
**Inconveniences:**

- small vertical movements of the base wire at the tensioning end.

**Advantages:**

- easy to manufacture.
- low cost.
- fast setup.
- fast tensioning mechanism.
- allows for an efficient wire anchoring knot (fisherman's knot).

Figure 3.8 Live end tensioning mechanism type III.



**Inconveniences:**

- small variations of the catenary of the wire can occur in long-term applications due to corrosion and dust accumulation on calibrated weights.
- friction of the sealed bearings can also vary with time, also causing slight variations of the shape of the wire.

**Advantages:**

- medium difficulty in manufacturing process.
- low cost.
- very fast setup.
- very fast and simple tensioning mechanism.
- no time consuming procedures required during testing/reading operations.
- no vertical movements of wire at tensioning end.
- allows for an efficient wire anchoring knot (fisherman's knot).

Figure 3.9 Live end tensioning mechanism type IV.

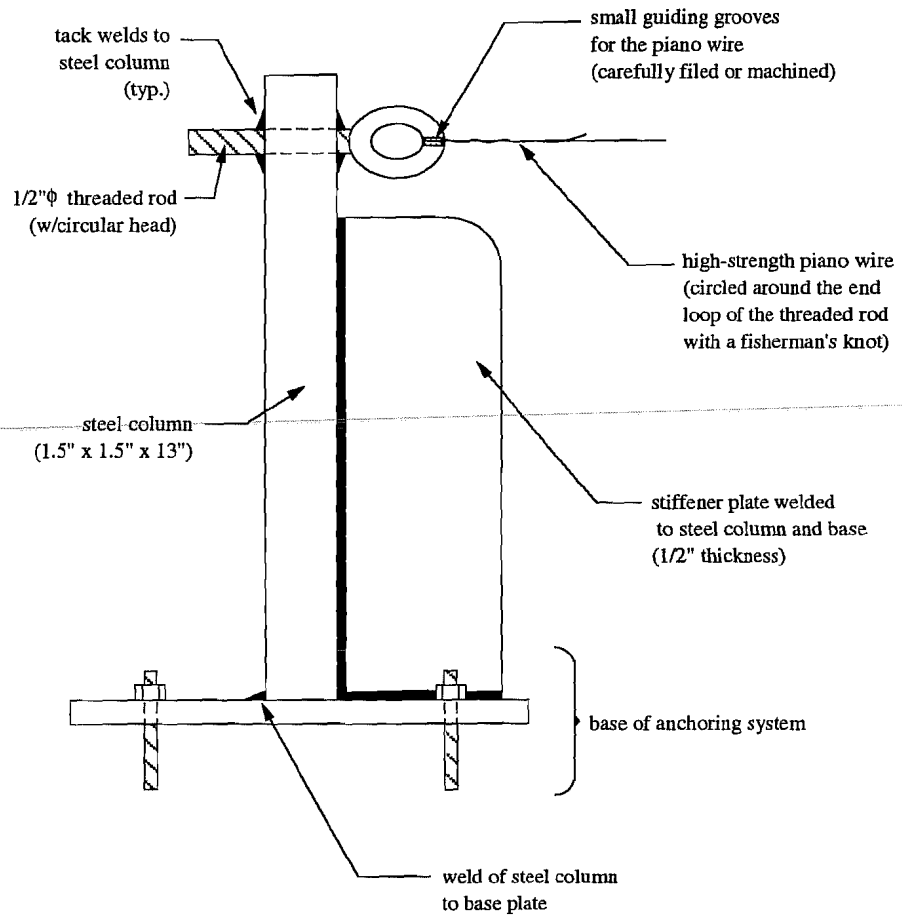


Figure 3.10 Typical dead end anchorage.

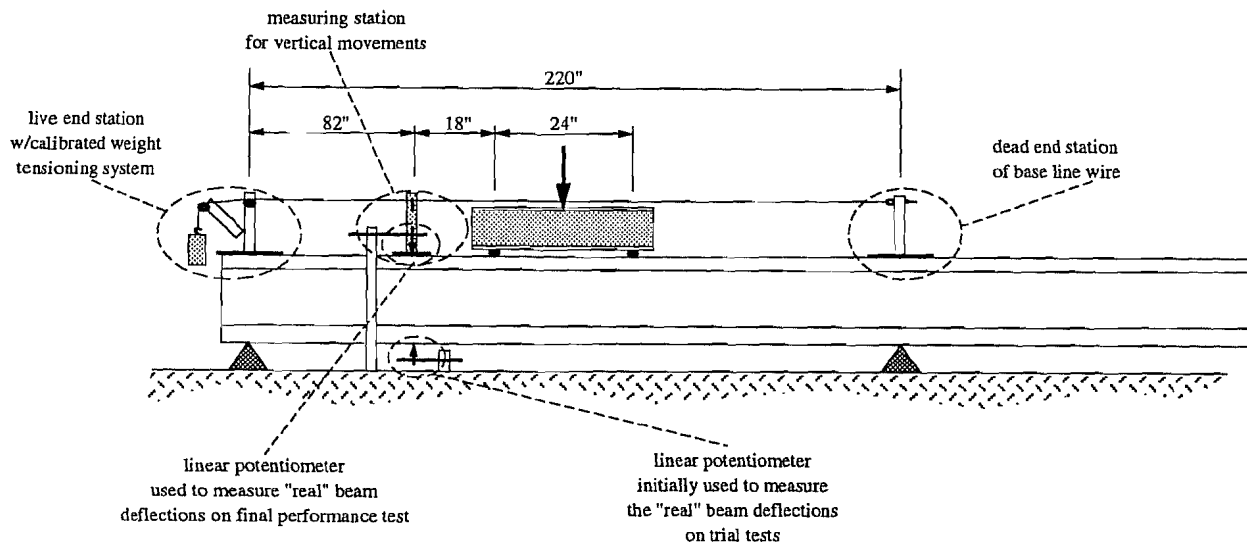


Figure 3.11 Typical short span test setup of deflection measuring systems.

directly above the supports. Four initial trial tests were performed by comparing the deflection system readings against the "real" beam deflections registered by a linear potentiometer automatically scanned with a computer-controlled data-acquisition system. As shown in Figure 3.11, the linear potentiometer of the trial tests measured the deflections of the bottom surface of the girder, directly below the place where the deflection-measuring systems were located. This was possibly not the same deflection as occurred at the top surface of the girder where the deflection systems were installed. However, since all trial tests were performed with the same reference, the errors introduced by the inadequate "real" pot deflection readings were approximately the same in each test.

Finally, these trial tests were also performed on a short-term basis with a maximum duration under two hours. Therefore, no conclusions about the stability of the readings with time could be drawn.

**3.2.1.3 Short-Span Test Results.** The most adequate tension adjusting method of the three types which were similar to Bradberry's consisted of the Type III system shown in Figure 3.8. The performance of this particular system was compared to the constant weight method of Figure 3.9 (system Type IV). Reading errors registered at each measuring stage during the short-span test of system Type III were compared to those of the short-span test of system Type IV. As shown in Figure 3.12, both line tensioning methods provided good levels of short-term accuracy. System Type III showed the single highest reading error of  $|0.021 \text{ inch}|$ . On the other hand, the largest reading error registered by the constant weight method was almost half of that, around  $|0.013 \text{ inch}|$ . Still, these two larger error extremes can be attributed to occasional operator misreadings or a similar type of accidental error. Ignoring the two sporadic

errors, it is highly probable that both systems can achieve about the same level of accuracy. Moreover, the average absolute reading errors for Type III and Type IV were only |0.0052 inch| and |0.0045 inch| respectively.

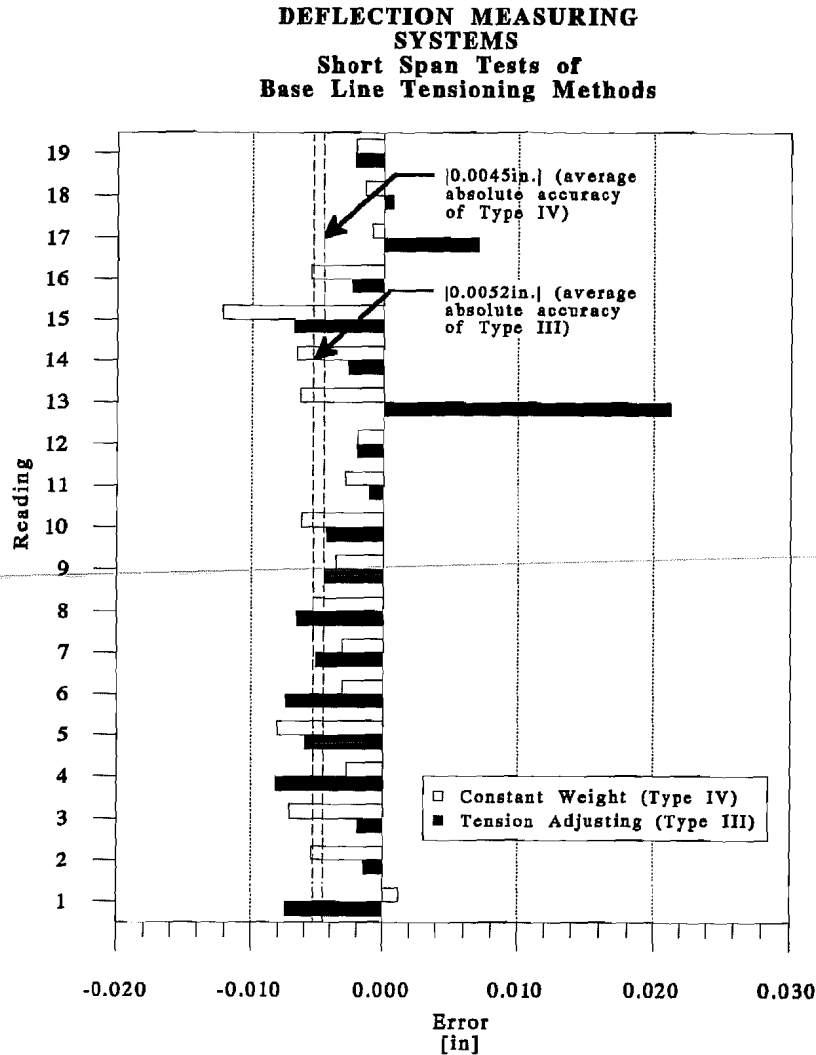


Figure 3.12 Comparison of performances of line tensioning methods.

Due to their resemblance in accuracy levels, installation, and manufacturing costs, the only difference between these two systems was therefore related to the level of difficulty of their tension-adjusting procedures. System Type III required rather tedious procedures for adjusting the tension of the base wire. On the contrary, the constant weight method directly self-adjusted the tension of the wire after each deflection of the girder (provided that the friction in the bearings was small enough to allow for the wire movements to occur). The high-quality sealed bearings were considered to have very low internal friction (enough to allow small movements

to occur). More importantly, they were considered to have only a minimal variation of their friction coefficients with time. This quality of the bearings should therefore ensure a high level of repeatability of readings with time.

The tensioning system Type IV was therefore recommended as the most adequate method for the baseline method of measurements of vertical deflections in box girder bridges. General recommendations about their manufacturing, installation, and use are included in Section 3.3.

**3.2.2 Reading Systems.** Once again, the two different reading systems used by Bradberry<sup>11</sup> and Pauw-Breen<sup>38</sup> were the basic systems tested and modified during the present laboratory investigations.

Bradberry's reading system was a small piece of a stainless steel high precision ruler bonded next to a similarly sized mirror. The mirror helped to accurately reproduce the same reading reference in the ruler (by taking each measurement when the base wire's image in the mirror was covered by the wire itself). This reading system was enhanced in the present project by purchasing stainless steel rulers with 1/100-inch divisions. This barely-perceptible level of reading resolution could be achieved by consistently reading the ruler mark defined by the top (or bottom) of the base wire, after proper alignment of the mirror image. However, the disadvantage of this method was the high occurrence of accidental reading errors. These were mainly due to the confusion associated with counting the number of 1/100-inch divisions to each reading mark. Another concern was related to the time and effort required for recording each deflection, which involved careful concentration and single-eye sighting.

In an ideal situation, the accuracy of the reading system based on the ruler and mirror assembly can only be improved to the lowest visible divisions of the ruler. Estimations of the 5/1000-inch divisions of a ruler are highly unlikely to be visible, unless a system of magnifying glasses is used. And even then, the error would be transferred to the variations of the reference level (since the mirror image of the wire can probably move (unnoticeably) more than 5/1000 inch). This limitation of the ideal system based on the ruler and mirror assembly inspired the investigators to examine other reading devices that can allow more accurate ideal determinations of the position of the base wire.

Pauw-Breen used a reading unit made of a ruler coupled with a vernier scale that reached measurement accuracies of 1/1000 inch.<sup>38</sup> The present investigators modernized this 1959 system model by replacing the old ruler by a currently available digital scale providing reading resolutions of 5/10,000 inch. The ruler used was a *Mitutoyo Digital Scale* with an 8-inch gage length. An aluminum extension arm was machined to fit a pair of screw holes existing in the moving part of the digital scale. This extension arm helped reach the location of the base wire, and its wide section allowed enough room for accidental lateral misalignments of the wire. The digital ruler with the fixed extension arm was tightly mounted to a 1-inch x 1-inch x 13-inch steel tube and a steel base. This deflection meter assembly would be expensive if it had to be permanently positioned at each reading station of each instrumented span. The digital scale alone was priced at \$150.00 in 1991. An alternative was to use a leveling base similar to that

in Pauw & Breen's portable deflection meter.<sup>38</sup> This base was made with two fixed screws and one leveling screw that worked in conjunction with a bubble level. However, the bubble level can substantially decrease the accuracy of the readings. Also, the leveling process of the meter at each measuring station can take long periods of time. A magnetic base was thus envisioned as a possible solution for the problems of accuracy and installation time. The foot of the steel tubing of the reading unit assembly (with the attached digital scale) was bolted to a strong magnet. The benchmark reading stations were therefore simplified to 4-inch x 4-inch x ½-inch square steel base plates secured to the concrete surface by four anchor bolts. A pair of guides were welded to the steel bases to reproduce the exact positioning of the magnets at each reading operation. The final system investigated is illustrated in Figures 3.13 and 3.14.

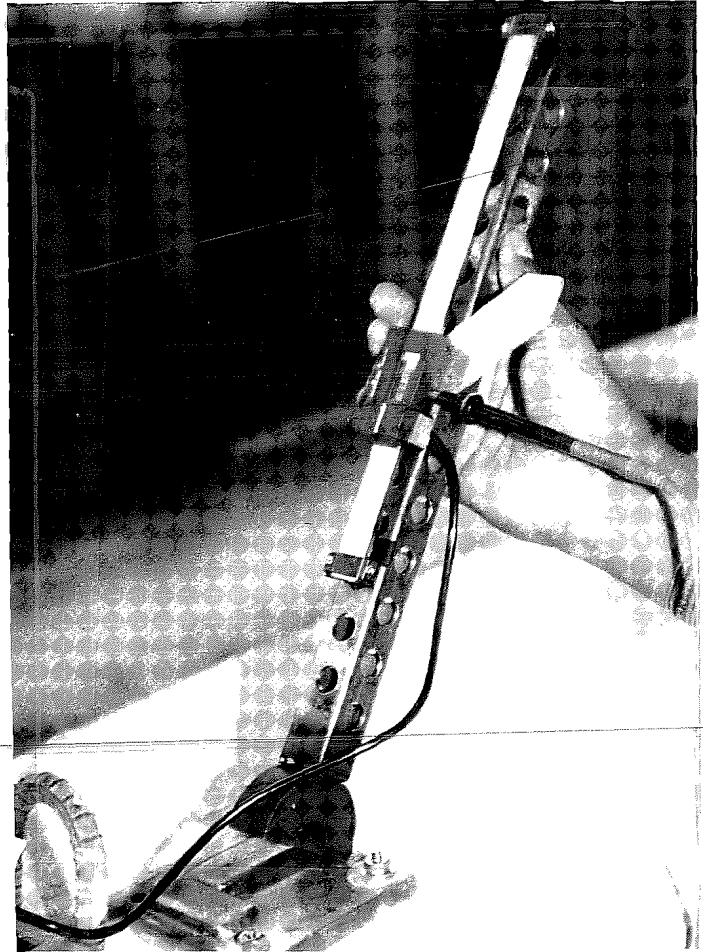


Figure 3.13 Portable reading unit of deflection measuring system (during installation to reading position).

The next problem encountered with the new digital deflection system was the difficulty in determining the exact moment when the extension arm of the scale "touched" the base wire. Small digital scale-induced pressure movements of 5/10,000 inch or even 1/1,000 inch of the base wire were easy to randomly produce from one reading to another. A consistent method for determining the exact moment when the scale touched the base wire was therefore needed. One solution that was successfully tested consisted of using a beeping sound that determined the electrical contact between the ruler's extension arm and the baseline wire. This was an easy solution that only required the installation of a small electrical wire extending from the dead or live end station to a place near each measuring station. One terminal of a standard hand-held voltmeter was connected to the reading unit assembly and the other terminal to the wire that was stretched to the live end station. When the reading unit assembly made contact with the baseline wire, a beep signaling the electrical shorting was produced by the voltmeter.

A final improvement in the deflection meter was the use of a semi-automated readout processor electrically connected to the digital scale. Digital scale manufacturers provide a mini-

processor that can store and print all readings of their digital scales by pressing a sensitive control switch located either at the scale or at the processor. This instrument is highly recommended for projects involving extensive deflection measurements because it provides several advantages:

- decreases the time necessary for sighting a reading and writing it on paper,
- can automatically store up to 11 readings from one single measuring position and print their statistical average (including maxima, minima, coefficients of variation, mean value, and standard deviation),
- eliminates reading errors of the operator (and errors due to illegible notes), and
- is battery operated and can be easily hand carried for field measurements.

The only disadvantage of the mini-processor is its cost. The *Mitutoyo Mini Processor BDP-100*, was priced at \$415.00 in July of 1991.

**3.2.3 Short-Span Performance of Final System.** The performance of the final version of the baseline system with the digital scale, the magnetic base, and the electrical system for determining contact of wire and meter was evaluated in a final short-span test. To check the accuracy of the readings, a linear potentiometer was installed next to the deflection meter station (as previously illustrated in Figure 3.11). The overall performance of the deflection meter during the complete loading test of the girder was compared to that of the linear potentiometer (which was automatically scanned with a computer-controlled data-acquisition system). The result of this overall performance check is shown in

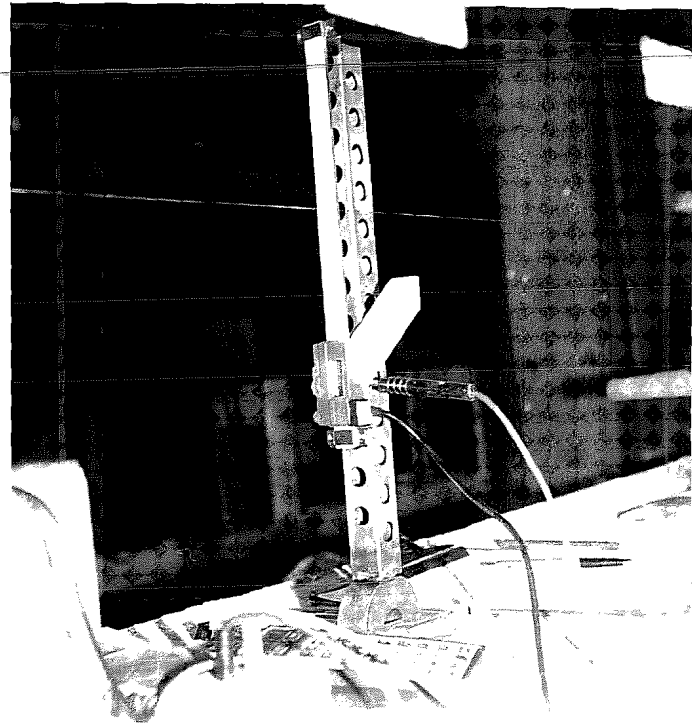


Figure 3.14 Portable reading unit of deflection measuring system (located in reading position).



Figure 3.15. Comparisons of each measurement obtained by the deflection meter with the corresponding value from the linear potentiometer (considered as the "real" deflection) gives an idea of the final accuracy of the modified baseline system. The result from this comparison is included in Figure 3.16. The highest reading error was  $|0.0082 \text{ inch}|$  in the 14th reading. However, an average of the absolute reading errors indicates  $|0.0024\text{-inch}|$  errors for each reading operation.

Another noticeable behavior discovered by examining Figure 3.16 is the occurrence of the consistent errors for the last four readings. These readings corresponded to girder deflections higher than 0.5 inch at the instrumented cross-section. A possible cause of these errors is the slight rotational movements experienced by the base plate of the reading station. As the girder deflected, the 4-inch x 4-inch steel base plate approximately moved tangent to the deflected shape of the girder at the instrumented section. The portable digital scale assembly was therefore installed at a small angle away from the vertical position when high levels of deflections occurred at the girder's cross-section. These errors are highly related to the maximum range of deflections to be experienced by the instrumented girder or span. It is concluded that the smaller the vertical movements of the instrumented station, the higher the level of accuracy of the measuring system, and vice versa, higher movements should produce smaller accuracies. Still, as shown by this short-span performance test, the maximum error of measurements taken beyond the cracking load of the concrete girder was well below the 1/100 inch desired accuracy level.

The short-term repeatability of measurements taken by two different operators during this short-span test was also investigated. The absolute differences between immediate readings taken by the different operators are included in Figure 3.17. It can be seen that the average error was only  $|2/1000 \text{ inch}|$ . However, the highest repeatability error reached the  $|5/1000 \text{ inch}|$  level.

After examining the results of the final short-span test it was concluded that the deflection measuring system provides an accuracy level that is much more sensitive than the desired 1/100 inch.

**3.2.4 Field Performance Test of Final System.** The last testing stage of the suggested baseline system was performed at a finished 100-foot typical span of Phase I-C of the San Antonio Y project. The overall accuracy of the deflection system was not addressed due to the difficulty for monitoring comparable "real" deflections of the structure. However, the field test was performed to indicate any other possible problems not envisioned during the installation and operation of the system.

Researchers evaluated the typical amount of time required for system installation, and for measuring span deflections at quarter- and mid-span stations. At the same time, the repeatability and the stability of the deflection readings were also investigated. These became a concern due to the longer spans of baseline wire required for field measurements in actual bridges.

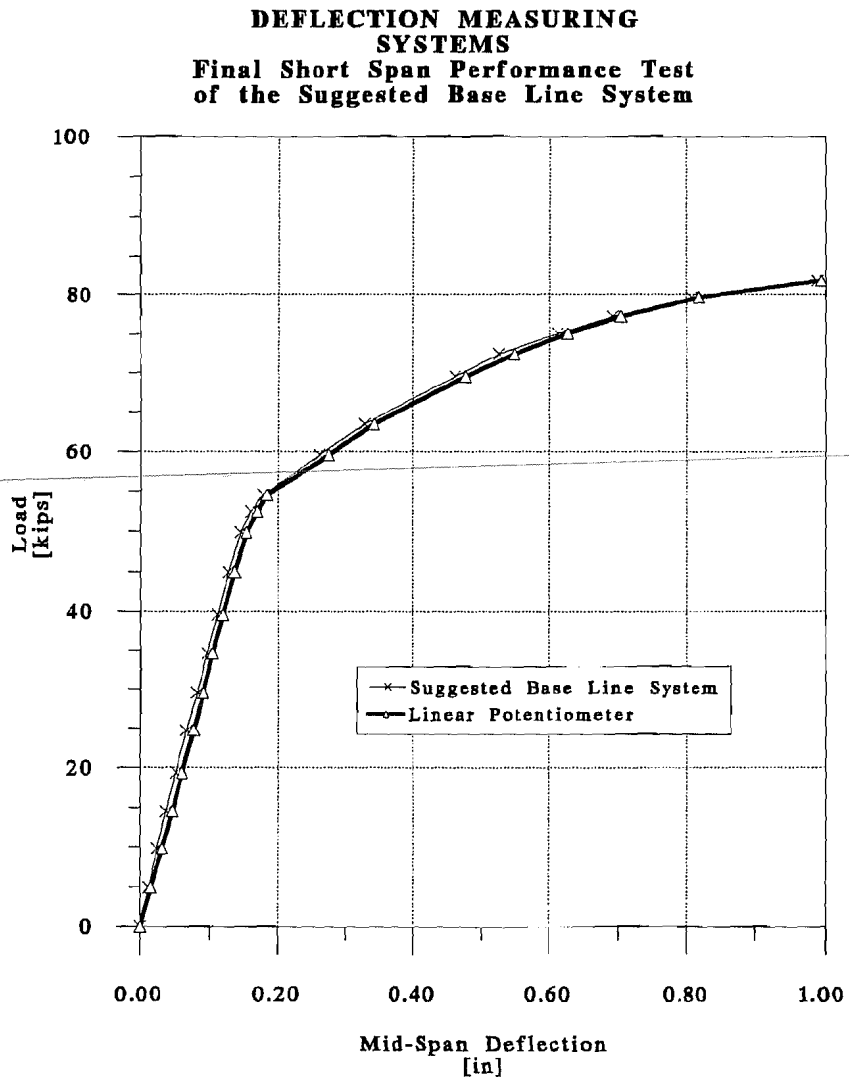


Figure 3.15 Overall performance of final deflection measuring system during short-span test.

**DEFLECTION MEASURING  
SYSTEMS  
Final Short Span Performance Test  
of the Suggested Base Line System**

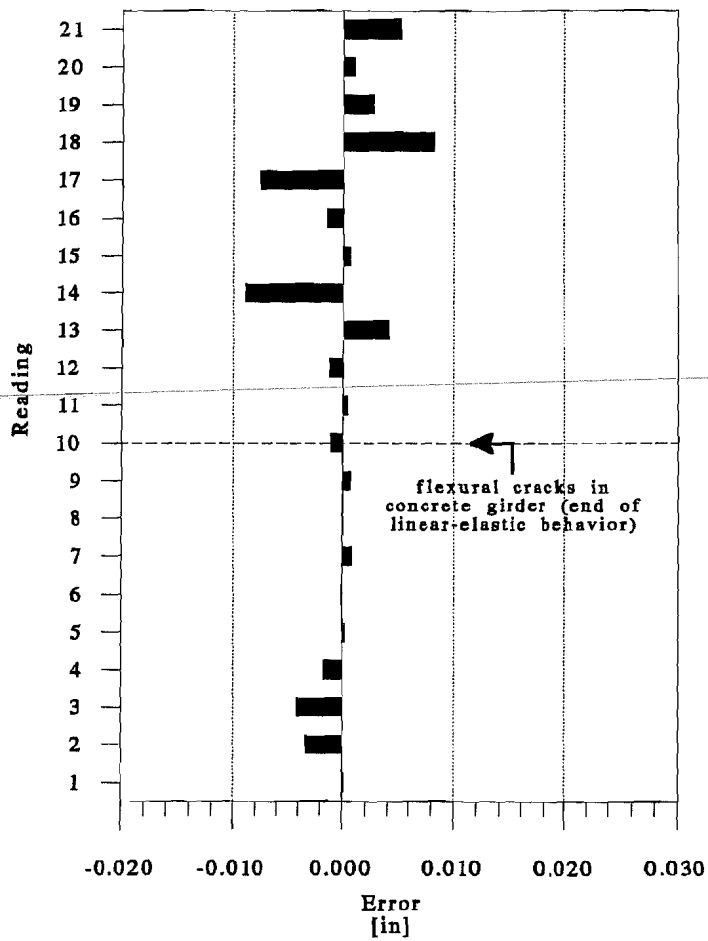


Figure 3.16 Reading errors of final deflection measuring system during short-span tests.

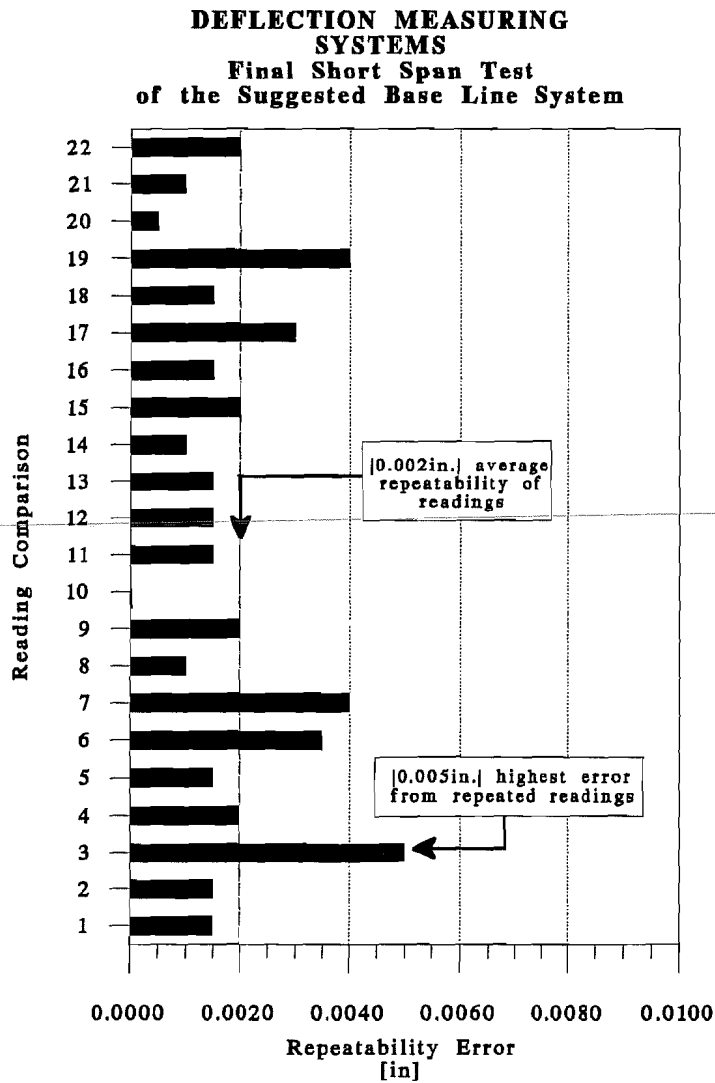


Figure 3.17 Repeatability errors of final deflection measuring system during short-span test using two different operators.

**3.2.4.1 Installation and Operation.** The system setup inside the concrete box girder bridge is illustrated in Figure 3.18. The instrumented span (C-35 of Project I-C) was the first one of six continuous spans. A secondary factor influencing the selection of this particular span was the interest in investigating the trend of vertical movements caused by subsequent stressing of the other continuous spans.

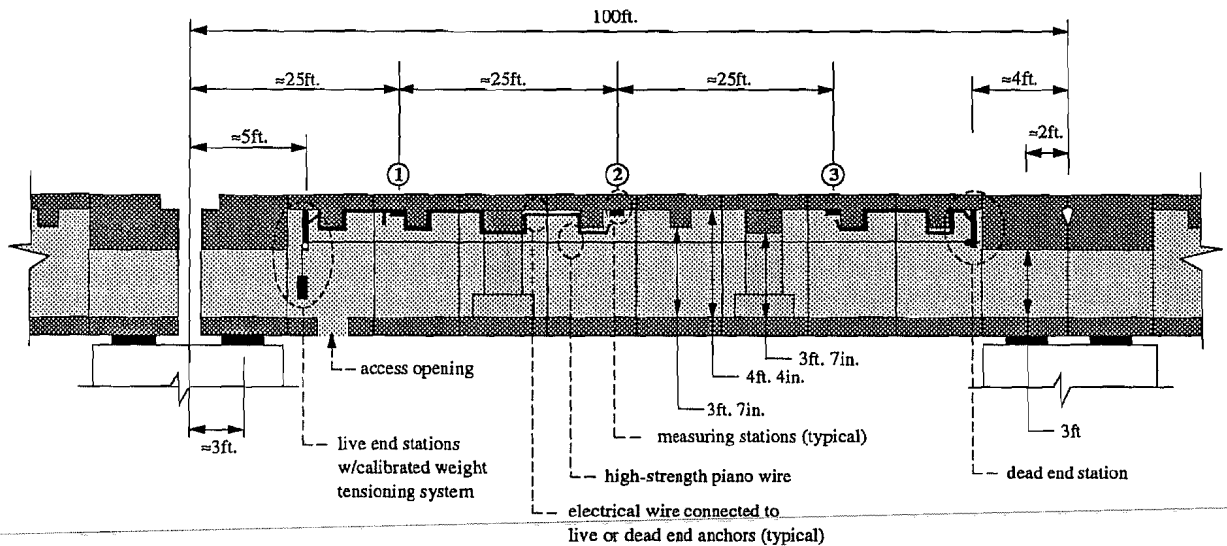


Figure 3.18 System setup inside box girder bridge.

The base plates of the reading stations (with the welded guides for correct positioning of the portable reading unit) were installed on the bottom (inner) surface of the top deck slabs of selected box girder segments, at the approximate distances shown in Figure 3.18. The plates consisted of 4-inch x 4-inch x 3/8-inch steel squares with four 5/16-inch holes drilled at their corners. The plates were fixed to the structure by special 1/4"  $\phi$  x 2.25-inch stainless steel mechanical anchors (manufactured by *Hilti*, of the type *Kwik Bolt II*, *AISI 304 & 316 Stainless Steel*, with 3/4-inch thread length and requiring one inch of embedment length in concrete).

Drilling of high-strength concrete was easily achieved with a concrete vibrating drill and special tungsten carbide drill bits. The initial use of regular drill bits was terminated since this considerably increased the installation efforts. Furthermore, regular drill bits only lasted for 3 or 4 drilling operations in high-strength concrete.

Live and dead end anchor assemblies were welded to their steel base plates and were permanently installed on the instrumented structure. The steel bases were similar to those used at the reading stations. The live and dead end anchors were not installed directly above the supports in this trial application (as shown in Figure 3.18) because they were designed for pier segments with larger height clearances. An electrical wire was connected from the live end

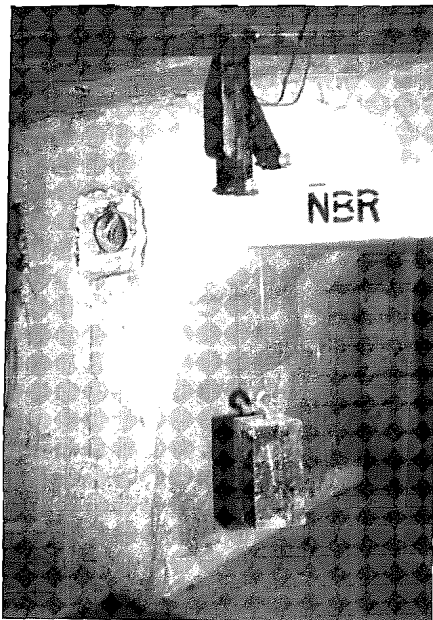


Figure 3.19 Live end anchor and calibrated weight inside the box girder bridge.



Figure 3.20 Digital scale measuring unit, mini-printer-processor, and voltmeter during sample reading operation inside box girder bridge.

station to places near each measuring station. This was part of the mechanism that helped determine the time of contact of the baseline wire and the extension arm of the digital scale.

Illustrations of the live end bracket assembly with the calibrated weight, and of a sample reading operation inside the box girder bridge are shown in Figures 3.19 and 3.20 respectively.

Despite the inconveniences produced by the small clearances existing inside the box girder segments (shown in Figures 3.18 and 3.20), the complete installation and the initial check of operation of the system was finished in approximately three hours.

**3.2.4.2 Measuring Times.** The components of the deflection system that were permanently left on-site were the live and dead end anchors, and the steel bases of each measuring station. Each reading day therefore required the following operations:

- Installation of the piano wire from dead end to live end station, where it was connected to the calibrated weight and hung on bearing guides.

- Translation of hand-held voltmeter, portable reading unit, and mini-processor-printer (optional) to location of each one of the three reading stations.
- Connection of the terminals of the voltmeter. One to the reading unit, and the other one to the "live" wire located next to each reading station (and connected to the live end station).
- Recording of readings from each one of the three stations.

Two operators (individually and in pairs) performed the outlined measuring day procedures on the single instrumented span. For a single operator, the total time employed varied from 18 minutes to 35 minutes. However, when a pair of operators worked together, the total time employed ranged from 9 minutes to 15 minutes.

One frequently difficult and time-consuming operation consisted of the installation of the piano wire from the dead end to the live end station. Unwinding long lengths of piano wire inside a box girder bridge with low vertical clearance was difficult. However, this initial problem was later avoided by installing proper lengths of piano wire on a large diameter reel built in the laboratory. The piano wire was not left on-site between measurements to avoid problems with the construction crew, and to avoid wire corrosion. The low clearance inside the instrumented box girder segments also contributed to increasing the total measuring time, and the effort required for moving along the span.

A decrease of the total reading time was provided by the mini-processor-printer, since it allowed for direct recording of several measurements at each reading station. This in turn produced more accurate reading averages and almost completely avoided reading errors from the operators.

In conclusion, the total time required for wire installation and recording of measurements at three stations of one 100-foot span averaged 12 minutes and 28 minutes for two operators and one operator respectively. This provided that operators used properly-coiled lengths of piano wire along with a mini-processor-printer.

**3.2.4.3 Repeatability of Readings.** After installing the deflection measuring system, the first investigation was to determine the accuracy at which measurements were repeated from one operator to another. For this purpose, the first operator took deflection readings of all three stations and immediately transferred the equipment to the second operator. An average of 15 minutes transpired between the first and the last reading of each station. No significant variation of the deflected shape of the instrumented span should have occurred in such a small lapse of time. The differences between each corresponding pair of measurements were therefore considered as repeatability errors of the system. Figure 3.21 shows the repeatability errors obtained from a comparison of 18 measurements. As expected, most of the largest errors from each measurement day were obtained at the mid-span station. However, the maximum error of

**DEFLECTION MEASURING SYSTEMS**  
**Field Test of Suggested Base Line System**

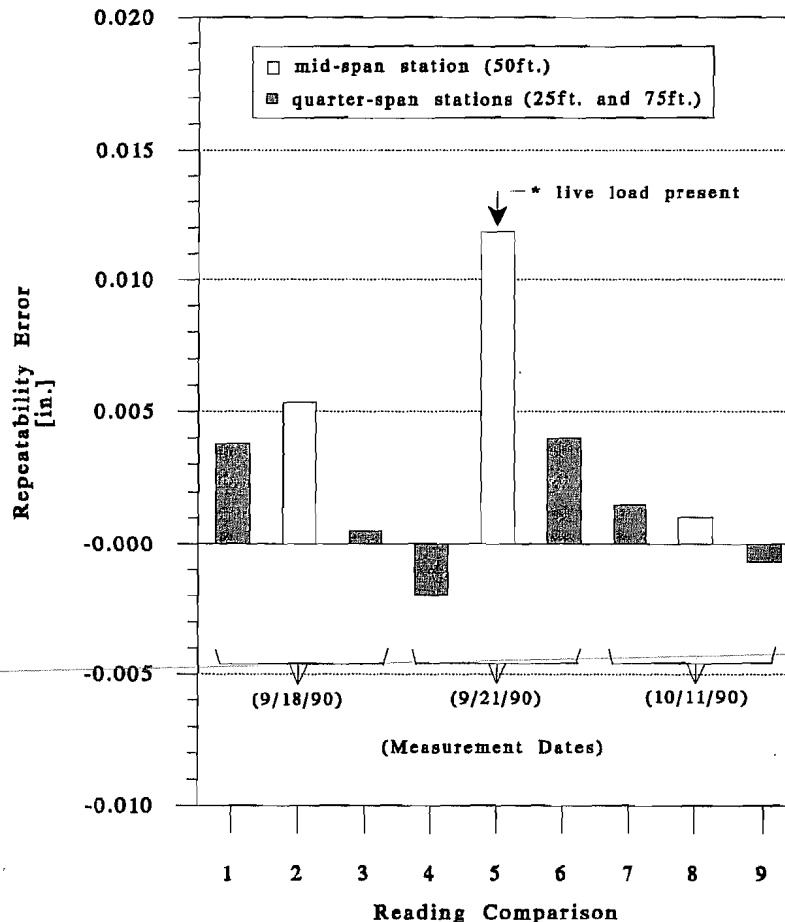


Figure 3.21 Repeatability of errors of final deflection measuring system during field test.

|0.0118 inch| obtained in the fifth reading comparison was believed to have been caused by a different source. A heavy-construction forklift was operating on top of the finished span, near the mid-span station, when the initial readings were taken. The machinery was not present during the station readings of the second operator. Ignoring this accidental error, the next poorest repeatable deflection reading only showed  $\approx$  |5/1000-inch| maximum disagreement. This is an acceptable degree of repeatability, and the recommended deflection measuring system is thus considered to be capable of determining 1/100-inch movements.

Although far from "perfect," practice does improve the accuracy of the measurements. The last set of readings performed by the same operators indicated a much lower average error. It is therefore important to develop the experience of the operators by making them follow well-defined standards while performing some initial sample measurements.



Observing Figure 3.21 and ignoring the reading discrepancy due to the live load, the next largest repeatability error occurred from comparisons of the mid-span measurements. These were evidently caused by the inaccurate determinations of the time when the deflection meter touched the base wire. The electrical-short-induced beeping of the voltmeter did not perform very efficiently. Furthermore, before the 10/11/90 set of readings in Figure 3.21, it was found that a new and unexpected electrical circuit existed between the live and dead end stations and each one of the anchor bolts of the measuring stations. This prevented the use of the voltmeter beeping system, and the readings were taken by sighting with one eye the instant when the extension arm of the digital scale touched the base wire. The |0.0015-inch| repeatability of these measurements was surprisingly high (see Figure 3.21). However, much more careful and time-consuming readings were necessary to be performed to obtain such high levels of repeatability.

It is still unknown what particular event caused the electrical shorting between the different stations. Although unlikely to occur, it is possible that each one of the anchored bolts of each one of the stations were embedded too deep in the segments and just reached the reinforcing bars. All of the bars of each segment have an electrical connection to each other. On the first two days of testing the segments were electrically isolated. However, on the third test day it seemed that the segments were probably electrically connected to the other segments at the time of installation of the metallic side railings along the wingtips at the top of the instrumented span. To prevent this problem, it is recommended that the anchors of each base plate be embedded to between 3/4 inch and 7/8 inch instead of the one-inch embedment length used in the trial field test.

**3.2.4.4 Stability of Readings.** It was beyond the budget of this study to prepare an accurate and stable system for measuring more "realistic" span deflections at the same locations of the measuring stations of the baseline system. This was mainly because the accuracy of the comparable system would at least have to be better and more repeatable than the 5/1000-inch short-span accuracy of the baseline system. No comparable measurements were therefore made to evaluate the long-span accuracy of the deflection system under investigation.

However, deflection measurements of the instrumented span were taken after each stressing operation of the following five continuous spans. Final measurements were also taken at 80 days after the erection of the instrumented span to verify the stability of the deflection measuring system.

To have some base of reference for the adequacy of the trend of measured vertical movements of the instrumented span, TxDOT engineers performed a detailed computer analysis of the span and provided their results to the researchers. A graphical comparison of the measured and calculated deflection values at each instrumented station and after each specific construction operation is included in Figures 3.22a and 3.22b. Readings taken after stressing of the instrumented span C-35 were considered as the reference shape for all future readings. Similarly, the calculated shape after stressing of the instrumented span was also taken as reference for further calculated values of span deflections.

**Vertical Movements of Span C-35**

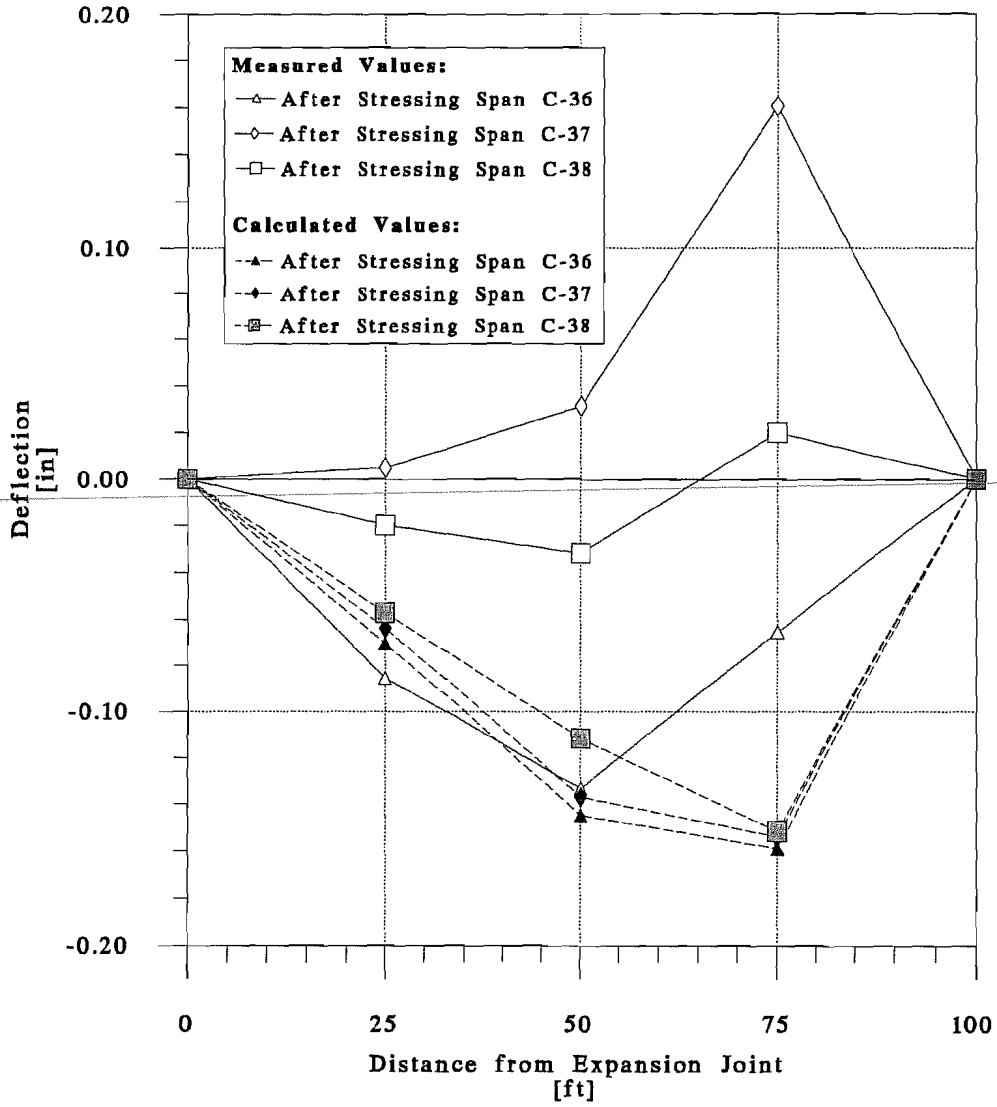


Figure 3.22a Measured and calculated deflections of span C-35.

### Vertical Movements of Span C-35

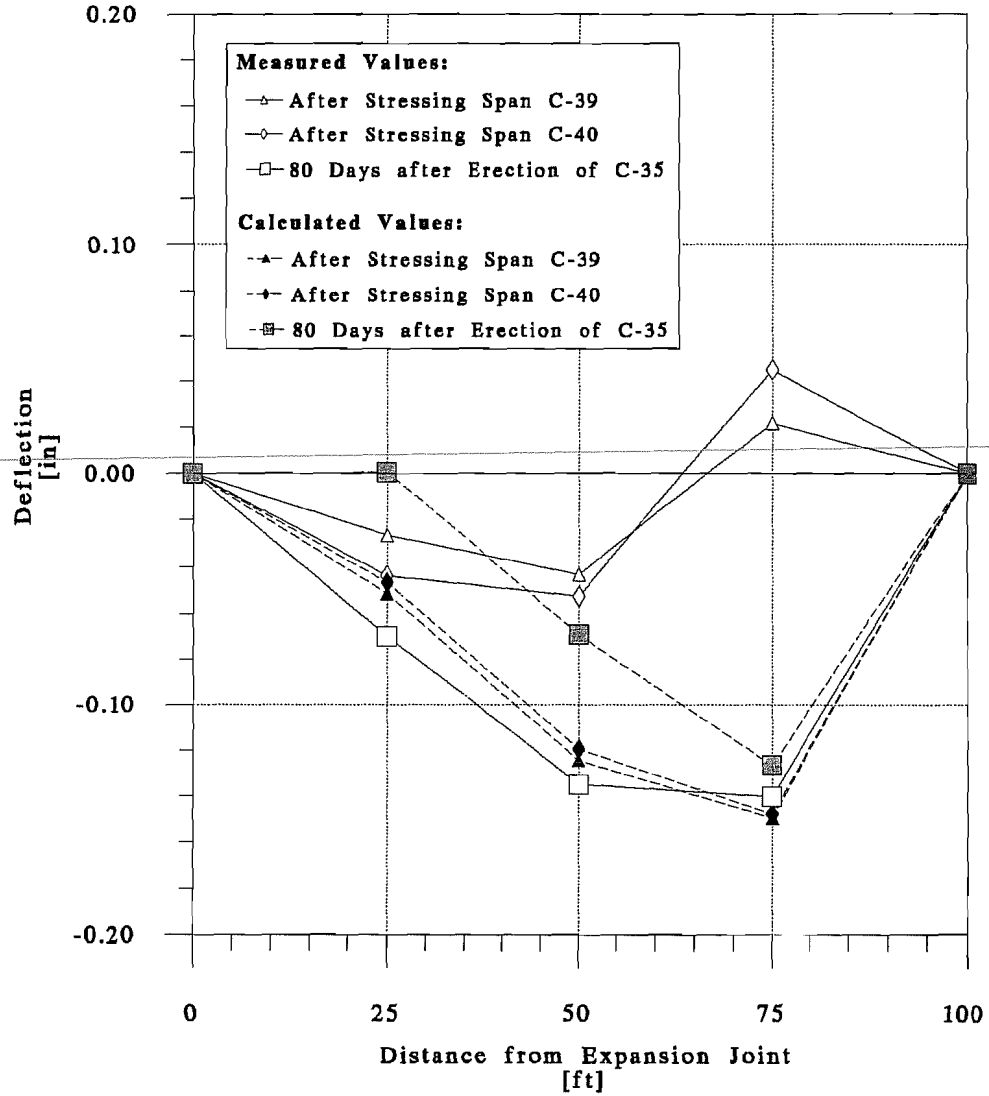


Figure 3.22b Measured and calculated deflections of span C-35.

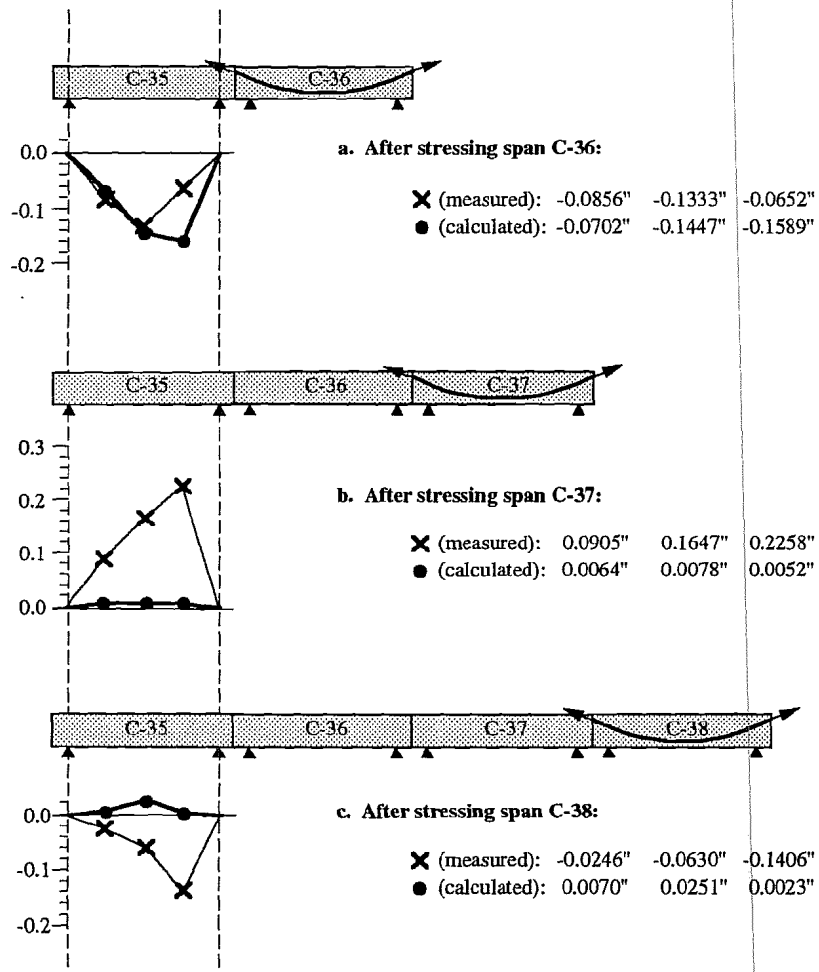
Despite the initial readings after stressing of the first continuous span (C-36), all the other measurements taken after erection of the following continuous spans showed noticeable discrepancies with the calculated estimates. At 80 days after erection of span C-35 though, the calculated values were once again close to the measured deflections. This was an interesting indication of a probable good performance of the deflection measuring system over an extended period of time. Furthermore, if the field measurements were indeed accurate, they also indicated a relatively good prediction of 80-day deflections by the analytical method used by TxDOT's designers. However, considerable differences between calculated and measured deflections were noticed between erection stages of continuous spans. Part of these differences were induced by predicted small vertical movements of the reference line. These movements were produced because the live and dead end anchors of the base wire were not installed directly above the supports. Also, the exact position of the wire at the live and dead ends was not checked.

Another source of errors could have been produced by temperature-induced vertical movements of the instrumented span. However, the field measurements corresponding to the erection stages of all continuous spans were approximately taken at the same time of the day and under similar ambient temperatures. The widest temperature difference occurred with the 80-day measurements that were taken at a lower ambient temperature.

To help determine the relevance of the predicted and measured deflection values, more graphical comparison plots are included in Figures 3.23a and 3.23b. Each vertical movement produced by a determined construction stage was plotted using as a reference the previously measured and calculated deflected shape of the instrumented span. Only comparison of vertical movements from the previous values are therefore plotted in Figures 3.23a and 3.23b. The graphics help one understand the overall adequacy of the trend followed by the measured vertical movements. They also show the slight inconsistency of the calculated values with the construction operation. The dead end bracket was located closest to Span C-36. The measurements indicate that the position of the knot at the dead end was varying as much as  $\pm 0.25$  inch. This indicates the importance of measuring the wire height immediately adjacent to the dead end.

Factors influencing the long-term performance of the baseline method were also investigated. Corrosion of the base plates at the measuring station was considered to be an important possible source of future problems. The final plates were therefore designed with non-corrosive *17-4 Stainless Steel*. Regular stainless steel plates were not used because these are not magnetic and would have not been compatible with the magnetic portable measuring unit. However, the bases of the live and dead end stations were designed with regular stainless steel plates.

Accidental damage of the dead or live end stations is possible during construction stages when different crews must travel inside the box girder segments. Each one of these stations -



**Note:**  
 Each set of values represents vertical movements from the previously measured and calculated shapes.

Figure 3.23a Measured and calculated vertical movements of span C-35 at different construction stages.

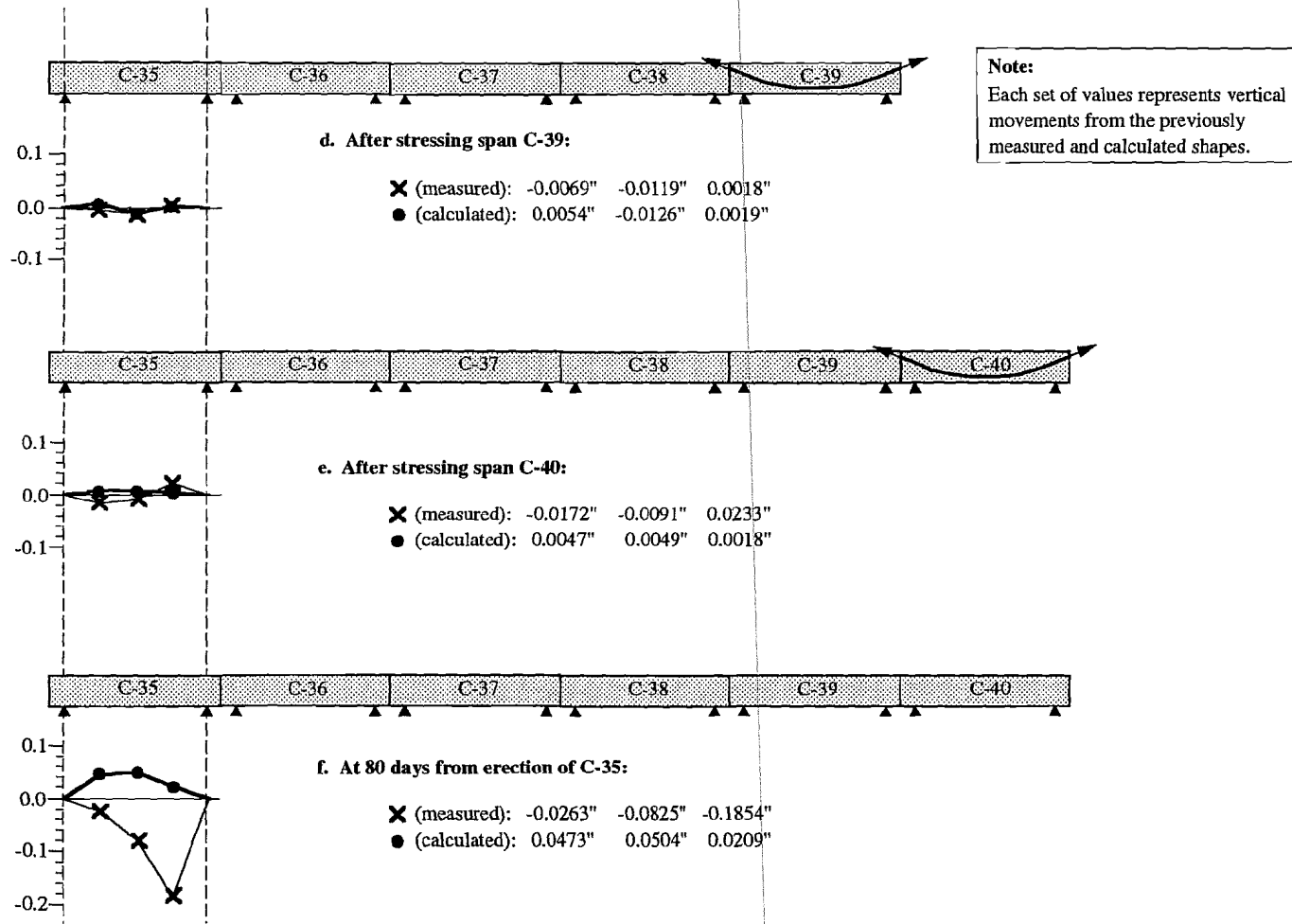


Figure 3.23b Measured and calculated vertical movements of span C-35 at different construction stages.

which are permanently left on site - was therefore designed to be attached to the concrete with four strong mechanical anchor bolts that can also be installed with epoxy as an added factor of stability.

The final factor influencing the long-term stability of readings is the possible physical damage of the portable reading unit with the digital scale. Any accidental movement of the extension arm attached to the digital scale will produce considerable errors. This unit should thus be carefully handled and stored. In addition, a reference calibrator should be constructed so that if a new unit must be made, readings can be transferred.

In conclusion, the deflection measuring system designed for field use in selected fully-instrumented spans of the San Antonio Y project is accurate and assumed to be stable for long-term readings. The approximate short-term accuracy of the selected system is expected to be »5/1000 inch. It is also considered possible to get close to a 1/100-inch accuracy level for medium-term readings of a few years. The system accuracy would be improved and reliability further assured if deflection measurements were also made at the dead and live end stations. It is possible that the disagreement between measured and calculated deformations in Figure 3.23 was due to a shifting of the wire elevation at the right end of the baseline. A more positive test was obtained from the actual field readings.

### 3.3 Recommendations

The method suggested for performing this type of field measurement was designed in this research program based on improvements of a previously developed system. The baseline system suggested by Pauw-Breen<sup>38</sup> in 1959 was ideal for the present instrumentation program since it complied with most of the initial requirements. The main advantages of the final version of the baseline system are:

- economical,
- easy to manufacture, install, and operate,
- accurate,
- good short- to medium-term stability, and
- simple technology.

Tests of this system were performed in laboratory-controlled conditions on short spans of up to 22-foot lengths. A final test was performed inside a selected 100-foot span of the San Antonio Y structure. Results from these trial tests were included in Section 3.2. A final description of the baseline system, and important suggestions for its proper selection, installation, and operation are included here.

**3.3.1 System Description and Selection.** The basic technology of the baseline method for measuring span deflections in bridges is very simple. It consists of measuring vertical movements of selected points of a span with respect to a reference line strung between the

abutments (or between locations just above the supports). A general description of the considerations that must be taken when designing each one of these components is included here.

**3.3.1.1 Baselines.** High-strength piano wire is suggested to be used as the reference line for this type of measurement. Sizing of the piano wire is closely related to the span length of the structure to be instrumented. Piano wires are usually sold in 0.5-pound rolls, so larger diameter wires have shorter lengths. For example, the maximum length of wires sold in 0.0310"  $\phi$  is  $\approx$  200 feet and for 0.0170"  $\phi$  is  $\approx$  650 feet. If the particular span to be instrumented is considerably longer than 110 feet, say beyond 200 feet, the proposed measurement system would need to be re-evaluated in terms of accuracy and repeatability of readings. The experience of the research team suggests that a 1/100-inch level of repeatability and accuracy can still be obtained with spans up to 200-foot length. Even for longer spans, it is likely that this system provides a better degree of accuracy than the traditional surveying methods.

A secondary factor regulating the ideal size of the piano wire is the portability of the calibrated weight that is hung at the live end (and used for stressing the wire). It is recommended to stress the piano wire to a level around 90% of its breaking strength. This is desired since small fluctuations of such a high level of stress should not provide any measurable variations in the catenary shape of the free length of the piano wire. To impose this level of stress in a piano wire requires heavy loads at the live end, for instance, the 0.0310"  $\phi$  wire needs  $\approx$  122 pounds to reach 90% of its breaking strength. This kind of load is obviously difficult to handle and also requires strong anchorages for the live and dead end stations.

Consideration of both of these factors (the free length of the wire and the calibrated load) influenced the decision for recommending the 0.017"  $\phi$  piano wires. These are sold in  $\approx$  650-foot lengths and only need a 37-pound weight to be stressed to 90% of the breaking strength. In the U.S., the place to purchase them is: *Schaff Piano Supply Co.*; located at: 451 Oakwood Rd., Lake Zurich, Illinois; Zip Code: 60047. The cost of piano wires is not a concern. As an example, in late 1990 each 0.5-pound roll of 0.031"  $\phi$  piano wire was purchased for \$3.70.

**3.3.1.2 Live End Stations.** These are composed of steel base plates, steel columns, and sealed bearings. Smaller bases are preferred to minimize the rotational movements produced by the span deflections. When large span deflections occur (usually only during ultimate strength tests performed in a laboratory, or during service load tests performed in the field), small errors are introduced by the rotation of the base plates. However, using the same size plates at the live and dead end anchors, and installing them directly above the supports should help decrease these errors. A suggested size for the base plates at both end anchors is 4-inch x 4-inch x 3/8-inch with 4-1/4"  $\phi$  holes drilled at their corners (for installation of the concrete anchorage bolts). These plates are recommended to be made of stainless steel members to avoid long-term corrosion problems.

The steel columns of the live ends should be made of regular steel tubing cut at variable heights. Square tubing of 1 inch x 1 inch (with  $\approx$  1/8-inch thickness) is recommended. Column stiffener plates can also be used to assure that the columns are not bent by the tension of the



base wire. The height of the tubing depends on the particular geometry of the span to be instrumented. For instance, the steel tubing at the dead end station of span A-44 had to be designed shorter than the other stations due to the increased thickness of the top deck slab at the expansion joint segment. Whenever possible, it is suggested to minimize the height of steel columns to decrease the errors attributed to rotations of the base plates. The steel tubes and optional stiffeners are recommended to be permanently welded to the base plates to avoid any accidental movements while left on site during construction operations. For this particular process, special stainless steel welding rods must be used (since the base plates are made of regular stainless steel).

The roller bearings are recommended to be of the sealed type to prevent friction variations with time. They should be tightly bolted to the steel columns. However, they should not be installed permanently to allow for their possible replacement in the future. An important characteristic of these bearings is that they should be grooved at the center of their outer circumference. These grooves should have  $\approx 1/16$ -inch depth and no more than  $1/16$ -inch width. They are recommended (one on each bearing) to serve as guides for the positioning of the base wires.

As mentioned earlier, the calibrated weights used to impose the proper level of stress to the base wires at the live end stations need to stress the wires to about 90% of their ultimate strength. A second condition in the design of these weights is that they should have a hook or a similar device helping to effectively anchor the piano wires.

**3.3.1.3 Dead End Stations.** These are similar to the live end stations, with the main difference that the bearings are replaced by a steel bolt with a circular loop at one end. This loop is ideal for anchoring the piano wire. An important consideration here is related to the type of knot used to anchor the piano wire to the steel loop. The traditional "fisherman's knot" worked the best in the trial tests with  $0.017''\phi$  wires and is therefore recommended. Furthermore, to avoid having small vertical variations of the place where the piano wire is anchored to the dead end loop, it is strongly suggested to machine some small grooved guides at the dead end anchors.

**3.3.1.4 Reading Stations.** These are 4-inch x 4-inch x  $1/4$ -inch square plates of a special steel used as bases for the portable reading units. Small steel tabs are suggested to be welded to the top surface of these steel plates to serve as reference guides for the magnet of the portable reading unit. Four  $1/4''\phi$  holes should also be drilled at each plate's corners for proper anchoring to the concrete. Another important characteristic related to these plates is that they cannot be made of regular stainless steel because it is not magnetic. As a solution, these plates should be made of *17-4 Stainless Steel* that is characterized by being magnetic and non-corrosive.

**3.3.1.5 Portable Reading Units.** These are made of a digital scale, a magnet, and a steel mounting column. The digital scales are recommended to have a  $5/10,000$ -inch resolution to obtain better levels of accuracy. A vernier adjustment would definitely improve the adequacy

of the scale, however, it is not imperative (since a 5/1000-inch accuracy was already obtained without a vernier micrometer). Digital scales of high resolution (at  $\approx$  8-inch lengths) are expensive. The scale to be used in the San Antonio Y instrumentation project is an 8-inch *Mitutoyo Digital Scale* priced at \$150.00 in July of 1991. Other digital scales of better accuracy are also available but at higher cost. For instance, *Swiss Precision Instruments, Inc.* offers the *Digital Height Gages* of 12-inch, 18-inch, and 24-inch lengths, and with 5/10,000-inch accuracy levels for \$468.00, \$676.00 and \$815.00 respectively (priced in late 1990). These types of gages are specifically made for baseline type of measurements and come with pre-attached extension arms and solid steel bases.

The digital scales (not purchased pre-assembled to a base and extension arm assembly, as in the case of the *Digital Height Gages*) should be tightly mounted (not permanently welded) to a steel column of the proper height. If solid, the weight of the steel column should be "lightened" by drilling several holes on all faces of the steel tubing. This is recommended as a method to decrease the downward force exerted by the weight of the portable unit on the magnetic bond system used at its base. An aluminum extension arm is also suggested to be mounted to the digital scale to allow for a wider range of lateral movements of the piano wire.

A strong magnet is suggested to be bolted to the base of the steel column. This method of securing the portable reading units to each reading station decreases considerably the total installation time and the portability of the reading stations without decreasing their accuracy and repeatability.

**3.3.2 Field Installation.** The field installation of the baseline system components requires the use of two electrical tools: a vibrating concrete drill and a portable drop-light. The drill is necessary for the installation of all the anchor bolts. Special tungsten carbide drill bits are strongly recommended, since in the trial tests the regular bits only worked well for 3 to 4 operations in high-strength concrete. The concrete anchorage bolts for the base plates of all stations should be made of strong, non-corrosive elements. *Hilti Kwik Bolt II, AISI 304 & 316 Stainless Steel* of 1/4-inch diameter and 3/4-inch threaded ends are recommended. The embedment length of these bolts, however, should be carefully controlled to less than 7/8-inch (ideally between 3/4 inch and 7/8 inch) to avoid establishing an electrical contact with the reinforcing bars. To increase the stability and mechanical strength of the anchor bolts, two-part epoxy mixes can also be used in their installation.

**3.3.3 Operation and Storage.** The first step for operation of the installed system is to tie the piano wire to the dead end station and unwind it to the live end station. The manufacturer-provided cage that holds each roll of piano wire is quite difficult to handle during the unwinding process of long lengths of wire. It is strongly recommended to manufacture a more practical piano wire cage assembly in the laboratory to prevent field problems. An important consideration for the handling of the piano wire is also to avoid producing any "kinks" due to excessive bending. When the piano wires are stressed to a level near their ultimate load, the locations damaged from excessive bending become critical failure areas where the wire

fractures. The "fisherman's knot" worked well at preventing this from happening in the connection of the piano wire to the dead end and to the calibrated load.

After proper unwinding of the piano wire, make sure that the bearings are not bound (or tighter than usual). Use light machine oil on the bearings when measurements are taken after long periods of time. Place the piano wire over the guiding grooves in the bearings and hang the calibrated weight very slowly to prevent overstressing the wire.

Before taking readings, make sure that the base plate of each reading station is clean and free of any metal particles (stuck to the plate due to its small residual magnetism). Take several readings from each station, and when averaging the results, do not include obvious misreadings. This is especially important when the method for determining the contact of the extension arm of the digital scale and the base wire is performed by single-eye sighting.

The portable reading unit should be stored and handled very carefully, as for any other high-precision instrument. Finally, it is strongly recommended that special light-weight, styrofoam-padded wooden cases be constructed for the portable reading units.

A battery-operated, portable, mini-processor-printer unit is suggested to be used for all the measurements. Most gage manufacturers provide a compatible processor that can be coupled with their digital gages. The use of the processor helps eliminating most operator errors and considerably increases the speed of measurements.

### **3. 4 Field Installation in the San Antonio Y Project**

#### ***3.4.1 Span Deflections.***

**3.4.1.1 Prefabrication.** All brackets, plates and two sliding digital rulers were fabricated in the laboratory. The height of the holding brackets was carefully determined taking into account the range of the sliding ruler, the depths of the top slab, which varied from typical segment to pier segment to expansion joint segment, and the vertical curvature of the spans. The weights used to tension the wires were also prefabricated. Two identical weights were fabricated for each span so a backup existed if one weight were lost.

**3.4.1.2 Installation.** All installation procedures took place at the erection site. The following is a list of operations:

1. The dead end and roller end brackets were attached to the underside of the top slab above the bearings using small expansion anchors. The holes for the expansion anchors were drilled with the cordless hammer drill. The cordless drill eliminated the need for a source of electricity.
2. The wire was strung and tensioned with a prefabricated weight.

3. The measuring plates were positioned carefully to ensure the measuring arm of the sliding ruler would properly contact the wire. The plates were attached with small expansion anchors.

The installation process took two workers approximately one hour.

**3.4.2 Truss Deflection System.** A similar baseline system was used to measure the deflections of the truss during erection operations. Figure 3.24 shows the dead end, live end and measuring brackets. The less precise ruler and mirror system was used to eliminate the need to attach and detach the measuring bracket, leaving hands free to maneuver on the erection truss.

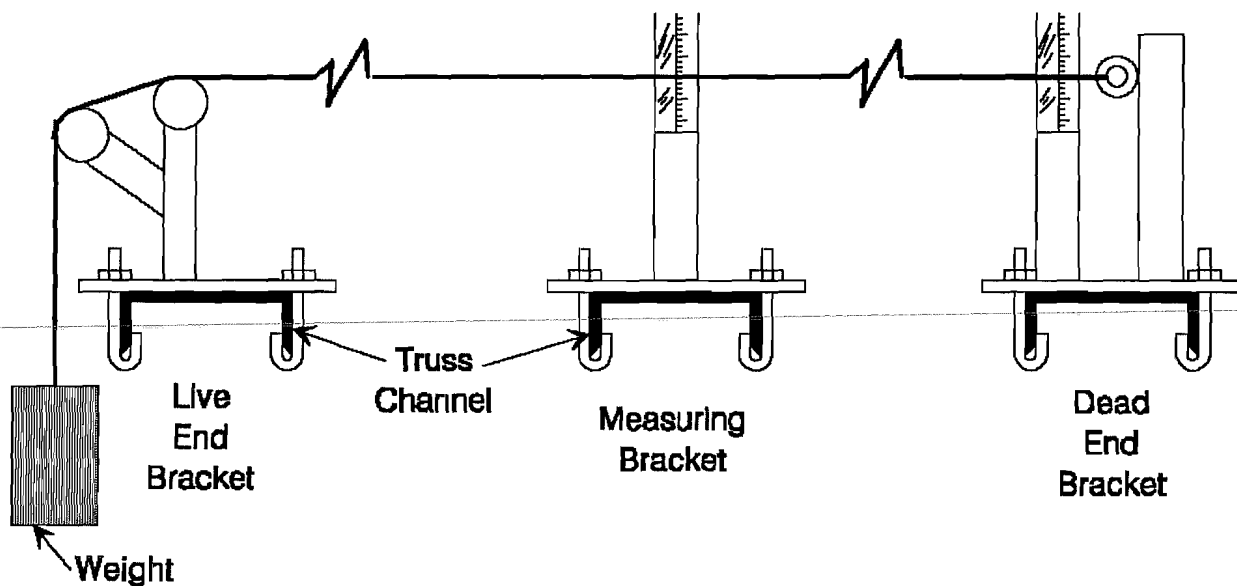


Figure 3.24 Truss deflection system.

The brackets were tightened down against channel braces which were located every 9'-8" along the truss. They were removable and replaceable so they could be arranged for each truss configuration (span lengths varied from 75 feet to 110 feet). The channel positions are shown in Figure 3.25. The reading locations were somewhat difficult to access, but overall the system worked quite well.

**3.4.3 Wingtip Deflection System.** A similar system was also used to measure transverse wingtip deflections caused by prestressing and by creep and shrinkage with time. Figure 3.26 shows the basic system arrangement. The dead and live end brackets were placed in the newly-cast concrete, and the measuring plates were also positioned. The digital sliding ruler was used, moving from measuring plate to measuring plate.

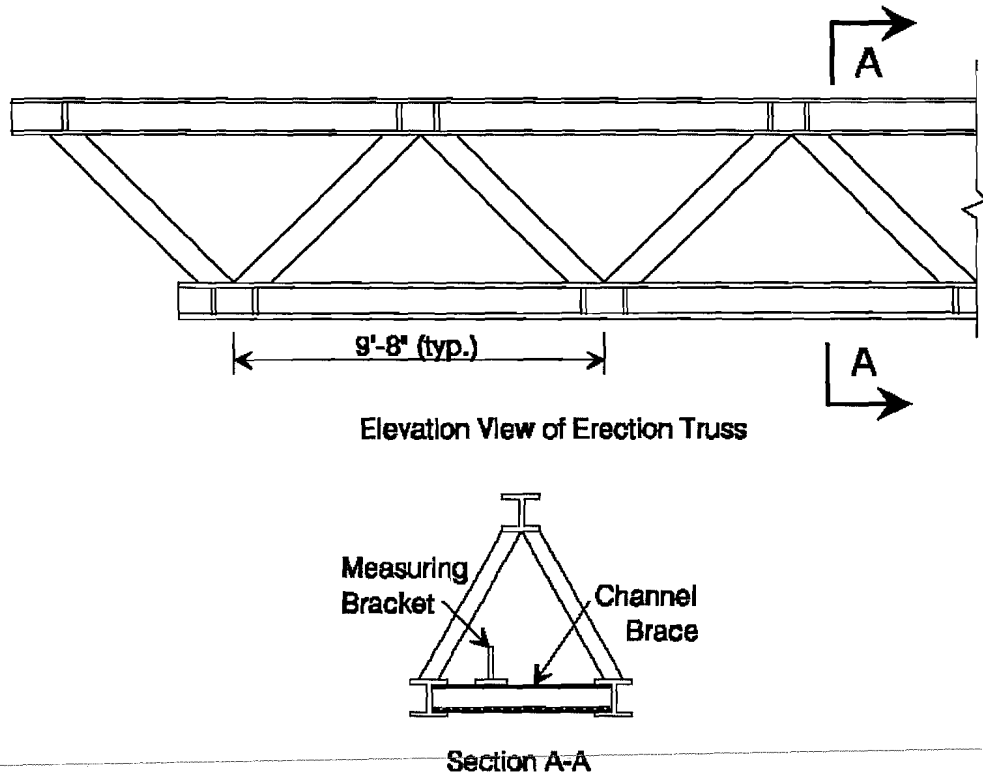


Figure 3.25 Truss schematic.

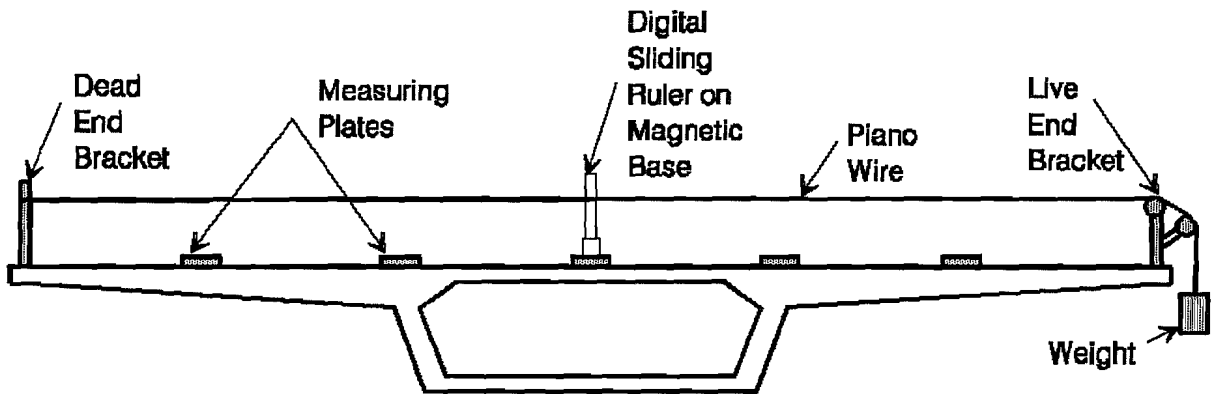
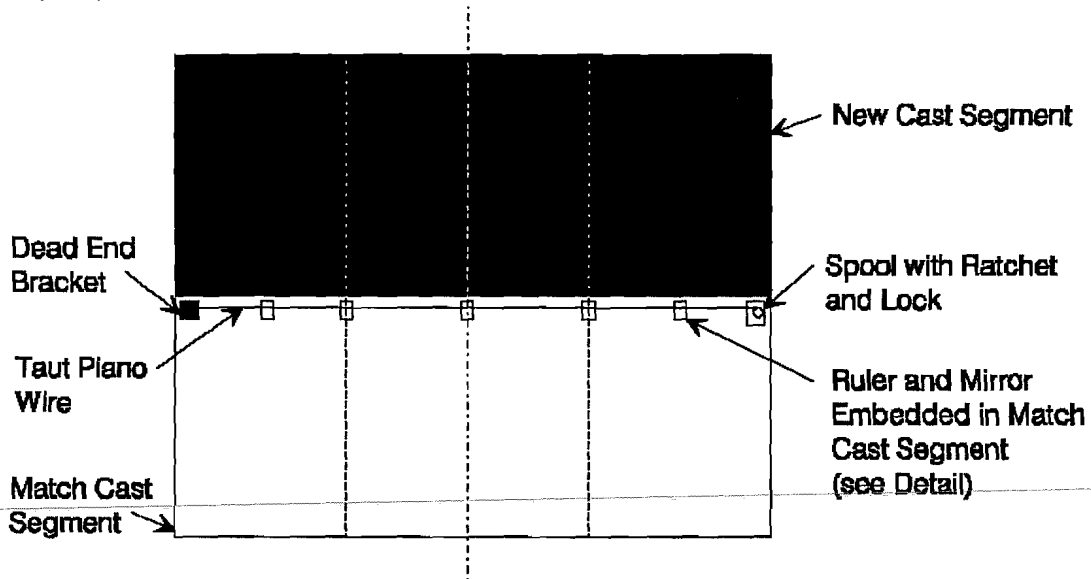


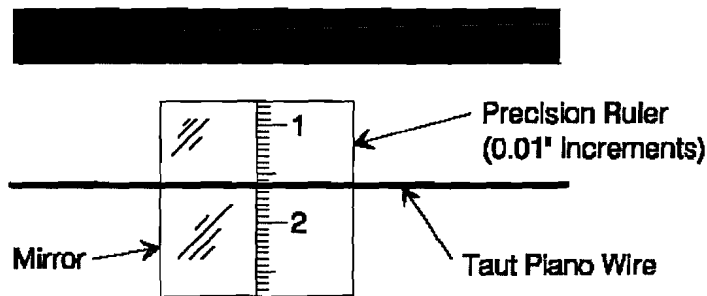
Figure 3.26 Wingtip deflection measurement system.

This system provided good information on the relative position of the measuring points. The instrumented segments were placed on the top level in storage so readings could continue with time.

**3.4.4 Segment Deformations during Match Casting.** A similar system was used to measure segment deformations during match casting. Figure 3.27 shows a schematic of the system. Since the measurements were horizontal and not vertical, the tension in the wire was not as critical. A spool with a ratchet and lock was used to tension the wire to an approximate level. At the dead end and live end brackets the wire was threaded through a guide groove to ensure it was always in the same position (see Figure 3.28). The system worked very well for measuring segment deformations.



Top View of  
New and Match Cast Segments



Detail

Figure 3.27 Deformation measurement system.

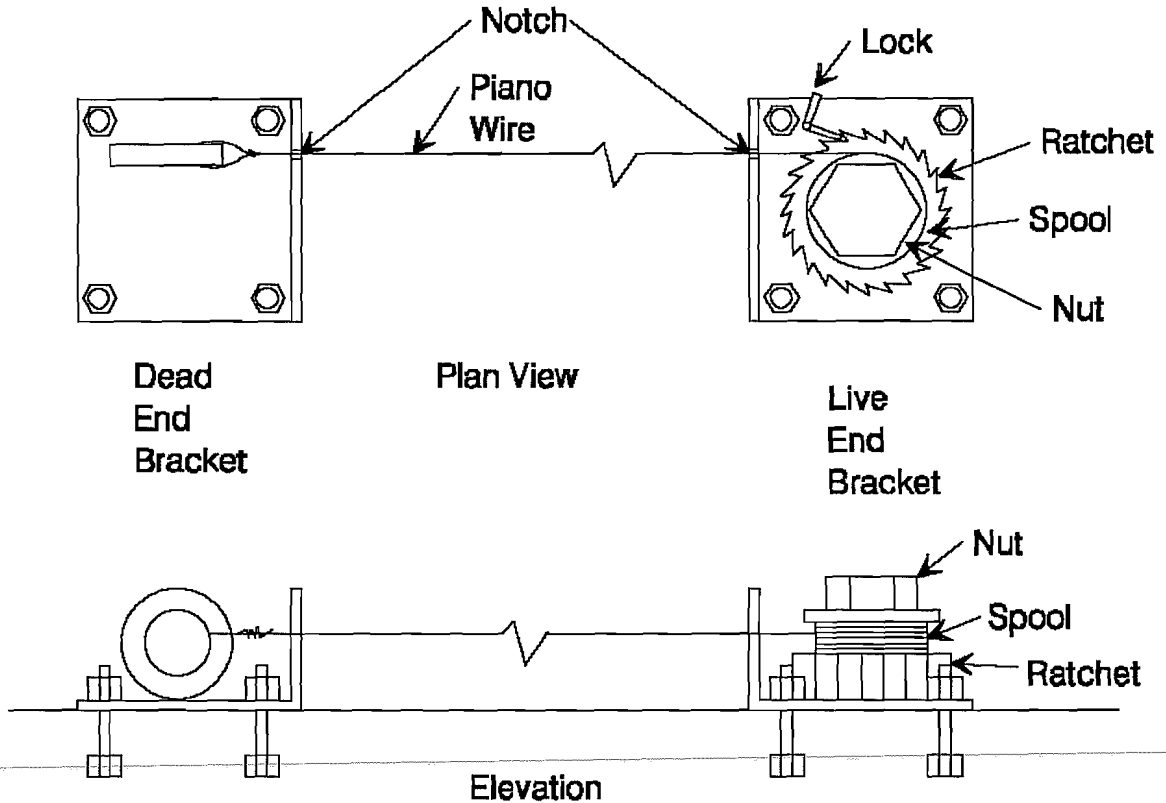


Figure 3.28 Segment deformation measurement system.

### 3.5 Performance

This system worked extremely well. The readings were fast, accurate, and repeatable, regardless of reader experience. Most readers found that shining a light behind the measuring arm enabled them to tell very precisely when the measuring arm came in contact with the wire.

A few problems occurred as follows:

**Wire Management:** The measuring wire is a #8 piano wire which comes in 300- to 400-foot lengths tightly coiled. Uncoiling a 110-foot length, without tangling, was a tedious and often frustrating task.

**Guide Bars on Measuring Plates:** One plate had a slight problem with the guide bars which ensure the measuring bracket is always placed in the same position. A weld was not ground completely and the measuring bracket sat on the weld, in an unstable position. With practice, the measuring bracket could always be held in the same position, but some readings from this plate are possibly in error.

**Bracket Removal:** In one instance a bracket was removed by construction workers. It apparently was in their way when placing closure pour formwork. Fortunately only a few days had elapsed before the removal was discovered. The bracket was replaced and readings continued. Since there is no assurance that the bracket was replaced in precisely the same location, the readings of changes in deflection for the few days the bracket was removed are considered lost.

### 3.6 Layouts

Figure 3.29 shows the layouts of the deflection measurement system. In three of the spans the deflections could not be read directly on the centerline of the box because a drainage pipe was to be installed directly on the centerline. The measurement brackets were therefore slightly offset.

### 3.7 Recommendations for Future Projects

This system worked quite well. Installation was simple and readings were very repeatable. Recommendations for improvement are:

1. Take great care in the fabrication of the measuring plates to ensure that the measuring bracket will always seat firmly in position.
2. Place a measuring plate near the roller end bracket (as well as the dead end bracket) so the position can be checked if the bracket is ever removed or damaged.



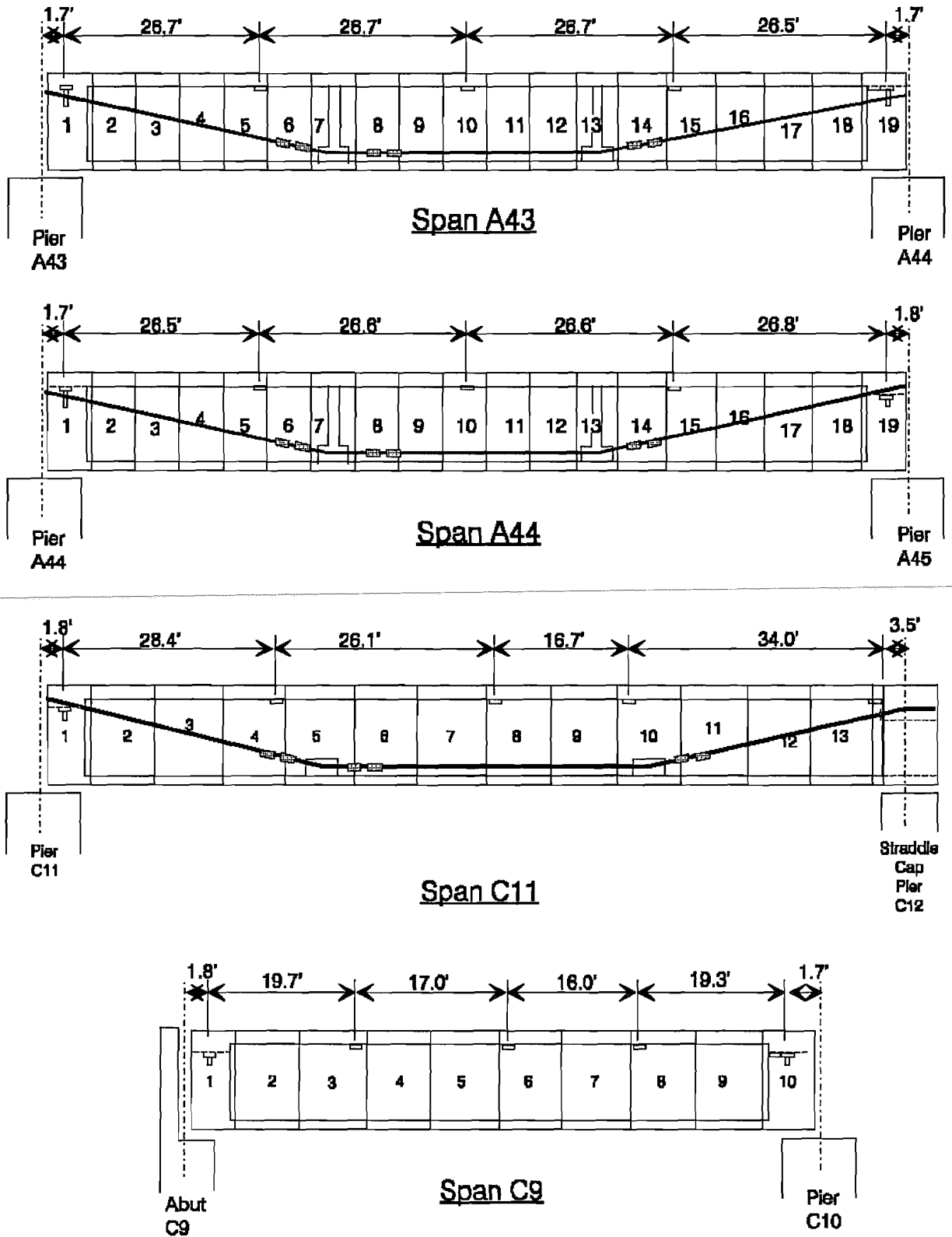
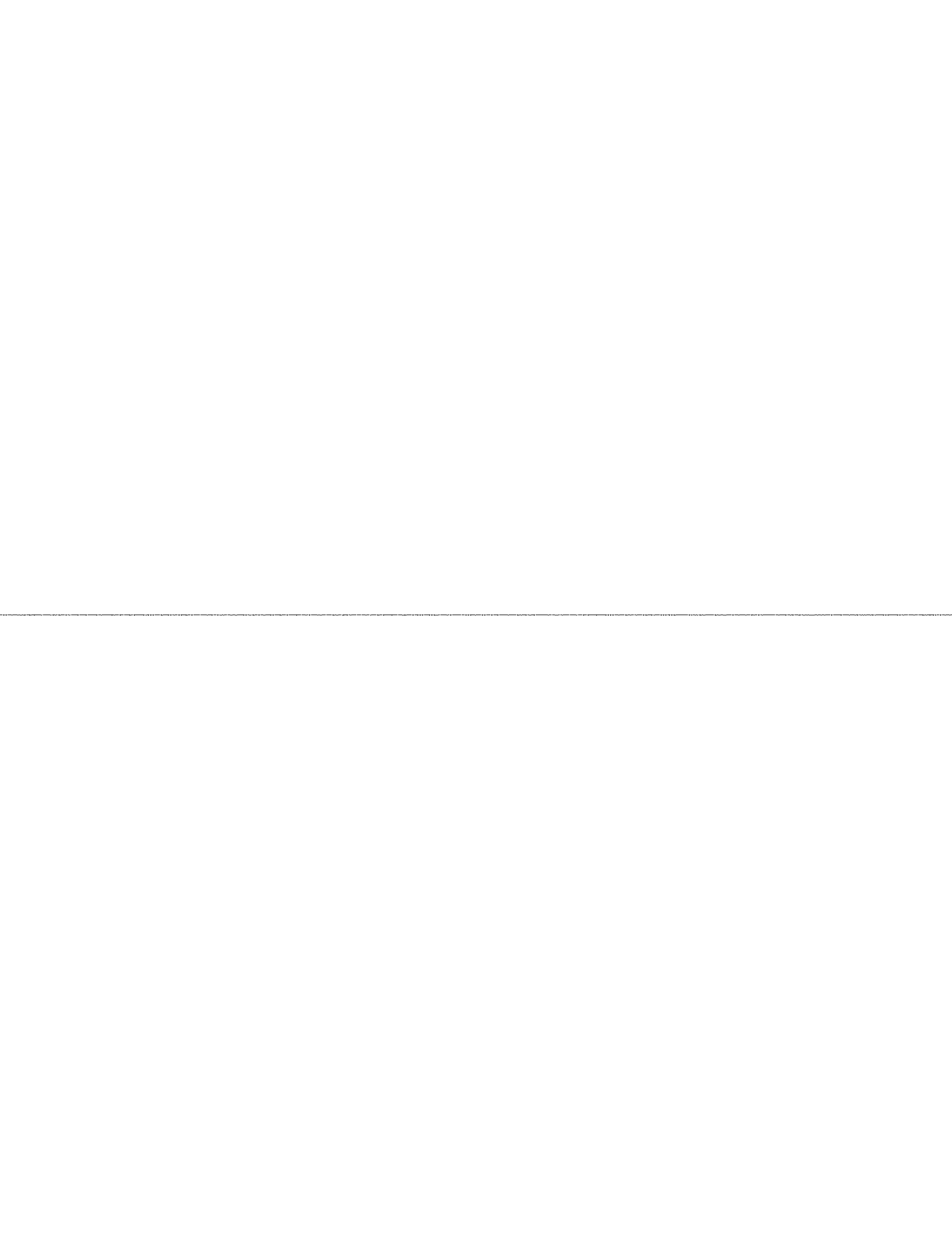


Figure 3.29 Deflection measurement system layouts.



## CHAPTER 4 CONCRETE TEMPERATURES

### 4.1 Review of Available Systems

Measurements of the thermal characteristics of bridge structures has lately become an important component of field instrumentation projects. Calculations of thermally-induced stresses in continuous prestressed concrete bridge structures can indicate a need for substantial additional prestress tendons. This is particularly true for the latest type of segmental box girder bridges because the special *AASHTO Guide Specification for the Design and Construction of Segmental Concrete Bridges*<sup>1</sup> requires consideration of thermal gradients in design. However, in only a few published cases were thermally-induced stresses considered as the main cause of cracking or joint openings in concrete bridges.<sup>56,21</sup>

In segmental concrete box girder bridges thermally-induced stresses might be significant in either the longitudinal or the transverse direction. In some precast segments, additional problems can result in the match-cast process due to the differential temperatures produced by the elevated and uneven heat of hydration between newly-cast and previously-cast segments as well as between large and small concrete elements (webs, top and bottom slabs, and cantilever wings). It is thus essential for a field instrumentation system of a novel segmental box girder structure (such as the San Antonio Y project) to measure the most important factors affecting the thermal response of the bridge.

Environmental factors, material properties, and geometric shapes can all influence the thermal response of a bridge structure. Some of these factors are shown in Figure 4.1. However, the most important mechanism of heat transfer in a bridge structure is usually considered to be the amount of solar radiation impinging upon the surface of the structure. This varies widely according to the angle at which the radiation passes through the atmosphere and the length of daylight. The intensity of solar radiation thus varies seasonally and daily (according to the time of day, degree of cloudiness, wind strength, etc.). A part of the total radiation that reaches a bridge is reflected, and part is absorbed by the structure and converted into heat. The amount of absorbed solar radiation depends on the type of surfacing of the bridge structure, particularly its color. Darker colors tend to absorb more solar radiation. However, previous research showed that a concrete surface with asphalt blacktop usually yields 10% lower temperatures than uncovered gray concrete surfaces.<sup>21</sup> This was explained to be possibly due to the insulating effect of the blacktop layer of asphalt.

Another important source of heat exchange for a bridge structure is the temperature of the surrounding atmosphere, which is transmitted to the concrete by convection and conduction (and is particularly dependent on wind speed and thermal conductivity of the material).

It will be helpful for designers to study the degree of influence that each one of the above-mentioned factors (solar radiation and ambient temperature) has on the non-linear

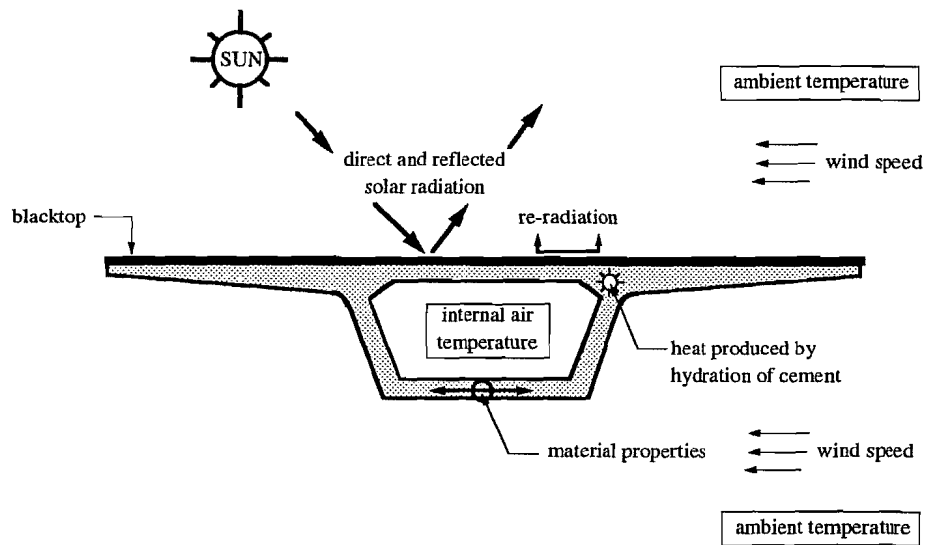


Figure 4.1 Factors influencing the thermal response of segmental box girder bridges.

temperature distribution of the different members of a typical concrete segment. The measurement of concrete temperatures is therefore crucial for determining the results of the heat exchange process.

**4.1.1 Objectives.** This section reviews some of the most popular instrumentation systems used for measuring concrete temperature and solar radiation. For each reviewed instrument, an evaluation of some of the most important information related to its method of installation, operation, and cost is included. Devices commonly available for measuring concrete temperature are included in Section 4.1.2, and a basic introduction to the measurement of solar radiation is included in Section 4.1.3. The final objective of this review is to help select the most appropriate devices for the instrumentation of concrete segmental box girder bridges.

High accuracy and sensitivity are not critical for these devices and their selection for a particular project is thus more dependent on cost and availability. Another factor of importance is the long-term stability of the selected system. No trial tests were considered necessary among the reviewed instrumentation devices for concrete temperatures since some of them have showed outstanding behavior in several reviewed short- to medium-term instrumentation projects. However, the selected solar radiation instrumentation system was installed on top of a finished span of the San Antonio Y bridges to check its overall behavior. This single field test helped familiarize the researchers with this seldom-used instrumentation device. Since measurements were only performed for understanding the operation of the solar radiation measuring device, no valid test conclusions were reached and no trial test reports are thus included in this chapter. Only a few recommendations about the installation and maintenance are included in Section 6.4.

In a thermal gradient instrumentation study of concrete bridges, measurements are needed to determine the type of temperature distribution occurring in different components of the

structure and across the thicknesses of each individual component. There are several instrumentation systems available for measuring temperature. The most widely-used devices are:

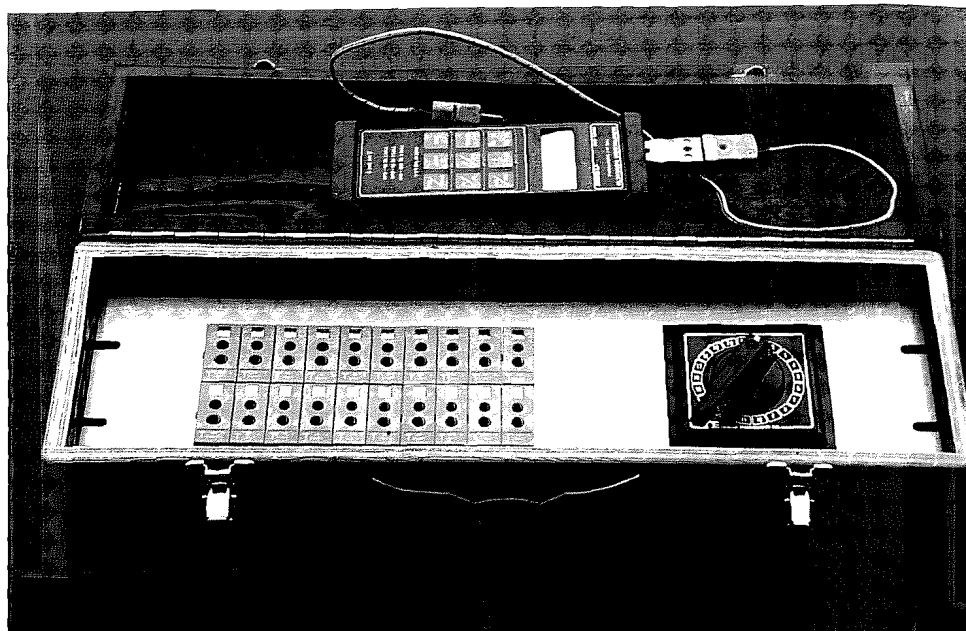
- thermocouple wires,
- thermistors,
- resistance temperature devices, and
- vibrating wire temperature sensors.

**4.1.2 Thermocouples.** These are by far the most widely-used devices for embedment in concrete structures. The operation of a thermocouple wire is simple. The voltage variations between two wires made of different materials and twisted together at one end is directly proportional to the temperature variations at the connection of the wires. The connection of the two wires (usually called the *measuring junction*) can be made either by twisting the wires together (see Figure 4.2c) or by fusing the two wire materials with an oxyacetylene flame. Both methods have worked well in previous instrumentation projects.

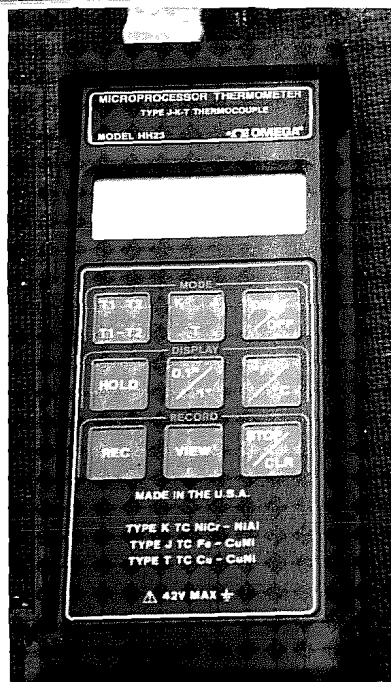
Measurements of the voltage variations between the two thermocouple wires cannot be made with regular voltmeters. This is because the connections to the voltmeter leadwires would produce another thermocouple junction of dissimilar metals which throws off the temperature measurements of the *measuring junction*. As shown in Figure 4.3, a reference temperature must be used at the connection of the voltmeter leadwires with the two thermocouple wires. Most of the measuring devices provided by thermocouple wire manufacturers have an electronically-controlled constant-temperature zone where the *reference junction* is performed. Most readout devices thus permit direct connection to each one of the thermocouple wires (provided that they are compatible with the type of materials used in the thermocouple wires). Calibrating charts are standard for each type of thermocouple wire. Temperature can thus be directly measured in °F or °C in most readout devices.

Several combinations of materials are available for thermocouple wires. The most common for embedment in concrete is copper-constantan (Type-T thermocouples). This is because both of these materials oxidize only mildly in aggressive environments such as concrete. Furthermore, thermocouple manufacturers also provide different types of insulating and overbraiding materials. Teflon is the preferred insulating material for concrete embedment due to its excellent moisture and abrasion resistance. Overbraiding of the thermocouple wires is optionally provided by most manufacturers. However, this is strongly suggested for field applications to increase the durability, flexibility, and abrasion protection of the thermocouple wires. Tinned-copper overbraids are recommended due to their relatively low cost and good performance. For applications different than in concrete, literature or suggestions from thermocouple manufacturers should be consulted due to the wide variety of combinations that can be made with the currently-available wires, insulations, and overbraids (see Table 4.1).

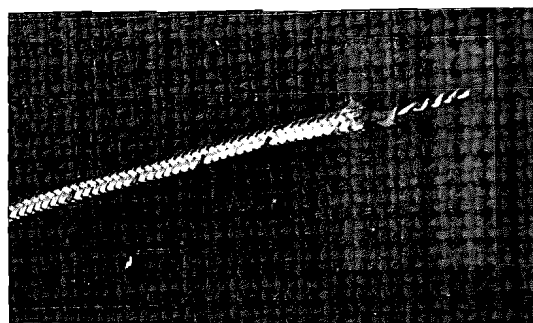
Thermocouples are also widely preferred since they can measure a wide range of temperatures at an accuracy level that is usually around  $\pm 1.0^{\circ}\text{C}$  ( $\pm 1.8^{\circ}\text{F}$ ). This is practical for



a. Portable multi-channel (19-channel) switching device for type T thermocouples.



b. Close-up of battery operated readout unit.



c. Close-up of a typical thermocouple measuring junction.

Figure 4.2 Typical thermocouple system for field instrumentation projects.

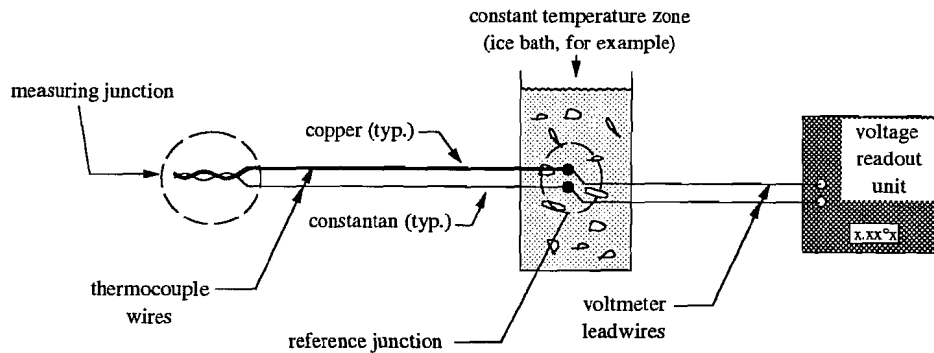


Figure 4.3 Principle of operation of thermocouples.

most structural engineering applications. Furthermore, there is a large selection of thermocouple readout equipment. Some are portable (battery operated) and can be used with specially manufactured multi-channel switching devices. A portable 19-channel switching device is shown in Figure 4.2a. This was easily assembled at the research facility (FSEL) with parts purchased from Omega Engineering, Inc. A battery-operated, standard portable readout unit (for Type J, K and T thermocouples) is also shown in Figure 4.2b.

Another important characteristic of thermocouples is their excellent suitability for automatic data acquisition. Most data-logger manufacturers provide the necessary reference junctions and calibration charts for each thermocouple wire type as standard options to their equipment. However, certain data-loggers need to be programmed to be able to record the thermocouple measurements in °F or °C.

Type-T thermocouples with the proper protection and installation can have excellent stability in concrete. The manufacturer-specified life of thermocouple systems with the proper insulation and overbraiding is usually around five years. However, in most of the reviewed field instrumentation projects much longer performance was obtained.

Typical costs of a standard thermocouple system for embedment in concrete and with a portable readout unit and multi-channel switching device are shown in Table 4.2. These prices are as of late 1990 and were obtained from Omega Engineering, Inc. They can be reached at: One Omega Dr., P. O. Box 4047, Stamford, CT 06907. Their current telephone number is: (203) 359-1660.

**4.1.3 Thermistors.** *Thermally sensitive resistors* are usually made of semiconductor materials that change their resistance with temperature (as shown in Figure 4.4). Absolute temperatures from thermistor resistance measurements (usually in Ohms) are obtained through

manufacturer charts. However, most thermistor manufacturers provide readout devices that can directly show temperatures in °F or °C. These instruments are relatively cheap and provide great levels of stability and accuracy. They are available in different sizes and shapes; the smaller ones are more adequate for the temperature corrections of other instrumentation devices. However, they have also been commonly used for embedment in boreholes in geotechnical instrumentation projects.

The semiconductors of a thermistor are highly sensitive to temperature differentials, while the two leadwires (that connect them to the readout units) are not as sensitive. This makes the thermistors highly-accurate and stable devices. A usual degree of accuracy for thermistors is  $\pm 0.1^\circ\text{C}$  ( $\pm 0.2^\circ\text{F}$ ). The range of temperatures that can be measured at such an accuracy level is usually considerable. Most manufacturers can offer the mentioned level of accuracy for a  $-80^\circ\text{C}$  to a  $+75^\circ\text{C}$  ( $-112^\circ\text{F}$  to  $+167^\circ\text{F}$ ) temperature range. Two-conductor long leadwires can usually be used without a drop in accuracy since the resistance of the leadwires varies only slightly with temperature. However, the resistance created by long lengths of leadwires should be subtracted from the total resistance readings of the thermistors to obtain absolute temperatures.

The largest inconvenience with thermistors is their lower degree of compatibility with automated data-acquisition systems. Since the variations of electrical resistance are quite large, only a few data-loggers supply the digital voltmeters necessary for obtaining such measurements. However, most manufacturers can provide affordable readout units, multi-channel switching devices, and data-loggers compatible to their thermistors. This type of thermometer can be purchased from several companies in the U.S.:

1. B.R. Jones & Assoc., P. O. Box 38, Normangee, TX 77871. Current telephone: (409) 396-9291.
2. Roctest, Inc., 7 Pond Street, Plattsburgh, NY 12901-0118. Current telephone: (518) 561-1192.

Table 4.1 Commonly available thermocouple wires, insulations, and overbraidings (from Omega Eng., Inc.).

Thermocouple Wire Types:
Iron-Constantan (Type J) Copper-Constantan (Type T) Chromel-Constantan (Type E) Chromel-Alumel (Type K)
Insulation Types:
Polymil Chloride High-Temperature Glass Kapton Teflon/Neoflon Silicone Rubber Glass Refrasil Nextel
Overbraiding Types:
304 Stainless Steel Inconel 600 Tinned Copper



3. Atkins Technical, Inc., 3401 S.W. 40th. Blvd., Archer Interchange (I-75), Gainesville, FL 32608. Current telephone: (904) 378-5555.

#### 4.1.4 Other Systems.

Less-common systems for measuring temperature variations in concrete structures consist of resistance temperature devices and vibrating wire temperature sensors.

Resistance temperature devices (also known as RTD's) are simple metal wire resistors connected to a readout unit through a three-leadwire system. As with the thermistors, these are also based on the principle that a wire's resistance varies in a directly proportional relationship with temperature. However, the temperature-induced resistance variations of an RTD are much smaller than for the thermistors, thus requiring the use of a three-leadwire, quarter-bridge Wheatstone bridge (necessary for avoiding the measurement of temperature differentials on the leadwires themselves). They are compatible with most automated

data-acquisition systems. However, since they require independent channels and quarter-bridge completion circuits, their application is more expensive than the other systems reviewed earlier in the present report. Manufacturers claim that these devices have excellent stability with time. In fact, their rated stability is usually in the neighborhood of 10 to 15 years. However, unless these devices are permanently connected to a portable readout unit or to an individual data-acquisition channel, errors can occur due to leadwire effects. The exact electrical resistances produced at the connections of the leadwires of each RTD to the different channels of a data-acquisition system cannot be accurately reproduced. A reduced accuracy level therefore exists in most practical applications of the RTDs. Not considering leadwire effects, an accuracy level about the same as obtained with thermistors ( $\pm 0.1^{\circ}\text{C}$  or  $\pm 0.2^{\circ}\text{F}$ ) is attainable.

Vibrating wire temperature sensors can also be used for concrete embedment. One of the most common types of vibrating wire sensors is the Carlson Elastic Wire Meter. Although

Table 4.2 Typical costs of a thermocouple system for use in concrete structures (from Omega Eng., Inc., prices from late 1990).

a. Thermocouple Wire: - Type T thermocouples - with Teflon/Neoflon Insultation - Size 20AWG - 500-foot spools	\$244.00
b. Thermocouple wire overbraids: (for the above-listed wire description) - Tinned Copper - 304 Stainless Steel - Inconel 600	\$85.00 \$127.00 \$212.00
c. Quick disconnect connectors for Type T thermocouples (each)	\$1.80
d. Hand-held thermometer for Type J/K/T thermocouples (battery operated, Type HH-23)	\$189.00
e. 19-channel portable switching device for Type T thermocouples (assembled at research facility, cost not including labor)	\$300.00

mainly used for measuring strains, this device provides the added benefit of measuring temperature.

Dedicated vibrating wire transducers also exist. They are usually made of a steel body to which a vibrating wire element is attached. The different coefficients of thermal expansion of the steel body and the vibrating wire enables a sensitive determination of temperature variations. Since signals consist of frequencies, no errors due to leadwire effects or other changes of resistance (caused by moisture penetration, temperature, or contact resistance) influence the stability and accuracy of these devices. The main problem related to these systems is that they are usually more expensive than the other temperature measuring devices that were reviewed here. Vibrating wire temperature sensors also require compatible readout units and data-loggers, which can be considerably expensive if non-compatible measurements of strain are performed for the same instrumentation project. High accuracy levels of less than  $\pm 0.1^{\circ}\text{C}$  ( $\pm 0.2^{\circ}\text{F}$ ) for temperature ranges of  $-40^{\circ}\text{C}$  to  $+160^{\circ}\text{C}$  ( $-40^{\circ}\text{F}$  to  $+320^{\circ}\text{F}$ ) can usually be obtained with these sensors.

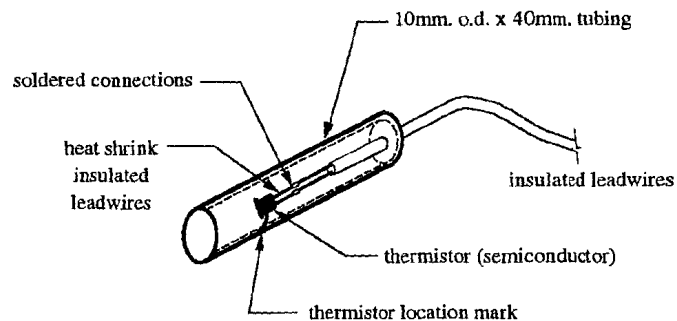


Figure 4.4 Typical thermistor for concrete embedment (from B.R. Jones Catalog).

## 4.2 Recommendations for Use with the San Antonio Y Project

The devices selected for measuring temperature variations inside concrete members on this project were thermocouple wires. Size 20AWG copper-constantan wires (thermocouple "Type-T") were selected due to their lower degree of oxidization and abrasion in aggressive environments. To further protect the thermocouple wires, it was recommended that they be insulated with Teflon/Neoflon compounds. These provide increased moisture protection and abrasion resistance. Finally, tinned copper overbraids were recommended for field applications to increase the physical protection and durability of the thermocouple wires. This type of overbraid is usually the least expensive and provides acceptable levels of protection.

To avoid any intermediate splices, the original thermocouple wires should be cut in proper lengths. Intermediate splices can form a secondary thermocouple junction that can introduce erroneous temperature readings. However, if splices become necessary, good procedures can be obtained from most thermocouple manufacturers. The temperature-measuring junction of copper-constantan thermocouple wires can be prepared by stranding both wires together or by fusing them with an oxyacetylene flame. To install a series of wires across the

thickness of certain box girder sections, each wire should be tightly taped to a strong plastic rod that can serve as a stabilizing base for the wires. The rods can then be tied to neighboring reinforcing steel bars at the required locations (as shown in Figure 4.5). These plastic rods will ensure that the thermocouple wires are kept at their predetermined locations during concrete casting. Alternatively, for individual thermocouple wires located along the bridge superstructure, high-strength fishing line can be used to tie each independent thermocouple to the reinforcing steel bars.

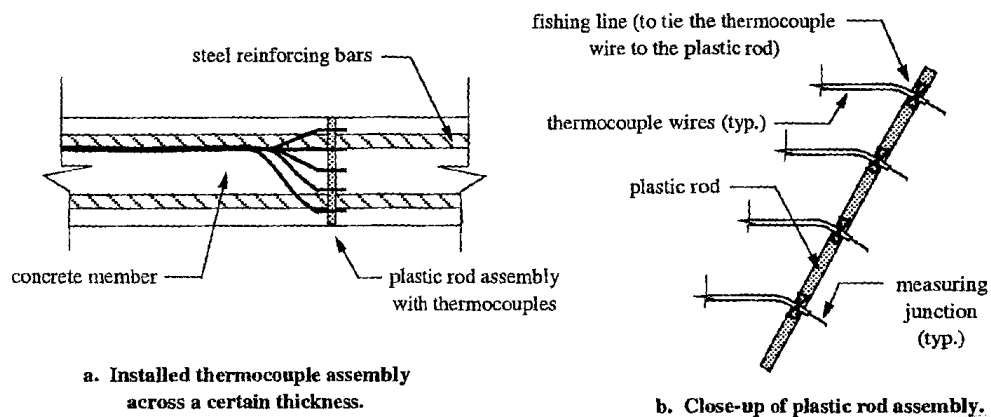


Figure 4.5 Installation of a series of thermocouple wires across the thickness of a concrete member.

When a thermocouple wire is installed near the concrete surface that is instrumented with strain-measuring devices, the thermocouple readings can provide important data for temperature-induced strains in the concrete.

Multi-channel switching devices are strongly recommended to be used in projects involving a considerable number of thermocouple wires. Since leadwire effects or contact resistance differentials do not decrease the accuracy of the thermocouples, highly-sophisticated automated data-acquisition systems are seldom needed. Portable multi-channel rotary switching devices for up to 39 channels can be easily assembled in most research laboratories at a very low cost. Groups of thermocouple wires placed in different spans can be plugged and unplugged at various times when readings are needed. The only problem with these arrangements will be the slow oxidization process of the reading junction terminals of each pair of unprotected thermocouple wires. This can only become a problem for long-term projects. To decrease the oxidization process at the end of the thermocouple wires, each group of wires can be kept inside foam-filled boxes containing several packets of silica gel desiccants.

### 4.3 Field Installation

As recommended, Type-T, copper-constantan, thermocouples were chosen to measure concrete temperatures. Two systems for reading the thermocouples were used. One was the manually-operated switch box (see Figure 4.2) to which a hand-held digital thermometer was attached. The other system was a Campbell 21X data logger. Eight thermocouples could be connected to the data logger and the logger programmed to read temperatures at set time intervals. The data could then be extracted with the notebook PC.

**4.3.1 Prefabrication.** All thermocouples were prefabricated prior to casting-yard activities. Prefabrication involved cutting the thermocouple wire to the proper length, stripping the wires and twisting them together at one end, stripping the wires and attaching a quick-connector to the other end, and labeling the thermocouple (see Figure 4.6).

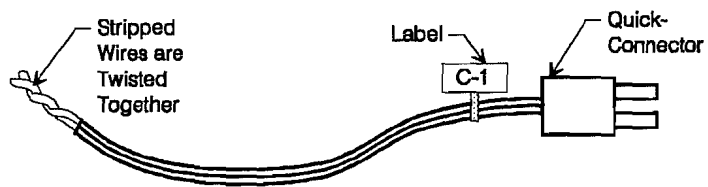


Figure 4.6 Thermocouple.

**4.3.2 Casting-Yard Operations.** All thermocouples were cast into the concrete. The following is the procedure for installation:

**Day 1:**

1. The reinforcing steel cage was normally completed by 12:00 to 2:00 pm. After the steel workers were finished the installation began.
2. Thermocouples were roughly positioned using cable ties to attach the wires to reinforcing steel near the thermocouples's final position.
3. The wires were threaded through the cage to a common exit point.

**Day 2:**

1. The cage was placed in the forms.
2. After the steel workers had made adjustments to the cage, the thermocouples were more precisely positioned using fishing line (see Figure 4.7).
3. As the concrete was cast, operations were monitored to ensure no damage to, or excessive movement of the gages.

### 4.3.3 Job-Site Operations.

#### 4.3.3.1 Manual Switch

**Box.** At the job site one of two methods was used to read the thermocouples. The first, the manual switch box, had the capacity to read 19 thermocouples, but temperatures had to be recorded by hand. This system was used on several occasions for in-depth temperature studies which compared concrete temperatures at many locations throughout the segment (web, wings, top, and bottom slabs) or compared temperatures in more than one segment.

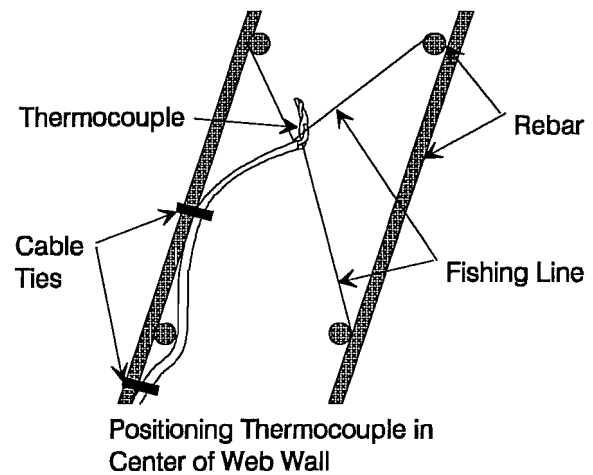


Figure 4.7 Positioning thermocouples with fishing line.

The job-site activities included arriving very early in the day to try to record the most uniform temperature distribution which normally occurred between 6:00 and 9:00 am. All the thermocouples were connected to the proper location on the switch box. The dial gage was switched from channel to channel and the temperatures recorded on a data sheet. The readings were made at each hour throughout the day. Each reading took about 5 minutes.

**4.3.3.2 Campbell Data Logger.** The second method of measuring thermocouples was the Campbell 21X data logger. The data logger can record up to 8 thermocouples, and can be programmed to read and record the temperatures at a given time interval. The web thermocouples of one segment were connected to the Campbell and it was programmed to read and record temperatures every half hour. This system was left in place for over one year.

In the field, the thermocouples were connected to the system and a program, written using the Campbell software, was downloaded to the Campbell through a notebook PC. Every month the data was extracted using the PC, and every other month the small batteries (8 each, size D) were replaced. Replacement required shutting off the system, replacing the batteries, reactivating the system, and downloading the program. The entire operation required approximately 10 minutes.

## 4.4 Performance

This system worked extremely well. Installation was relatively easy, the thermocouples were very hardy, with only a few not responding, and both reading systems were easy and accurate. No major problems occurred with this system.

#### 4.5 Instrumentation Layouts

Figure 4.8 shows the thermocouple layouts. Thermocouples were installed for two purposes: to read horizontal thermal gradients during match casting and to read vertical thermal gradients due to climatic conditions.

#### 4.6 Recommendations for Future Projects

Generally, the system worked extremely well. Installation was very easy and the data was quite reliable. The only recommendations concern the use of the Campbell data logger. The system could have been even easier if it had been connected to a modem to allow remote data retrieval. Another improvement would be to use longer-lasting batteries, or some kind of solar cell charger or trickle charger to eliminate the need to replace the batteries so often.

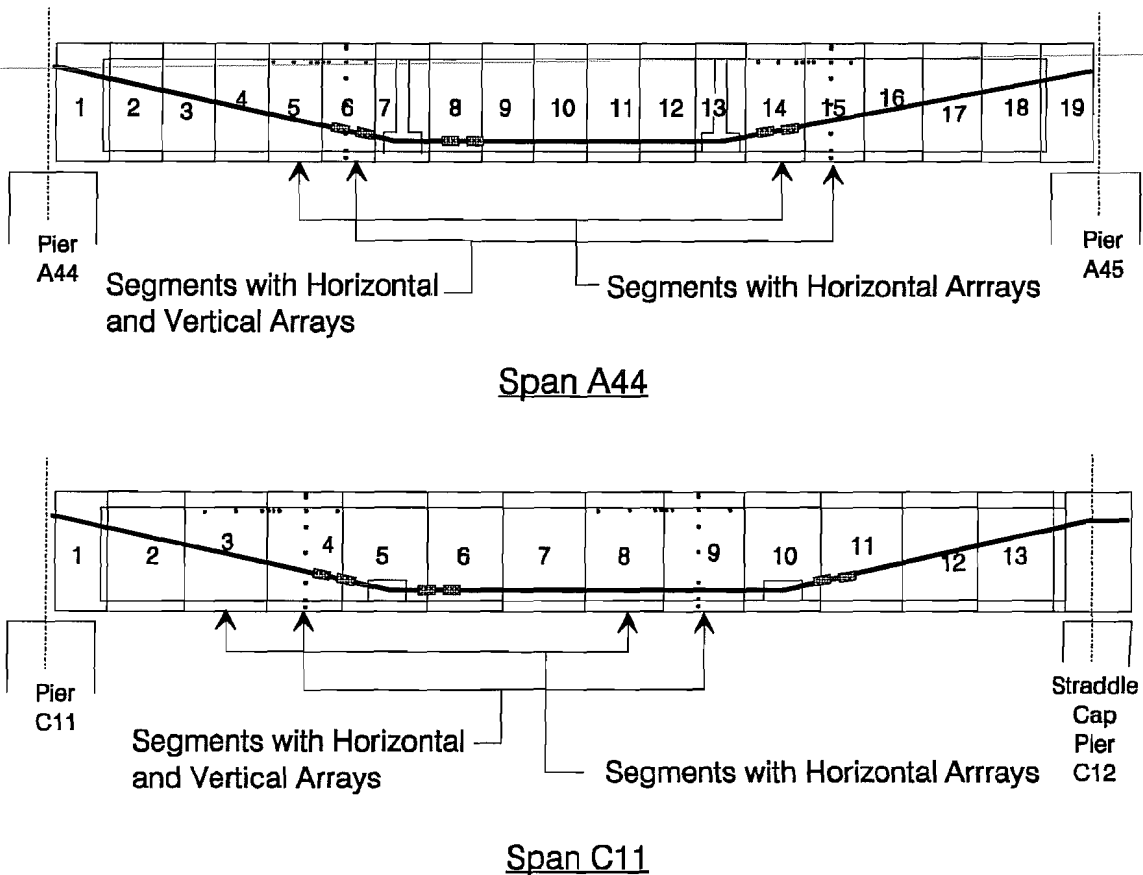
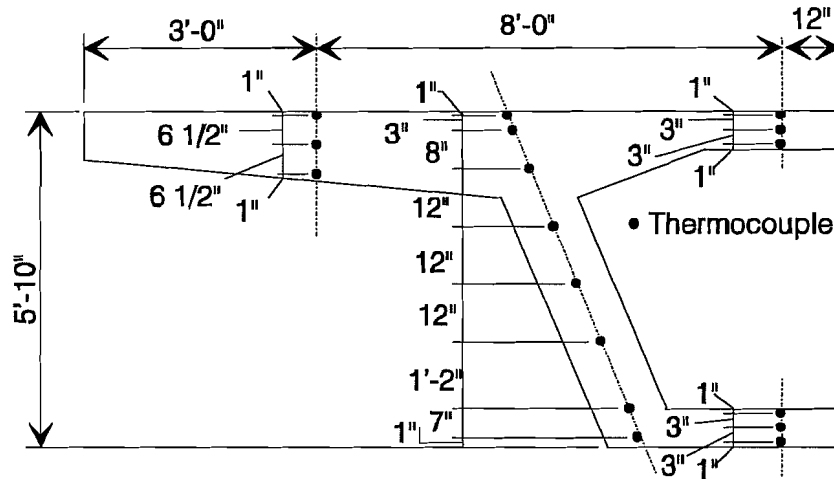
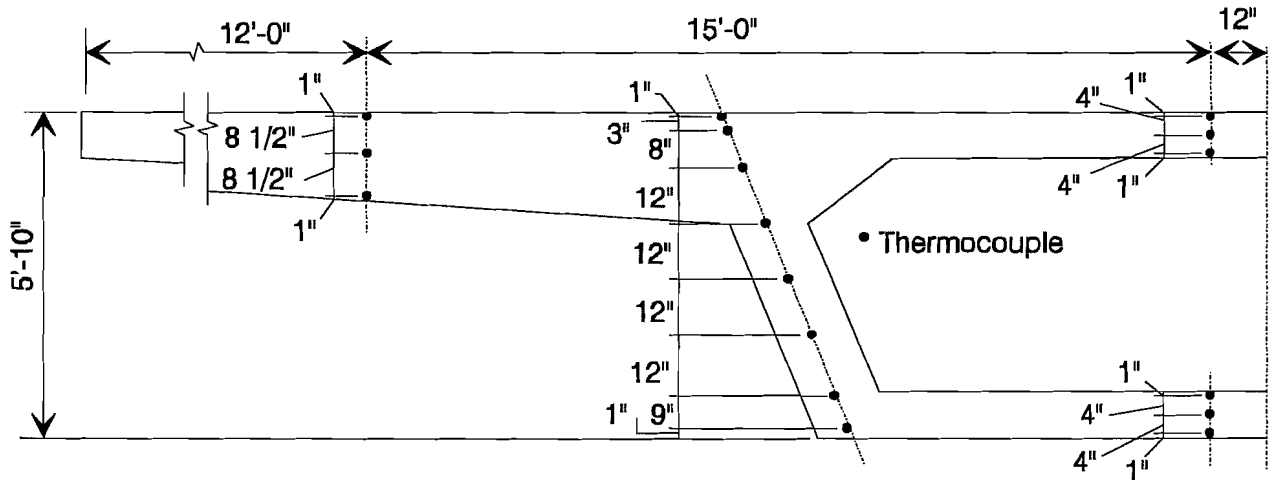


Figure 4.8a Thermocouple layouts.



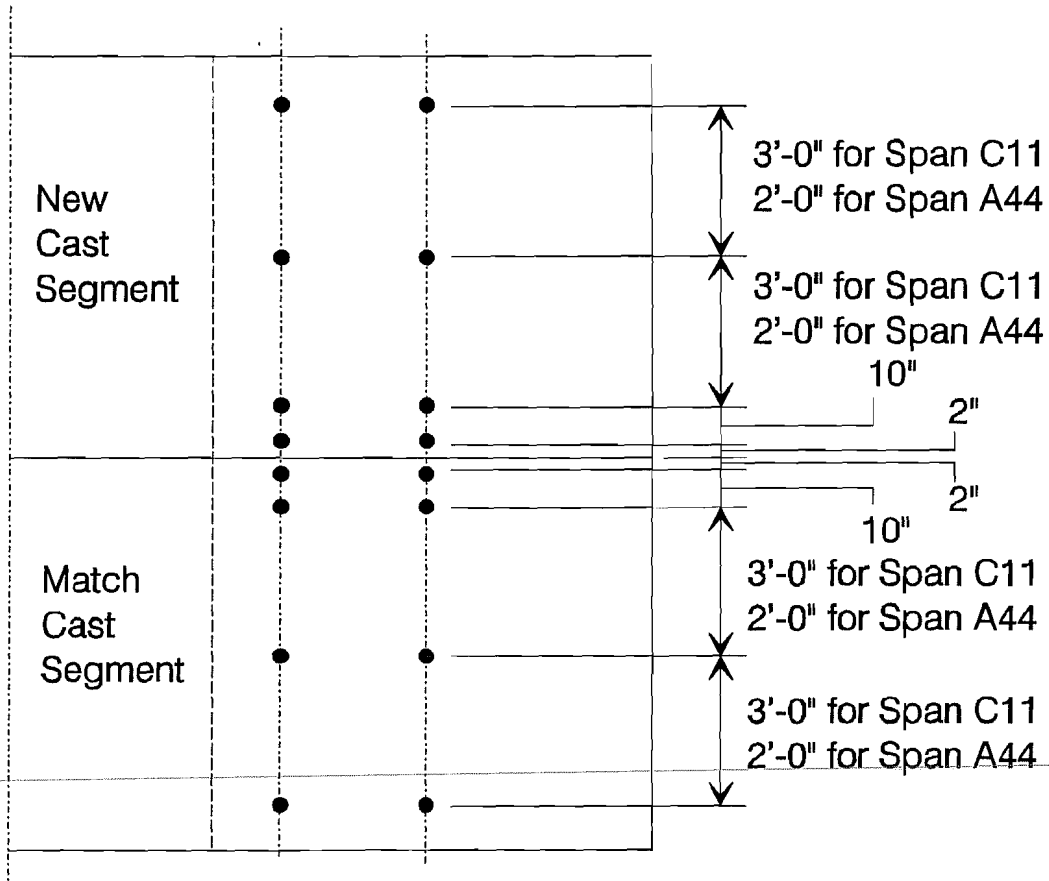
Segments 11C-4 and 11C-9  
Vertical Thermocouple Layout



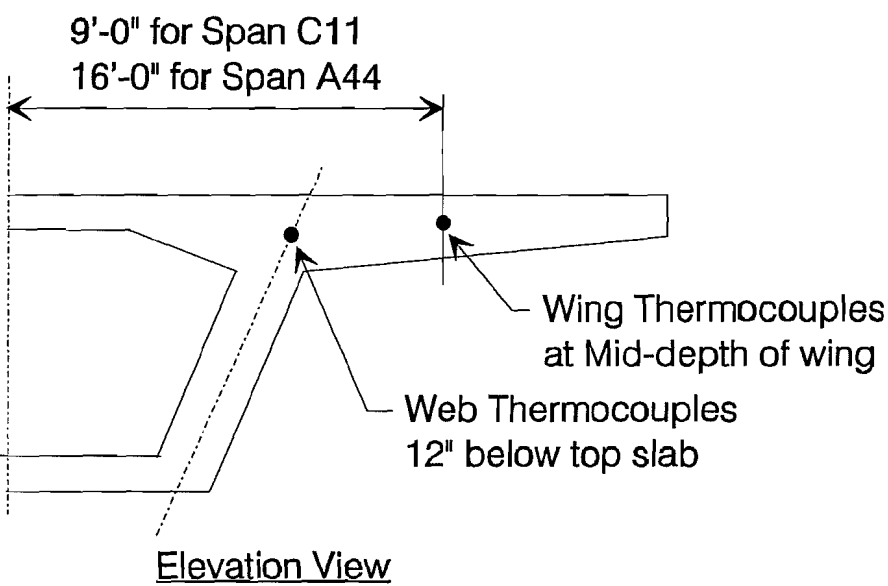
Segments 44A-6 and 44A-15  
Vertical Thermocouple Layout

Vertical arrays were placed at the longitudinal mid-point of the segment

Figure 4.8b Thermocouple layouts.



Top View of Segments



Elevation View

Figure 4.8c Typical horizontal thermocouple layout.



## CHAPTER 5 CONCRETE STRAINS

### 5.1 Review of Available Systems

Strains in concrete are seldom used directly in structural engineering design computations. They are often used by designers for estimating the state of stress in many types of structures, since the ability of a material to carry applied loads is normally expressed in terms of stress. The knowledge of local stresses in concrete structures is necessary for designing structural components which will use the least amount of material at their greatest efficiency.

Stress is a basic mathematical concept - force over a unit area - and not amenable to measurement. With the understanding of Hooke's law, the measurement of the physical entity of strain of materials is an important tool for engineering research. The relationship between strain and stress, known as the "modulus of elasticity" (or Young's modulus of elasticity), is linear at service loading states for most structural engineering materials. The average intensity of stress in a body subjected to some external loads can therefore be estimated by measuring the resulting strains and multiplying them by the known modulus of elasticity of the material.

In the particular case of concrete structures, estimating of concrete stresses is quite difficult due to three complicating factors:

1. Inaccurate modulus of elasticity,
2. Presence of strains not directly related to stress, and
3. Measurement of local strain variations.

**Inaccurate Modulus of Elasticity.** It is difficult to get a good estimate of the modulus of elasticity of composite materials such as concrete. Significant errors can result from this uncertainty. Between two different concrete batches, variations of the modulus of elasticity are widespread and obvious. Even for the same concrete batch, factors such as air voids, trapped moisture, and variation in compaction and curing conditions can also influence the modulus of elasticity from one point to another.

Published data from a previous field instrumentation program of a segmental prestressed concrete bridge<sup>29</sup> was evaluated by the present researchers. Values for the concrete modulus of elasticity of twelve 6-inch x 12-inch control cylinders taken from three different segments (different concrete batches) of a single span were obtained following ASTM Specification C39.<sup>6</sup> This small sample showed a maximum  $\pm 10\%$  variation of the average concrete modulus of elasticity considered for the analytical studies. However, when only considering control cylinders taken from casting of each instrumented segment, the variation of the average modulus was calculated at  $\pm 2\%$ . This is in accordance with initial tests of control cylinders taken from the San Antonio Y project, where the variation of the average segment modulus seems to be near 1.7%.

**Presence of strains not directly related to stress.** With respect to strain variations, not all strains in concrete are induced by external load related stress. Other influencing factors are:

1. Creep (changes of strain under a constant state of stress),
2. Shrinkage and swelling (changes in strain due to moisture changes in the concrete),
3. Temperature (changes in strain due to temperature variations in the concrete and in the strain gage material), and
4. Curing effects (changes which occur during concrete curing).

In prestressed concrete structures, creep is one of the most influential factors. Previous studies indicate that the importance of creep increases substantially when stresses are above about 60% of the ultimate strength of the concrete.<sup>36</sup> The duration of the instrumentation program is another important consideration to have in mind when dealing with creep and shrinkage strains. If the research is limited in time, creep and shrinkage-induced strains in concrete may not significantly influence the final results.

The rate of creep and shrinkage of concrete structures are known to be influenced by several factors.<sup>4</sup> These are mix design parameters, type of aggregate, fineness of cement, and environmental conditions during and after set (such as relative humidity, moisture content, ambient air temperature, etc.). The companion material tests of concrete, recommended in Chapter 8, are included to more accurately determine the actual state of stress of the instrumented spans of the San Antonio Y structure.

In precast segmental bridge construction, changes due to shrinkage should be smaller than cast-in-place structures. This is because much of the shrinkage strain of precast segments occurs in very early periods, while they are kept in the storage yard. The level of creep in cast-in-place structures also tends to be much higher than in precast structures, which are more mature when stressed. This is because concrete loaded at a young age creeps more than older concrete. It is therefore expected that in precast segmental bridge structures, and for the duration of a field instrumentation project, only creep and not shrinkage is expected to be a major factor.

**Measurement of local strain variations.** Finally, due to the non-homogeneity of concrete, local variations of strains occur from one point to another. As a general rule most investigations in structural concrete are designed to measure average strains thus avoiding the errors introduced by local variations of the material. Past investigations related to this effect suggest the use of gage lengths at least 5 times the maximum aggregate dimension.<sup>9</sup> These gage lengths should be able to allow strain measurements without significant errors due to local variations in the concrete material.

**5.1.1 Objectives.** The basic goal of this section is to investigate the availability and performance of the most widely-used methods for monitoring concrete strains in structures. The only way to measure this property of concrete is with "strain gages."

There are several types and variations of strain gages available. One of the best classifications has been proposed by Dunicliff<sup>15</sup> who divided them in two groups:

1. Embedment strain gages, and
2. Surface strain gages.

For the examination of performance of strain gages some qualifications must be met. An interesting description of necessary conditions for an "ideal" strain gage was proposed by Perry and Lissner.<sup>40</sup> These conditions, along with an explanation are:

1. Extremely small size. This is necessary in order to avoid modifying the actual behavior of the element to be instrumented.
2. Insignificant mass. This is also necessary to avoid modifying the actual behavior of the element to be instrumented.
3. Easy to attach to the member being analyzed. This is mainly for practicality.
4. Highly sensitive to strain. The possibility of measuring strain with extra sensitivity is desirable.
5. Unaffected by temperature, vibration, humidity, or other ambient conditions likely to be encountered in testing elements under service loads. This is to avoid measuring strains induced by factors other than applied loads.
6. Capable of indicating both static and dynamic strains.
7. Capable of remote indication and recording. This enhances the practicality of measuring and analyzing data.
8. Inexpensive.
9. Characterized by an infinitesimal gage length. By definition, strains are usually related to a single point in an element.

This review of an "ideal" gage provides an understanding of the ultimate objectives pursued by instrumentation engineers. The following survey of available concrete strain

instrumentation devices explains the most important characteristics of each system, along with known data about their performance.

**5.1.2 Embedment Systems.** Instruments that are embedded in concrete to measure stress through bonding introduce a new source of error known as the *inclusion effect*. A disturbance of the actual strain field could be caused by the inclusion of a strain gage in the concrete. The measured strains could be significantly different than the ones that would occur if the gage were not present. The degree of disturbance of actual strains due to the inclusion effect is directly related to the relative ratio of gage to concrete stiffness.<sup>9</sup>

Tests related to the inclusion effect of strain gages embedded in concrete were reported by Loh.<sup>26</sup> A generally good conformance is achieved by a gage that has a modulus similar to the concrete surrounding it. In these cases, the strain measurements will be correct. When the stiffnesses are different, some errors will be introduced. Their magnitude will then depend on the geometry of the gage. The stiffness of a gage is usually expressed in terms of the modulus of elasticity of a material which would form a solid cylinder of the same stiffness as the gage, when this cylinder has a diameter equal to the outside diameter of the tube of the gage.

A graphical description of the inclusion effect based on Loh's analytical expressions was prepared by Bakoss<sup>9</sup> and is shown in Figure 5.1.

The analytical formulas included in the graph of Figure 5.1 are approximate and based on a linear-elastic behavior of the materials. The graph relates the longitudinal axial strain in a cylindrical inclusion (strain gage) to the longitudinal strain which would occur in the same direction in the matrix material if the inclusion were not present.

Several strain gages of the embedment type were initially reviewed for this project. The main details of each system evaluated are provided here.

**5.1.2.1 Vibrating Wire Strain Gages.** These are the usually preferred type of gages for most long-term instrumentation programs due to their good performance and stability. However, their greatest disadvantage is their high cost which becomes a concern for large instrumentation projects. An important addition to the total cost for implementing vibrating wire gages for an instrumentation project is the need of special readout units. This could be expensive if portability and automated multi-channel operations are desired.

The vibrating wire technology measures strain from variations in the natural frequency of a high-strength steel wire. An advantage of these gages is that variations in resistance of the lead wires do not affect the readings of frequency. Inclusion effects are also minimized since most commercial vibrating wire gages have similar stiffness to that of commonly-used concrete materials. Signal long-term stability is not a major concern for these types of gages. Previous studies indicate negligible long-term zero drifts.<sup>55,9</sup> However, small sources of zero drift are

still possible due to wire corrosion, creep of the vibrating wire under tension, external source of gage vibration, or slippage at the wire clamping points.<sup>15</sup> A summary of the main technical characteristics of typical commercial vibrating wire strain gages is shown in Table 5.1.

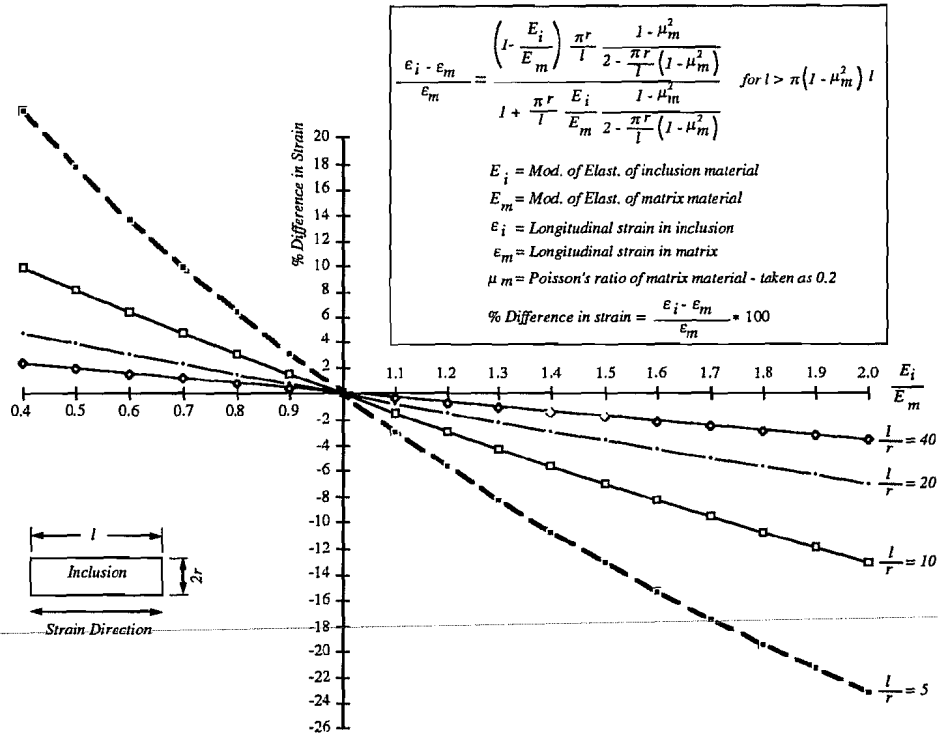


Figure 5.1 Strain errors produced from inclusion effect of different materials and sizes (after Bakoss<sup>9</sup>).

Table 5.1 Technical data of typical vibrating wire strain gages for embedment in concrete.

<b>Gage Manufacturer:</b>	Irad Gage		Geokon, Inc.	
<b>Distributor:</b>	Roctest, Inc.		Geokon, Inc.	
<b>Gage Model:</b>	EM-5	EM-3	VCE-4200	VCE-4210
<b>Current Cost (p/unit):</b>	≈\$150.00	≈\$200.00	≈\$95.00	≈\$275.00
<b>Gage Length (in):</b>	6.63	3.63	6	10
<b>Flange Diameter (in):</b>	0.875	0.875	0.75	2
<b>Strain Range (μΕ):</b>	±3000	±3000	±1500	±1500
<b>Avg. Sensitivity (μΕ):</b>	0.3	0.2	1	0.5
<b>System Accuracy Range (μΕ):</b>	±5-50			

There are two different classes of gages that are based on the vibrating wire technology, the commercial prefabricated gages and the sister bar type of gages (sometimes called rebar

*strainmeters*). A schematic and sample of the first type of gage are shown in Figure 5.2. The usual configuration of a sister bar type of vibrating wire gage is presented in Figure 5.3. Several companies offer vibrating wire strain gages. Some of them are:

1. Rocrest, Inc., Irad Gage Division, 7 Pond Street, Plattsburgh, NY 12901. Current telephone (518) 561-3300.
2. Geokon, Inc., 48 Spencer Street, Lebanon, NH 03766. Current telephone (603) 448-1562.
3. Gage Technique Ltd., P.O. Box 30, Trowbridge, Wilts BA14 8YD, England, Great Britain.

**5.1.2.2 Electrical Resistance Strain Gages.** These gages are the basic component of many concrete strain measuring devices. The electrical resistance gaging technology was explained in Chapter 3.

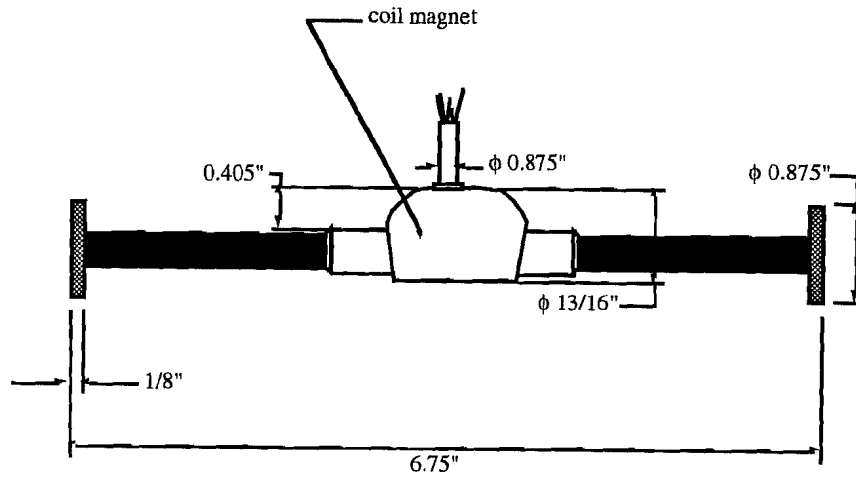
Most concrete embedment strain gages based on electrical resistance foil gages are relatively inexpensive. One problem is that very strict guidelines for installation and moisture protection must be followed to achieve satisfactory long-term stability. Varying degrees of errors can also occur due to the previously-mentioned *inclusion effect*. Other gages within this group consist of: Mustran Cells and Plastic Encased Embedment Gages.

**Mustran Cells.** These were originally developed by L. Reese and student researchers from the Center for Highway Research of the University of Texas at Austin. The original name stands for *Multiplying strain transducers*.<sup>10</sup> They are based on electrical resistance strain gages bonded to specially-fabricated steel bars with 1/4-inch threaded ends. In the design phase of these gages very careful measures were taken to match the relative stiffness of the gage with the average stiffness of concrete. This reduces the errors from the *inclusion effect* to a minimum.

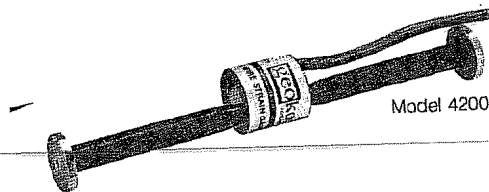
Mustran Cells were reported to have worked well in drilled shaft tests performed by its creators.<sup>10</sup> Acceptably low levels of gage drift were encountered in the initial applications. However, long-term stability of these gages could be difficult and costly to obtain. Table 5.2 shows approximate technical data for the original Mustran Cells, as reported by the manufacturers. Costs are excluded since no correct estimates are presently available. The multiplication of strains and the robustness of the cells present two great advantages for structural investigations in large concrete elements.

Table 5.2 Technical data of original Mustran Cells.

Gage Model:	Type I	Type II
Active Gage Length (in):	7	8.5
Flange Diameter (in):	2.5	2.5
Strain Range ( $\mu\epsilon$ ):	1500	1500
Avg. Sensitivity ( $\mu\epsilon$ ):	1	1
System Accuracy Range ( $\mu\epsilon$ ):	$\pm 10-50$	



a. Dimensions of Irad Gage Model EM-5 (courtesy of Rocrest, Inc.)



b. Standard Geokon gage Model VCE-4200 (courtesy of Geokon, Inc.)

Figure 5.2 Typical commercial embedment-type vibrating wire gages.

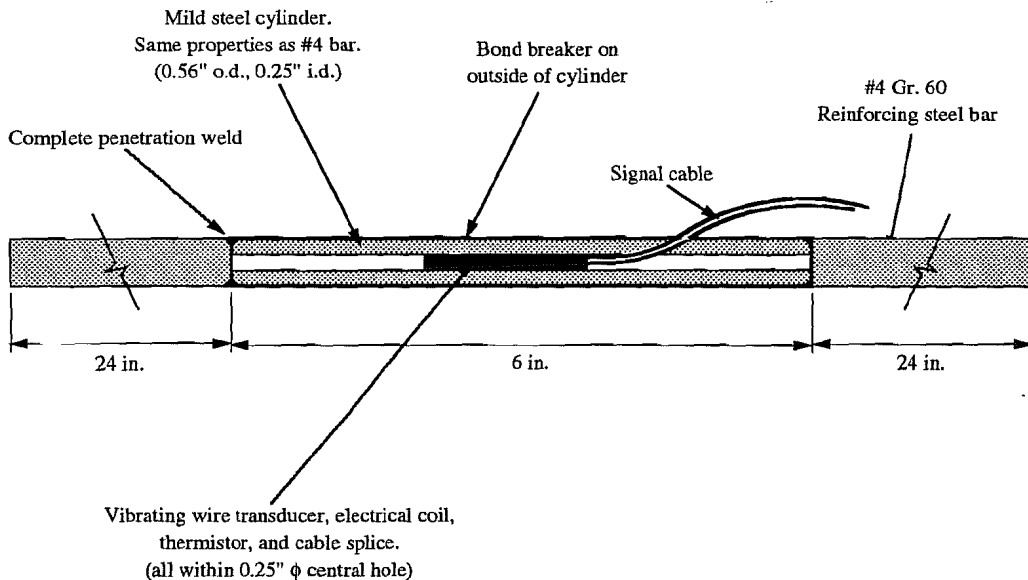


Figure 5.3 Typical sister bar vibrating wire strain gage (after Dunicliff<sup>15</sup>).

The original design of the Mustran Cells seems expensive and complicated, particularly in the moisture protection system based on liquid nitrogen pressure. This gage protection scheme can probably be replaced by a more easily applicable method such as any of the epoxy-based moisture and physical protection methods suggested by leading electrical resistance strain gage manufacturers. Due to their size, the original cells are limited to applications in large concrete structures. This imposes another limitation for their effective use in segmental concrete box-girder bridge structures.

Smaller, cheaper, less complicated gages can be easily built based on the original Mustran Cell design procedure and the new moisture protection methods. However, further detailed testing of any modified Mustran Cell system would be necessary to determine their sensitivity, gage factor, and accuracy. Illustrations of the original Mustran Cells and an example of a modified system used on previous projects at Ferguson Structural Engineering Laboratory are shown in Figure 5.4. Although these gages are not commercially available, they could be easily manufactured in-house at most structural engineering laboratories.

**Plastic Encased Embedment Gages.** (Also described as *Embedment Gages* by some researchers, and as *Polyester Mold Gages* by some manufacturers.) These gages consist of a standard wire-type resistance strain gage attached to leadwires, and hermetically sealed between thin resin plates. These plastic plates are usually coated with a rough grid surface to provide good bond. They are longer than traditional foil electrical resistance strain gages, and they are specifically manufactured for embedment in large structural concrete masses where uniaxial strains are expected, such as columns, piles, or drilled shafts.

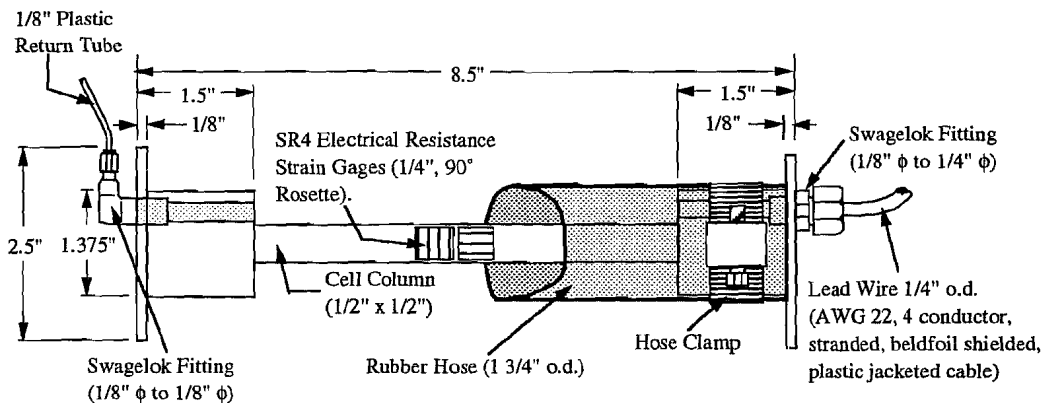
Problems related to gage drift (due to temperature) and moisture penetration (causing low resistance to ground) were reported in previous studies.<sup>51</sup> These studies have also concluded that the method of compensating temperature effects with a "dummy" unstrained gage was not an effective alternative. Further tests with carefully sealed dummy gages confirmed these conclusions.<sup>10</sup> Investigations are still needed for developing an effective method of temperature compensation and for reducing the drift of these gages.

The level of accuracy of the system can be improved by precasting them into small concrete cylinders, as suggested by Vijayvergiya.<sup>51</sup> However, as with other electrical resistance strain gages, these can only be reliable for short-term investigations.

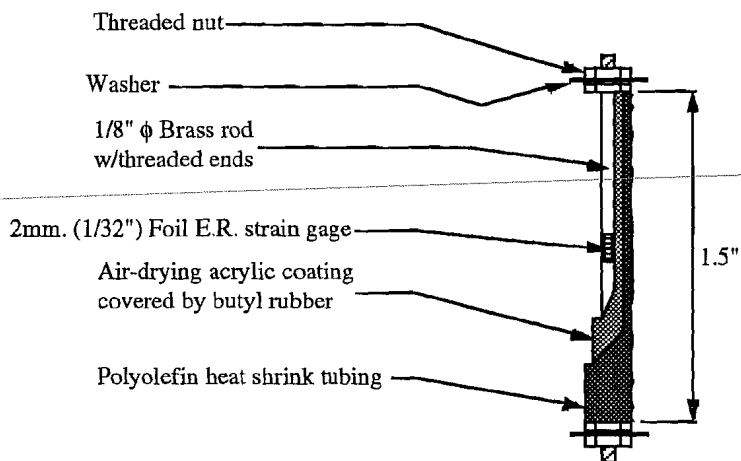
A widely-known manufacturer of these type of gages is Tokyo Sokki Kenkyujo Co. (TML) represented in the United States by Texas Measurements, Inc., P.O. Box 2618, College Station, TX 77841. Current telephone: (409) 764-0442.

**5.1.2.3 Carlson Elastic Wire Strain Meters.** These gages are also based on direct measurements of variations in the electrical resistance of an electrical conductor. In this case however, the conductor is an unbonded elastic wire, as shown in Figure 5.5. These devices are

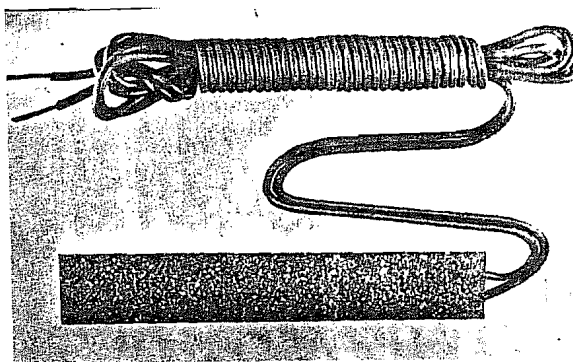




a. Original Type II Mustran Cell. (after Reese [63]).



b. Modified Mustran Cell. (after Falconer [95]).



c. Polyester Mold Gage: TML Model PML-60 (courtesy of TML).

Figure 5.4 Concrete embedment strain gages based on the electrical resistance technology.

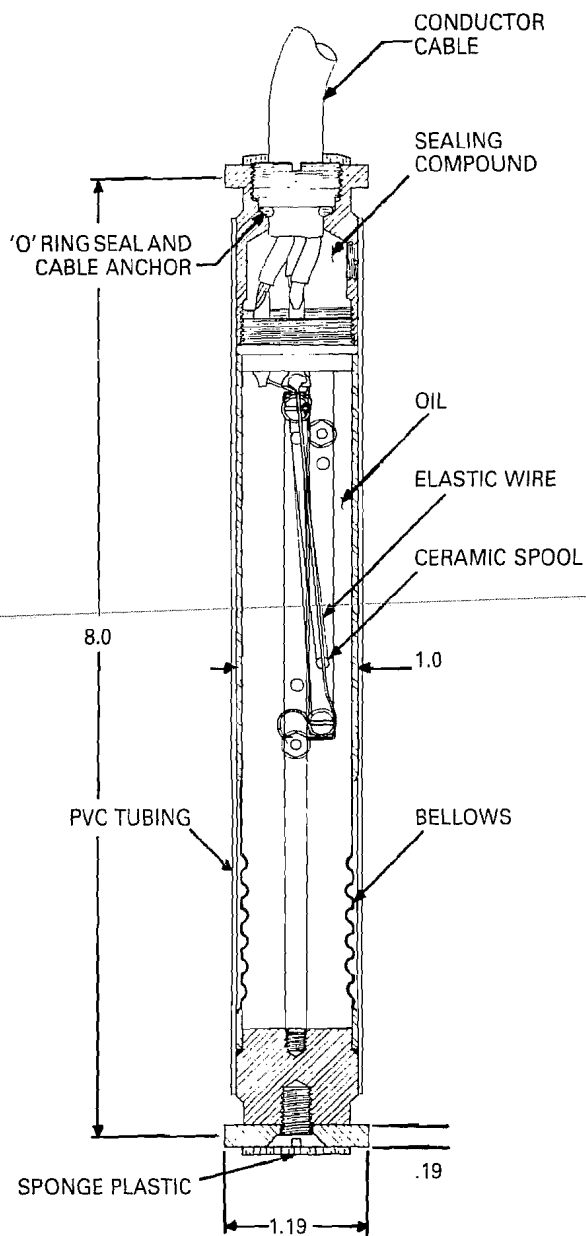


Figure 5.5 Typical Carlson Elastic Wire Meter (courtesy of B.R. Jones and Associates, Inc.).

characterized by their long-term stability. To improve their stability and moisture protection the elastic wires are heat treated during manufacturing and the complete inner tubing is filled with oil and hermetically sealed. The main longitudinal body of the sensor is covered by a smooth PVC tubing to prevent bonding with concrete. Since the main frame of the sensor is made of steel, very small temperature corrections need to be made to account for the difference of thermal coefficients of expansion between steel and the surrounding concrete. This is only necessary when very precise measurements are important.

The instrument's design uses two separate elastic wires, one providing increased resistances with increasing strain while the other one indicates decreased values with increasing strains. Measuring the ratio of these two resistances maximizes accuracy and reduces temperature effects. These are claimed to be the most widely-used concrete strain measuring devices in this country.<sup>15</sup> However, their high cost is a limiting factor for large instrumentation projects. Carlson Elastic Wire Strain Meters are mostly used in 8-, 10-, or 20-inch gage lengths. Smaller, more economical gages are available in 4-, 8-, and 10-inch gage lengths. Technical data for the most widely-used gages are indicated in Table 5.3.

Table 5.3 Technical data of other strain gages for embedment in concrete.

Gage Type:	Polyester Mold		Carlson Strain Meter	
Gage Manufacturer:	TML		Carlson/R.S.T. Inst., Inc.	
Distributor:	Texas Measurements, Inc.		B.R.Jones & Assoc., Inc.	
Gage Model:	PML-60	PML-120	A10	M10
Current Cost (p/unit):	≈\$15	≈\$25	≈\$207.00	≈\$127.00
Gage Length:	125mm	125mm	10in	10in
Gage Width:	13mm	13mm	1.19in	0.88in
Strain Range (μϵ):	20000	20000	2100	1600
Avg. Sensitivity (μϵ):	1	1	2.9	5.8
System Accuracy Range (μϵ):	±10-50		±20-75	

These gages can be purchased from:

1. Carlson Instruments, Inc., 1190-C Dell Avenue, Campbell, CA 95008.  
Current telephone: (408) 374-8959.
2. B.R. Jones & Assoc., P.O. Box 38, Normangee, TX 77871. Current telephone: (409) 396-9291.
3. Texas Measurements, Inc., P.O. Box 2618, College Station, TX 77841.  
Current telephone: (409) 764-0442.

**5.1.3 Surface Strain Systems.** Problems related to the *inclusion effect* are negligible in surface-mounted concrete strain gages. In general, most gages within this category provide slightly less accuracy and sensitivity than the embedment gages but they usually have larger strain ranges. Gages of this type were separated according to their method of measuring strains into mechanical, vibrating wire, and electrical resistance devices.

**5.1.3.1 Mechanical Devices.** This is one of the most widely-used classes of devices for measuring strains in concrete. Advantages similar for all gages within this group are related to their simple behavior, low cost, robustness, ease of installation, and lack of need of special waterproofing procedures. Problems are related to the need for adequate access to the element to be instrumented, lack of automated readouts, and lower accuracy. Reported devices representing this group are composed of Demec Extensometers and Whittemore Gages.

**Demec Extensometers.** Their name is derived from *demountable mechanical extensometers* and were developed by the Cement and Concrete Association in England.<sup>15</sup> As shown in Figure 5.6, they consist of an invar bar with conical locating points at each end, one fixed and the other one pivoting on a knife edge. The pivoting movement is transmitted to a 0.002 mm resolution dial indicator via a lever arm.

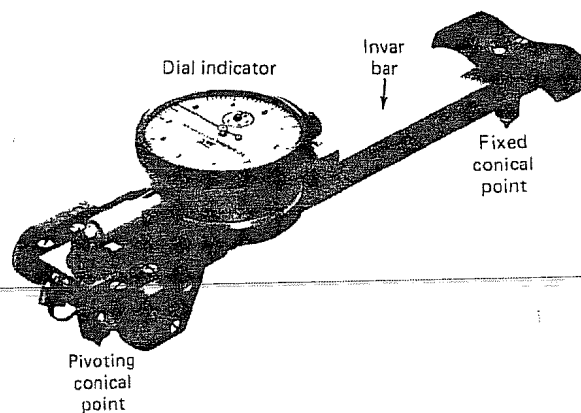


Figure 5.6 Demec extensometer (after Dunning<sup>15</sup>).

Gages are usually custom manufactured for each order and could have different gage lengths. The most common gages are of 100, 200, and 400 mm lengths.

An important disadvantage of these gages is related to their manufacture and availability. The only place of manufacture is in England and it can take 3 to 6 months for completing a purchase order from the United States (from time ordered to time of receiving the gage). Experiences of the present author with these gages also demonstrated that the spring at the pivoting end can wear out within a few years of field use, and the gage would have to be recalibrated for useful accuracy.

A separate invar bar is supplied with each gage so as to measure a standard reference reading. Temperature strains of the Demec extensometer and zero drift are minimized by recording initial measurements of the standard reference bar and surface temperature measurements in the concrete. Small stainless steel locating discs with a central conical indentation are installed on the surface of the element to be measured. These are supplied by the gage manufacturer in standard circular stainless steel units of 6 mm diameter, and 1 mm thickness. Long-term stability of these gages is feasible but also depends on the bonding method of the locating discs to the concrete surface. The actual level of accuracy varies according to gage length and reading carefulness. For 200 mm gages (with standard sensitivities of  $8.1\mu\epsilon$ )

accuracies of  $16\mu\epsilon$  have been found feasible in field measurements. Technical data for typical Demec extensometers are included in Table 5.4.

Table 5.4 Technical data for typical Demec extensometers.

<b>Gage Manufacturer:</b>	W.H. Mayes and Son (Windsor) Ltd.		
<b>Gage Model:</b>	100	200	400
<b>Current Cost (p/unit, inc. standard bar):</b>	≈\$902.00	≈\$950.00	≈\$1064.00
<b>Gage Length (mm):</b>	100	200	400
<b>Strain Range (<math>\mu\epsilon</math>):</b>	±50000	±20250	±10000
<b>Avg. Sensitivity (<math>\mu\epsilon</math>):</b>	20	8.1	4
<b>System Accuracy Range (<math>\mu\epsilon</math>):</b>	±12-60		

The only manufacturer known by the present author for these gages is W. H. Mayes and Son (Windsor) Ltd., Vansittart Estate, Arthur Road, Windsor, Berkshire, SL4 1SD, England, Great Britain. Their current telephone is 44-753-864756.

**Whittemore Gages.** These are similar to Demec extensometers, but provide a significantly lower degree of accuracy.<sup>15</sup> They were formerly manufactured and marketed by Baldwin-Lima-Hamilton Corporation (now BLH Corp.). The new generation of Whittemore gages are now manufactured by Soiltest, Inc., and available in 4-, 6-, 8-, and 10-inch gage lengths. These gages are marketed under the name of *Multi-Position Strain Gages*. Their advertised average sensitivity is of  $\approx 50\mu\epsilon$ . As with the Demec extensometers, *Multi-Position Gages* are built around a calibrated dial indicator with a 0.002 mm reading resolution. Their frame is different since they are made of aluminum-magnesium alloy. Invar master bars can be purchased separately for checking master settings of the main gage. When using these gages extra care should be given to temperature-induced strains in the gage itself, the concrete, and in the master reference bar since all will be different. Previous applications of these mechanical gages to prestressed concrete I-girder bridges reported some difficulties due to temperature differentials between the top surface of the bridge and underneath.<sup>19</sup>

Other problems such as long-term stability of the guiding points, and mechanical wear with time are also present in these types of strain gages. One great advantage of Whittemore gages over Demec extensometers is their availability, since they are stocked in the United States.

These gages can be obtained from Soiltest, Inc., Materials Testing Division, 2205 Lee Street, Evanston, IL 60202. Their current telephone is (800) 323-1242. Current prices for these gages are shown in Table 5.5.

### 5.1.3.2 Vibrating Wire Strain Gages.

These are based on the same principle previously described in Section 5.1.2.1. They are normally attached to the concrete's surface by bolting to precast threaded studs or holes. Their long-term stability is more severely dependent on the method of attachment of the gages than on zero drift of the vibrating wire, since frequency readings are very stable. Surface-mounted vibrating wire gages are costly, with prices similar to those of the embedment gages. The elevated price of these gages is a considerable limitation for their use in large instrumentation projects.

Table 5.5 Current prices of Whittemore gages (from Soiltest, Inc.).

Multi-Position Strain Gage (Eng. Units):	\$680.00
Invar Master Bar (English Units):	\$121.00
Strain Gage Punch Bar:	\$171.00
Contact Points:	\$13.00
Brass Inserts (100 units):	\$82.00
Contact Seats:	\$3.00

Most of these gages are provided with a mechanism for adjusting the initial tension in the vibrating wire. Wire tension is regulated according to the expected range of strains to be measured in the concrete surface. An additional device incorporated with most commercial gages is a thermistor that supplies simultaneous temperature data at each reading. Data from typical gage manufacturers is shown in Table 5.6. These gages could be obtained from the same manufacturers previously listed in the section of vibrating wire embedment gages.

Table 5.6 Technical data for typical surface-mounted vibrating wire strain gages.

<b>Gage Manufacturer:</b>	Irad Gage		Geokon, Inc.	
<b>Distributor:</b>	Roctest, Inc.		Geokon, Inc.	
<b>Gage Model:</b>	SM-5A	SM-5B	VSM-4000	VK-4100
<b>Current Cost (p/unit):</b>	≈\$140.00	≈\$250.00	≈\$95.00	≈\$95.00
<b>Gage Length (in):</b>	5.88	5.08	5.875	2
<b>Thermistor (yes or no):</b>	Y	Y	Y	Y
<b>Strain Range (µε):</b>	3300	3300	3000	2500
<b>Avg. Sensitivity (µε):</b>	0.3	0.3	1	0.5
<b>System Accuracy Range (µε):</b>	±5-50			

**5.1.3.3 Electrical Resistance Strain Gages.** Some of the foil-type electrical resistance gages are directly bonded to specially-prepared concrete surfaces. Due to the method of preparation of the concrete surface and the difficulty of protecting the gages against external elements, bonded foil type gages are only reliable for short-term measurements. These gages also have the same problems previously outlined for the electrical resistance strain gage technology.

Concrete surface preparation is usually done by vigorously removing all loose particles on a surface about one inch larger than each dimension of the gage that is being used. Sometimes light sanding is required. A thin film of a normal-set epoxy that hardens at ambient temperature is placed as the base for the strain gage. Once the epoxy has hardened, standard cyanoacrylate adhesives provided by gage manufacturers can be used for final bonding of the gage to the prepared surface. This surface preparation is not stable for long-term measurements. It is only recommended for a maximum of one or two weeks, provided that the installed system is not subjected to large temperature differentials. After installing the gage and leadwires a moisture and physical protection system should be used around the final system.

Since these gages are for direct bonding to the concrete surface, their size is longer than regular foil gages. The rule of thumb for using a concrete gage of about 5 times the diameter of the largest aggregate requires gage lengths of 2 to 5 inches. Longer gage lengths are usually better for full-scale investigations since a better average strain behavior can be measured. Typical data from leading electrical resistance strain gage manufacturers is shown in Table 5.7.

Table 5.7 Technical data of surface bonded foil electrical resistance strain gages.

<b>Gage Manufacturer:</b>	Measurements Group Vishay		Tokyo Sokki Kenkyujo Co., Ltd.	
<b>Distributor:</b>	Micro Measurements Division		Texas Measurements, Inc.	
<b>Gage Model:</b>	20CBW	40CBY	PL-90	PL-120
<b>Current Cost (p/unit):</b>	≈\$17.00	≈\$34.00	≈\$4.00	≈\$6.00
<b>Gage Length:</b>	2in	4in	60mm	120mm
<b>Matrix Width:</b>	0.32in	0.33in	8mm	8mm
<b>Strain Range (με):</b>	up to 20,000		up to 2,000	
<b>Avg. Sensitivity (με):</b>	1	1	1	1
<b>System Accuracy Range (με):</b>	±1-5 (short-term only)			

**5.1.3.4 Fiber Optical Strain Gages.** These gages have not yet been used for measuring strain in concrete structures. Originally developed as a prototype for measurements in very aggressive environments (in terms of temperature and electromagnetic fields), commercial use of this technology can be expected in the near future. Several approaches to measuring strain could be followed by the principles of fiber optics. Two different fiber optical devices were investigated during the present survey of state-of-the-art systems for measuring strain.

Extensive research for a possible commercialization of a particular type of fiber optical gage is presently under development in the Mechanical Engineering Department of The University of Texas at Austin, under the direction of A. B. Buckman. Initial reports of the status of this research were expected to be published in 1991.

A different fiber optical gage has been developed and successfully tested in a parallel study performed by the Center for Electromechanics (CEM) from the University of Texas at Austin.<sup>22</sup> This is among the first successful experimental applications of a fiber optical strain gage based on the principle of interferometry. Most previous reports consisted of prototype models and of studies of gage accuracy and sensitivity.

The basic principle of operation of interferometric fiber optic strain gages is shown in Figure 5.7. A laser beam (with sufficient coherent light length) is launched into a directional coupler. This coupler splits the light beam into two others of approximately the same intensity, and propagates them into two similar lengths of single-mode fibers. Both light beams later reflect off the mirrored path ends and return to the directional coupler to recombine as the interfered output. This output produces visible fringes on certain devices such as oscilloscopes. If the optical pathlength through one fiber is changed with respect to the other, the fringes will shift. This amount of fringe shift is proportional to the relative change in optical pathlengths. By observing the motion of fringes in the oscilloscope, the optical pathlength changes can be determined with great accuracy. Simple studies on prototype tests of these gages reported up to  $0.4\mu\epsilon$  accuracies.<sup>13</sup> No valid range of accuracy was obtained from CEM's fiber optic strain gage since only a single successful test was performed to date. However, the gage along with the reading equipment utilized had sensitivities in the order of  $0.1\mu\epsilon$ .

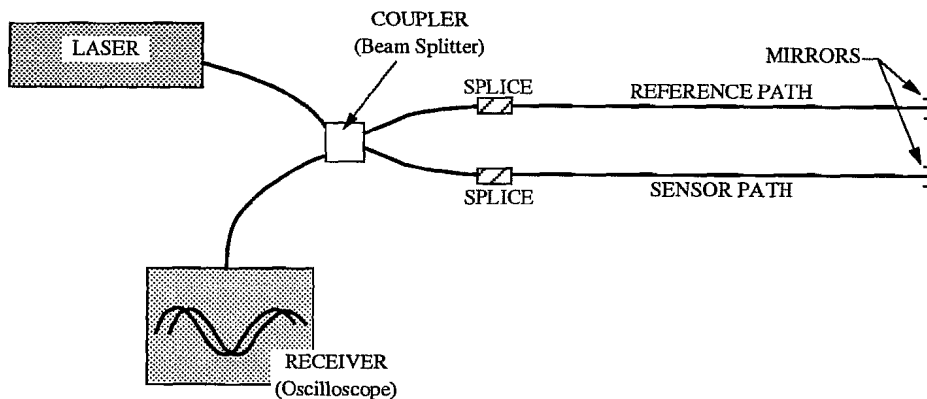


Figure 5.7 Principle of interferometric fiber optic sensors.

Present technology for these gages only allows them to be used for short-term dynamic tests. The phase shifts on the fringes of the oscilloscopes need to be counted as the test is being performed, and no recording or automated systems are presently available for unattended operation. A second disadvantage is the very brittle consistency of the fibers. During bonding of the fibers used in the CEM testing program, only one out of three survived installation. The fibers also need physical protection along their full length. Johnson, from CEM, threaded the fibers through a small heat shrink type of plastic, but this was still quite delicate.<sup>22</sup> However delicate,



these gages have one of the highest levels of strain sensitivity and can be used in extreme environmental and electromagnetic conditions. The tests at CEM required maximum temperature ranges of  $-196^{\circ}\text{C}$  to  $200^{\circ}\text{C}$ , under a maximum magnetic field of 30Tesla in a 30 ms. timeframe. The surviving fiber optic gage only failed at failure of the specimen.<sup>22</sup>

## 5.2 Trials of Instrumentation Systems

All concrete strain measuring devices reviewed in Section 5.1 were considered for testing trials. Vibrating wire gages and Carlson meters were eliminated due to their high costs and because of unavailability of laboratory support equipment. Mechanical extensometers and Mustran Cells appeared to be the most satisfactory devices for the present project. Mustran Cells however, were set aside because of the high expenditure necessary for achieving long-term stability of the low electrical signals. Demec extensometers and Whittemore gages were serious contenders, but the availability of Demec extensometers at the research facility made this system the best one to choose for trial tests.

Demec mechanical extensometers were selected for refinement in the following areas:

1. More durable method of bonding locating discs to concrete surfaces,
2. ~~Need for increasing the operating speed for taking measurements, and~~
3. Better repeatability of readings.

**5.2.1 Demec Gages: Bonding Methods.** One of the main problems with Demec extensometers is directly related to the long-term stability of the guiding points bonded to the concrete's surface. Previous field studies found long-term stability problems with the frequently-used method of surface gluing of locating discs provided by the gage manufacturer.<sup>42,11</sup>

Several methods for bonding locating discs of Demec gages to the concrete surface were therefore tested under laboratory and field conditions. The following is a general description of the different systems investigated:

1. Surface bond:
  - with quick setting epoxy
  - with cyanoacrylates
2. Concrete embedment bond:
  - stainless steel bolts
  - stainless steel pins
3. Drilled concrete bond:
  - epoxied stainless steel bolts
  - epoxied stainless steel pins
  - mechanical wedging bolts
  - mechanical nailed inserts

Some of the guide points for the Demec gages were custom made at Ferguson Laboratory. Bonding systems were evaluated in two areas of concern: ease of installation and long-term stability in aggressive environments.

**5.2.1.1 Ease of Installation.** In addition to actual installation problems, this factor also takes into account the difficulties encountered for the manufacture of the new Demec locating points. Several systems were found inadequate just after installation due to misalignment. Others did not survive through concrete casting and formwork stripping operations. The effectiveness of the installed system is thus another factor of importance to be considered within the overall factor of ease of installation. A final analysis of the systems investigated in trial tests is shown in Table 5.8.

Table 5.8 Ease of installation of different bonding methods of Demec locating points.

Bonding Methods	Advantages	Disadvantages
Surface Bond	<ul style="list-style-type: none"> <li>• Relatively cheap</li> <li>• No special manufacturing</li> <li>• No overlapping with construction operations</li> <li>• Short installation process</li> <li>• Least concrete disruption</li> <li>• No formwork modifications</li> <li>• Good final alignment</li> </ul>	<ul style="list-style-type: none"> <li>• Long periods of time to receive locating discs from manufacturer</li> <li>• Loss of bond with time and exposure</li> </ul>
Concrete Embedment	<ul style="list-style-type: none"> <li>• Medium cost</li> <li>• Low concrete disruption</li> </ul>	<ul style="list-style-type: none"> <li>• Requires special manufacture</li> <li>• Difficult installation process</li> <li>• Overlapping w/const. operations</li> <li>• Requires formwork modification</li> <li>• Poor final alignment</li> <li>• Problems at casting</li> </ul>
Drilled Concrete	<ul style="list-style-type: none"> <li>• Medium cost</li> <li>• No overlapping with construction operations</li> <li>• No formwork modifications</li> </ul>	<ul style="list-style-type: none"> <li>• Requires special manufacture</li> <li>• Medium difficulty in installation process</li> <li>• Some chipping on concrete surface</li> <li>• High concrete disruption</li> <li>• Medium final alignment</li> </ul>

Surface bonding of the original Demec locating discs proved to be the best method with respect to ease of installation. They are easy to attach and provide one of the best final alignments. The movement of the pivoting endpoint of the Demec extensometer is restricted to a certain range. Good alignment of the guide points is thus necessary for measuring the full range of possible strains in the concrete specimens. Surface bonding of the original Demec locating discs also provided the least amount of concrete disruption.

The initial specimens with concrete embedment systems had serious difficulties related to stability during concrete casting operations. Several methods to improve their formwork attachment were later designed. Labor-intensive methods of installation that required drilling of the formwork had successful stability during concrete casting and formwork stripping. However, they had problems with the final alignment of the drilled Demec guide points. Even at the final testing of the most successful method of installation, four out of six guide points were out of range for the Demec gage. Drilling two off-centered indentations on each one of the custom-manufactured inserts was later found to greatly reduce misalignment problems. A schematic of the final method used for embedment in concrete is shown in Figure 5.8.

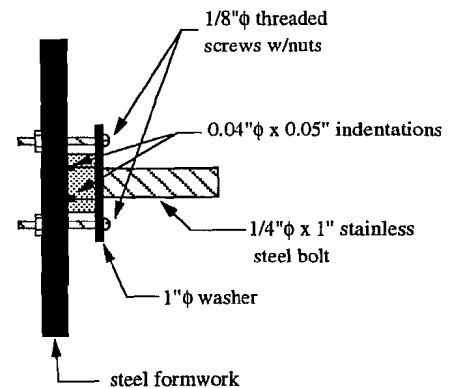


Figure 5.8 Concrete embedment method.

Indentations used as guide points for the Demec gages were manufactured at the research facility. A drill press with precision finger chucks was used in the manufacturing process. The drill bits were of straight shank size 60 ( $.040''\phi$ ) of  $\approx 0.8$ -inch usable flute length (stub length). Cobalt drill bits broke easily and only worked well for an average of 12 holes. Slightly more expensive tungsten carbide bits improved performance to 60-80 holes before breaking. Minimum drill depth was the depth at which the ends of the conical points from the Demec gages would reach the base of the drilled hole ( $\approx 0.05$  inch). These custom-manufactured locating points did not cause a measurable decrease in reading accuracy. The same manufacturing system for custom guide points was also used in some specimens of the drilled concrete bonding methods. No major disturbances of the concrete were caused by embedment methods. Inclusion effects were also small since the strains of the inserted material were relatively small compared to the strains in the concrete between guide points.

Adequate performance was obtained with most drilled concrete methods. Some problems of chipping of the concrete's surface were found with systems that required larger diameter holes. Drilling in high-strength concrete was performed with tungsten carbide masonry drill bits and special electric hammer drills. In general, the final alignment of guide points was better than with embedment methods. Improved alignment was obtained with drilled inserts of smaller diameter. Drilling smaller holes was easier, produced low concrete disruption, improved accuracy, and provided less room for misalignment. A picture of the four types of inserts used in the drilled concrete systems is shown in Figure 5.9. Varying degrees of concrete disruption were introduced by these methods. The present investigation did not address their degree of influence but assumed this to be negligible for 200 mm gage lengths. Certain errors were introduced with this assumption and more research can be helpful in this particular area.

### 5.2.1.2 Long-Term Stability.

This was a more important factor of consideration for the present investigations. Five 7-inch x 13-inch x 3-inch concrete specimens were cast with a design mix of  $f'_c = 5500$  psi. A general description of the systems tested for long-term stability is included in Table 5.9. An indication of the size and type of inserts is also included in the same table. The systems of "Mechanical Stainless Steel Inserts" (Table 5.9: #3.1 & #3.2) and "Mechanical Wedging Bolts" (Table 5.9: #3.5 & #3.6) consisted of modified commercially-available anchors for concrete. Anchors used were *Rawl Zamac Nailin* (stainless steel type w/mushroom head) of  $1/4"$   $\phi$  x 1 inch for systems #3.1 and #3.2, and *Hilti Quick Bolts* (also stainless steel) of  $1/4"$   $\phi$  x 1 inch for systems #3.5 and #3.6. Locating indentations for the Demec gages were drilled at the laboratory under the same procedures outlined previously.

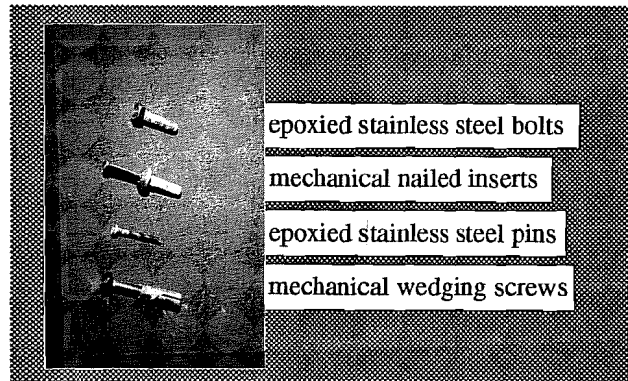


Figure 5.9 Inserts for drilled concrete methods.

Table 5.9 Description of systems tested for long-term stability.

SYSTEM CODE: NUMBER & NAME	INSERT DESCRIPTION	BONDING METHOD
<b>1. Surface Bond:</b> 1.1 Epoxied Demec Discs	Orig. Demec Discs	Type IV Epoxy
<b>2. Concrete Embedment Bond:</b> 2.1 Stainless Steel Bolts 2.2 Non-Stainless Steel Bolts 2.3 Stainless Steel Pins	$1/4"$ $\phi$ x 1" $1/4"$ $\phi$ x 1" $1/8"$ $\phi$ x 1"	Precast Precast Precast
<b>3. Drilled Concrete Bond:</b> 3.1 Epoxied & Mechanical Stainless Steel Inserts 3.2 Mech. Stainless Steel Inserts 3.3 Epoxied Stainless Steel Pins 3.4 Epoxied Stainless Steel Bolts 3.5 Epoxied Mech. Stainless Steel Wedging Bolts 3.6 Mech. Stainless Steel Wedg. Bolts	$1/4"$ $\phi$ x 1" $1/4"$ $\phi$ x 1" $1/8"$ $\phi$ x 1" $1/4"$ $\phi$ x 1" $1/4"$ $\phi$ x 1" $1/4"$ $\phi$ x 1"	Type V Epoxy & Mechanical Anchorage Mechanical Anchorage Type V Epoxy Type V Epoxy Type V Epoxy & Mechanical Anchorage Type V Epoxy

Systems of "Stainless Steel Pins" (Table 5.9: #2.3 and #3.3) consisted of original Demec discs welded in the laboratory to stainless steel rods of  $1/8"$   $\phi$  x 1 inch lengths. Special stainless

steel rods were used for the welding process to avoid corrosion at the welds. Finished samples of each one of these special systems were shown in Figure 5.9. The epoxy used for bonding complied with Texas Highway Department Type V Specifications.<sup>49</sup> Tests were performed with *Industrial Coating Model A-103* two-part epoxy donated by the Material Testing Division of the Texas Highway Department.

Long-term stability testing was performed according to ASTM Specification D-2933-74 (1986) "Corrosion Resistance of Coated Steel Specimens (Cyclic Method)".<sup>5</sup> Thirty-five freeze-thaw cycles with a salt-water solution were performed on the five concrete test specimens. According to specifications, this was approximately equivalent to more severe conditions than two years of inland Florida exposure. After this initial cycling the specimens were left outside the laboratory for a period of one year. A final report of the failures and problems encountered with the different systems is included in Table 5.10.

Table 5.10 Final report on long-term stability of Demec guiding systems.

SYSTEM CODE (Table 4.2)	ORIGINAL QUANTITY TESTED (& gage length)	SPECIMEN	STABILITY REPORT:		
			AFTER CASTING	AFTER FREEZE/THAW	AFTER ONE YEAR
1.1	2-100mm	3	OK	OK	2-Debonded
2.1	2-200mm	1 & 3	1-Bad	OK	OK
	3-100mm	4 & 5	1-Bad	OK	OK
2.2	3-200mm	2 & 3	OK	3-Corr	--
	3-100mm	2	3-Bad	3-Corr	--
2.3	2-200mm	1 & 3	1-Bad	OK	1-Scaled
	3-100mm	4 & 5	1-Bad	OK	OK
3.1	2-200mm	1 & 2	OK	OK	OK
	3-100mm	4 & 5	2-Bad	OK	OK
3.2	2-200mm	1 & 2	OK	OK	OK
	3-100mm	4 & 5	2-Bad	OK	OK
3.3	2-200mm	1 & 3	OK	OK	OK
	3-100mm	4 & 5	OK	OK	OK
3.4	2-200mm	1 & 2	OK	OK	OK
	6-100mm	4 & 5	OK	OK	OK
3.5	2-200mm	2 & 3	OK	OK	1-Corroded
3.6	1-200mm	3	OK	OK	OK
	3-100mm	5	OK	OK	OK

All of the non-stainless steel systems were corroded at the end of the cyclic period ( $\approx 2$  years equivalent exposure). Some of these systems were still giving reasonable readings. However, at the end of one year exposure (equivalent to a three-year period) all readings became unstable. More than 43% of the original number of concrete embedment systems were initially cast out of range, while only 15% of the drilled concrete systems were misaligned at initial

setting. Surface bonded Demec discs worked well initially. However, at the end of the three-year equivalent testing period some of them started debonding.

Results from these tests of Demec systems suggested that drilled concrete methods are more appropriate for long-term instrumentation projects. Stainless steel inserts (Table 5.9: #3.1) were finally selected as the most adequate system.

Although cheaper and easier to install, surface bonding systems were not selected since they become unbonded with time. Wear and tear from periodic measurements was also considered to be a secondary factor influencing the long-term behavior of surface bonded systems. This factor was not properly reproduced on the test specimens and could have been the reason for such a relatively long stability of the surface bonded systems. Systems based on embedment methods were too complicated to install, and they also presented serious problems of initial misalignment of locating points.

**5.2.2 Demec Gages: Increases in Operating Speed.** All demec extensometers are furnished with a high resolution dial indicator mounted to the top of their frame. A considerable amount of time is usually necessary for the reading process of a group of gage points, since very careful attention must be taken to avoid reading errors. Even for experienced people this reading process takes up some valuable time due to the small guide marks on the dial indicators. The present researchers attempted to find an automated method or set of instructions that would speed up the reading process without increasing the randomly occurring reading errors. The system that was finally envisioned involved the replacement of the original dial indicator by a "friendlier" digital indicator now available in the market. This was assumed to be an obvious growth of the old mechanical technology.

The original dial indicators of the Demec extensometers are custom built for the Demec gage manufacturer based on standard dimensions of commercially available dial indicators. Demec dial indicators have a 0.5-inch range and a 0.002 mm (0.000787-inch) reading resolution. The project researchers used a *Mitutoyo Digimatic Indicator Model 543-135* as a replacement. The installation of this new system only required special machining for the four mounting screws at the base. The new digital indicator was slightly larger, but it fit well in the flat mounting plate of the Demec extensometer. The final system is shown in Figure 5.10.

Proper usage of the new system would have required a careful recalibration of the extensometer so as to find the new gage factor. However, to carry out the initial goals of the present testing phase (i.e. to examine speed in reading operations) a recalibration was not necessary.

Tests were performed with a field investigation of span C-35 of Phase I-C of the San Antonio Y elevated highway project. Sets of thirteen, nine and five Demec locating discs were distributed in three different cross sections on the top surface of the 100-foot span as shown in Figure 5.11. All gage points were the standard Demec locating discs directly bonded to the concrete with quick-setting epoxy resins. No sophisticated bonding methods were used since the

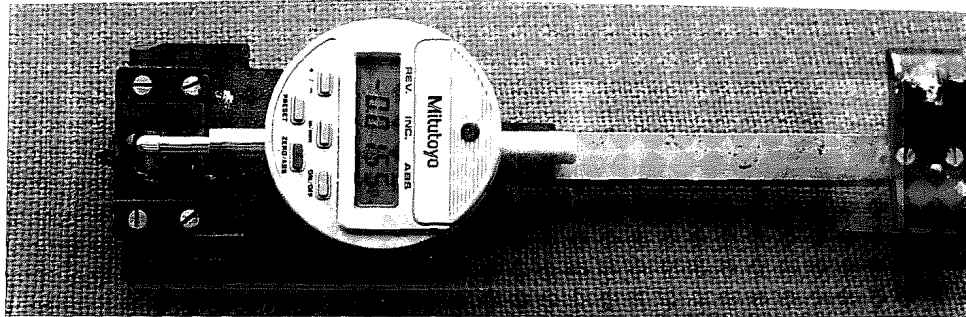


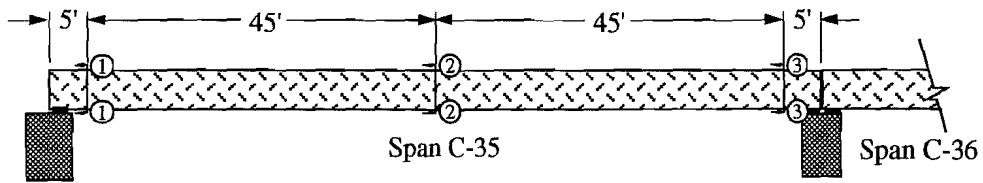
Figure 5.10 Modified Demec extensometer.

test involved only short-term measurements. It was the intention of this testing trial to observe the daily variation of surface strains in the concrete due to temperature, and to observe the performance of the modified Demec extensometer. Both Demec extensometers used, standard and modified, were of 200 mm gage length. Readings from the modified (but uncalibrated) Demec extensometer were not accurate and were taken for the sole purpose of addressing speed improvements.

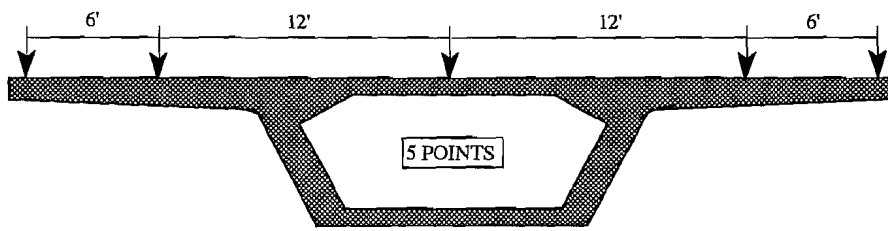
Test results, shown in Figure 5.12, show a consistent increase in speed of the reading operations of the modified gage. Each vertical scale value on this graph represents the time necessary for performing a single strain reading (as averaged from a series of 13 readings). It was safely concluded from this initial test that digital dial indicators provide an average 22% increase in speed for a single reading step. As shown in Figure 5.12, this amounts to about 2.6 sec of an average 11.6 sec standard Demec reading. This benefit is consistent with the increase in cost, since the addition of the digital indicator represented a 20% increment of the original cost of the 200 mm Demec gage (about  $\approx$ \$194.00 price increase).

The reduction of random reading errors of the modified Demec extensometer represents a secondary factor of benefit. This was not addressed by the present researchers and is recommended for further study.

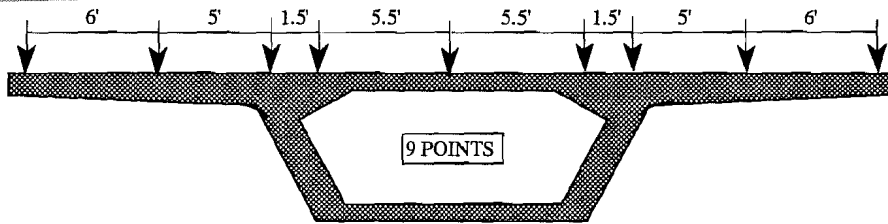
After a thorough investigation of newer digital dial indicators, models providing better resolution were found available. The indicator used for the reading speed tests had a 0.0127 mm (0.005-inch) resolution, much cruder than the 0.002 mm (0.0008-inch) resolution of the original Demec dial indicators. Digital dial indicators with much higher precision were investigated. The *Mitutoyo Digimatic Indicator Model 543-180* provides a resolution of 0.0001 mm (0.00005-inch). If properly installed and calibrated, these digital indicators can achieve a considerable improvement on the original sensitivity of the standard Demec extensometers. The present researchers performed no tests related to improvements of sensitivity, but strongly recommend them for future investigations. The higher resolution indicator represents 34% cost of the original price of a 200 mm Demec extensometer ( $\approx$ \$320.00). Installation costs were calculated at 10% increase ( $\approx$ \$100.00), and calibration would require an additional investment of 32% of



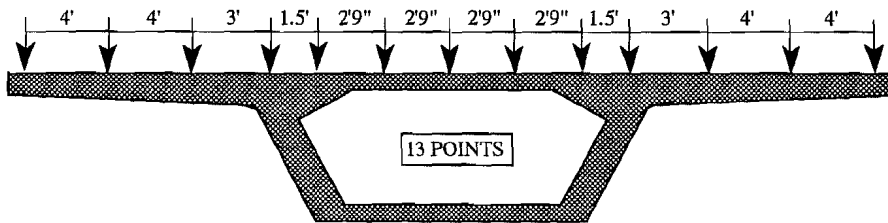
a. Longitudinal Cross Section



b. Section 1-1



c. Section 2-2



d. Section 3-3

\* all arrowheads indicate the center of a pair of Demec locating discs set for 200mm. gage length

Figure 5.11 Location of Demec points on test span C-35.



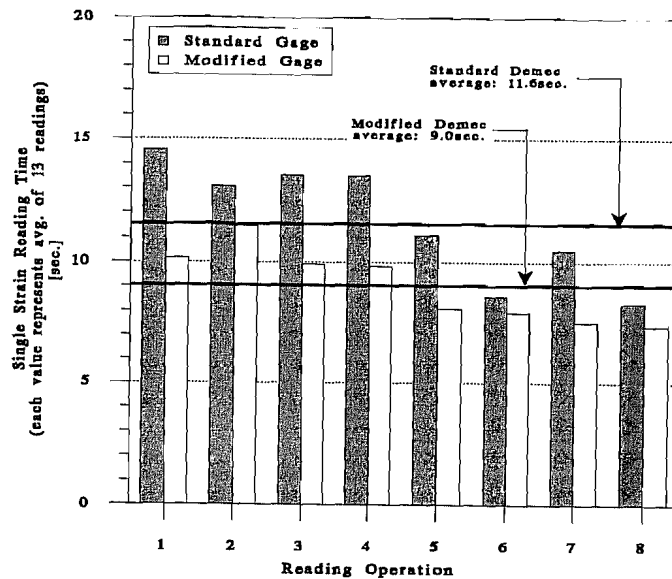


Figure 5.12 Comparison of reading speed of modified and standard Demec gages.

the gage price ( $\approx \$304.00$ ). This total investment of 76% of the original 200 mm gage price can be cost effective by the addition of the following benefits:

1. Improved sensitivity (in the order of 100 to 200%),
2. Faster operation (about 20% per reading step), and
3. Reduced possibility for random reading errors.

Two methods of gage calibration were considered by the present project researchers:

1. Shipment of complete modified gage to the original manufacturer in England for purposes of recalibration, or
2. Construction of a gage calibration device based on a workable model designed by Pauw and Breen for The University of Missouri.<sup>39</sup>

The use of either of these two methods for proper gage calibration would have required longer time than available. Time and budget limitations precluded the use of modified Demec extensometers with digital dial indicators in the present project.

**5.2.3 Demec Gages: Repeatability.** The 200 mm Demec extensometers have been found to reach  $16\mu\epsilon$  in reading repeatability when special care was followed in the reading operations.

Throughout the different tests performed with Demec gages, the following factors were found to influence the repeatability of gage readings:

1. Positioning of the Demec extensometer with respect to the locating points. Variations between the two possible locations of the Demec gage on each set of locating points introduced small errors. These were probably associated with irregularities in the geometry of the gage and the conical holes in the locating points.
2. Variations of gage pressure while holding in place to obtain strain readings. This is particularly important for inclined surfaces, when some pressure must be exerted on the gage to make it fit well in the conical holes of the locating points. Errors due to this factor increase if different operators alternate gage readings. Different operators should standardize their gage pressure for readings on inclined surfaces. For horizontal surfaces the only pressure should be the weight of the gage itself. This will minimize errors due to pressure differentials between different operators.

### 5.3 Recommendations for Use with the San Antonio Y Project

The selected method of monitoring concrete strains for this instrumentation project was based on the Demec Extensometer. Several recommendations for the proper operation of this type of instrument are summarized in this chapter.

Standard Demec extensometers can have good stability of measurements and efficiency, provided that they are properly calibrated, installed, and operated. Guidelines for achieving acceptable long-term stability of measurements with Demec extensometers are included in this section.

**5.3.1 Installation of Locating Points.** According to results from the trial tests, the system of "Epoxied Mechanical Stainless Steel Inserts" was selected as the most favorable for the present project.

Inserts recommended for use are the *Rawl Zamac Nailin* (stainless steel type w/mushroom head)  $1/4" \phi$  x 1 inch length (sold in boxes of 100 units). As shown in Figure 5.13, these devices are composed of a receptacle and a stainless steel nail insert. To use the *Nailin* as Demec locating discs requires pre-drilling of the indentations used as guiding points at the head of the stainless steel nails. Drilling should not be performed at the center location in the head of the inserts. Off-centered guiding holes allow better positioning of the nails so as to stay within the measurement range of the Demec gages. Drilling of the guiding holes is recommended to be performed in a drill press with special high precision adaptors. Use of a straight shank size 60 ( $0.040" \phi$  x 0.8 inch usable flute length) tungsten carbide bit gives good performance. A drilling

depth of 0.05 inch should be the minimum for these indentations to prevent the points of the Demec gage from touching the steel at the base of the hole.

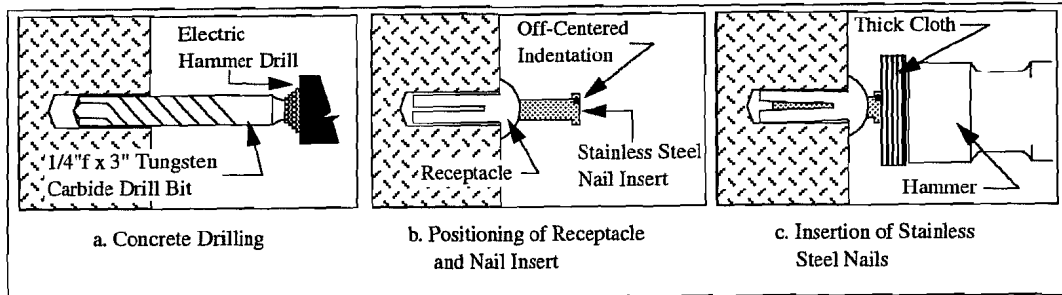


Figure 5.13 Installation of recommended Demec guiding system.

The heads of the pre-drilled stainless steel nails should be protected with a thick cloth during insertion, to prevent physical damage of the indentations. Concrete drilling is better performed with a tungsten carbide masonry drill bit ( $1/4"$   $\phi$ ,  $\approx 2$  inch usable flute length) and an electric hammer drill.

Use of epoxy is encouraged. When utilized, epoxies complying with the Texas Highway Department Type V Epoxy Specifications should be used. *Industrial Coating A-103* two-part epoxy worked well in the trial tests.

**5.3.2 Corrections for Temperature Differentials.** Two important temperature-related sources of errors should be avoided in field measurements of concrete strain with Demec extensometers.

First of all, in segmental box girder structures large temperature differentials are usually present between the top slab surface and the interior of the box girders. Errors associated with different temperature strains of the Demec extensometer, standard reference bar, and concrete surface should be avoided.

Errors due to temperature could also be present if the different expansions of invar steel and concrete are not considered in the data reduction. This second problem is important in cases where extreme temperature differentials are expected, such as in long-term instrumentation projects. Long-term instrumentation projects in Texas can expect to find temperature differentials in the order of  $80^{\circ}\text{F}$  between summer and fall. This can introduce significant errors.

To avoid errors from temperature differentials, the following considerations are recommended:

1. The initial standard reference bar reading should be taken before the first set of locating point readings, but after the Demec extensometer and the standard reference bar have reached the same ambient temperature as the location of the first set of guiding points. For segmental box girder bridges, where one set of locating points is usually installed in the outside top deck slab and another in the inside of the box girders, two widely different ambient temperatures are usually present. When available reading time is an important factor, then two different sets of Demec extensometers and standard reference bars should be used. One set should be allowed to operate at standard ambient temperature on the inside of the box girder, and the other on the top surface.
2. The Demec extensometer and the standard reference gage are both made of invar steel. Thermal coefficient of expansion for invar is approximately  $0.8 \times 10^{-6}$  units per  $^{\circ}\text{F}$ , and that of concrete varies from 5 to  $6.5 \times 10^{-6}$  units per  $^{\circ}\text{F}$ . For each temperature differential of  $10^{\circ}\text{F}$  about  $8\mu\epsilon$  will be induced by temperature strains of the gage itself, and  $50\mu\epsilon$  to  $65\mu\epsilon$  due to expansion of concrete. The best method for avoiding differential expansion errors is to implement an organized set of reading operations and data reduction when utilizing Demec extensometers. A suggested methodology for reading operations is included in Section 5.3.3. Data-reduction procedures can vary widely according to the researcher's depth of knowledge of standard electronic spreadsheets. Any method that follows a consistent reduction should be acceptable.

**5.3.3 Operating Instructions.** The following reading operations are suggested:

1. Allow Demec extensometer and standard reference bar to achieve the same ambient temperature as the instrumented concrete surface.
2. Set dial indicator of Demec at an initial value. This initial value should normally be the zero mark of the dial indicator.
3. Get initial reference reading ( $\epsilon_{st,o}$ ) of standard bar (use the average of three readings).
4. Get readings from each instrumented location on the surface of the concrete ( $\epsilon_{ci,o}$ ), again averaging a set of three readings if possible.
5. Measure the average ambient temperature  $T_o$ , or concrete surface temperature at time of initial readings at location of first set of points.
6. At a later time, after finishing the next set of readings (following steps a through e), the corrected concrete strain at each location of similar

ambient temperature on the concrete surface can be obtained with the following formula:

$$\epsilon_{icorr} = (\epsilon_{ci,j} - \epsilon_{ci,o}) + (T_j - T_o) * (a_{in} - a_c) + (\epsilon_{st,j} - \epsilon_{st,o})$$

where:

- $\epsilon_{icorr}$ : corrected concrete strain differential of guiding point i ( $\mu\epsilon$ )
- $\epsilon_{ci,j}$ : jth concrete strain reading of guiding point i ( $\mu\epsilon$ )
- $\epsilon_{ci,o}$ : initial concrete strain reading of guiding point i ( $\mu\epsilon$ )
- $T_j$ : jth concrete surface temperature reading ( $^{\circ}F$ )
- $T_o$ : initial concrete surface temperature reading ( $^{\circ}F$ )
- $a_{in}$ : thermal coefficient of expansion of invar steel ( $0.8 \mu\epsilon/^{\circ}F$ )
- $a_c$ : thermal coefficient of expansion of concrete ( $5.5 \mu\epsilon/^{\circ}F$ , suggested)
- $\epsilon_{st,j}$ : jth strain reading of standard invar reference bar ( $\mu\epsilon$ )
- $\epsilon_{st,o}$ : initial strain reading of standard invar reference bar ( $\mu\epsilon$ )

Final operating recommendations of the Demec extensometers are related to:

1. Repeatability, and
2. Handling and Storage.

**5.3.3.1 Repeatability.** Gage readings should be performed following the most standardized methods of operation. This has been found to have a direct influence on the repeatability of gage readings.<sup>11</sup> Standards for reading operations should be set in the following areas:

1. The positioning of the Demec extensometer's fixed point should be the same for all subsequent readings of the same locating points. This avoids measuring strain related to differences in seating conditions.
2. Pressure on the Demec extensometer while reading the strain values at each point should be constant for all subsequent readings. For strain readings on horizontal surfaces it is recommended to avoid using any more pressure than the weight of the Demec extensometer (for 200 mm or larger gages). On inclined surfaces, all operators in charge of strain readings should standardize the pressure exerted on the Demec gage. This can be done by taking several successive readings at one particular location until all operators achieve strain values within the acceptable level of repeatability.

**5.3.3.2 Handling and Storage.** Demec gages should be treated with all the carefulness required for precision mechanical instruments. The spring at the pivoting ends wears out rapidly in field applications and recalibration is costly and time consuming. When the pivoting end is worn out, the old gage should be replaced with a recalibrated gage. Strain correction readings should be taken from each location with the new and old gages. Standard

reference bars should also be kept clean and in good condition to avoid the introduction of wearing errors in the reference readings.

#### 5.4 Field Installation

All installation processes occurred at the casting yard. After the segments were removed from the match cast position, they were taken to a "make-ready" area where they were inspected and repaired as necessary. After the make-ready crew was finished with the segment, the researchers installed the Demec locating discs. A battery-operated hammer drill was used so no electricity was required for the operation. Each of the 15 instrumented segments had between 20 and 22 pairs of discs and these required approximately 1-1/2 hours for installation.

#### 5.5 Performance

Generally the Demec system worked very well. Compared to other systems for measuring concrete strain, a great deal of data can be generated for a relatively small cost. The system is not, however, without problems. The following is a brief description of some of the troubles:

1. *Human Error*: As mentioned earlier, there is a great deal of variability in reading Demec gages, depending on how the gage is held and how much pressure is applied. An experienced reader can get very repeatable results ( $\pm 16\mu\epsilon$ ). An inexperienced reader will not do as well, and when more than one reader takes the same set of readings those readings can vary significantly. It is therefore imperative that one experienced gage reader takes all readings on a particular set of gages.
2. *Locating Disc Misalignment*: Because of the method of disc installation, there was some fluctuation in the orientation of the holes. For best results, the holes in the discs must be oriented exactly perpendicular to the surface of the concrete. This ensures a repeatable reading (see Figure 5.14). If the discs are not oriented properly, the risk for reader error increases because the pressure applied to seat the extensometer in the holes becomes more critical.
3. *Time-Consuming*: Taking Demec readings was the most time-consuming aspect of the instrumentation program. One reader and one recorder could read 55 to 65 gages in 40-45 minutes.
4. *Damage with Time*: The gages became dirty with time which caused inaccurate readings. If dust, grime, or grout got into the precise holes on the locating discs, the extensometer would not seat properly and the

reading would be in error. Initially, great care was taken to clean the holes before the readings were made. This also was quite time consuming.

The final damage to the discs occurred due to their proximity to the joints. Before the asphalt topping could be laid, the epoxy squeeze out at every joint had to be ground down to the level of the concrete. As the epoxy was ground, so were locating discs close to the joint. All points on the top surface of the box were lost except in two segments where the points were more remote from the joints.

Generally, it can be concluded that Demec gages are a fine tool for short-term strain readings, if the points are carefully located and read by an experienced operator.

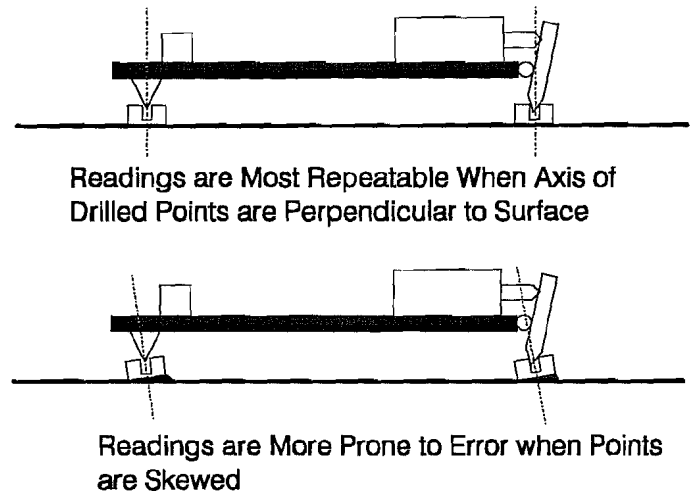


Figure 5.14 Proper and improper Demec point attachment.

## 5.6 Instrumentation Layouts

Figure 5.15 shows the layouts of the surface strain gages. During stressing operations one reader and one recorder measured the top slab points and another pair measured the points inside of the box.

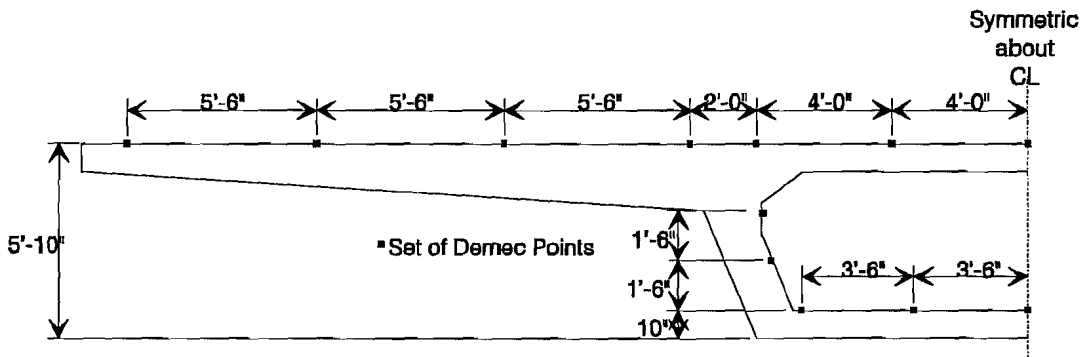
## 5.7 Recommendations for Future Projects

The Demec gage system gave good results for short-term readings and less reliable results for long-term readings. This system is definitely the most economical, especially if a large number of readings is desired. It is also a very labor-intensive system and the readings cannot be made remotely.

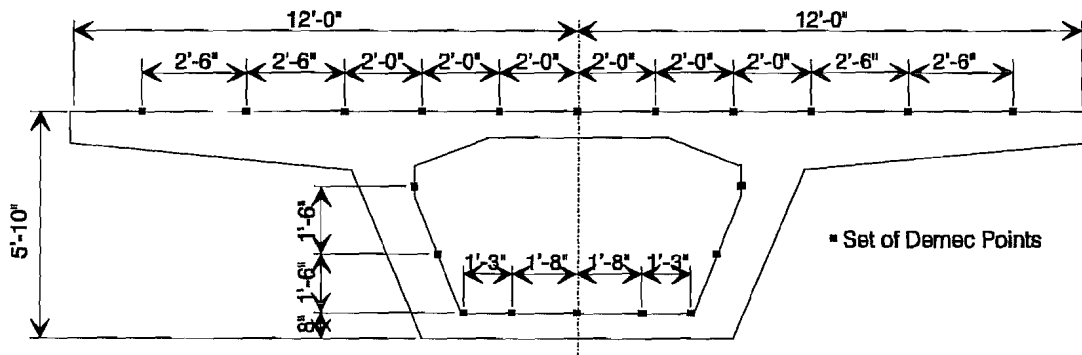
The following recommendations could help improve these readings:

1. If Demec gages are used:
  - (a) Always have a set of readings read with the same gage by the same experienced reader.

- (b) Protect the Demec points from getting dust, dirt, grout, etc. in the point.
2. If a remote system is desired, investigate concrete insert electrical resistance gages<sup>16</sup> or vibrating wire gages. Surface strain gages would be too susceptible to damage.



Spans A43 and A44 Demec Point Layout



Span C11 Demec Point Layout

Figure 5.15a Demec point layouts.



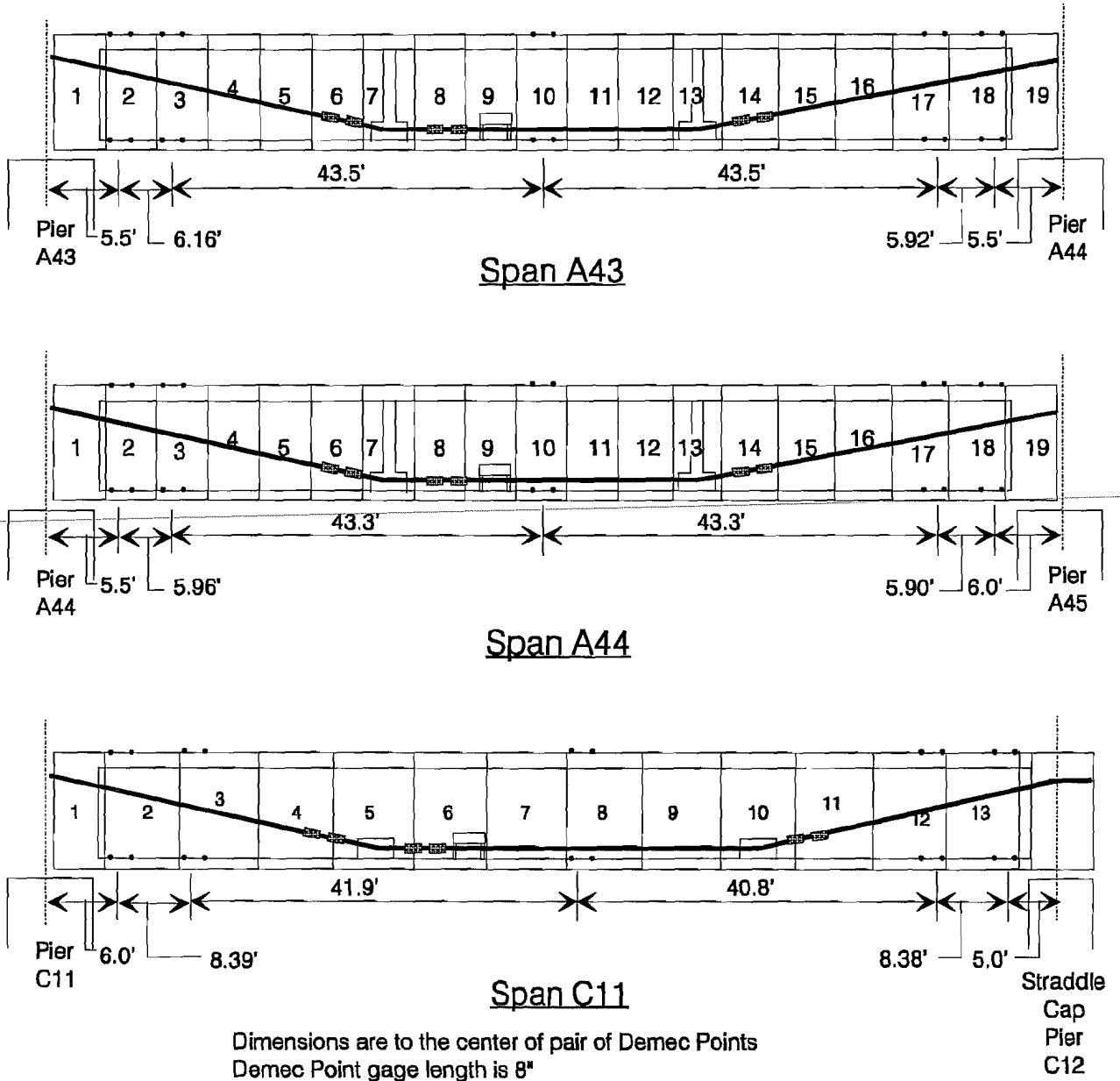
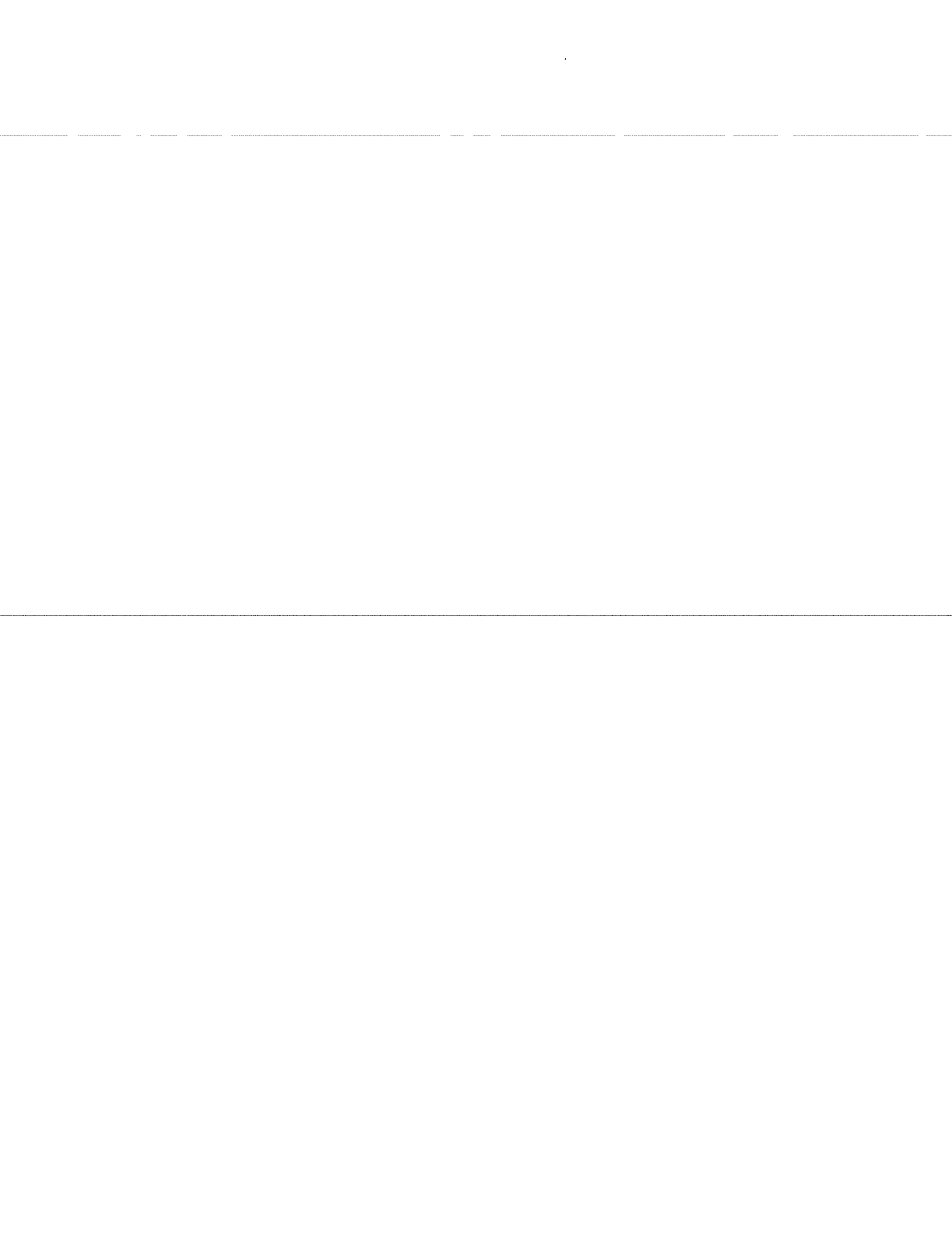


Figure 5.15b Demec point layouts.



## CHAPTER 6 OTHER MEASUREMENTS

### 6.1 Reinforcing Steel Strain Gages

**6.1.1 Recommendations.** Techniques for the use of electrical resistance strain gages in steel reinforcing bars were not investigated due to the good performance experienced in previous laboratory tests at Ferguson Laboratory. In the San Antonio Y structures, reinforcing bars were to be instrumented only for short-term investigations during initial loading of tendons. However, to assure proper functioning, and always when long-term stability is also needed, most recommendations established previously for the strain gage instrumentation of the prestressing strands should be followed:

1. Epoxy Preparation. Same as in Section 2.3.1.2.
2. Surface Preparation. Modify instruction 2.1 in Section 2.3.1.2 as follows:
  - 2.1 Grind off the ribs of the reinforcing bar leaving a smooth area for installation of the strain gage. Spray degreaser CSM-1 on a section slightly larger than the grind area.
3. Gage Installation. Same as in Section 2.3.1.2.
4. Epoxy Mixing and Placing. Same as in Section 2.3.1.2.
5. Gage Clamping. Modify. Cut a small piece of thin neoprene rubber (Measurements Group FN Neoprene Rubber) and cover the installed gage. Use an adequate hose clamp to exert an even pressure over the area of the gage. Follow the same curing conditions indicated in Section 2.3.1.2.
6. Soldering and Gage Protection. Same as in Section 2.3.1.2. Gage protection should work better considering the smoother surface of the reinforcing bars.
7. Data Reduction. Modify. When establishing load levels at each instrumented reinforcing bar, use the modulus of elasticity that was obtained from the companion steel reinforcing bar material tests and not the manufacturer values (see the Material Test Recommendations in Section 8.1.3).

### ***6.1.2 System Installation in the San Antonio Y Project.***

**6.1.2.1 Prefabrication.** Well ahead of casting and erection the lead wires which connect the reinforcing steel strain gages to the permanent data-acquisition system were cut to length, labeled, and soldered to amphenol connectors.

**6.1.2.2 Casting Yard Activities.** Normally the reinforcing steel cage for the following day's segment was completed between 12:00 and 2:00 pm the previous day. As soon as the steel workers were through with their work the researchers were given access to the cage. The following is the process of gage installation:

#### ***Day 1:***

1. The bars to be gaged were marked and the locations were sanded down to create a smooth flat surface for the gage.
2. The surfaces of all locations (8 to 12 places) were prepared and the gages set in position with cellophane tape.
3. A batch of epoxy was mixed and applied to the gages. The gages were clamped into position by encircling the bar with a layer of vinyl and then a small hose clamp.
4. The epoxy was allowed to cure for at least six hours.
5. After the epoxy had cured the hose clamps and vinyl were removed and the lead wires were soldered onto the gages. These lead wires were just long enough to extend out of the cage with three to four feet extra. All lead wires were carefully labeled.
6. The waterproofing was applied, and lead wires were secured to the reinforcing steel.

#### ***Day 2:***

1. The placing of the cage into the form was carefully monitored to preclude damage to the gages. The workers were also watched and reminded of the gages. In both deviators and diaphragms there is a great deal of congestion and bars are moved to allow placement of post-tensioning hardware and ducts. The workers took reasonable care to not damage the gages during this process.
2. The casting process was also observed. The lead wires were monitored to ensure they extended out of the concrete.

**Day 3:**

1. After casting, the gages were checked to see if they survived the casting operations. In the two diaphragms only one of 24 gages did not survive. In the three deviators, however, only 19 of 28 gages survived. No additional gages were lost between completion of casting and erection.
2. The lead wires were covered in black plastic and secured with duct tape to protect them while the segments were in storage.

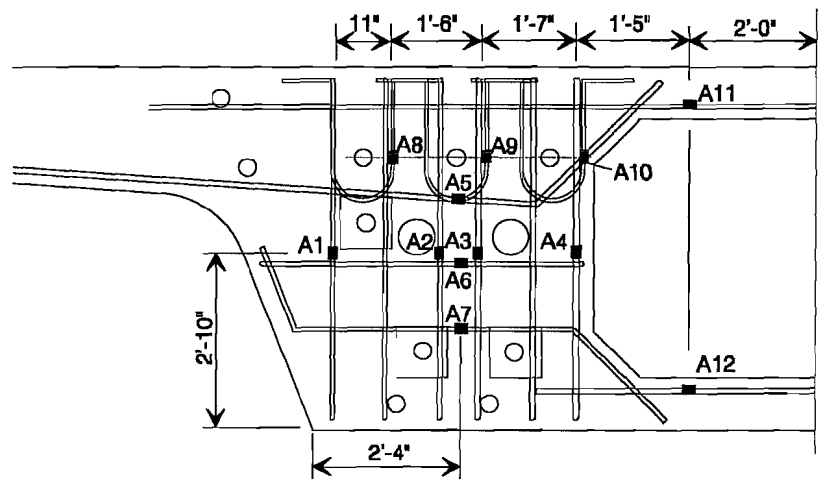
**6.1.2.3 Erection Site Activities.** At the erection site, on day three of the instrumentation installation, the prefabricated lead wires were soldered to the short leads extending out of the segments. The connections were waterproofed and the leads connected to the data-acquisition system. Data was collected at 20-second intervals during stressing and at 1½-hour intervals after that.

**6.1.3 Performance.** This system worked reasonably well, but was not without some difficulties. Since all of the gaging work was done outside in the casting yard, weather often posed a problem. The gages had to be temporarily protected from rain with black plastic on a few occasions. Also, working with the soldering iron and lights was impossible during rainstorms.

The amount of reinforcement adjustment in the diaphragms and deviators is substantial, and it was difficult to monitor the activities of the form crews at all times. A few well-placed hammer blows or crowbar pries destroyed some of the gages. In the future a greater number of redundant gages would be wise.

Overall, the system worked well and produced good data.

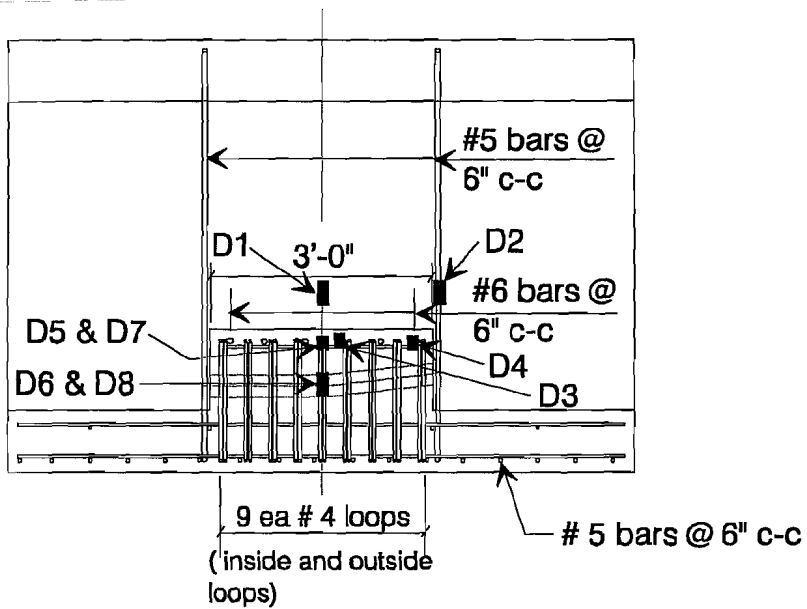
**6.1.4 Instrumentation Layouts.** Figure 6.1 shows the locations and designations of the



**Reinforcing Steel Strain Gage Layout  
Pier Segments 43A-1 and 44A-1**

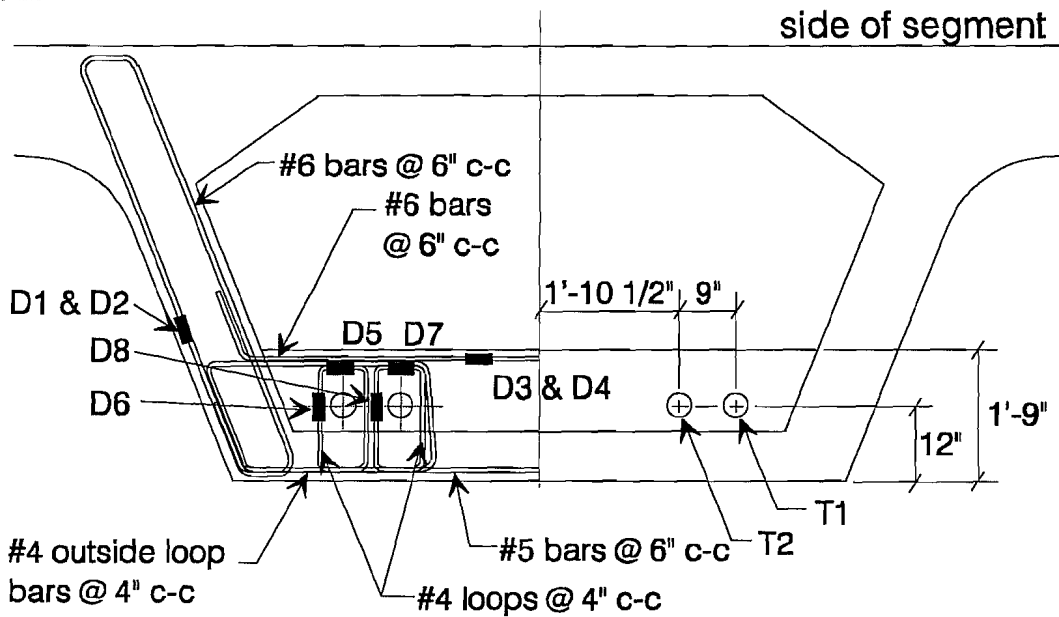
Gages are on the layer of reinforcing steel farthest from the anchor heads (most up station)

Figure 6.1a Reinforcing steel strain gage layouts.



Segment 11C-5 Section View

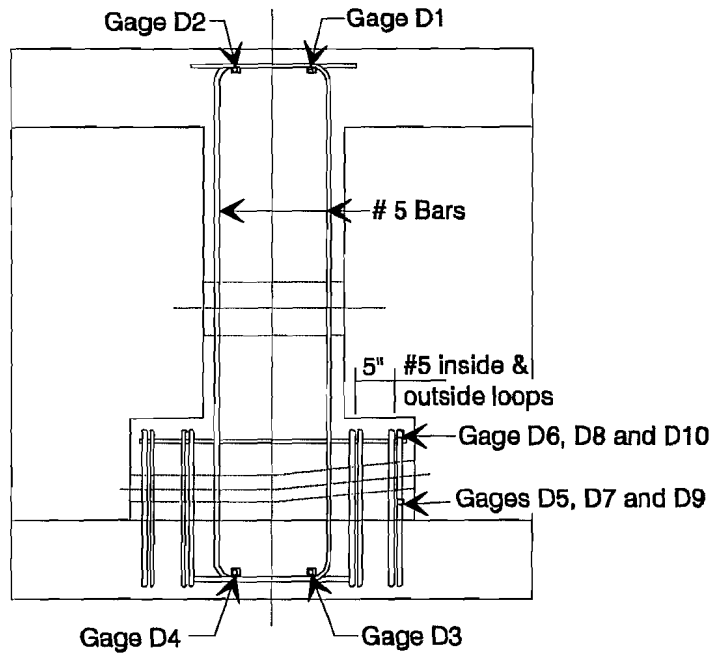
Gages are on North side of segment



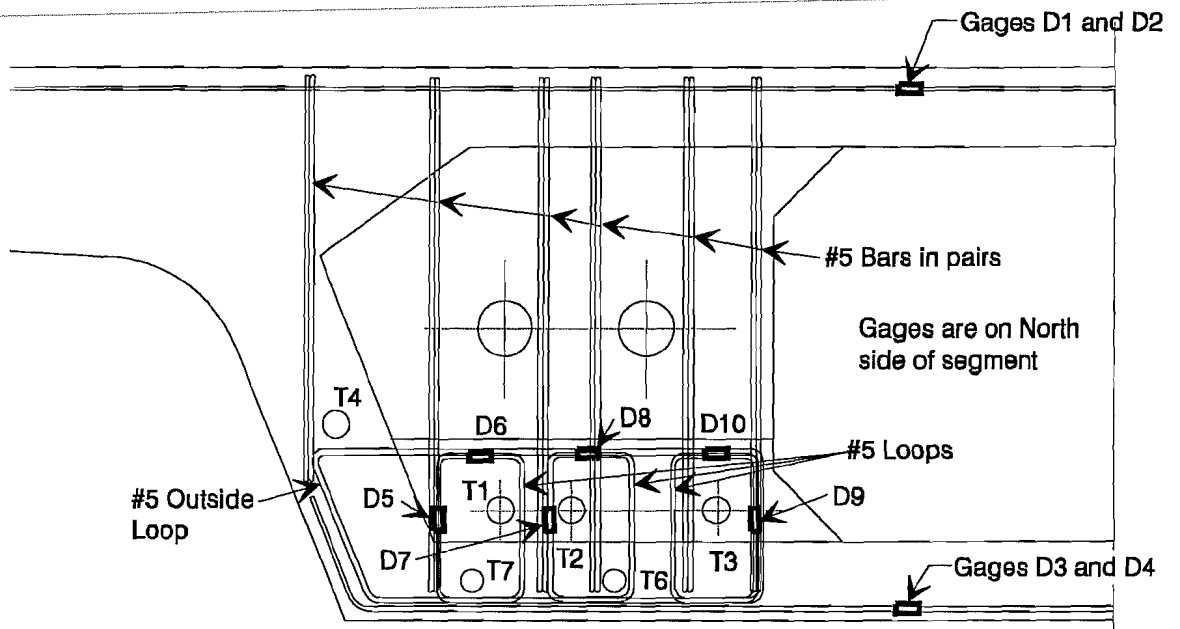
Segment 11C-5 Deviator Segment Elevation View

Typical segment bars not shown for clarity

Figure 6.1b Reinforcing steel strain gage layouts.



**Segment 44A-7 and 43A-7**  
**Section View**



**Segments 43A-7 & and 44A-7**  
**Deviator Segment Elevation View**

Typical segment bars not shown for clarity

Figure 6.1c Reinforcing steel strain gage layouts.

reinforcing steel strain gages. Gages in deviators were given a "D" designation and those in the anchorage zones an "A".

**6.1.5 Recommendations for Future Projects.** The reinforcing steel gage performed very well. Their only drawback is their susceptibility to damage during casting. The placement of redundant gages could help remedy the problem.

## 6.2 Joint Openings

In segmental box girder bridges it is usually desirable to instrument critical joints between concrete segments to check if any displacements occur. Because of the conservative design criteria and the use of epoxy joints, it was not expected that joints would actually open in the San Antonio Y bridges. However, joints between certain segments have opened considerably in the earlier applications of this bridge technology, particularly with dry joints.<sup>56</sup> Monitoring of displacements across the joint of two concrete segments is a simple measuring process that can be performed with relatively inexpensive instruments. A number of previous laboratory investigations related to box girder bridges have successfully used devices called *calibrated crack monitors* to measure these movements. These are introduced here in more detail.

**6.2.1 Recommendations.** Calibrated Crack Monitors have been traditionally marketed for measuring crack widths in concrete members. However, they can also be used very efficiently for the measurement of joint openings between concrete segments (which can basically be treated as cracks).

They are simple measuring devices composed of two Plexiglass acrylic plates of approximately 4 inches L x 1 1/4 inches W (as shown in Figure 6.2). One of these plates is usually white with a black colored grid of 40 mm x 20 mm (calibrated in millimeters). The other plate is transparent and fits on top of the first one. This top plate has two red-colored cross hairs centered over the zero marks of the bottom grid. The installation of the plates involves careful attachment to each side of a joint between two concrete segments. In short-term projects, the plates can be attached with any two-part epoxy adhesive. However, long-term projects should avoid this method of installation since epoxy adhesives have shown low long-term durability when used on concrete surfaces. An alternative is to use some type of mechanical anchoring devices combined with two-part epoxy products.

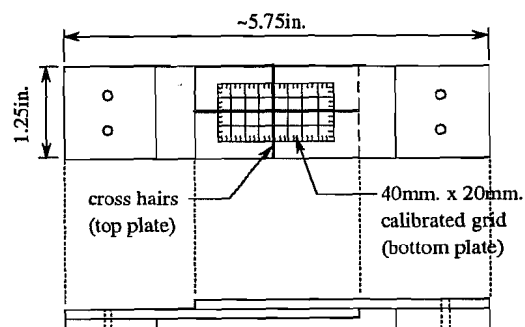


Figure 6.2a Avongard calibrated crack monitor: typical dimensions.



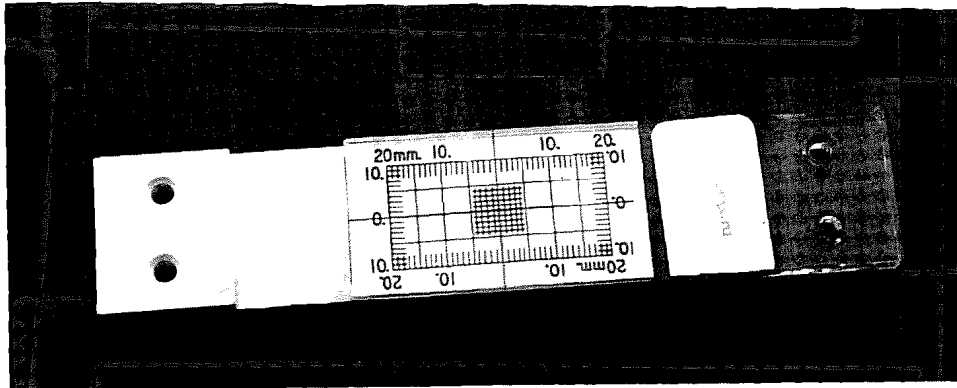


Figure 6.2b Avongard calibrated crack monitor: appearance.

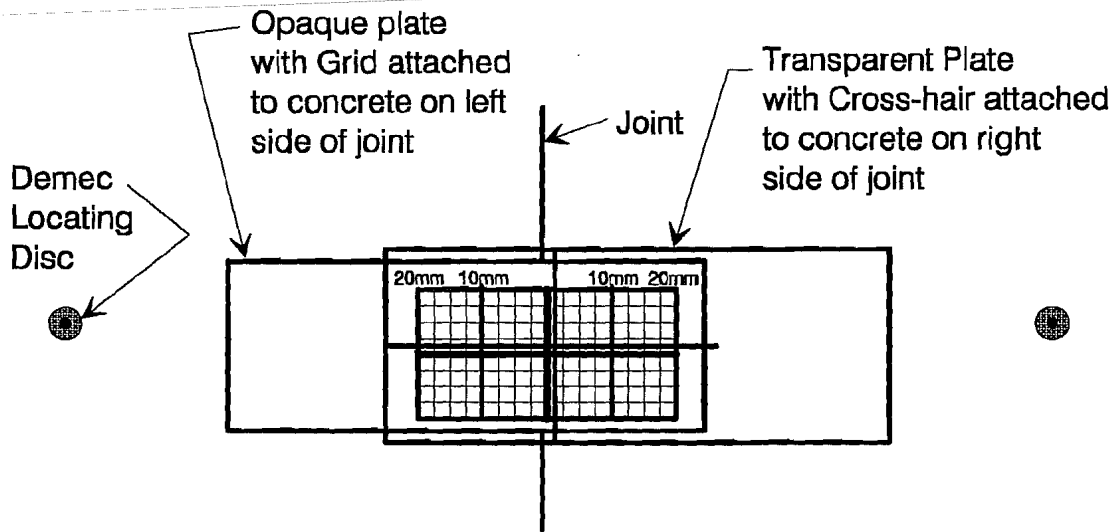
Vertical and horizontal movements can be estimated to 0.5 mm (0.02 inch) with these crack monitors. To obtain a greater degree of accuracy, mechanical strain-measuring devices can also be employed at the same locations where the crack monitors are placed. A pair of Demec locating discs can be easily installed near each calibrated crack monitor.

The crack monitors have a registered patent in the U.S. and are manufactured by a single company. The lack of competition makes this product more expensive than expected. A single calibrated crack monitor cost \$12.50 in early 1991. They can be purchased from Avongard Products U.S.A., located at: 2836 Osage, Waukegan, IL 60087. Their current telephone number is: (708) 244-6685.

To measure any separation of segments across their joints, *calibrated crack monitors* are recommended to be supplemented with Demec extensometers. Locating these two systems across a joint will provide a very reliable source of information about joint openings. Demec extensometers will provide a more accurate measurement of movements. However, the maximum measurable range of a Demec extensometer is very limited. In the unexpected case of large openings, the crack monitors will be essential instrumentation devices.

The calibrated crack monitors should be installed with some type of mechanical anchorage and two-part epoxy adhesives to ensure their long-term stability. The recommended methods from Section 5.3.1 should be used for anchoring the Demec locating discs near each crack monitor. Either the 100 mm or the 200 mm gage lengths of Demec extensometers will work well for these measurements. The operating instructions mentioned previously in Section 5.3.3 should be followed for these readings.

**6.2.2 Field Installation in the San Antonio Y Project.** As recommended, a dual measurement system was used to measure joint openings. Both grid crack monitors and Demec gages were used (see Figure 6.3). In this way, a strain might be associated with the point at which a joint opens.



The opaque plate and transparent plate are not connected and can move independent of each other in any direction

Figure 6.3 Grid crack monitor and Demec points.

The grid crack monitors and Demec gages were installed after the temporary post-tensioning operations were completed. The instrumentation was installed on the inside of the web walls so the gages could be read from inside the box. The joints were marked for the positions of the grid crack monitors and Demec points, normally one very close to the bottom slab and one very close to the top slab. A pair of Demec points, without a grid crack monitor, was also positioned at mid-height of the web. Both the grid crack monitors and the Demec points were attached using a quick-setting two-part epoxy glue (Atlas by Atlas Minerals and Chemicals Inc.). In some cases the epoxy buildup at the joint was excessive, so plastic plates were used to elevate the grid crack monitor slightly so it could span over the epoxy (see Figure 6.4). The installation of monitors and gages for 3 to 4 joints took approximately one hour.

**6.2.3 Performance.** This system performed reasonably well. Installation was simple and only a few points and monitors were damaged. The only problem was that the movements of the joints were so small that changes in the readings on the grid crack monitors were almost imperceptible. The Demec points, however, gave good readings of the changes in compressive strain across the joints.

**6.2.4 Instrumentation Layouts.** Figure 6.5 shows the layouts of the joint opening measurement system. Due to the high cost of the grid crack monitors, only one web wall in each span was instrumented. Since all but one span were symmetric, one web wall was considered adequate.

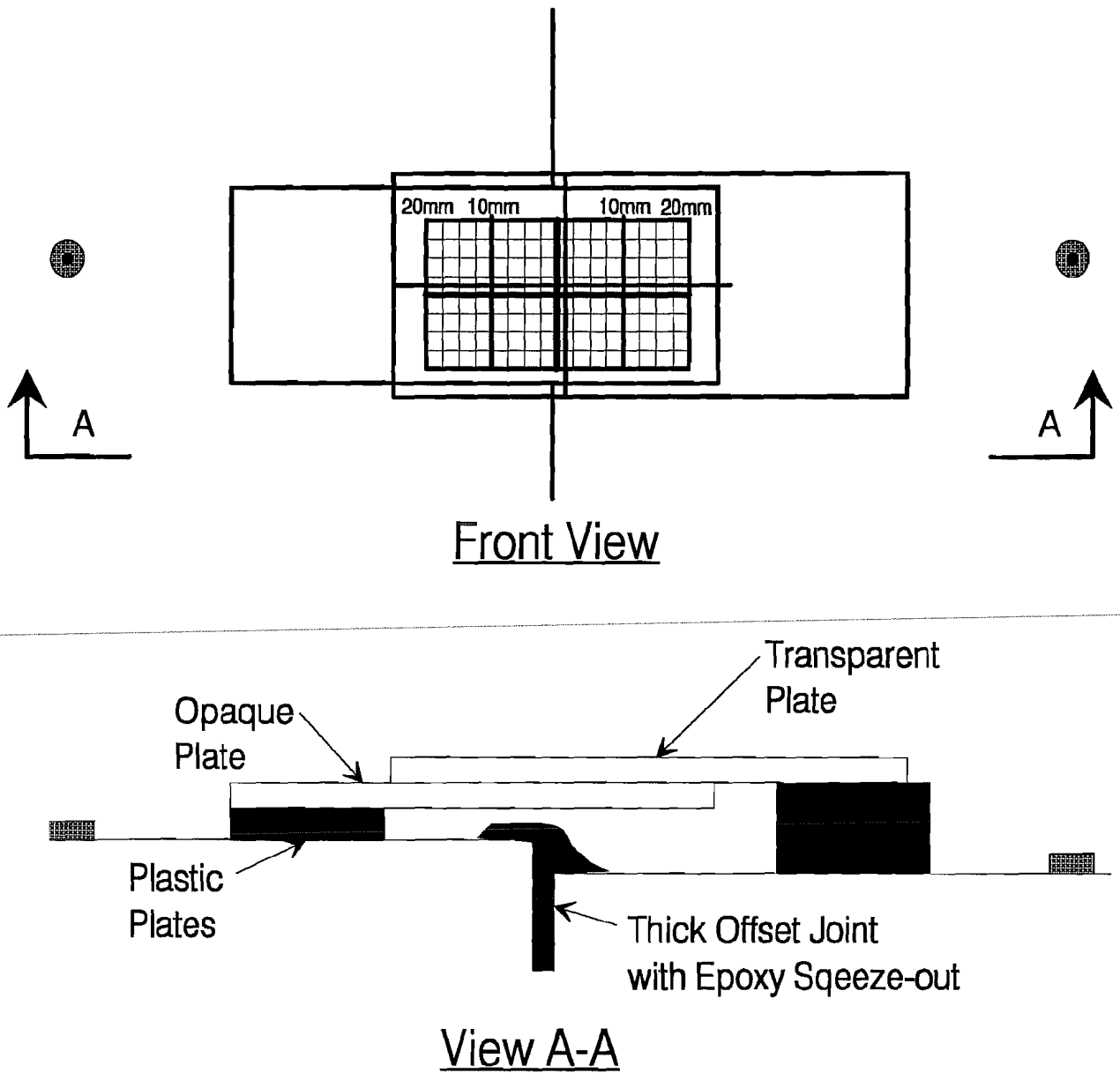


Figure 6.4 Grid crack monitor at offset joint.

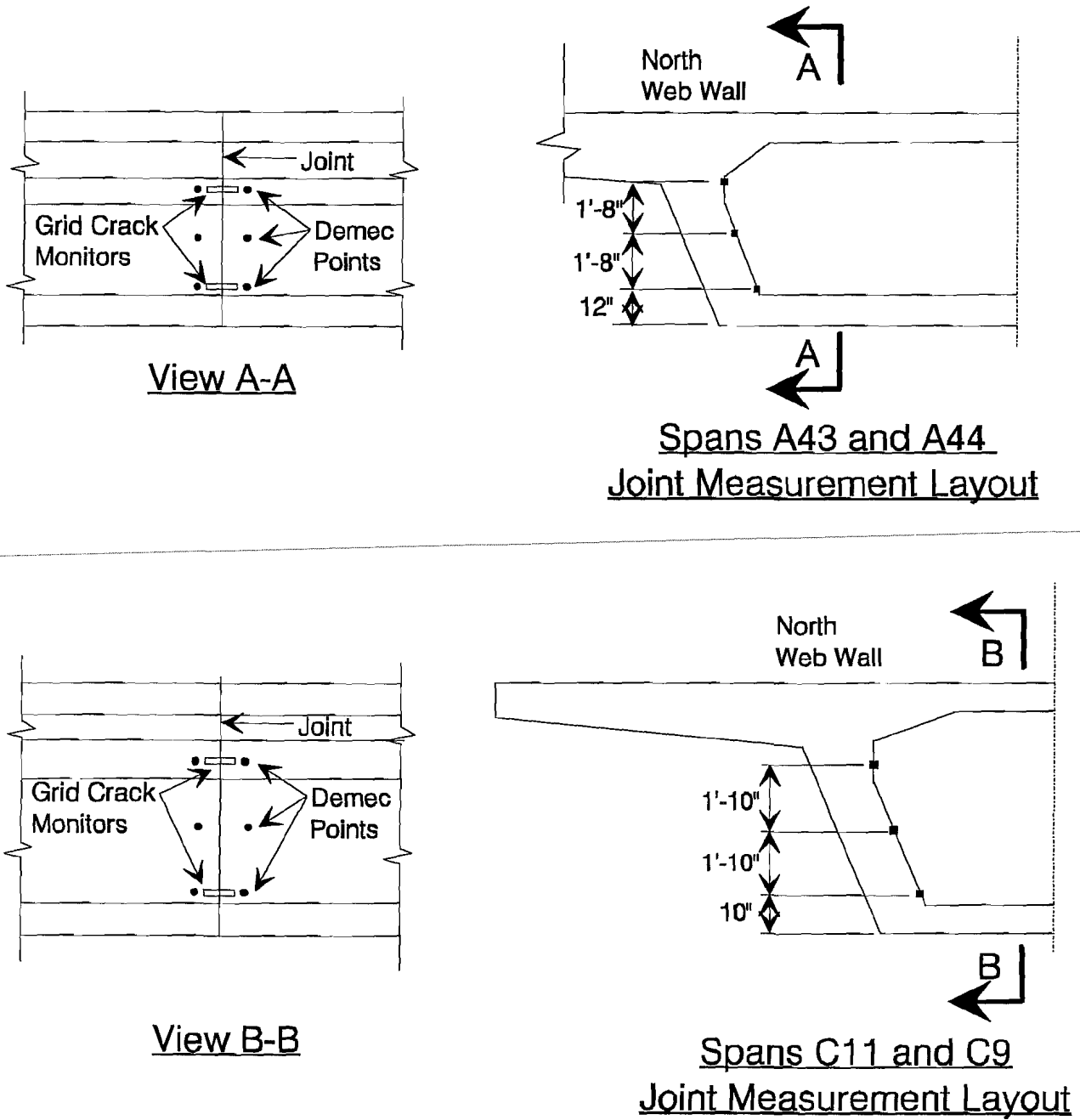


Figure 6.5a Joint movement instrumentation layouts.

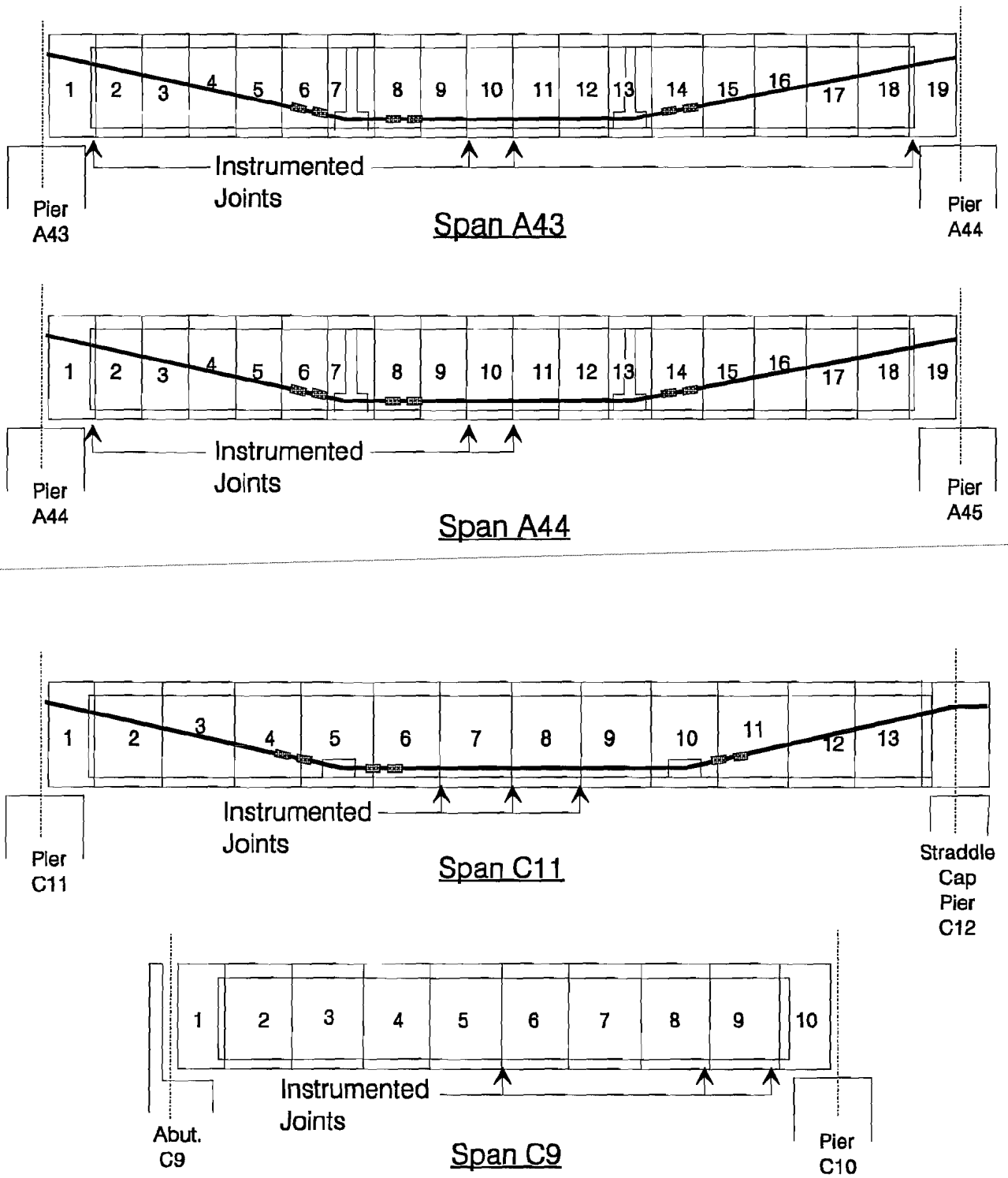


Figure 6.5b Joint movement instrumentation layouts.

### 6.3 Bearing Movements

Another physical quantity usually desired to be measured in segmental concrete bridges is the load imposed at the supports of each span. These measurements can be easily achieved with hydraulic or electronic load cells. However, in these cases the high-priced load cells would have to be left permanently in the bridge structures. This is a very expensive alternative for any large bridge instrumentation program. The present investigators thus avoided the use of load cells due to their high cost. However, these measurements can probably be indirectly determined by measuring the deformation of the fabrica bearing pads at each support. These measurements can be performed easily and at a very low cost with the help of high-resolution caliper gages. This process is further explained in Section 6.3.1.

It is interesting to note that despite investigations in laboratory-controlled environments, most of the previously-reviewed projects (mainly the field instrumentation projects) did not perform this kind of measurement. According to U.S. representatives of Freyssinet International, some European bridge structures implemented Freyssinet's *flat-jacks* to measure load variations in a few supports. However, no literature was obtained from these applications.

**6.3.1 Recommendations.** Caliper gages are usually present in every well-equipped machine shop. They are used for the measurement of internal diameters of tubes, or for measuring internal grooves and recesses. They are offered in different gage lengths. The larger gages can be ideal for accurately measuring the vertical movements between the bottom of the pier segment and the top plane surface of the piers (as occurring near a fabrica bearing pad). The approximate behavior of the fabrica bearing pads can be obtained from their manufacturers. This information combined with measured vertical deformations can give an approximation of the loads imposed to each bearing pad. The accuracy of these loads will obviously be quite low. However, serious overloadings or loading differentials among the bearing pads of a single span can still be expected to be determined with this type of measurement. None of the reviewed instrumentation projects (in laboratory as well as in field applications) have applied these measurements before. The San Antonio Y project provided the first conclusions about their use and applicability for a field instrumentation project.

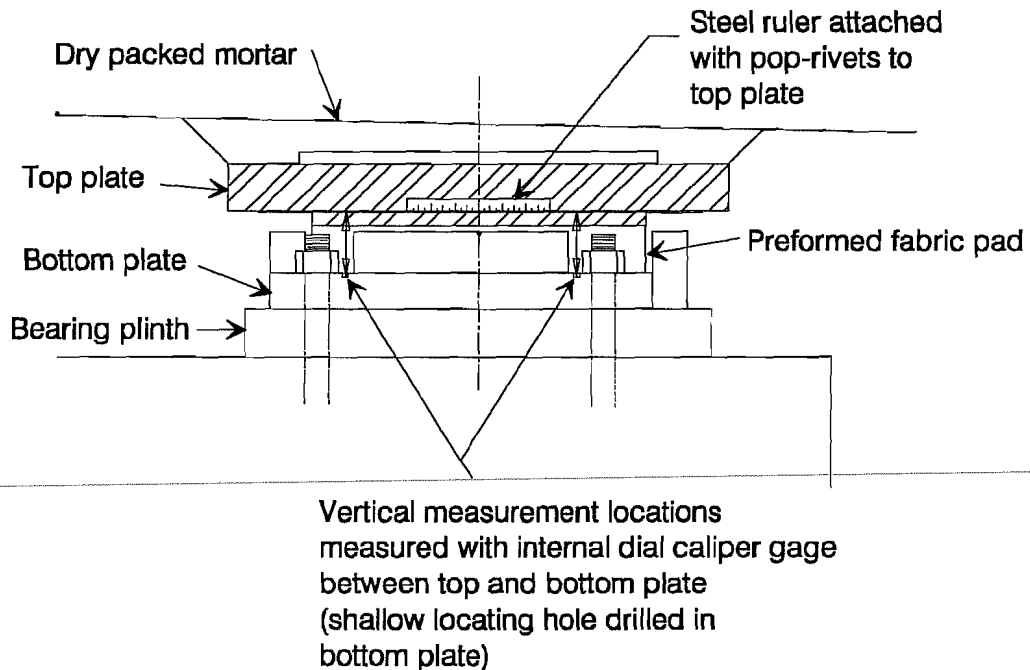
Caliper gages can be obtained from most machine shop precision tool manufacturers. They are offered with digital readouts or with dial indicators. Resolutions of 5/10,000 inch can be obtained with most gages. The larger calipers can measure movements of up to 0.8 inch. However, these larger calipers (of the dial indicator type) can cost up to \$400.00, and up to \$650.00 for digital calipers with 2/10,000 inch resolution.

This is a novel application to be investigated for reliability in this instrumentation project. No laboratory trials have been made with this system and some rules and recommendations are expected to appear in the near future.

High-resolution caliper gages can be ideally used for measuring the vertical deformations of the neoprene bearing pads located at the support of each span. This information, along with

the material data for the neoprene pads, can be helpful for determining the loads imposed at each support.

**6.3.2 Field Installation.** The system was installed on one pair of bearings at the most accessible location, Abutment C9 (see Figure 6.6). While the bearings were in the storage area, the shallow holes for the internal dial caliper gages were drilled, the ruler was attached to the top plate with pop-rivets, and the reference line on the bottom plate was scored.



Typical Sliding Bearing Detail

Figure 6.6 Bearing measurement details.

In the field, measurements began immediately after the span was lowered onto its bearings.

**6.3.3 Performance.** The system worked reasonably well, except for some problems with the internal dial caliper gage which behaved erratically in cold or humid weather. The readings, unfortunately, were inconclusive. The bearing moved longitudinally only 1/4 inch. (For the first six months it did not move at all.) Vertical readings showed a steady rate of creep for the first year. It is difficult to separate small strains due to load redistribution from the constant strains related to creep.

**6.3.4 Instrumentation Layouts.** As mentioned previously, the system was installed on only one pair of bearings due to the need for easy accessibility. Figure 6.6 shows the final instrumentation configuration.

**6.3.5 Recommendations for Future Projects.** The bearing measurement system was not completely successful. The longitudinal movement system is simple to install and read but can only be used on bearings which are easily accessible. The vertical readings were somewhat erratic and the nature of fabrica pads is such that it is difficult to isolate the effects of load changes and pad creep.

## 6.4 Solar Radiation

Radiation is the transfer of energy produced by a disorganized propagation of photons. Any body continually radiates photons at random directions, phases and frequencies. Photons can travel in any wavelength of the electromagnetic wave spectrum. Only the photons traveling at a small part of the spectrum affect the human eyes as visible light. Available instrumentation devices for measuring the amount of radiation impinging upon a flat surface usually vary according to the range of the electromagnetic wave spectrum that they measure. Within them, the most accurate devices are those that use cosine corrected functions to account for the angular incidence of the radiation rays (coming from all angles of a hemisphere) on a flat surface.

Instruments that measure the solar radiation received from a whole hemisphere have the specific name of *pyranometers*. These instruments are suitable for measuring the energy flux density of both direct beam and diffuse sky radiation passing through a horizontal plane of known unit area (thus measuring global sun plus sky radiation). In general, pyranometers are not generally useful when installed under artificial lighting or to measure reflected radiation. However, these devices are effective for most applications in concrete structures where the largest amount of radiation comes from direct solar rays. Some of them are even effective for more dedicated thermal engineering research (such as the *Eppley Precision Spectral Pyranometer*). These devices provide measurements of radiation density flux in units of cal./(m<sup>2</sup> x min).

Only one type of pyranometer was actually purchased and operated by the present research project. This was the LI-200SZ Pyranometer Sensor manufactured by LI-COR Inc. (shown in Figure 6.7). The manufacturer is located at: 4421 Superior St., P.O. Box 4425, Lincoln, NE 68504. Their current telephone number: (402) 467-3576.

**6.4.1 Recommendations.** The device selected for measuring the amount of solar radiation impinging upon the top of the deck slabs was the LI-200SZ Silicon Photodiode Pyranometer. The operation of this device is relatively simple when connected to automated data-loggers. It can also be operated with a multimeter (measuring millivolts) provided that a 140Ω (max.) resistor is installed across the leads of the coaxial cable of the pyranometer. The



millivolt output can be directly related to units of  $cal/(m^2 \times min)$  by knowing the calibration constant of the pyranometer sensor.

The greatest inconvenience associated with the pyranometer is that it should be sent back to the manufacturer for recalibration every two years. It should also be stored and treated very carefully in order to maintain its original accuracy for each two-year period. The top of the sensor should always be cleaned of dust before each operation. The pyranometer should be installed on a leveled surface. Leveling can be achieved easily with the optional mounting and leveling fixtures offered with the pyranometer. Finally, these devices are very sensitive to any form of shade. They should be positioned so they only become affected by shade provided by clouds and not shade induced by localized elements (such as construction machinery, trees, etc.).

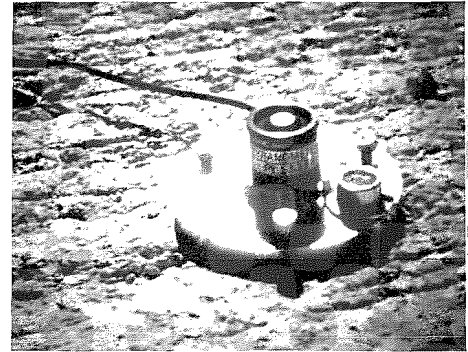


Figure 6.7 LI-200SZ Pyranometer.

**6.4.2 Field Installation on the San Antonio Y Project.** The solar radiation device was installed only three times during the course of the project and several problems were encountered. Twice it was connected to the permanent data-acquisition system through an auxiliary connection. On the first occasion, the lead wire which was brought from the laboratory was too short to extend from the data-acquisition system through an opening at the pier and up onto the deck. An attempt was made to field splice in an additional wire, but it was ineffective.

The second occasion was hindered by a programming error. The constant, by which the voltage difference is multiplied, was input incorrectly and as a result the numbers were too large for the system to store. Only the first few readings, when the solar radiation levels were very small, were recorded.

On the third occasion the solar pyranometer was connected to the Campbell which was used for thermocouple readings. Everything proceeded smoothly and excellent data was obtained.

**6.4.3 Performance.** With proper preparation and programming this is a fine system. The only problem is the inability to leave it in place for any length of time. When it was in use it was placed on the top deck where it was exposed to construction traffic. It was monitored constantly to ensure it was not damaged. For this device to be more effective, a location needs to be found where the pyranometer will collect the data required, but not need constant attention to prevent theft or damage.

---

**6.4.4 Recommendation for Future Projects.** As mentioned, this is a good system if properly programmed. A permanent safe position should be found for the device so more complete data can be collected.

---

## CHAPTER 7

# DATA ACQUISITION SYSTEMS

### 7.1 Review of Available Systems

Dedicated data-acquisition systems are usually the single most expensive investment of a field instrumentation project. The function of data-acquisition systems is to gather signals from different instrumentation devices, condition some of the collected signals, and record, transmit, or display the processed data. Most of the field instrumentation projects reviewed used portable manual readout units in their data-acquisition process. However, some field projects and most of the laboratory investigations used sophisticated automated data-acquisition systems (sometimes referred to as ADAS).

Practically each instrumentation device reviewed in the preceding chapters is offered with a compatible portable manual readout unit. Some of these units can be combined with manually-operated multi-channel switching devices. However, these systems are not recommended for large instrumentation projects employing several input channels that must be scanned at regular intervals. Manually-obtained data needs to be keyed into electronic spreadsheets for final analysis. This introduces a new level of operational error and a time-consuming operation for projects involving several instrumentation devices. A more important problem occurs with measurements of small electrical resistances (such as from ER-gages and load cells) due to the variation of the contact resistance that occurs in the connections to each channel. In long-term readings, large errors can be introduced from the variation in the contact resistances of the connections. These electrical resistance variations can occur due to oxidization of terminals, temperature differentials, variation of the type of electrical contact produced by each connector, etc. The best way of avoiding these errors is by using permanent (i.e. for the duration of the project) connections to each channel. However, this is expensive and inefficient when a large number of channels are needed. A different solution is to use some other type of almost perfectly reproducible electrical contact. One electrical connection that can be reproduced accurately through different contacts is to immerse the connecting leadwires in a solution of mercury. This method is evidently impractical and dangerous due to the health-threatening effects of mercury. However, an accurate reproduction of connections can also be obtained with gold-plated connectors (usually employed inside several multi-channel switching devices).

The best method for acquiring data from a large number of instrumentation devices is to use a commercial automated data-acquisition system. There is a wide variety of systems available, ranging from data-loggers to computer-controlled data controllers. The data-loggers are characterized by simply scanning and recording data from different types of instruments at user programmable time intervals. Data can be recorded in internal random access memory (RAM-memory), hard disc memory, floppy disks, tape cartridges, or some systems can even be coupled with external modems and send data directly to a remote computer (located in a research laboratory for example) through a dedicated phone line. Prices of these systems vary widely according to the type and amount of data storage, number and type of devices that can be

scanned, availability of internal programs (written in ROM modules and used to reduce data processing or programming), operating environment, etc.

Data controllers are similar to data-loggers but provide additional interfacing and basic programming that can control the operation of certain equipment based on the variations of the measured data. These are more sophisticated and expensive equipment and are seldom used in structural engineering investigations.

Battery-operated data-loggers are usually preferred for field instrumentation projects. Only a few field projects can be supplied with a regular source of electricity. Even when electricity is available, provisions must be made to prevent voltage surges, voltage drops, or occasional power outages that can alter the normal operation of the system. Line stabilizers, surge suppressors, and uninterruptible backup power supplies should be used with expensive data-acquisition systems connected to regular AC electricity (to protect their delicate internal circuitry).

For the present project, several types of available data-acquisition systems were investigated. A portable data-logger was desirable because it would avoid the dependence on regular sources of electricity and the extra investments of power backup and system protection devices. Moreover, battery-powered data-loggers can usually be operated in harsher environmental conditions (in terms of moisture and temperature) than AC systems that are mainly designed for laboratory use.

After a review of previously-used data-loggers and after an investigation of the currently available technology, the present researchers decided to purchase a low-cost system offered by Campbell Scientific. Part of the reason for purchasing this equipment was that a very efficient field system built around a portable data-logger was previously designed by researchers of the present laboratory.<sup>41</sup>

The previous researchers considered the *Campbell Scientific 21X* to be a cost-efficient battery-powered type of data-logger. An extensive development of software needed for interactive programming and data retrieval was prepared for this system. This software program was found incompatible for the presently desired application and the development of a new one would have considerably increased the final cost of the data-acquisition system. However, Campbell Scientific recently developed a low-cost PC-compatible software kit that includes the necessary wiring for connecting their data-logger to the serial port of any personal computer. This kit also includes some basic software that helps considerably in the processes of programming, remote communication, and data retrieval of the data-loggers offered by this company. Costs of the purchased equipment from Campbell Scientific are included in Table 7.1.

Table 7.1 Late 1990 prices for data-acquisition components offered by Campbell Scientific, Inc.

a. 21XL Micrologger (w/40K RAM & PROM module).	\$1900.00
b. 16-channel 4-wire input multiplexer (AM416, no enclosure).	\$475.00
c. Optically isolated RS-232 interface (to PC serial port).	\$130.00
d. Data acquisition software package.	\$200.00

However, these costs do not include the extra equipment necessary for the construction of the field-operational data-acquisition system built for the San Antonio Y project. Other expenditures were related to:

- the internal quarter bridge completion circuitry (necessary for the electrical resistance strain gages),
- high-quality connectors (to ensure good resistance to moisture and physical damage), and
- labor time needed for soldering the internal wiring of all data-logger channels to the proper poles in the connectors, and for construction of the box enclosure.

Important wiring information about the quarter bridge Wheatstone completion circuits (designed by the present researchers) is included in Appendix A. This information can be helpful for future similar projects since the completed system was very affordable considering the extensive number of quarter bridge ER-gage channels that it can handle.

Future instrumentation projects desiring different data-loggers can consult with several companies. First of all, most of the previously-mentioned manufacturers of specific monitoring devices offer some type of data-acquisition system. Other companies more dedicated to the production of data-acquisition systems (rather than specific instrumentation devices) are:

1. Campbell Scientific, Inc., P. O. Box 551, Logan, UT 84321. Current telephone: (801) 753-2342.
2. Optim Electronics, Middlebrook Tech Park, 12401 Middlebrook Rd., Germantown, MA 20874. Current telephone: (301) 428-7200.
3. Hewlett-Packard, 1820 Embarcadero Road, Palo Alto, CA 94303.
4. National Instruments, 6504 Bridge Point Parkway, Austin, TX 78730-5039. Current telephone: (512) 794-0100.
5. Contec Microelectronics U.S.A., Inc., 2010 N. First Street, Suite 530, San Jose, CA 95131. Current telephone: (408) 436-0340.

## 7.2 System Selection

A battery-powered data-acquisition system based on the *Campbell Scientific 21X Micrologger* was purchased for the project. The following considerations influenced the decision for purchasing this particular system:

1. Factors supporting an automated system:
  - operational errors are usually associated with the data-recording procedures of manually-operated systems,
  - time-consuming operations are involved in the data-recording procedures of manual systems, and
  - large long-term errors can be introduced due to the variation of contact resistances that occur in the connections of electrical resistance strain gage channels.
  
2. Factors supporting a battery-operated system:
  - independence from a reliable source of AC electricity,
  - avoidance of line stabilizers, surge suppressors, and uninterruptible power supplies, and
  - ability to operate in a harsher range of environmental conditions (in terms of moisture and temperature).
  
3. Factors supporting the Campbell Scientific equipment:
  - data-loggers, PC-interfacing kit and software for programming and data retrieval all offered at low comparative costs,
  - ability to work with a large number of ER-gage channels (with quarter bridge Wheatstone circuits),
  - ability to accept input from a great variety of sensors, such as: thermocouples, LI-200SZ Pyranometer (for solar radiation measurements), ER-based strain gages, load cells and pressure transducers, LVDTs, etc.

Beyond the cost of the actual data-logger, multi-channel switching devices, PC interfacing kit, and data-retrieval software, other important expenses are associated with the fabrication of the bridge completion circuits. The high sensitivity of the measurements related to variations of electrical resistances (such as those of ER-gages) gave a priority to the automation of these particular channels. A very large number of electrical resistance strain gages were initially designed to be used in each instrumented span of the San Antonio Y project (up to 66 channels on two spans and up to 34 channels on the third one). However, this number is low when considering that all concrete strains were designed to be instrumented with mechanical extensometers. Most of the reviewed field instrumentation and laboratory projects also used an

elevated number of electrical resistance sensors (when compared to the other devices that were used in the same project).

A certain type of Wheatstone completion circuit is necessary to be coupled with each channel of the data-acquisition system to measure the very low electrical signals provided by the electrical resistance strain gages or load cells. Most of the ER-gages used in concrete structures are based on  $120\Omega$  or  $350\Omega$  resistors and require some type of Wheatstone bridge completion circuit. The most widely-used Wheatstone bridge for ER-gages is the three-leadwire, quarter-bridge completion circuit. To build this, it is necessary to have three high-precision resistors for each ER-gage channel (as shown in Figure 7.1). Similar precision resistors need to be installed in the same arm of the Wheatstone bridge where the electrical resistance strain gage is to be placed. The second arm is usually designed with the same resistors for simplicity. The  $350\Omega$  (@0.01%) precision resistors cost about \$7.50 apiece (as of July 1990). Each completion circuit thus costs around \$22.50. Up to 16 quarter bridge channels were advertised to be handled by each AM416 relay multiplexer unit (this is the multi-channel switching unit that can be connected to the 21X data-logger). For the initially desired 166 quarter bridge completion circuits the total cost of completion circuits alone would have been about \$3,735.00. Evidently, the completion boxes would have comprised a highly-priced component of the instrumentation project.

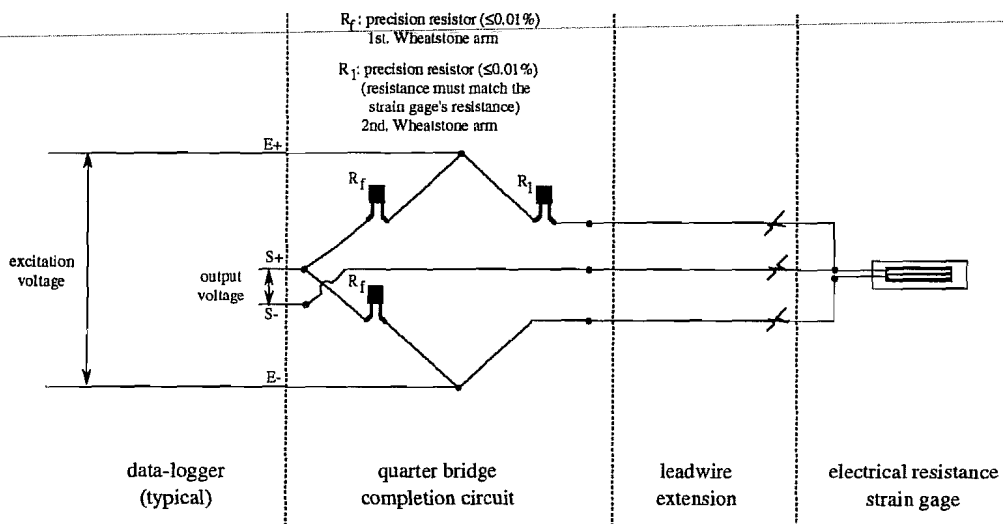


Figure 7.1 Three-leadwire, quarter-bridge Wheatstone completion circuit typically needed for most data-loggers.

As a savings alternative, the researchers investigated the possibility of directly wiring quarter bridge circuitry between the data-logger and each AM416 multiplexer. If this was possible then a single completion circuit could be used for each group of 16 ER-gage channels. The only disadvantage was that all 16 channels of each multiplexer wired in a quarter bridge configuration to the data-logger could not be used for other types of measurements.

An initial design of the envisioned quarter bridge circuitry was provided by the engineers of Campbell Scientific.<sup>47</sup> The researchers from FSEL learned the operation principles of the data-logger and redesigned the original circuitry provided by Campbell Scientific.<sup>50</sup> The first finding was that a simple completion bridge can be formed between the data-logger and each multiplexer. A secondary, yet equally important, finding was that each multiplexer could actually handle double the 16 original number of quarter bridge channels mentioned by Campbell Scientific (provided that the data-logger is programmed and wired in accordance to the new design). With these findings, the total cost of the completion circuits necessary for the originally-designed 166 ER-gage channels of the project was reduced from \$3,735.00 to \$360.00.

Three portable data-acquisition systems were designed (one for each span to be instrumented). A general description of these systems is included here. However, a more detailed analysis of these systems is included in Appendix A.

The two larger data-acquisition systems were similar. Each one of these two was composed of a single 21X Micrologger, two AM416 Multiplexers, and an internal PC Interface Kit. The third system only had a single AM416 Multiplexer since it was prepared for use in the span with less instrumentation. Each system was designed to be powered by an external hookup to a 12V marine-type battery that was calculated to last about two weeks at the scan rate, excitation level, and number of channels to be used by each large-size data-acquisition system. The final design included a provision for replacing the battery without cutting the power to the data-logger. This was accomplished by providing a secondary external battery port that can be connected to a replacement battery before cutting off the old one. The side panel of each system was also designed with two button-activated indicators. The first one was a voltmeter that checked the charge of the main battery, and the second one was a scan rate signal light that indicated if the system was properly scanning channels. These two control devices were incorporated based on a previous system designed by Post et al.<sup>41</sup>

In each system, all the connections to the different gage channels were designed with high-quality, silver-plated military standard amphenol connectors. These were used to ensure the long-term stability of the external electrical connections. Heat shrink plastic tubes were used to cover all internal connections from the data-logger to the multiplexers and to the connectors. Special Polyethylene foam panels were used to enclose the data-logger and multiplexers inside each portable system. Packages of silica gel dehydrators were also placed inside each system to help prevent moisture accumulation. The portable boxes of each system were built at FSEL with ½-inch marine plywood sheets.

The small data-acquisition system was completed first and it was checked on a short-term laboratory trial test using four 350Ω ER-gages. The gages were alternated through all the available channels of the system. This test showed that the system was completely functional. Initial tests were performed on one of the larger data-acquisition systems and also indicated satisfactory behavior. All necessary details for the construction and operation of these systems are evaluated in Appendix A. These can be helpful for future similar endeavors.



### **7.3 System Installation in the San Antonio Y Project**

As recommended, three complete systems were fabricated and tested in the laboratory. Also, lockable security enclosures were built to protect the systems from theft and damage. In the field the installation was quite simple. The security box was fastened to the inside of the span with small expansion anchors. The data-acquisition box was placed in the enclosure and the lead wires were connected. The large marine battery was also placed in the security box and connected to the system.

All programming was done well ahead of time, and the programs tested in the laboratory. Using the software provided with the data-logger, the programming was extremely easy. Programs are listed in Appendix B. Downloading the programs to the data-logger and retrieving data was also quite easy.

### **7.4 Performance**

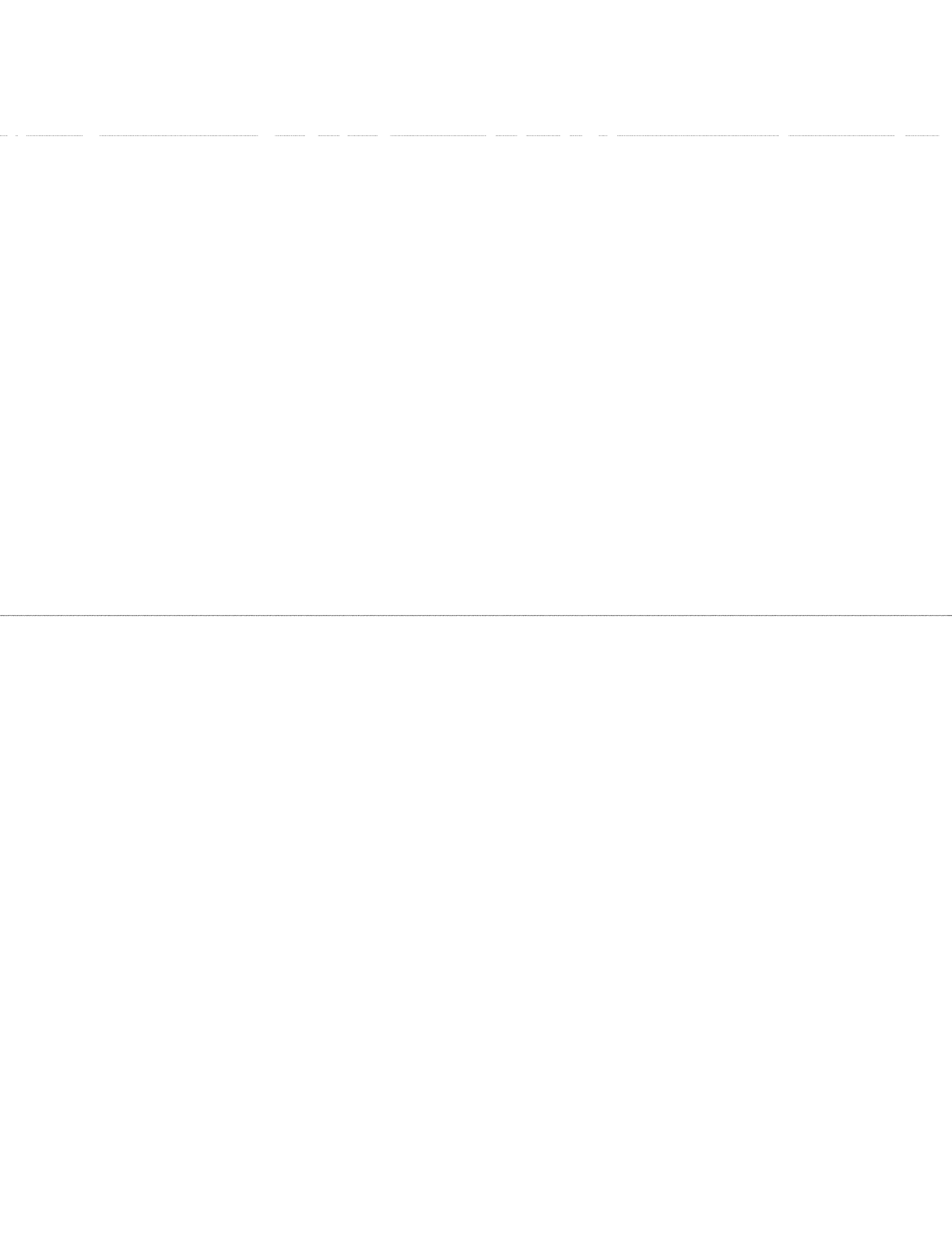
The Campbell data-acquisition system was extremely effective. For a relatively low cost, very good data was produced. There were no major field difficulties to report; however, some refinements could improve the system. One system was flooded unexpectedly due to water accumulating in the box girder in a heavy rainstorm before end expansion joints were sealed.

### **7.5 Recommendations for Future Projects**

The system could be improved by the following modifications:

1. Connection of the system to a phone line and modem to enable remote data retrieval. The Campbell programming is fully adaptable to modem data retrieval.
2. Connection of the battery to a trickle charger, either through a solar collector or through an AC power line. This would eliminate the battery replacement difficulties.
3. Use connectors other than amphenol. Amphenol connectors are extremely expensive and extremely tedious to connect and disconnect. Other types should be investigated.
4. Place the data-acquisition system in a very safe location well above high water level. The possibility of water leaking into the box should be considered in finding a secure position for the system.

These recommendations should improve the performance of the data-acquisition system.



## CHAPTER 8 COMPANION MATERIAL TESTS

Every structural instrumentation program must consider companion material tests to check values of several properties that cannot be accurately obtained with code-established empirical procedures. These tests are essential in concrete structures. The following suggestions have been prepared from a literature survey of past field investigations.

### 8.1 Recommendations

**8.1.1 Concrete.** Companion material tests of concrete are suggested as an aid for more accurately determining the state of stress of the instrumented spans of the San Antonio Y structure. These concrete tests are suggested for estimating the highly variable parameters of:

modulus of elasticity,  
creep, and  
shrinkage.

Several factors have been found to influence the actual creep and shrinkage of concrete structures as previously mentioned. The influence of creep and shrinkage in segmental concrete bridges has been studied in several previous investigations. Most of these tests measured considerable creep and shrinkage strain variations among specimens stored inside, on top, and underneath the box girder segments. Bryant<sup>12</sup> found that specimens on top and under the box girders experienced similar creep, but those inside the bridge experienced 15% more creep. Shrinkage was found to be more dependent on location. The specimens inside the box girders had 100% more shrinkage than those on the top slab, and 25% more than specimens under the bridge.<sup>12</sup> Bryant also found that the CEB-FIP<sup>14</sup> and ACI<sup>3</sup> predictions for creep and shrinkage were both about 25% of the experimental values.<sup>12</sup> Although size of the concrete elements also plays an important role in creep and shrinkage test results, there is a well-defined dependence on location that should be considered. Japanese shrinkage tests further found that unstressed web elements inside the same span of a box girder bridge but located at opposite ends had differences of up to 40%<sup>23</sup>. These previous tests suggest the following considerations for the concrete material tests of the San Antonio Y structures:

1. Creep Tests.
  - 1.1 Cylindrical specimens (6-inch x 12-inch) should be taken during casting operations of each instrumented segment of the selected spans. These should be properly labeled and left near or inside the box girder segments during the time they are in storage.
  - 1.2 Creep specimens should be loaded on special frames that comply with ASTM C512 specifications.<sup>7</sup> Due to problems related to

transportation, theft, and possible tinkering of creep frames left on the job site, these tests can be developed in a field outside the Austin laboratory facilities. The environmental conditions should be generally similar to those in San Antonio. Creep specimens should be loaded as closely as possible to the stressing day of corresponding spans. Properly-calibrated load cells are highly recommended as load monitoring devices during initial loading of creep specimens.

- 1.3 Each specimen should be gaged in two diametrically opposite positions and readings should follow the recommended procedures for 200 mm Demec extensometers (see Section 5.3.2).

## 2. Shrinkage Tests.

- 2.1 Shrinkage specimens should be taken from concrete used in the locations where strain readings will be taken in the structure. The size of these specimens depends on the gage length of the instrumentation device to be used on them (which should be the same as the device to be used in the actual field measurements of concrete strains). Since 200 mm Demec extensometers were planned to be used in the field measurements, 6-inch x 12-inch cylinders or 6-inch x 12-inch x 3-inch rectangular beams are recommended. Each specimen should be properly labeled and should undergo similar environmental conditions as the sections of the structure that will be monitored. For example, specimens monitoring concrete behavior at inner web locations should be stored inside the box girders.

- 2.2 Each specimen should be gaged in at least two locations following the recommended procedures for assuring long-term stability of the locating points of 200 mm Demec extensometers (see Section 5.3.1).

## 3. Modulus of Elasticity.

- 3.1 Specimens for these tests should be taken during casting operations of each instrumented segment of the selected spans. The size of these specimens usually depends on the most available testing machine. Since the contractor's San Antonio casting yard has a testing machine for 4-inch x 8-inch cylindrical specimens, this is the recommended size. This size of specimens also facilitates handling.

3.2 Tests should be performed at the following days:

- 7 days after casting,
- 28 days after casting, and
- at day of initial stressing of tendons.

**8.1.2 Prestressing Steel.** Laboratory testing should be performed with at least two samples taken out of each prestressing strand roll to be used in the instrumented spans. The important parameters obtained from these tests consist of the values for the strand's modulus of elasticity determined by the epoxy sleeves and the electrical resistance strain gages. These two separate values can be obtained with single companion material tests of strand specimens instrumented with both measurement systems. General recommendations regarding the single-strand material tests consist of the following:

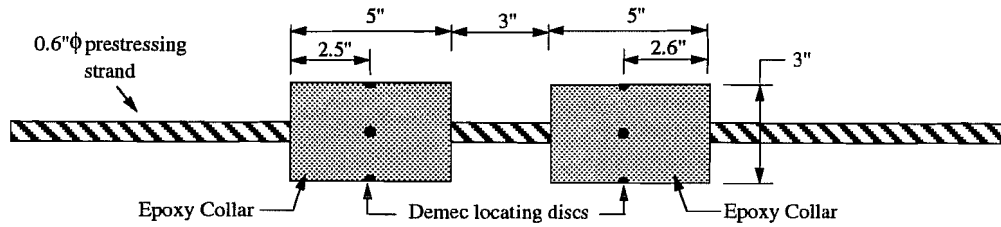
- The length of the specimen directly depends on the testing machine to be used. A good rule is to use specimens no shorter than 4½ feet.
- Use standard single-strand anchorage hardware. Pre-load the specimen to about  $0.50f_{pu}$  to properly seat the wedges on each wire. Unload back to zero and start testing.
- A properly calibrated load cell or universal test machine should be used for obtaining corresponding live or dead end loads. Average strand stresses should be obtained by considering the nominal cross-sectional strand area.
- In the data-reduction process, only consider the data points that correspond to stress values between 20% and 80% of ultimate.

**8.1.2.1 Epoxy Sleeves.** For the San Antonio Y instrumentation project, the single-strand tests with epoxy sleeves will only be performed as companion material tests. These will be necessary for determining the modulus of elasticity that corresponds to the strain measurements from the epoxy sleeve system. The modulus determined from epoxy sleeve readings should only be slightly larger than that given by the strand manufacturer.

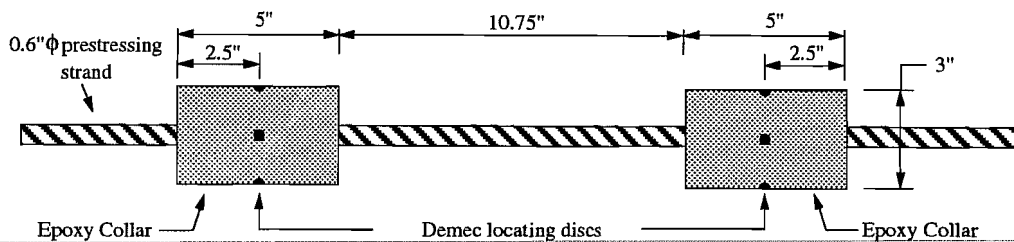
Two different setups can be followed according to the gage length of the Demec extensometer to be used in the field instrumentation project. Figure 8.1 illustrates these two possible systems. The following specific guidelines only apply to the shorter epoxy sleeve system. However, they can be easily modified for the longer one.

1. For ease of installation in structural engineering laboratories, the 3-inch x 6-inch standard plastic cylinders for concrete tests are ideal for single-strand epoxy sleeve molds. The only modification is that a 0.5-inch or

0.6-inch diameter circle (according to the size of strand being tested) should be drilled at the bottom of each plastic mold.



a. Final schematic of single strand epoxy sleeve system for 200mm. Demec extensometers.



b. Final schematic of single strand epoxy sleeve system for 400mm. Demec extensometers.

Figure 8.1 Schematic of finished single-strand epoxy sleeve systems.

2. To maintain the tops of the plastic molds concentric with the prestressing strand, two 2.885-inch o.d. circles should be cut from a 0.5-inch thick plywood sheet. These plywood caps should have a central 0.5-inch or 0.6-inch diameter hole according to the size of the strand to be instrumented.
3. Each mold and cap pair should be slipped onto the prestressing strand specimen and placed so as to have a space of approximately 2.75 inches between the top of the lower plastic mold and the bottom of the upper plastic mold (10.5 inches when using 400 mm extensometers). The small spaces between the strand and the circular holes at the bottom of both molds should then be covered with silicone. A minimum drying period of one hour is recommended for the silicone.
4. With the strand specimens in an upward position, the proper epoxy mix (same as that to be used in the actual field tests) should be poured into the plastic molds. The molds should only be filled up to a level one inch

below their tops. The minimum epoxy-curing time suggested by the manufacturer should be followed.

5. After cutting the plastic molds from the epoxy collars, at least two pairs of demec locating points should be placed around the sleeves according to the distances shown in Figure 8.1. Since only short-term tests are necessary, these locating points can just be bonded to the surface of the epoxy collars.
6. During testing, the strain readings of the epoxy sleeves should be taken very carefully, preferably according to the recommendations included in Section 5.3.2 for Demec extensometers.
7. In the data-reduction process, a straight line fit of all acceptable data should finally provide the average modulus of elasticity determined from the epoxy sleeve readings. This is the modulus that should be used for converting the modified field measurements of epoxy sleeve strain readings to average stresses.

**8.1.2.2 Electrical Resistance Strain Gages.** Companion material tests of prestressing strands with electrical resistance strain gages should be performed according to the following guidelines:

1. Each specimen should be gaged with a minimum of 4 ER-gages similar to those to be used for the actual field testing. Install these gages at one single cross-section in the middle of the specimen, preferably between the two epoxy collars. If possible, also install every pair of gages on diametrically opposed wires of the prestressing strand.
2. In the data-reduction process, compute the average of the strain readings obtained from each ER-gage and for each loading step. Make a linear regression of the acceptable data points, without requiring the line to pass through the origin of coordinates. Use the slope of this line as the modulus of elasticity for estimating stress levels from field strain readings of ER-gages.

**8.1.3 Reinforcing Steel.** These companion material tests are expected to be much simpler than for concrete and prestressing steel. Reinforcing steel material tests are more important for laboratory testing of structural components, when specimens are usually loaded to failure. In most cases, the material tests of reinforcing bars reveal slightly different yield points. However, such a high level of stress is evidently not expected in field instrumentation projects of actual structures.

Some recommendations for these tests are:

- Specimens should be taken from the same batch of reinforcing steel bars that will be instrumented with strain gages.
- Instrumentation should consist of a single strain gage per specimen, installed according to the recommended procedures of Section 6.1.1.

## 8.2 Field Applications in the San Antonio Y Project

Generally all recommended tests were performed as part of the field project. This section outlines differences from the recommendations and problems encountered in the field.

**8.2.1 Concrete.** Creep tests were performed as recommended. Three pairs of 6-inch x 12-inch cylinders from each instrumented span were placed in creep frames outside the laboratory in Austin. In conjunction with each pair of creep cylinders, one 6-inch x 12-inch cylinder was monitored as a companion shrinkage specimen. The creep and shrinkage tests were initiated within one week of the span erection.

~~Compressive strength was checked with 4-inch x 8-inch cylinders. The contractor tested cylinder strength on every segment the morning after casting, and after 28 days in a water bath. This information was provided to the investigators. In addition, compressive strength on pairs of cylinders from 5 segments per span was tested at 28 days and at the time of erection. These cylinders were stored with their respective segments, and so were exposed to the same climatic conditions.~~

Tensile strength was checked with 4-inch x 8-inch cylinders from 3 to 5 segments per span. The strengths were tested at 28 days and at the time of erection.

The modulus of elasticity of 6-inch x 12-inch cylinders from 3 pairs of cylinders per span was tested at the time of erection.

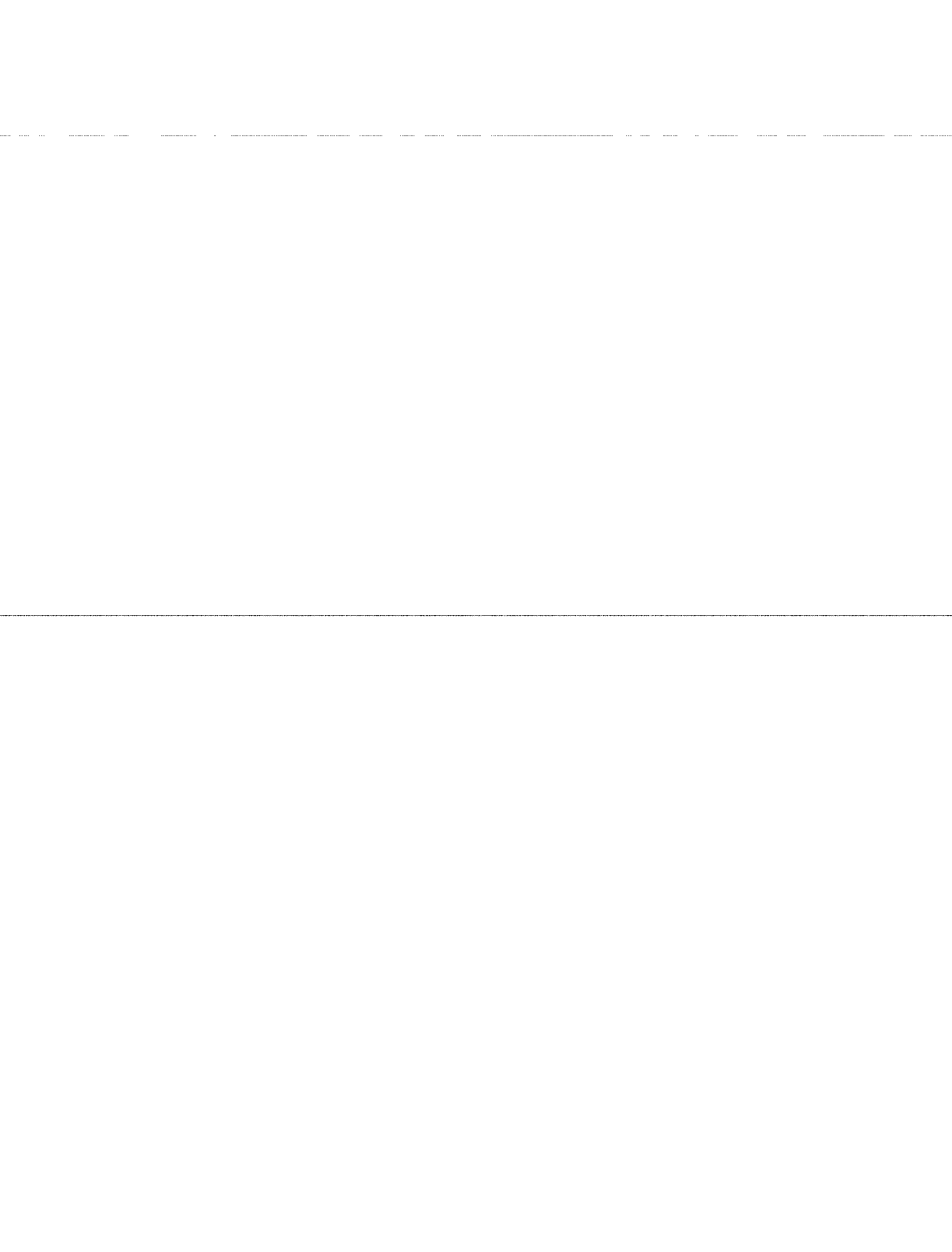
The coefficient of thermal expansion was checked with three 6-inch x 12-inch cylinders from each of the spans with thermocouples.

One problem in the concrete testing was the proper marking and storage of cylinders. Initially the cylinders were placed in storage with their corresponding segment. Due to construction schedules, a great deal of rearranging of segments in storage took place. Some cylinders were misplaced or thrown away by the storage yard crews. Other cylinders had problems because the ink used to mark them faded considerably. Better care of cylinders is recommended for future projects.



---

**8.2.2 *Prestressing Steel and Reinforcing Steel.*** Tests of reinforcing steel and prestressing steel were carried out as recommended.



## CHAPTER 9

### CONCLUSIONS AND RECOMMENDATIONS

This study has provided valuable information on field instrumentation systems for the study of segmental concrete bridges, particularly those erected with span-by-span techniques. Systems have been recommended which were used with great success in the study of four spans of the San Antonio "Y" Project, Phase IIC. The results of this study are presented in other publications.<sup>46</sup>

The final recommendations for instrumentation systems for the study of segmental concrete bridges with external tendons are as follows:

1. **External tendon forces:** Dual measurement system with mechanical extensometer locating points on epoxy collars and electrical resistance strain gages, on individual wires of the tendon, hooked to a permanent data-acquisition system (see Section 2.3).
2. **Span deflections and segment deformations:** Taut wire baseline system with the wire tensioned with a dead weight and the changes in deflection measured with a digital sliding ruler (see Section 3.3).
3. **Concrete temperatures:** Type T (copper vs. constantan) thermocouples cast into the concrete and read with either a manual switch box and a hand-held thermometer or with a dedicated Campbell Scientific 21X Micrologger (see Section 4.2).
4. **Concrete strains:** Demec mechanical extensometer with locating points on nail inserts which provide both a mechanical and epoxy connection to the concrete (see Section 5.3).
5. **Reinforcing steel strains:** 350 $\Omega$  electrical resistance gages, adhered with a long-life, two-part epoxy, and connected to a permanent data-acquisition system (see Section 6.1.1).
6. **Joint openings:** Grid crack monitors and demec points (see Section 6.2.1).
7. **Bearing movements:** Inside calipers for vertical movements and precision rulers for longitudinal and transverse movements (see Section 6.3.1).
8. **Solar radiation:** LI-200SZ Pyranometer Sensor by LI-COR hooked to a Campbell Scientific 21X Micrologger (see Section 6.4.1).

9. **Data acquisition system:** Campbell Scientific 21X Micrologger with AM416 Multiplexers (see Section 7.2).

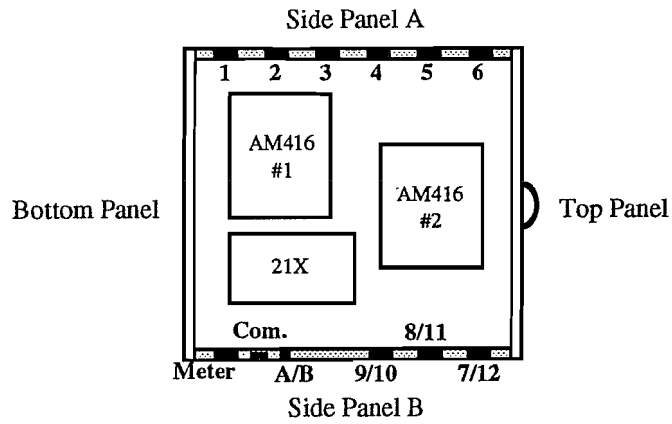
These systems, used in conjunction with required companion material tests (see Chapter 8), have provided excellent data in San Antonio. With some modifications and refinements, even better information can be obtained in future projects. With continued collection of lab and field data, the *AASHTO Guide Specification* and the state-of-the-art of segmental concrete bridge design and construction will continue to evolve and improve.

---

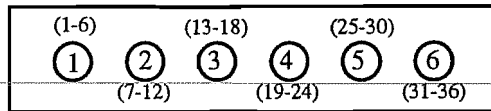
**APPENDIX A**  
**WIRING DIAGRAMS**

---

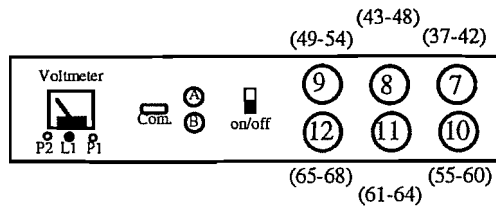
**II. Plan View:**



**III Side Panel A:**



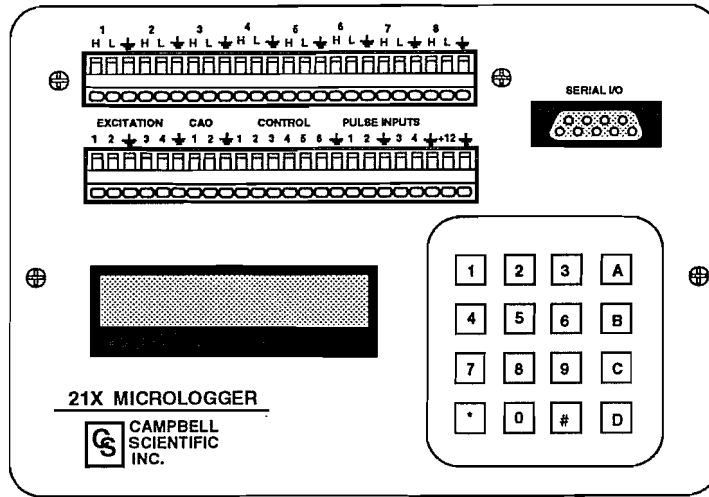
**IV. Side Panel B:**



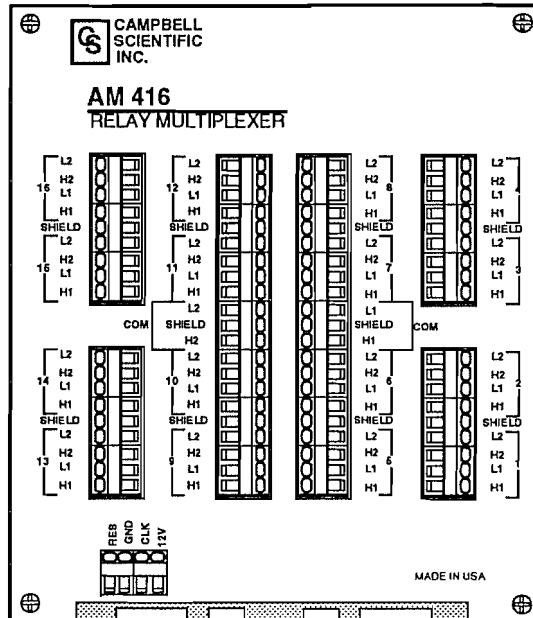
**Description:**

- L1: Scan light
- P1: Switch activating scan light
- P2: Switch activating voltmeter
- Com.: Standard 9-contact serial receptacle (type RS232)
- A/B: Amphenol 2-contact receptacles (type MS-3102A-14S-9S)
- 1 - 12: Amphenol 20-contact receptacles (type MS-3102A-28-16S)
- \* Channel numbers in parentheses

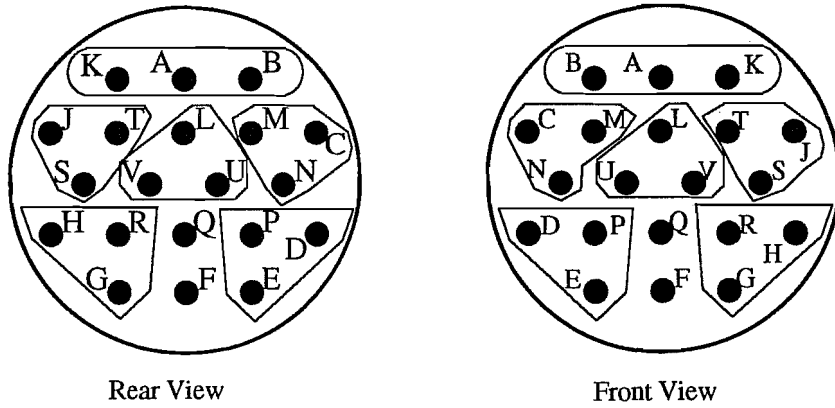
V. Data-logger 21X



VI. Multiplexer AM416



VII. Typical Wiring of Connectors #1 through #10



Amphenol 20-contact receptacle

**Strain Gage  
Channel Number**

**1**      K --> S-  
          A --> E+  
          B --> E-

**2**      J --> S-  
          T --> E+  
          S --> E-

**3**      L --> S-  
          V --> E+  
          U --> E-

**Strain Gage  
Channel Number**

**4**      M --> S-  
          C --> E+  
          N --> E-

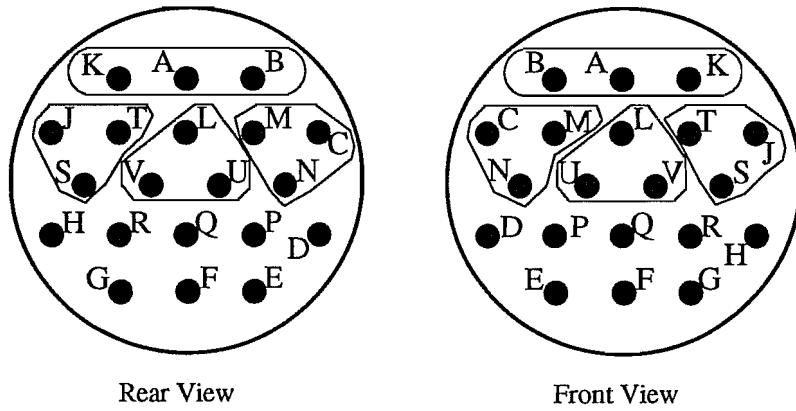
**5**      H --> S-  
          R --> E+  
          G --> E-

**6**      P --> S-  
          D --> E+  
          E --> E-

Q --> not connected  
F -->



VIII. Wiring of Connector #11



Amphenol 20-contact receptacle

Strain Gage  
Channel Number

**61** K --> S-  
A --> E+  
B --> E-

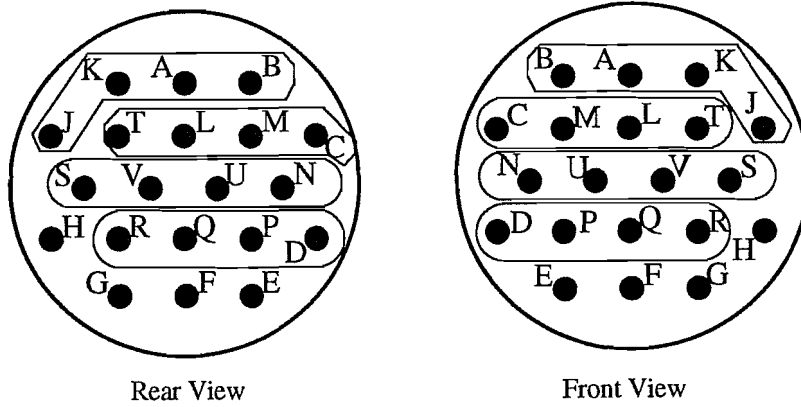
**62** J --> S-  
T --> E+  
S --> E-

**63** L --> S-  
V --> E+  
U --> E-

**64** M --> S-  
C --> E+  
N --> E-

H -->  
R -->  
G -->  
P --> not connected  
D -->  
E -->  
Q -->  
F -->

**IX. Wiring of Connector #12**



Amphenol 20-contact receptacle

**Strain Gage  
Channel Number**

**65** A --> E+  
 B --> S-  
 J --> E-  
 K --> S+

**66** M --> E+  
 C --> S-  
 T --> E-  
 L --> S+

**Strain Gage  
Channel Number**

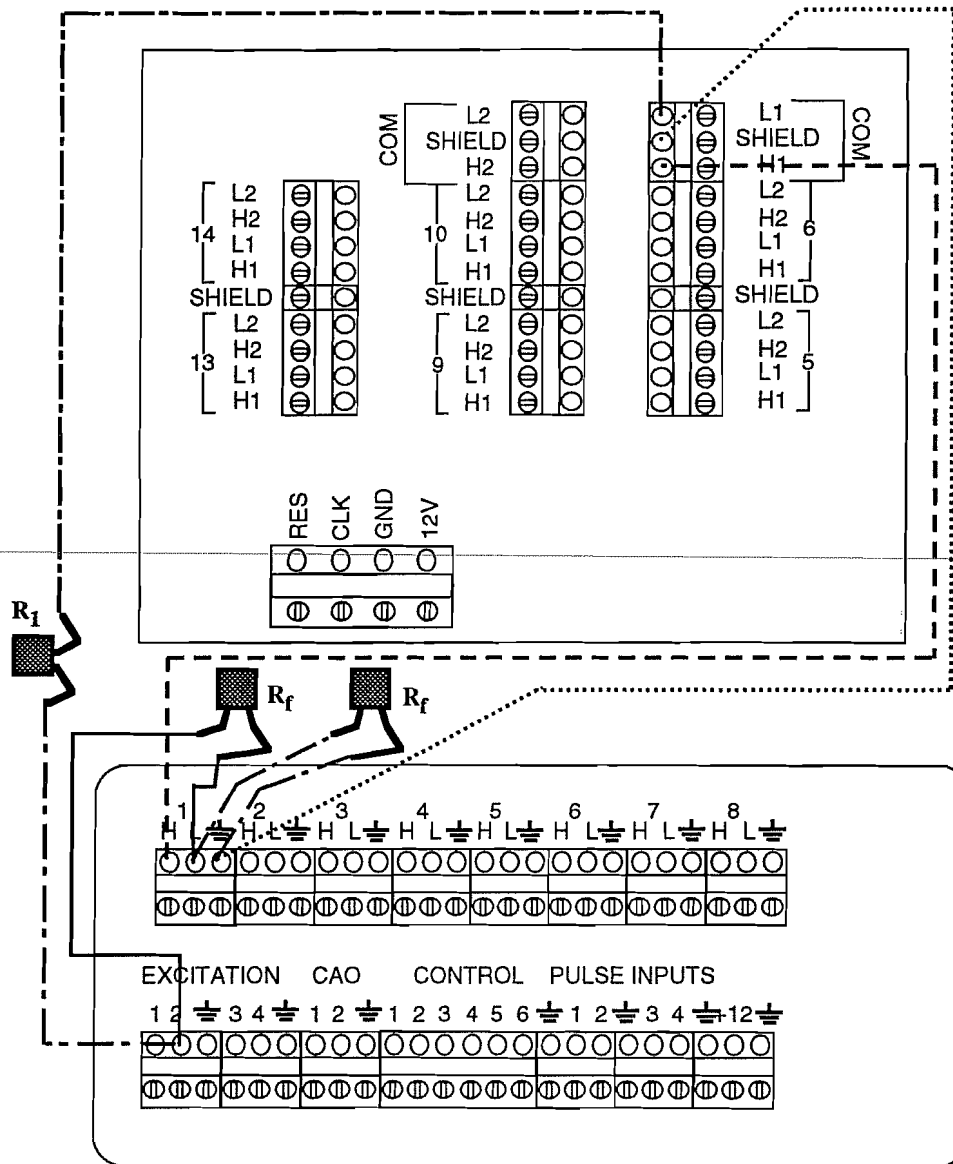
**67** U --> E+  
 N --> S-  
 S --> E-  
 V --> S+

**68** P --> E+  
 D --> S-  
 R --> E-  
 Q --> S+

H --> Control #4  
 G --> Control #5  
 F --> Pulse Input #3  
 E --> Pulse Input #4

**X. Internal connection circuit between Campbell and Multiplexers**

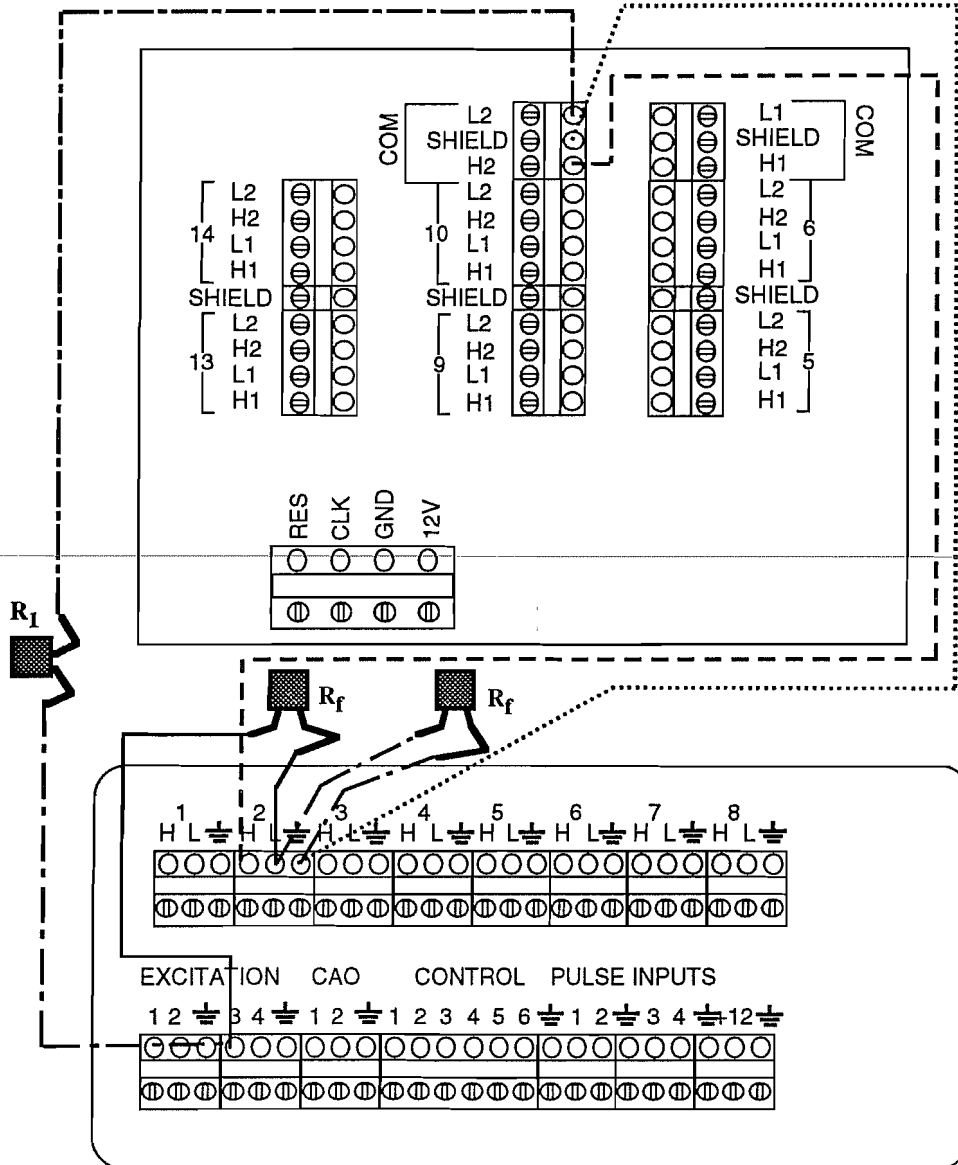
**10.1 Quarter bridge completion circuit with Multiplexer #1, channels H1-L1:**



Notes:

- $R_f$ : 350Ω (0.01%) Precision Resistor - 1st. Wheatstone arm
- $R_1$ : 350Ω (0.01%) Precision Resistor - 2nd. Wheatstone arm

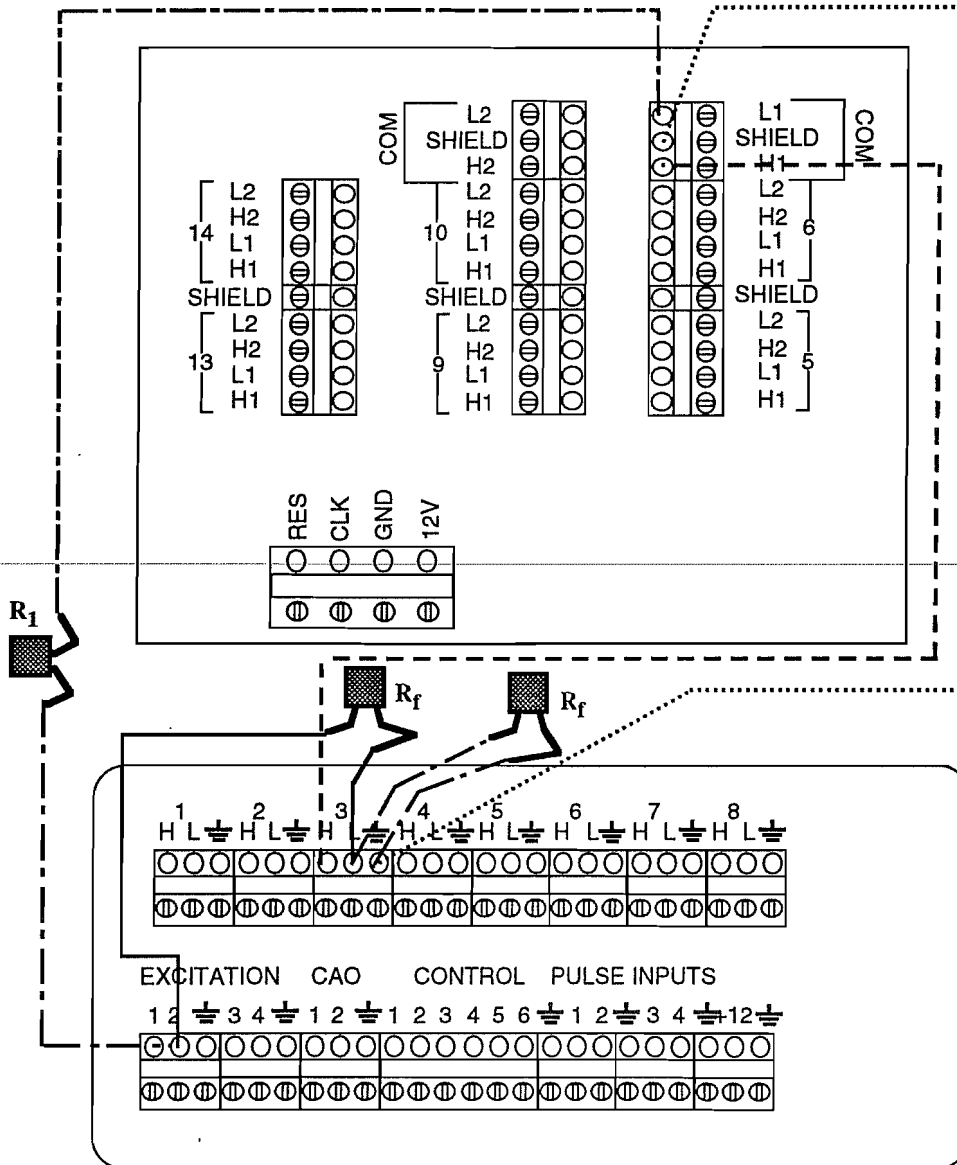
10.2 Quarter bridge completion circuit with Multiplexer #1, channels H2-L2:



Notes:

- R<sub>f</sub> : 350Ω (0.01%) Precision Resistor - 1st. Wheatstone arm
- R<sub>1</sub> : 350Ω (0.01%) Precision Resistor - 2nd. Wheatstone arm

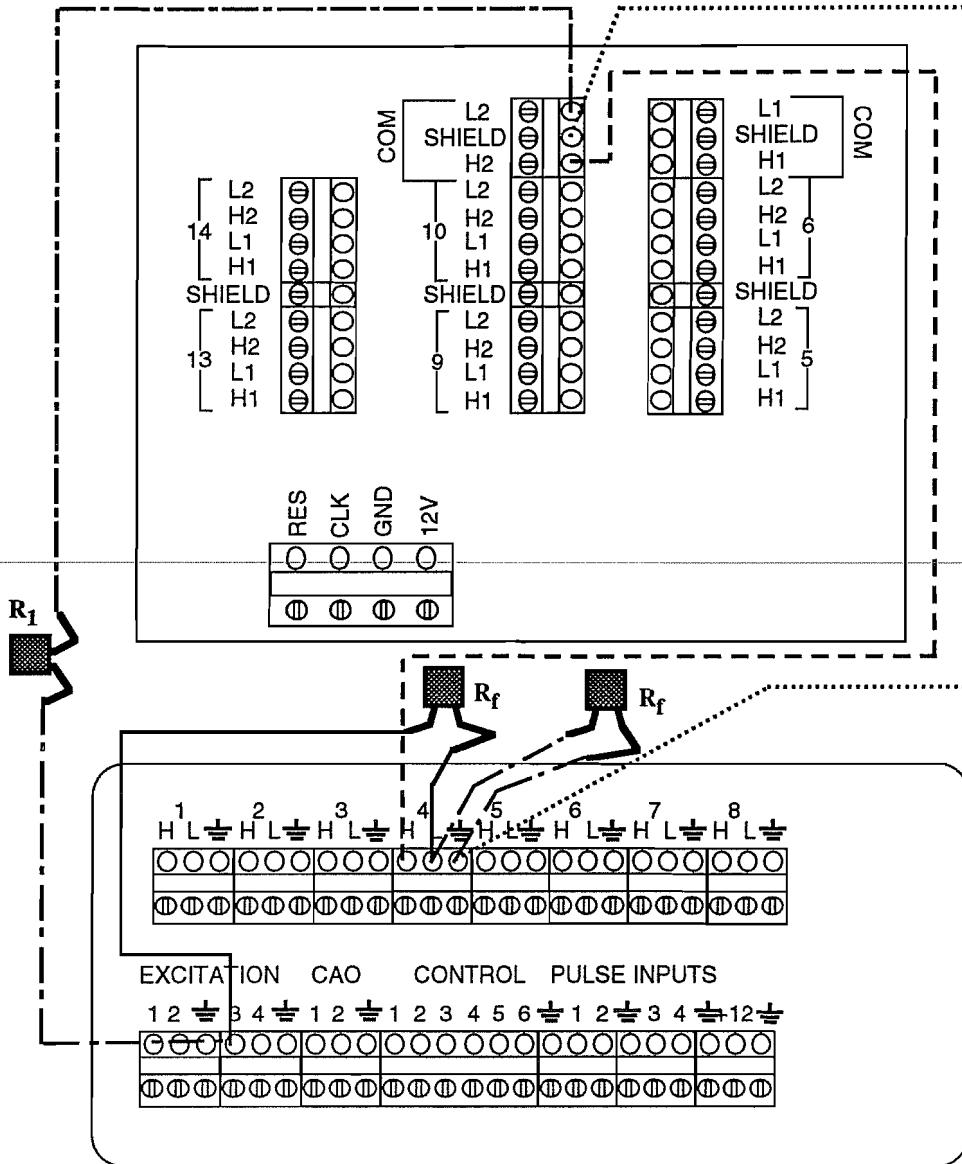
10.3 Quarter bridge completion circuit with Multiplexer #2, channels H1-L1:



Notes:

- $R_f$ : 350 $\Omega$  (0.01%) Precision Resistor - 1st. Wheatstone arm
- $R_1$ : 350 $\Omega$  (0.01%) Precision Resistor - 2nd. Wheatstone arm

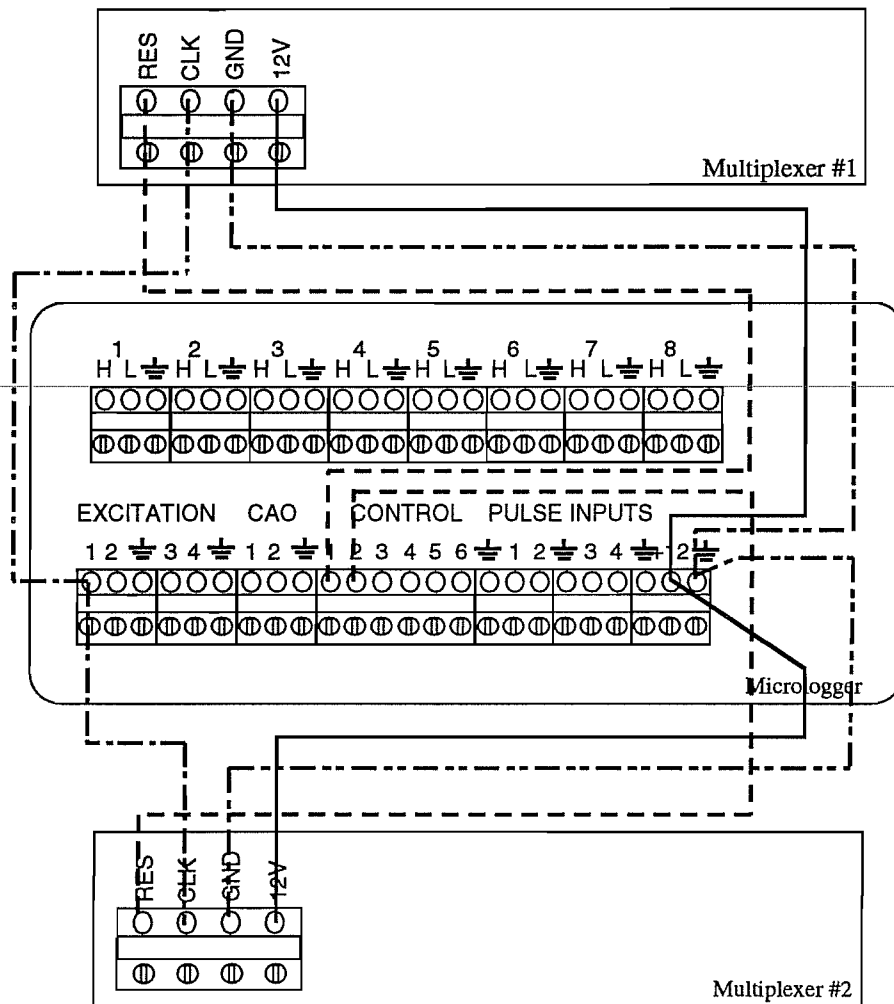
10.4 Quarter bridge completion circuit with Multiplexer #2, channels H2-L2:



Notes:

- R<sub>f</sub>: 350Ω (0.01%) Precision Resistor - 1st. Wheatstone arm
- R<sub>1</sub>: 350Ω (0.01%) Precision Resistor - 2nd. Wheatstone arm

10.5 Typical connections between Micrologger 21X and AM416 Multiplexers:



## XI. Detailed Internal Wiring between Multiplexers, Datalogger and Connectors

### 11.1 Multiplexer #1:

Connector Number	Channel Number	Connector Letter Code	Wire Type	Wire Color	Multiplexer Channel	
1	1	K	S-	Red	1- 1H	
		A	E+	White	1- 1L	
		B	E-	Black	1/2- Ground	
	2	2	J	S-	Red	1- 2H
			T	E+	White	1- 2L
			S	E-	Black	1/2- Ground
	3	3	L	S-	Red	2- 1H
			V	E+	White	2- 1L
			U	E-	Black	1/2- Ground
	4	4	M	S-	Red	2- 2H
			C	E+	White	2- 2L
			N	E-	Black	1/2- Ground
	5	5	H	S-	Red	3- 1H
			R	E+	White	3- 1L
			G	E-	Black	3/4- Ground
6	6	P	S-	Red	3- 2H	
		D	E+	White	3- 2L	
		E	E-	Black	3/4- Ground	
2	7	K	S-	Red	4- 1H	
		A	E+	White	4- 1L	
		B	E-	Black	3/4- Ground	
	8	8	J	S-	Red	4- 2H
			T	E+	White	4- 2L
			S	E-	Black	3/4- Ground
	9	9	L	S-	Red	5- 1H
			V	E+	White	5- 1L
			U	E-	Black	5/6- Ground
	10	10	M	S-	Red	5- 2H
			C	E+	White	5- 2L
			N	E-	Black	5/6- Ground
	11	11	H	S-	Red	6- 1H
			R	E+	White	6- 1L
			G	E-	Black	5/6- Ground
12	12	P	S-	Red	6- 2H	
		D	E+	White	6- 2L	
		E	E-	Black	5/6- Ground	



Connector Number	Channel Number	Connector Letter Code	Wire Type	Wire Color	Multiplexer Channel
3	13	K	S-	Red	7- 1H
		A	E+	White	7- 1L
		B	E-	Black	7/8- Ground
	14	J	S-	Red	7- 2H
		T	E+	White	7- 2L
		S	E-	Black	7/8- Ground
	15	L	S-	Red	8- 1H
		V	E+	White	8- 1L
		U	E-	Black	7/8- Ground
	16	M	S-	Red	8- 2H
		C	E+	White	8- 2L
		N	E-	Black	7/8- Ground
	17	H	S-	Red	9- 1H
		R	E+	White	9- 1L
		G	E-	Black	9/10- Ground
18	P	S-	Red	9- 2H	
	D	E+	White	9- 2L	
	E	E-	Black	9/10- Ground	
4	19	K	S-	Red	10- 1H
		A	E+	White	10- 1L
		B	E-	Black	9/10- Ground
	20	J	S-	Red	10- 2H
		T	E+	White	10- 2L
		S	E-	Black	9/10- Ground
	21	L	S-	Red	11- 1H
		V	E+	White	11- 1L
		U	E-	Black	11/12- Ground
	22	M	S-	Red	11- 2H
		C	E+	White	11- 2L
		N	E-	Black	11/12- Ground
	23	H	S-	Red	12- 1H
		R	E+	White	12- 1L
		G	E-	Black	11/12- Ground
24	P	S-	Red	12- 2H	
	D	E+	White	12- 2L	
	E	E-	Black	11/12- Ground	

Connector Number	Channel Number	Connector Letter Code	Wire Type	Wire Color	Multiplexer Channel
5	25	K	S-	Red	13- 1H
		A	E+	White	13- 1L
		B	E-	Black	13/14- Ground
	26	J	S-	Red	13- 2H
		T	E+	White	13- 2L
		S	E-	Black	13/14- Ground
	27	L	S-	Red	14- 1H
		V	E+	White	14- 1L
		U	E-	Black	13/14- Ground
	28	M	S-	Red	14- 2H
		C	E+	White	14- 2L
		N	E-	Black	13/14- Ground
	29	H	S-	Red	15- 1H
		R	E+	White	15- 1L
		G	E-	Black	15/16- Ground
30	P	S-	Red	15- 2H	
	D	E+	White	15- 2L	
	E	E-	Black	15/16- Ground	
6	31	K	S-	Red	16- 1H
		A	E+	White	16- 1L
		B	E-	Black	15/16- Ground
	32	J	S-	Red	16- 2H
		T	E+	White	16- 2L
		S	E-	Black	15/16- Ground

### 11.2 Multiplexer #2:

6	33	L	S-	Red	1- 1H
		V	E+	White	1- 1L
		U	E-	Black	1/2- Ground
	34	M	S-	Red	1- 2H
		C	E+	White	1- 2L
		N	E-	Black	1/2- Ground
	35	H	S-	Red	2- 1H
		R	E+	White	2- 1L
		G	E-	Black	1/2- Ground
	36	P	S-	Red	2- 2H
		D	E+	White	2- 2L
		E	E-	Black	1/2- Ground

Connector Number	Channel Number	Connector Letter Code	Wire Type	Wire Color	Multiplexer Channel
7	37	K	S-	Red	3- 1H
		A	E+	White	3- 1L
		B	E-	Black	3/4- Ground
	38	J	S-	Red	3- 2H
		T	E+	White	3- 2L
		S	E-	Black	3/4- Ground
	39	L	S-	Red	4- 1H
		V	E+	White	4- 1L
		U	E-	Black	3/4- Ground
	40	M	S-	Red	4- 2H
		C	E+	White	4- 2L
		N	E-	Black	3/4- Ground
	41	H	S-	Red	5- 1H
		R	E+	White	5- 1L
G		E-	Black	5/6- Ground	
42	P	S-	Red	5- 2H	
	D	E+	White	5- 2L	
	E	E-	Black	5/6- Ground	
8	43	K	S-	Red	6- 1H
		A	E+	White	6- 1L
		B	E-	Black	5/6- Ground
	44	J	S-	Red	6- 2H
		T	E+	White	6- 2L
		S	E-	Black	5/6- Ground
	45	L	S-	Red	7- 1H
		V	E+	White	7- 1L
		U	E-	Black	7/8- Ground
	46	M	S-	Red	7- 2H
		C	E+	White	7- 2L
		N	E-	Black	7/8- Ground
	47	H	S-	Red	8- 1H
		R	E+	White	8- 1L
		G	E-	Black	7/8- Ground
	48	P	S-	Red	8- 2H
		D	E+	White	8- 2L
		E	E-	Black	7/8- Ground
9	49	K	S-	Red	9- 1H
		A	E+	White	9- 1L
		B	E-	Black	9/10- Ground

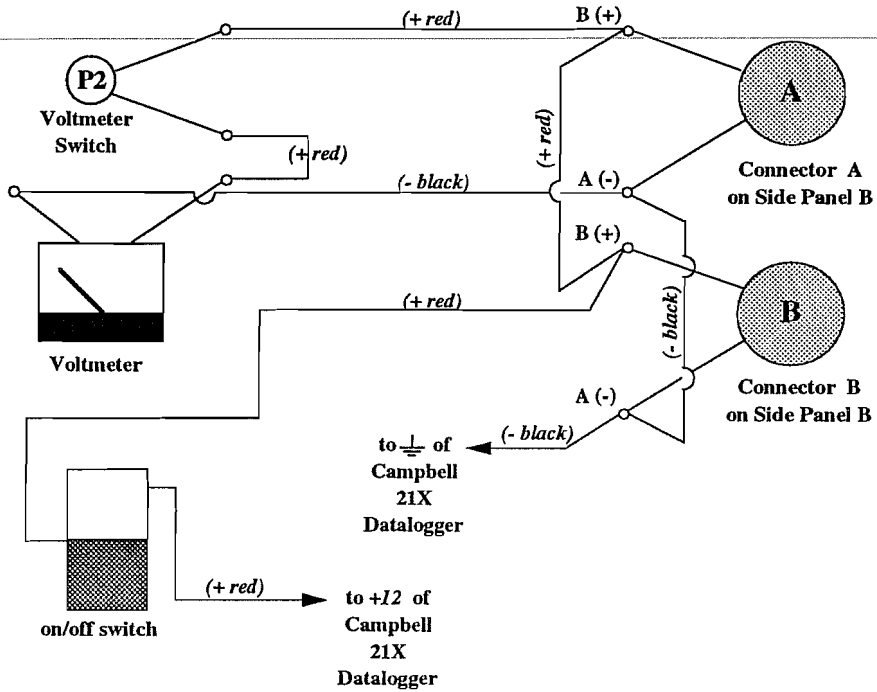
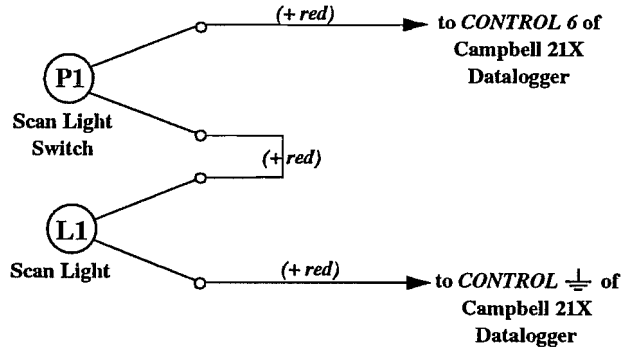
Connector Number	Channel Number	Connector Letter Code	Wire Type	Wire Color	Multiplexer Channel
9	50	J	S-	Red	9- 2H
		T	E+	White	9- 2L
		S	E-	Black	9/10- Ground
	51	L	S-	Red	10- 1H
		V	E+	White	10- 1L
		U	E-	Black	9/10- Ground
	52	M	S-	Red	10- 2H
		C	E+	White	10- 2L
		N	E-	Black	9/10- Ground
	53	H	S-	Red	11- 1H
		R	E+	White	11- 1L
		G	E-	Black	11/12- Ground
	54	P	S-	Red	11- 2H
		D	E+	White	11- 2L
		E	E-	Black	11/12- Ground
10	55	K	S-	Red	12- 1H
	56	A	E+	White	12- 1L
		B	E-	Black	11/12- Ground
		J	S-	Red	12- 2H
	57	T	E+	White	12- 2L
		S	E-	Black	11/12- Ground
		L	S-	Red	13- 1H
	58	V	E+	White	13- 1L
		U	E-	Black	13/14- Ground
		M	S-	Red	13- 2H
	59	C	E+	White	13- 2L
		N	E-	Black	13/14- Ground
		H	S-	Red	14- 1H
	60	R	E+	White	14- 1L
		G	E-	Black	13/14- Ground
		P	S-	Red	14- 2H
	61	D	E+	White	14- 2L
		E	E-	Black	13/14- Ground
		K	S-	Red	15- 1H
11	62	A	E+	White	15- 1L
		B	E-	Black	15/16- Ground
		J	S-	Red	15- 1H
	T	E+	White	15- 1L	
	S	E-	Black	15/16- Ground	

Connector Number	Channel Number	Connector Letter Code	Wire Type	Wire Color	Multiplexer Channel
11	63	L	S-	Red	16- 1H
		V	E+	White	16- 1L
		U	E-	Black	15/16- Ground
	64	M	S-	Red	16- 2H
		C	E+	White	16- 2L
		N	E-	Black	15/16- Ground

### 11.3 Campbell 21X:

Connector Number	Channel Number	Connector Letter Code	Wire Type	Wire Color	Multiplexer Channel	
12	65	A	E+	Red	E4	
		B	S-	White	5L	
		J	E-	Black	5- Ground	
	66	K	S+	Green	5H	
		M	E+	Red	E4	
		C	S-	White	6L	
	67	T	E-	Black	6- Ground	
		L	S+	Green	6H	
		U	E+	Red	E4	
		N	S-	White	7L	
		S	E-	Black	7- Ground	
		V	S+	Green	7H	
	68	P	E+	Red	E4	
		D	S-	White	8L	
		R	E-	Black	8- Ground	
		Q	S+	Green	8H	
	<b>Other connections:</b> (same connector #12)		H	(-)	Red	Control-4
			G	(-)	Red	Control-5
		E	(-)	Green	Pulse In-3	
		F	(-)	Green	Pulse In-4	

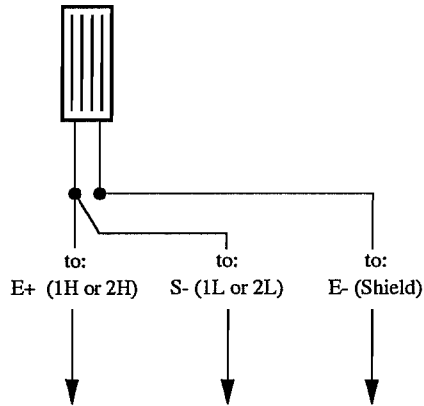
**XII. Detailed Internal Wiring between Switches, Battery Connectors, and Datalogger**



**XIII. Wiring from Data Acquisition Box to Typical Sensors**

**13.1 Electrical Resistance Strain Gages (only for 350W)**

--all three leadwire, quarter-bridge Wheatstone circuits--



**Available Combinations:**

Connector Number	Connector Labels		
#1 through #10 (channels 1 thru 60)	A	K	B
	T	J	S
	V	L	U
	C	M	N
	R	H	G
	D	P	E
#11 (channels 61 thru 64)	A	K	B
	T	J	S
	V	L	U
	C	M	N

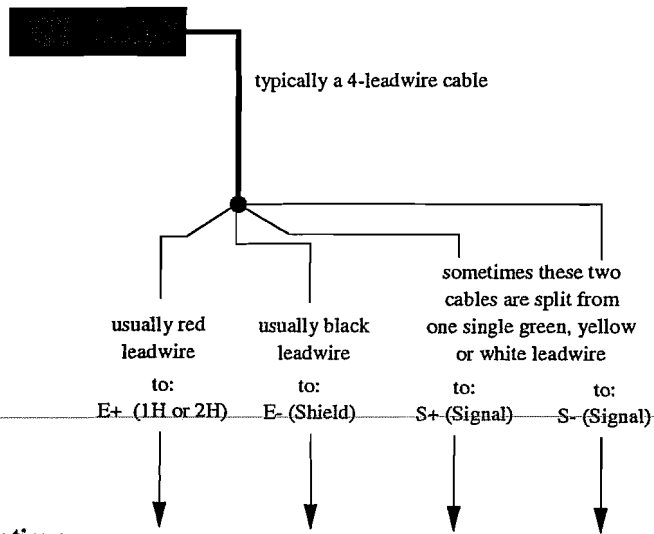
**Notes:**

\* a total of 64 channels are available for this type of sensor.

\*\* four additional channels can be employed if the completion circuits (one for each channel) are prepared externally from the data acquisition box. These additional sensors can then use Channels 65 through 68.

**13.2 Pressure Transducer, Linear Potentiometers (LVDTs)**

--electrical resistance, 3 or 4-leadwire, full-bridge Wheatstone circuits--



**Available Combinations:**

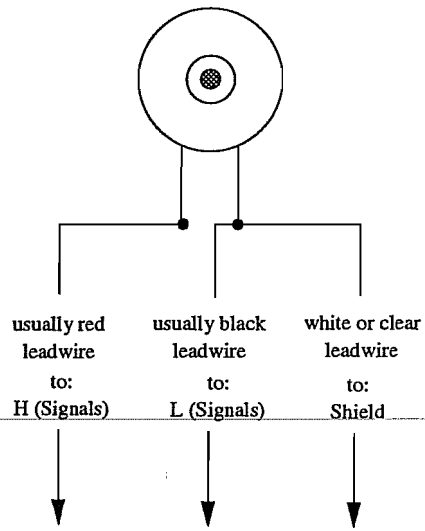
Connector Number	Connector Labels			
#12 (channels 1 thru 4)	A	J	K	B
	M	T	L	C
	U	S	V	N
	P	R	Q	D

**Notes:**

\* a total of 4 channels are available for this type of sensor.



**13.3 LI-200SZ Pyranometer**



**Available Combinations:**

Connector Number	Connector Labels		
#12 (channels 1 thru 4)	K	B	J
	L	C	T
	V	N	S
	Q	D	R

**Notes:**

\* a total of 4 channels are available for this type of sensor.

### 13.4 Other Sensors

#### *a. Thermocouples*

The Campbell 21X Micrologger was originally designed to measure up to 8 differential thermocouple channels (of the type T, E, K, or J). Each AM-416 Multiplexer was originally designed to handle up to 32 additional differential thermocouple channels (only if each group of 16 or all 32 channels are of the same thermocouple type T, E, K, or J)<sup>(1)</sup>. The reference junction of the differential thermocouple measurements made by the Campbell 21X is the panel temperature (since each 21X has an internal sensor that determines the panel temperature).

However, with the new portable data acquisition boxes, thermocouple measurements are no longer available. This is because an added thermocouple junction will exist at the connections between the external thermocouple wires and the connectors located in the portable data acquisition box side panels.

#### *b. Thermistors*

Measurements of this type of sensor consist of electrical resistance readings. Single-ended channels can be used (up to 16 on each 21X and up to 64 on each AM-416). The new portable data acquisition boxes can still perform thermistor measurements using the available channels on connector #12. Up to eight thermistors can thus be used on each data acquisition box. The same wiring suggested by accompanying Campbell Instruments literature should be used. Campbell Scientific, Inc. offers two types of thermistors fully compatible to their dataloggers (the 107- and the 108-*Thermistors* sold for \$40.00 and \$44.00 respectively according to mid-1990 price sheet).

#### *c. Relative Humidity*

Campbell Scientific, Inc. offers the 207 *Temperature and RH Probe* (\$200.00 each on mid-1990 price sheet) that can still be used with the new portable data acquisition box. The same

---

<sup>(1)</sup> If thermocouples were grounded at about the same ground potential of the 21X, then single-ended thermocouple measurements can be performed and the available number of channels will double from the previously given numbers (each 21X could thus handle up to 16 single-ended channels and each AM-416 up to 64 single-ended channels).

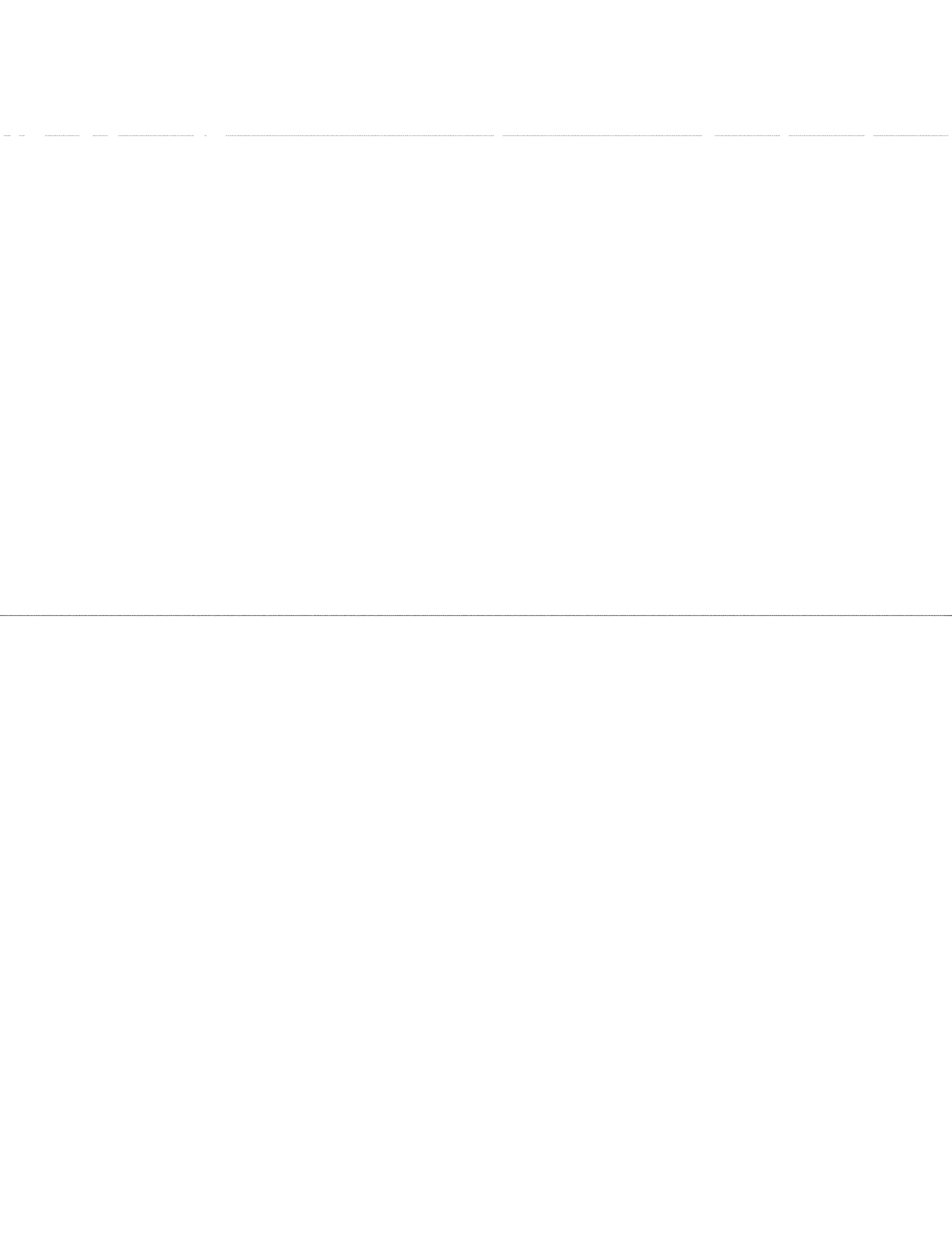
---

instructions provided in the Campbell literature applies to the available channels of connector #12.

*d. Wind Speed and Direction*

These sensors can still be used with each portable data acquisition box. The Campbell Scientific *014A Wind Speed Sensor* and the *024A Wind Direction Sensor* cost \$275.00 and \$393 in mid-1990.

---



## APPENDIX B

### PROGRAMS FOR CAMPBELL SCIENTIFIC 21X MICROLOGGER

Program: Span CC11 Stressing

Flag Usage:

Input Channel Usage:

1H & 1L Multiplexer pass 1  
2H & 2L Multiplexer pass 2  
3H & 3L Pressure Transducer  
4H & 4L Solar Radiation  
5H & 5L Auxilliary Full Bridge  
6,7,8 Empty

Excitation Channel Usage:

1 Clock Multiplexer  
2 Multiplexer pass 1  
3 Multiplexer pass 2  
4 Full Bridge Channels

Continuous Analog Output Usage:

None

Control Port Usage:

1 Multiplexer  
6 LED

Pulse Input Channel Usage:

None

Output Array Definitions:

*1	Table 1 Programs
01:60	Sec. Execution Interval
01:P17	Panel Temperature
01:37	Loc : PANTEMP
02:P20	Set Port
01:1	Set high
02:6	Port Number

---

03:P10	Battery Voltage
01:36	Loc : BATVOLT
04:P20	Set Port
01:1	Set high
02:1	Port Number
05:P87	Beginning of Loop
01:0	Delay
02:16	Loop Count 32 strain gages
06:P22	Excitation with Delay
01:1	EX Chan
02:1	Delay w/EX (units=.01sec)
03:1	Delay after EX (units=.01sec)
04:5000	mV Excitation
07:P6	Full Bridge
01:1	Rep
02:3	50 mV slow Range
03:1	IN Chan
04:2	Excite all reps w/EXchan 2
05:5000	mV Excitation
06:1--	Loc : Strain Gage #1
07:1	Mult
08:0	Offset
08:P6	Full Bridge
01:1	Rep
02:3	50 mV slow Range
03:2	IN Chan
04:3	Excite all reps w/EXchan 3
05:5000	mV Excitation
06:17--	Loc : Strain Gage #2
07:1	Mult
08:0	Offset
09:P95	End
10:P20	Set Port
01:0	Set low
02:1	Port Number

---

11:P6 Full Bridge  
 01:1 Rep  
 02:3 50 mV slow Range  
 03:3 IN Chan  
 04:4 Excite all reps w/EXchan 4  
 05:5000 mV Excitation  
 06:33 Loc : Pressure Transducer  
 07:1 Mult  
 08:0 Offset

12:P6 Full Bridge  
 01:1 Rep  
 02:3 50 mV slow Range  
 03:4 IN Chan  
 04:4 Excite all reps w/EXchan 4  
 05:5000 mV Excitation  
 06:34 Loc : Solar Radiation  
 07:1 Mult  
 08:0 Offset

---

13:P6 Full Bridge  
 01:1 Rep  
 02:3 50 mV slow Range  
 03:5 IN Chan  
 04:4 Excite all reps w/EXchan 4  
 05:5000 mV Excitation  
 06:35 Loc : Auxilliary  
 07:1 Mult  
 08:0 Offset

14:P20 Set Port  
 01:0 Set low  
 02:6 Port Number

15:P86 Do  
 01:10 Set high Flag 0 (output)

16:P77 Real Time  
 01:10 Hour-Minute

17:P70 Sample  
 01:16 Repls  
 02:1-- Loc

246

18:P70      Sample  
01:16      Reps  
02:17--    Loc

19:P70      Sample  
01:5        Reps  
02:33--    Loc

20:P        End Table 1

\*2         Table 2 Programs  
01:0.0000   Sec. Execution Interval

01:P        End Table 2

\*3         Table 3 Subroutines

01:P        End Table 3

\*4         Mode 4 Output Options  
01:00      Tape/Printer Option  
02:00      Printer Baud Option

\*A         Mode 10 Memory Allocation  
01:40      Input Locations  
02:40      Intermediate Locations

\*C         Mode 12 Security (OSX-0)  
01:00      Security Option  
02:0000    Security Code

Permanent Storage Locations

Storage #	Connection #	Gage Designation
1	1-1	T1SL1
2	1-3	T2SL1
3	1-5	T1SM1
4	2-1	T2SM1
5	2-3	T1SD1
6	2-5	T2SD1



7	3-1	T1NL1
8	3-3	T2NL1
9	3-5	T1NM1
10	4-1	T2NM1
11	4-3	T1ND1
12	4-5	T2ND1
13	5-1	D1
14	5-3	D3
15	5-5	D5
16	6-1	D7
17	1-2	T1SL2
18	1-4	T2SL2
19	1-6	T1SM2
20	2-2	T2SM2
21	2-4	T1SD2
22	2-6	T2SD2
23	3-2	T1NL2
24	3-4	T2NL2
25	3-6	T1NM2
26	4-2	T2NM2
27	4-4	T1ND2
28	4-6	T2ND2
29	5-2	D2
30	5-4	D4
31	5-6	D6
32	6-2	D8
33	6-1W	PRESSURE TRANSDUCER
34	6-2W	SOLAR RADIATION
35	6-3W	AUXILLIARY
36	-	BATTERY VOLTAGE
37	-	PANEL TEMPERATURE

Input Location Assignments (with comments):

Key:

T=Table Number

E=Entry Number

L=Location Number

T:E:L:

1:7:1:        Loc : Strain Gage #1

1:8:17:      Loc : Strain Gage #2

1:11:33:     Loc : Pressure Transducer

1:12:34: Loc : Solar Radiation  
1:13:35: Loc : Auxilliary  
1:3:36: Loc : BATVOLT  
1:1:37: Loc : PANTEMP

Program:Span AA44 Stressing

Flag Usage:

Input Channel Usage:

1H & 1L Multiplexer 1 pass 1  
2H & 2L Multiplexer 1 pass 2  
3H & 3L Multiplexer 2 pass 1  
4H & 4L Multiplexer 2 pass 2  
5H & 5L Pressure Transducer  
6H & 6L Solar Radiation  
7H & 7L Auxilliary Full Bridge  
8H & 8L Auxilliary Full Bridge

Excitation Channel Usage:

1 Clock Multiplexer  
2 Multiplexers 1 & 2 pass 1  
3 Multiplexers 1 & 2 pass 2  
4 Full Bridge Channels

Continuous Analog Output Usage:  
None

Control Port Usage:

1 Multiplexer 1  
2 Multiplexer 2  
6 LED

Pulse Input Channel Usage:  
None

Output Array Definitions:

\*1 Table 1 Programs  
01:30 Sec. Execution Interval

---

01:P17      Panel Temperature  
01: 68      Loc : PANTEMP

02:P20      Set Port  
01:1      Set high  
02:6      Port Number

03:P10      Battery Voltage  
01:69      Loc : BATVOLT

Clock Multiplexer #1 and read Gages 1-32

04:P20      Set Port  
01:1      Set high  
02:1      Port Number

05:P87      Beginning of Loop  
01:0      Delay  
02:16      Loop Count 32 strain gages

---

06:P22      Excitation with Delay  
01:1      EX Chan  
02:1      Delay w/EX (units=.01sec)  
03:1      Delay after EX (units=.01sec)  
04:5000    mV Excitation

07:P6      Full Bridge  
01:1      Rep  
02:3      50 mV slow Range  
03:1      IN Chan  
04:2      Excite all reps w/EXchan 2  
05:5000    mV Excitation  
06:1--      Loc : Strain Gage #1  
07:1      Mult  
08:0      Offset

08:P6      Full Bridge  
01:1      Rep  
02:3      50 mV slow Range  
03:2      IN Chan  
04:3      Excite all reps w/EXchan 3  
05:5000    mV Excitation  
06:17--    Loc : Strain Gage #2

250

---

07:1 Mult  
08:0 Offset

09:P95 End

10:P20 Set Port  
01:0 Set low  
02:1 Port Number

Shut down Multiplexer #1, Clock Multiplexer #2 and  
read gages 33-64

11:P20 Set Port  
01:1 Set high  
02:2 Port Number

12:P87 Beginning of Loop  
01:0 Delay  
02:16 Loop Count

---

13:P22 Excitation with Delay  
01:1 EX Chan  
02:1 Delay w/EX (units=.01sec)  
03:1 Delay after EX (units=.01sec)  
04:5000 mV Excitation

14:P6 Full Bridge  
01:1 Rep  
02:3 50 mV slow Range  
03:3 IN Chan  
04:2 Excite all reps w/EXchan 2  
05:5000 mV Excitation  
06:33-- Loc :  
07:1 Mult  
08:0 Offset

15:P6 Full Bridge  
01:1 Rep  
02:3 50 mV slow Range  
03:4 IN Chan  
04:3 Excite all reps w/EXchan 3  
05:5000 mV Excitation

---

06:49--	Loc :
07:1	Mult
08:0	Offset
16:P95	End
17:P20	Set Port
01:0	Set low
02:2	Port Number
18:P6	Full Bridge
01:1	Rep
02:3	50 mV slow Range
03:5	IN Chan
04:4	Excite all reps w/EXchan 4
05:5000	mV Excitation
06:65	Loc : Pressure Transducer
07:1	Mult
08:0	Offset
19:P6	Full Bridge
01:1	Rep
02:3	50 mV slow Range
03:6	IN Chan
04:4	Excite all reps w/EXchan 4
05:5000	mV Excitation
06:66	Loc : Solar Radiation
07:1	Mult
08:0	Offset
20:P6	Full Bridge
01:1	Rep
02:3	50 mV slow Range
03:7	IN Chan
04:4	Excite all reps w/EXchan 4
05:5000	mV Excitation
06:67	Loc : Auxilliary
07:1	Mult
08:0	Offset
21:P20	Set Port
01:0	Set low
02:6	Port Number

252

---

22:P86      Do  
01:10      Set high Flag 0 (output)

23:P77      Real Time  
01:10      Hour-Minute

24:P70      Sample  
01:16      Reps  
02:1--      Loc

25:P70      Sample  
01:16      Reps  
02:17--      Loc

26:P70      Sample  
01:16      Reps  
02:33--      Loc

27:P70      Sample  
01:16      Reps  
02:49--      Loc

---

28:P70      Sample  
01:5        Reps  
02:65--      Loc

29:P        End Table 1

\*2        Table 2 Programs  
01:0.0000    Sec. Execution Interval

01:P        End Table 2

\*3        Table 3 Subroutines

01:P        End Table 3

\*4        Mode 4 Output Options  
01:00      Tape/Printer Option  
02:00      Printer Baud Option

\*A            Mode 10 Memory Allocation  
 01:72        Input Locations  
 02:72        Intermediate Locations

\*C            Mode 12 Security (OSX-0)  
 01:00        Security Option  
 02:0000     Security Code

Permanent Storage Locations

Storage #	Connection #	Gage Designation
1	1-1	T1NL1
2	1-3	T2NL1
3	1-5	T3NL1
4	2-1	T1SL1
5	2-3	T2SL1
6	2-5	T3SL1
7	3-1	T1NM1
8	3-3	T2NM1
9	3-5	T3NM1
10	4-1	T1SM1
11	4-3	T2SM1
12	4-5	T3SM1
13	5-1	T1ND1
14	5-3	T2ND1
15	5-5	T3ND1
16	6-1	T1SD1
17	1-2	T1NL2
18	1-4	T2NL2
19	1-6	T3NL2
20	2-2	T1SL2
21	2-4	T2SL2
22	2-6	T3SL2
23	3-2	T1NM2
24	3-4	T2NM2
25	3-6	T3NM2
26	4-2	T1SM2
27	4-4	T2SM2
28	4-6	T3SM2
29	5-2	T1ND2
30	5-4	T2ND2
31	5-6	T3ND2
32	6-2	T1SD2
33	6-3	T2SD1

---

34	6-5	T3SD1
35	7-1	D1
36	7-3	D3
37	7-5	D5
38	8-1	D7
39	8-3	D9
40	8-5	A1
41	9-1	A3
42	9-3	A5
43	9-5	A7
44	10-1	A9
45	10-3	A11
46	10-5	T6NM1
47	11-1	T6SM1
48	11-3	T6NM3
49	6-4	T2SD2
50	6-6	T3SD2
51	7-2	D2
52	7-4	D4
53	7-6	D6
54	8-2	D8
55	8-4	D10
56	8-6	A2
57	9-2	A4
58	9-4	A6
59	9-6	A8
60	10-2	A10
61	10-4	A12
62	10-6	T6NM2
63	11-2	T6SM2
64	11-4	T6SM3
65	12-1	PRESSURE TRANSDUCER
66	12-2	SOLAR RADIATION
67	12-3	AUXILLIARY FULL BRIDGE
68	-	PANEL TEMPERATURE
69	-	BATTERY VOLTAGE

---



---

**Input Location Assignments (with comments):**
**Key:**

T=Table Number

E=Entry Number

L=Location Number

**T:E:L:**

1:7:1:        Loc : Strain Gage #1  
 1:8:17:       Loc : Strain Gage #2  
 1:14:33:       Loc :  
 1:15:49:       Loc :  
 1:18:65:       Loc : Pressure Transducer  
 1:19:66:       Loc : Solar Radiation  
 1:20:67:       Loc : Auxilliary  
 1:1:68:        Loc : PANTEMP  
 1:3:69:        Loc : BATVOLT

**Program: Temperature Gradient Measurement****Flag Usage:****Input Channel Usage:****Excitation Channel Usage:****Continuous Analog Output Usage:****Control Port Usage:****Pulse Input Channel Usage:****Output Array Definitions:**

\*1            Table 1 Programs  
 01:1800       Sec. Execution Interval  
  
 01:P17        Panel Temperature  
 01:1           Loc : Panel Temperature  
  
 02:P14        Thermocouple Temp (DIFF)  
 01:1           Rep  
 02:1           5 mV slow Range  
 03:1           IN Chan  
 04:1           Type T (Copper-Constantan)  
 05:1           Ref Temp Loc  
 06:2           Loc :  
 07:1.8        Mult  
 08:32         Offset

03:P14 Thermocouple Temp (DIFF)  
01:1 Rep  
02:1 5 mV slow Range  
03:2 IN Chan  
04:1 Type T (Copper-Constantan)  
05:1 Ref Temp Loc  
06:3 Loc :  
07:1.8 Mult  
08:32 Offset

04:P14 Thermocouple Temp (DIFF)  
01:1 Rep  
02:1 5 mV slow Range  
03:3 IN Chan  
04:1 Type T (Copper-Constantan)  
05:1 Ref Temp Loc  
06:4 Loc :  
07:1.8 Mult  
08:32 Offset

05:P14 Thermocouple Temp (DIFF)  
01:1 Rep  
02:1 5 mV slow Range  
03:4 IN Chan  
04:1 Type T (Copper-Constantan)  
05:1 Ref Temp Loc  
06:5 Loc :  
07:1.8 Mult  
08:32 Offset

06:P14 Thermocouple Temp (DIFF)  
01:1 Rep  
02:1 5 mV slow Range  
03:5 IN Chan  
04:1 Type T (Copper-Constantan)  
05:1 Ref Temp Loc  
06:6 Loc :  
07:1.8 Mult  
08:32 Offset

07:P14 Thermocouple Temp (DIFF)  
01:1 Rep  
02:1 5 mV slow Range  
03:6 IN Chan

04:1	Type T (Copper-Constantan)
05:1	Ref Temp Loc
06:7	Loc :
07:1.8	Mult
08:32	Offset
08:P14	Thermocouple Temp (DIFF)
01:1	Rep
02:1	5 mV slow Range
03:7	IN Chan
04:1	Type T (Copper-Constantan)
05:1	Ref Temp Loc
06:8	Loc :
07:1.8	Mult
08:32	Offset
09:P2	Volt (DIFF)
01:1	Rep
02:2	15 mV slow Range
03:8	IN Chan
04:9	Loc :
05:0.13004	Mult
06:0.0000	Offset
10:P86	Do
01:10	Set high Flag 0 (output)
11:P77	Real Time
01:110	Day,Hour-Minute
12:P70	Sample
01:9	Reps
02:1--	Loc
13:P	End Table 1
*2	Table 2 Programs
01:0.0000	Sec. Execution Interval
01:P	End Table 2

---

*3	Table 3 Subroutines
01:P	End Table 3
*4	Mode 4 Output Options
01:00	Tape/Printer Option
02:00	Printer Baud Option
*A	Mode 10 Memory Allocation
01:28	Input Locations
02:64	Intermediate Locations
*C	Mode 12 Security (OSX-0)
01:00	Security Option
02:0000	Security Code

Input Location Assignments (with comments):

Key:

T=Table Number

E=Entry Number

L=Location Number

---

T:E:L:

1:1:1:      Loc : Panel Temperature

1:2:2:      Loc :

1:3:3:      Loc :

1:4:4:      Loc :

1:5:5:      Loc :

1:6:6:      Loc :

1:7:7:      Loc :

1:8:8:      Loc :

1:9:9:      Loc :

## REFERENCES

1. AASHTO, *Guide Specification for the Design and Construction of Segmental Concrete Bridges*, 1989.
2. AASHTO, "Interim Specifications for Segmental Bridges," American Association of State Highway and Transportation Officials, 1989.
3. ACI Committee 209, "Effects of Concrete Constituents, Environment, and Stress on the Creep and Shrinkage of Concrete," Special Publication SP-27, American Concrete Institute, Detroit, Michigan, 1971.
4. ACI Committee 209, "Prediction of Creep, Shrinkage, and Temperature Effects in Concrete Structures," Design for Creep and Shrinkage of Concrete Structures, Special Publication SP-76, American Concrete Institute, Detroit, Michigan, 1982.
5. American Society for Testing Materials, "Corrosion Resistance of Coated Steel Specimens (Cyclic Method)," American Society of Testing Materials, Designation D-2933-74 (Reapproved 1986).
6. American Society for Testing Materials, "Standard Test Method for Compressive Strength of Cylindrical Concrete Specimens," Specification C39-72, Philadelphia, PA, 1972.
7. American Society for Testing Materials, "Standard Test Method for Creep of Concrete in Compression," Specification C512-87, Philadelphia, PA, August 1987.
8. Baber, T. T., and Hilton, M. H., "Field Monitoring of the I-295 Bridge Over the James River Bridge -- Instrumentation Installation and Construction Period Studies," Interim Report, Virginia Transportation Research Council (Jointly Sponsored by the University of Virginia and the Virginia Department of Transportation), Charlottesville, Virginia, Report No. VTRC 88-R23, April 1988.
9. Bakoss, S. L., Burfitt, A. J., and Cridland, L., "The Measurement of Strain in Concrete with the Embedment Type Vibrating Wire Gauge," The New South Wales Institute of Technology, School of Civil Engineering, Civil Engineering Monograph No. C.E. 76/2 M.E., Sydney, Australia, 1976.
10. Barker, W. R., and Reese, L. C., "Instrumentation for Measurement of Axial Load in Drilled Shafts," Center for Highway Research, The University of Texas at Austin, Research Report No. 89-6, November 1969.

11. Bradberry, T. E., *Time dependent Deformation of Long Span Prestressed Concrete Beams Having Low Relaxation Strands*, M.S. Report, The University of Texas at Austin, May 1986.
12. Bryant, A. H., Wood, J. A., and Fenwick, R. C., "Creep and Shrinkage in Concrete Bridges," RRU Bulletin 70, National Roads Board, Wellington, New Zealand, 1984.
13. Butter, C. D., and Hocker, G. B., "Fiber Optics Strain Gauge," *Applied Optics*, Vol.17, No. 18, September 1978, pp. 2867-2869.
14. Comité Euro-International du Béton - Fédération Internationale de la Précontrainte, *CEB-FIP Model Code for Concrete Structures 1978*, 1978.
15. Dunncliff, J., *Geotechnical Instrumentation for Monitoring Field Performance*, John Wiley and Sons, Inc., New York, 1988.
16. Falconer, B.A. "Post-tensioning Anchorage Zones in Bridge Decks", Masters Thesis, University of Texas at Austin, May 1990.
17. Favre, R., Charif, H., and Markey, I., "Observation a Long Terme de la Déformation des Ponts," Institut de Statique et Structures - Béton Armé et Précontraint (IBAP), Ecole Polytechnique Fédérale de Lausanne, Projet de Recherche 86/88, October 1990.
18. Fellenius, B. H., "Ignorance is Bliss," *Geotechnical News*, Vol. 2, No. 4, December 1984, pp. 14-15.
19. Gamble, W. L., "Long-Term Behavior of a Prestressed I-Girder Highway Bridge in Champaign County, Illinois," University of Illinois at Urbana-Champaign, Structural Research Series No. 470, Report No. UILU-ENG-79-2019, Research Project No. FHWA/IL/UI/180, August 1979.
20. Hanna, T. H., *Field Instrumentation in Geotechnical Engineering*, Trans Tech Publications, First Edition, 1985.
21. Imbsen, R. A., Vandershaf, D. E., Schamber, R. A., and Nutt, R. V., "Thermal Effects in Concrete Bridge Superstructures," NCHRP Research Report No. 276, Transportation Research Board, Washington, D.C., September 1985.
22. Johnson, M. J., *Fiber Optic Interferometer Sensor for Strain Measurements in High Magnetic Fields and Cryogenic Environments*, M. S. Thesis, The University of Texas at Austin, May 1991.

23. Kokobu, M., Gogo, Y., Ozaka, Y., Okamura, H., and Momoshima, S., "Measurements of Creep and Shrinkage in Actual Prestressed Concrete Bridges," International Association for Bridge and Structural Engineering, Symposium: Design of Concrete Structures for Creep, Shrinkage, and Temperature Changes, Madrid 1970, pp. 19-26.
24. Koretsky, A. V., and Pritchard, R. W., "Critical Assessment of the International Estimates for Relaxation Losses in Prestressing Strands," University of Queensland, Department of Civil Engineering, Research Report No. CE25, St. Lucia, Australia, June 1981.
25. Littlejohn, G. S., "Acceptance Criteria for the Service Behaviour of Ground Anchorages," Ground Engineering, Vol. 14, No. 3, April 1981, pp. 26-36.
26. Loh, Y. C., Internal Stress Gages for Cementitious Materials, SESA, Proceedings Vol. 11, No. 2, 1954, pp.13- 28.
27. Lutz, B. A., *Measurement of Development Length of 0.5 Inch and 0.6 Inch Diameter Prestressing Strand In Fully Bonded Concrete Beams*, M. S. Thesis, The University of Texas at Austin, May 1991.
28. Markey, I., "Hydrostatic Levelling System for the Measurement of Bridge Deformation," Publication No. 134, Institut de Statique et Structures - Béton Armé et Précontraint (IBAP), Ecole Polytechnique Fédérale de Lausanne, November 1989.
29. Marshall, V., and Gamble, W. L., "Time Dependent Deformations in Segmental Prestressed Concrete Bridges," Research Report No. UILU-ENG-81-2014, SRS-495, University of Illinois at Urbana-Champaign, Department of Civil Engineering, Urbana, IL, October 1981.
30. McGregor, R. J. G., *Evaluation of Strength and Ductility of a Three Span Externally Post-Tensioned Box Girder Bridge Model*, Ph. D. Dissertation, The University of Texas at Austin, August 1989.
31. Measurements Group, *Manual of Technical Reports*, Strain Gage Technical Data, Strain Gage Listings, Technical Tips and Instruction Bulletins.
32. Measurements Group, "Optimizing Strain Gage Excitation Levels," Technical Note TN-502, 1979.
33. Measurements Group, "Strain Gage Applications with M-Bond AE-10/15 and M-Bond GA-2 Adhesive Systems," Instruction Bulletin B-137-13, Raleigh, North Carolina, 1979.
34. Measurements Group, "Surface Preparation for Strain Gage Bonding," Instruction Bulletin B-129-6, Raleigh, North Carolina, 1976.

35. Miessler, H. J., and Levacher, F. K., "Monitoring Stressing Behaviour with Integrated Optical Fiber Sensors," 13th IABSE Congress, Helsinki, International Association for Bridge and Structural Engineering, June 1988.
36. Neville, A. M., *Creep of Plain and Structural Concrete*, London, 1983.
37. Orsat, P., and Bertel, J. C., "Measurement of Forces Actually Applied on Rebars Anchor-Bolts or Strands with Tensiomag," International Association of Bridge and Structural Engineering, IABSE Proceedings, 5th Annual International Bridge Conference (IBC), June 13-15, 1988, Pittsburgh, Pennsylvania, pp. 51-56.
38. Pauw, A., and Breen, J. E., "Field Testing and Analysis of Two Prestressed Concrete Girders," The University of Missouri Bulletin, Volume 60, Number 52, Columbia Missouri, November 1959.
39. Pauw, A., and Breen, J. E., "Structural and Economic Study of Precast Bridge Units - Instrumentation," Technical Report No. 1, The University of Missouri, Department of Civil engineering, 1957.
40. Perry, C. C., and Lissner, H. R., *The Strain Gage Primer*, McGraw-Hill Book Company, Inc., New York, Second Edition, 1962.
41. Post, J., Tahamassebi, B., and Frank, K. H., "Estimating Fatigue Life of Bridges," The University of Texas at Austin, Center for Transportation Research, Report No. 464-1F, March 1988.
42. Poston, R. W., Bradberry, T. E., and Breen, J. E., "Load Tests of a Pretensioned Girder Bridge near Happy, Texas," Research Report No. 921-1F, Center for Transportation Research, The University of Texas at Austin, April 1985.
43. Preston, H. K., "Testing of 7-Wire Strand for Prestressed Concrete -- The State of the Art," Journal of the Prestressed Concrete Institute, Vol. 30, No. 3, May-June 1985, pp. 134-155.
44. Radloff, B. J., *Bonding of External Tendons at Deviators*, M. S. Thesis, The University of Texas at Austin, December 1990.
45. Richardson, J. E., "Field-Measured Post-Tension Prestress Loss in Stress-Relieved Strands," California Department of Transportation (CALTRANS), Report No. FHWA/CA/SD-84/02, Sacramento, CA, June 1984.
46. Roberts, C.L., "Measurement Based Revisions for Segmental Bridge Design and Construction Criteria", Doctoral Dissertation, University of Texas at Austin, December 1993.



47. Telephone conversations and electronic FAX transmittals with Mark Hatfield, Applications Engineer, Campbell Scientific, Inc., June/July 1990.
48. Telephone conversations with Mr. Frank Dominico of Sika, Inc., during August and September of 1990.
49. Texas Department of Highways and Public Transportation, Material Specification D-9-6110, Epoxy Adhesive Type V.
50. The final completion bridge circuitry between the 21X-data-logger and each AM416-multiplexer was designed with the assistance of Johaan Ernest, Electronic Shop Assistant for FSEL, August/September 1990.
51. Vijayvergiya, V. N., *Load Distribution for a Drilled Shaft in Clay Shale*, Ph.D. Dissertation, The University of Texas at Austin, Austin, Texas, November 1968.
52. White, C. D., *Observations and Evaluation of the Composite Wing Girder Bridge at Bear Creek*, M. S. Thesis, The University of Texas at Austin, May 1984.
53. Wolff, R., and Miesslerer, H. J., "New Materials for Prestressing and Monitoring Heavy Structures," *Concrete International*, American Concrete Institute, Vol. 11, No. 9, pp. 86-89, September 1989.
54. Yates, D. L., *A Study of Fretting Fatigue in Post-Tensioned Concrete Beams*, M. S. Thesis, The University of Texas at Austin, May 1988.
55. Ziadat, G. S., and Waldron, P., "Measurement of Time-Dependent Behaviour in the River Torridge Bridge," Report No. UBCE/C/87/4, University of Bristol, November 1987.
56. Ziadat, G. S., and Waldron, P., "Segmental Construction of Concrete Bridges: A State-of-the-Art Report," Report No. UBCE/C/86/1, University of Bristol, Department of Civil Engineering, December 1986.
57. Zumbrennen, L. G., *Behavior of Statically Loaded Prestressed Concrete Girders With 0.5 Inch Diameter Debonded Strands*, M. S. Thesis, The University of Texas at Austin, May 1991.

